

January 2016

A Human-Centered Approach for the Design of Perimeter Office Spaces Based on Visual Environment Criteria

Iason Konstantzos
Purdue University

Follow this and additional works at: https://docs.lib.purdue.edu/open_access_dissertations

Recommended Citation

Konstantzos, Iason, "A Human-Centered Approach for the Design of Perimeter Office Spaces Based on Visual Environment Criteria" (2016). *Open Access Dissertations*. 1222.
https://docs.lib.purdue.edu/open_access_dissertations/1222

This document has been made available through Purdue e-Pubs, a service of the Purdue University Libraries. Please contact epubs@purdue.edu for additional information.

**PURDUE UNIVERSITY
GRADUATE SCHOOL
Thesis/Dissertation Acceptance**

This is to certify that the thesis/dissertation prepared

By Iason Konstantzos

Entitled

A HUMAN-CENTERED APPROACH FOR THE DESIGN OF PERIMETER OFFICE SPACES BASED ON VISUAL
ENVIRONMENT CRITERIA

For the degree of Doctor of Philosophy

Is approved by the final examining committee:

Athanasios Tzempelikos

Chair

Qingyan Chen

Panagiota Karava

Robert Proctor

To the best of my knowledge and as understood by the student in the Thesis/Dissertation Agreement, Publication Delay, and Certification Disclaimer (Graduate School Form 32), this thesis/dissertation adheres to the provisions of Purdue University's "Policy of Integrity in Research" and the use of copyright material.

Approved by Major Professor(s): Athanasios Tzempelikos

Approved by: Dulcy M. Abraham

Head of the Departmental Graduate Program

11/28/2016

Date

A HUMAN-CENTERED APPROACH FOR THE DESIGN OF PERIMETER OFFICE
SPACES BASED ON VISUAL ENVIRONMENT CRITERIA

A Dissertation

Submitted to the Faculty

of

Purdue University

by

Iason Konstantzos

In Partial Fulfillment of the

Requirements for the Degree

of

Doctor of Philosophy

December 2016

Purdue University

West Lafayette, Indiana

For my parents

ACKNOWLEDGEMENTS

My PhD has been quite a journey, full of experiences, unforgettable moments, exciting accomplishments and stressful disappointments, endless nights of work under strict deadlines and creative moments. Reaching the finish line gives me mixed feelings, excitement for the things I've accomplished but also slight nostalgia, thinking that soon I'll head my own path in a different place, far from the warm environment of Purdue University. Coming from an entirely different background, I found myself in a whole new world working in the field of Building Science. In that, the help of my advisor, Athanasios Tzempelikos has been priceless; he helped me gradually build a solid background, he was always available any time I needed him, and most importantly, he transmitted to me his enthusiasm of advancing the field with quality research. Also, I would like to thank my committee members, Qingyan Chen, Panagiota Karava and Robert Proctor, for their invaluable comments on the course of my research work. Each one coming from a different background, together they formed an ideal expert group in the field of indoor built environment and human comfort.

My work would be not possible without the support of ALCOA foundation and the funding they provided for my research. Also I'd like to mention the valuable help of Lutron Electronics, and especially Brent Protzman and Sam Chambers for supplying our laboratories with equipment, sharing with us concerns of the industry related to our field

and collaborating with us for solving problems. Also, Matt Miller and Bill Hooper from Kawneer Inc. for giving me the chance to apply my skills to actual industry products and for their valuable comments, Viracon Inc. and Charles Boyer, as well as PPG industries for equipping our laboratories.

Of course, although a PhD cycle is a lonely journey, it would be impossible without the support of my colleagues, and especially Ying-Chieh Chan, who from my first day at Purdue was always there to guide me as a more senior PhD student. Also, I would like to thank my parents, who formed me as the person I am, provided me with everything I needed to pursue my future, and was always there for me, and this Thesis is definitely dedicated to them. Last, but not least, I'd like to thank my dear wife, Xiaoqi, for her unconditional support. Not only she has been always by my side, happy to deal with my extreme schedules and stress, but she also provided me with an invaluable colleague, having a rare understanding of my field and sharing with me her comments throughout the course of my research.

TABLE OF CONTENTS

	Page
ABSTRACT.....	ix
CHAPTER 1. INTRODUCTION.....	1
1.1 Background.....	1
1.2 Motivation - Objective	2
1.3 Document Overview.....	5
CHAPTER 2. LITERATURE REVIEW	8
2.1 Evolution of Daylight Glare Indices.....	8
2.2 Daylight Glare Probability (DGP).....	12
2.3 HDR imaging for daylight glare evaluation	15
2.4 Daylight Glare measurement and experimental studies	21
2.5 Daylight Glare Modeling Approaches.....	26
2.6 Occupant-related daylight glare studies – Validations of indices - Interactions	34
2.7 Spatial Considerations – Recommendations	43
2.8 Comfort-oriented Control Implementation.....	45
2.9 Daylight metrics	46
2.10 Window Views and Related Studies – Quantity and Quality of View	47
2.11 Research gaps and aims of Thesis	50
CHAPTER 3. METHODOLOGY	55
3.1 Experimental methodology	55
3.1.1 Façade Engineering Labs (Architectural Engineering facilities at Bowen Laboratories).....	55
3.1.2 Living Labs – Herrick Laboratories.....	63
3.1.3 Private offices– Herrick Laboratories	64

3.2	Shading controls	67
3.3	HDR imaging.....	68
3.3.1	Methodology A – LMK system	68
3.3.2	Methodology B – Calibration of regular dSLR cameras	74
3.3.3	Methodology C – Including the solar corona through window shades	80
3.4	Simulation Methodology	83
3.4.1	Incident illuminance on facade	85
3.4.2	Interior illuminance calculations.....	85
3.4.2.1	Ray tracing method	85
3.4.2.2	Daylight transmission through shading.....	86
3.4.2.3	Radiosity calculations	88
3.4.3	Glare calculation module	90
3.4.4	Model Validation	92
CHAPTER 4. EXPERIMENTAL AND SIMULATION ANALYSIS OF DAYLIGHT GLARE PROBABILITY IN OFFICES WITH DYNAMIC WINDOW SHADES		96
4.1	Introduction	96
4.2	Experimental results of DGP under variable sky conditions.....	96
4.2.1	Correlations between DGP and work plane illuminance	97
4.2.2	DGP-vertical illuminance correlations and contrast influence discussion .	99
4.2.3	Experimental assessment of shading control efficiency in terms of glare	102
4.3	Generalization of results – DGP simulation for dynamic shading	104
4.3.1	Annual correlations between DGP and work plane illuminance	105
4.3.2	Annual DGP-vertical illuminance correlations, DGPs applicability and contrast discussion	107
4.3.3	Daylight Glare Probability with the sun within the field of view	109
4.3.4	Annual evaluation of shading control efficiency towards glare	112
4.4	Discussion.....	114
4.5	Recommendations for fabric selection to avoid daylight glare	117
CHAPTER 5. VISUAL COMFORT EVALUATIONS WITH HUMAN SUBJECTS		119

5.1 Preliminary study for the evaluation of discomfort predictors in open plan offices	120
5.1.1 Introduction - Procedure	120
5.1.2 Correlations between visual comfort preferences and known indices	126
5.1.3 General Impressions.....	132
5.2 Preferred indoor illuminance and DGP ranges in private offices with manual visual environment controls	136
5.2.1 Introduction.....	136
5.2.2 Results.....	138
5.3 Discussion.....	142
CHAPTER 6. DAYLIGHT GLARE EVALUATION WITH THE SUN IN THE FIELD OF VIEW THROUGH WINDOW SHADES	143
6.1 Introduction	143
6.2 Methodology.....	145
6.2.1 Experimental setting, measurements and instrumentation.....	145
6.2.2 Shading fabrics.....	148
6.2.3 Angular fabric transmission properties and direct vertical illuminance on the eye	149
6.2.4 Experimental procedure, tests and surveys.....	151
6.3 Results	154
6.3.1 General impact of fabric properties on glare	154
6.3.2 Vertical illuminance, DGP and respective comfort ranges.....	157
6.3.3 Correlation of discomfort sensation with existing illuminance- and luminance-based metrics	160
6.3.4 Modification of the DGP coefficients for cases with the sun in the field of view through roller shades.....	163
6.3.5 Formulation of a new illuminance-based metric for assessing daylight glare with the sun in the field of view through roller shades.....	166
6.4 Conclusion.....	170

CHAPTER 7. A METHOD FOR QUANTIFYING VIEW CLARITY THROUGH WINDOWS WITH SHADING FABRICS.....	173
7.1 Introduction and Experimental Methodology	173
7.2 Questionnaires – Data collection.....	178
7.3 Total scores and fabric rankings.....	181
7.4 Descriptive statistics	183
7.5 An empirical model for predicting the view clarity index.....	185
7.6 Analysis of variance results.....	189
7.7 General Impressions	193
7.8 Visual comfort, color and transparency preferences	195
7.9 Limitations.....	197
CHAPTER 8. DESIGN RECOMMENDATIONS	200
8.1 Introduction	200
8.2 A suite of metrics for the holistic evaluation of the visual environment.....	201
8.2.1 Visual Comfort Autonomy (VCA)	201
8.2.2 Lighting Energy Performance	204
8.2.3 Connection to the outdoors	205
8.3 Using the suite of metrics as a triple visual environment criterion	209
8.3.1 A private office case study.....	210
8.3.2 Application in open-plan offices – A case study	212
8.4 Discussion - Limitations	216
CHAPTER 9. FUTURE WORK	219
9.1 Development of a standard framework for glare evaluations	219
9.2 Glare evaluation with the sun visible through diffuse fabrics.....	219
9.3 Fabric selection guidelines	220
9.4 Luminance and glare evaluation using smartphones.....	220
REFERENCES	222
VITA.....	232
PUBLICATIONS.....	233

ABSTRACT

Konstantzos, Iason. Ph.D., Purdue University, December 2016. A Human-Centered Approach for the Design of Perimeter Office Spaces Based on Visual Environment Criteria. Major Professor: Athanasios Tzempelikos.

With perimeter office spaces with large glazing facades being an indisputable trend in modern architecture, human comfort has been in the scope of Building science; the necessity to improve occupants' satisfaction, along with maintaining sustainability has become apparent, as productivity and even the well-being of occupants are connected with maintaining a pleasant environment in the interior. While thermal comfort has been extensively studied, the satisfaction with the visual environment has still aspects that are either inadequately explained, or even entirely absent from literature. This Thesis investigated most aspects of the visual environment, including visual comfort, lighting energy performance through the utilization of daylight and connection to the outdoors, using experimental studies, simulation studies and human subjects' based experiments.

Visual discomfort is mostly associated with discomfort glare, which can be evaluated using a variety of available different indices with known strengths and weaknesses. Most of the latter are based on the luminance distribution of the visual field. Obtaining the luminance distribution is a complex procedure, either on an experimental or simulation level; experimental acquisition involves the use of dSLR cameras and HDR imaging, along with a series of image processing, calibrations and calculations, while it

faces challenges in cases of measuring the solar corona, due to its extreme peak luminance level. This leads to time consuming procedures with questionable accuracy. Also, when it comes to simulations, a detailed luminance mapping of the interior involves time consuming renderings, which makes annual simulations slow and inefficient. This Thesis uses three different experimental methodologies for luminance acquisition in order to provide accurate and fast measurements, even for the case of the sun being included in the field of view, and also utilizes a hybrid ray-tracing and radiosity lighting model to improve the effectiveness of annual discomfort modeling with the minimal compromise in terms of accuracy. The experimental methodology has been evaluated in preliminary human subjects testing in real office spaces in order to validate its effectiveness and also give some preliminary results and directions for the next parts.

Daylight Glare Probability is the most recent visual discomfort index, and currently considered to be the most reliable, as it is extracted by human subjects experimentation. However, the specific conditions under which it was proposed and its behavior in specific cases have raised some concerns in terms of its effectiveness in different conditions, especially when it comes to roller shades and the sun being included in the field of view. This Thesis used experimental and simulation analysis to evaluate the behavior of Daylight Glare Probability under different shading controls, investigate the effectiveness of the simplified index DGPs and pointed out inconsistencies in special cases, like facing the sun through roller shades.

To address the inconsistencies identified, an extended human subjects study was performed, in order to evaluate visual discomfort in the special case of the sun being visible through shading fabrics. Discomfort thresholds are extracted for important interior

illuminance and luminance metrics, and a variety of widely used glare indices are evaluated in terms of their prediction performance. Two new discomfort metrics are proposed, DGPmod and GlareEV, to be used in a dual function form only for the cases of the sun being visible through shading fabrics.

As the quality of view is highly subjective and connected to a lot of non-quantifiable parameters, its only measurable aspect, the visual clarity has been investigated. By developing a scoring system based on a combination of subjective and objective questions, human subjects' surveys have been used to find that visual clarity is a function of the fabrics' most common properties, the openness factor and visible transmittance. Through the use of the developed equation, the View Clarity Index (VCI), architects can have an understanding about the visual clarity in the design phase.

Finally, in the lack of a unified design methodology based on the visual environment, the newly obtained knowledge of this Thesis has been combined to propose the Visual Environment Index, a design framework based on three main visual environment factors: visual comfort, lighting energy performance and connection to the outdoors. In that scope, a suite of three metrics are introduced, the Visual Comfort Autonomy (VCA), to account for the portion of annual working hours under conditions of comfort, the Continuous Daylight Autonomy to cover the lighting energy savings, and the Effective Outside View (EOV), to quantify the connection to the outdoors. Using these three metrics in the framework of VEI can help architects make decisions in terms of façade configurations, shading controls or even positional layouts in private or open plan offices.

CHAPTER 1. INTRODUCTION

1.1 Background

The architectural trends of the second half of the twentieth century are still dominating the commercial construction trends globally, involving office spaces, in private or open-plan layouts, parts of high-rise buildings with large facades, aiming to improve the satisfaction of occupants (Figure 1.1).



Figure 1.1 Open plan office with large glazing surfaces (Harvard Business Review)

The use of such components leads to the gradual advance of Building Science, considered today to be one of the most important aspects of construction, as office spaces need to be more efficient in terms of both energy savings and productivity. Improvements in energy efficiency are achieved by a thorough study of the thermal and visual aspects of the

building, starting from the envelope's material design, glazing dimensioning and selection, and continuing to the level of equipment, including HVAC, lighting and shading systems and controls. On the other hand, the improvement of productivity is directly connected to the advancements in terms of thermal and visual aspects of comfort. Comfort oriented use of building science aims to create spaces that are pleasing for their occupants, provide healthy conditions and at the same time keep negative environmental influence at a minimal level.

While thermal comfort is a relatively well studied field, the visual aspects of comfort are in certain levels still unclear. Glare, either in the degree of discomfort or disability, is considered to be the most important factor affecting visual comfort, however other involved topics include light adequacy, contrast within the visual field, and even the connection to the outdoors (view) in terms of quantity and quality. Visual comfort is more difficult to assess, as it gets affected immediately when related conditions are met, unlike thermal sensation, which in most cases shows a relatively transient behavior. That makes the design of visual comfort-targeted controls complicated, as except for the fact that it requires consideration of short time steps, it involves also the balance between shading and overall lighting controls. Also, visual comfort frequently interferes with energy efficiency, as while the excessive use of daylight through windows can minimize lighting energy use, at the same time it creates non-comfortable, and often even intolerable conditions.

1.2 Motivation - Objective

Focusing on comfort involves a great challenge, as essentially it mixes two entirely different aspects; an advanced quantitative approach towards uncovering interactions and

investigating the behavior of all involved environmental parameters and at the same time a thorough study of the human perception of comfort, and how it is interacting with the above. Therefore, advanced simulations and extensive laboratory research need to be applied in order to cover the quantitative side. Human-centered studies, involving test subjects and even implementing psychology and psychophysics concepts, need to accompany the quantitative side, either to validate its findings, or to direct the next necessary steps towards an efficient alignment of the goals of building science with the needs of human occupants. In addition, while comfort is the main focus of related literature, there are also other aspects that contribute to the overall satisfaction of occupants, such as the concept of the connection to the outdoors. This rather ambiguous factor, in general incompatible with glare, the leading constraint of comfort, is usually not addressed although it has been proven to be important for the occupants' satisfaction.

A human-centered approach towards designing office spaces is the main objective which involves a cycle of advancement of all of the above-mentioned factors simultaneously. Analyzing thoroughly the known methods of quantifying visual comfort, understanding any interdependencies and limitations involved, designing energy-efficient visual system controls based on these findings, validating the findings with human subjects, and identifying the connection with environmental variables, are important parts of the required research steps. In addition, the ambiguity, which is an essential part of the concept of comfort, often requires statistical processing, in order to extrapolate general trends from experiments of limited laboratory capacity.

The overall objective of this thesis is to propose a holistic design framework based on the visual environment. This will cover the three main factors that affect it, visual

comfort, lighting energy performance and the connection to the outdoors. This framework will give architects the opportunity to choose optimal façade configurations and orientations, during the design or retrofit phase, as well as the options to perform cost-effective but efficient changes during the operation phase, such as selecting optimal positioning layouts, shading controls or combinations of the above. In the path to make such a framework possible, a series of gaps in our knowledge towards the visual environment need to be filled.

Concerning visual comfort, it is necessary to improve current measurement methodologies, introduce automation techniques to make them more efficient, and also develop advanced daylight and glare modeling methodologies which will allow to generalize the experimental findings for any type of dynamic façade systems, spaces and orientations. Also, the investigation of the behavior of current daylight and glare metrics as discomfort predictors is needed, covering all possible cases, including the much scarcely studied case of having the sun in the field of view through shading fabrics. All these need to be evaluated in combined experimental, simulation and human subjects studies.

In terms of the lighting energy performance, shading control approaches need to be investigated based on their combined performance in both daylight provision and comfort, in both experimental and simulation levels, as well as using human subjects. Having efficient control strategies, using thresholds validated by human subjects and implementing them in the holistic framework will allow optimal design in terms of energy and comfort.

Finally, about the ambiguous factor of the connection to the outdoors, as its psychological aspect (quality of scenery etc.) is out of the focus of such a framework, its

two main quantifiable options need to be investigated; the amount of view, in terms of the portion of the visual field that gets connected to the exterior through the fenestration, and the clarity of view, covering the interferences to the view caused by the complex fenestration systems, if any.

Shedding light in all the aforementioned topics will lead to the development of the Visual Environment Index, a holistic framework that will allow design based on the visual environment.

1.3 Document Overview

Chapter 2 contains an extensive literature review about visual comfort, the most important glare indices, HDR imaging and glare experimental studies, as well as about the most widely used simulation methods.

Chapter 3 includes a detailed view of the methodology for this Thesis. It is split in 4 parts: 3.1 covers the experimental methodology and descriptions of the experimental facilities. 3.2 describes all shading control approaches that are used extensively throughout this thesis. 3.3 covers the HDR imaging methodology for obtaining accurate luminance mapping and image processing to acquire daylight glare metrics. 3.4 includes the simulation methodology for generalization of experimental findings with respect to daylight glare. The latter covers an overview of the daylighting model, using a hybrid ray tracing and radiosity approach that includes detailed daylight transmission through complex fenestration systems, and consideration of dynamic shading controls in an annual analysis. A glare calculation module, based on DGP, is integrated with the daylighting module for daylight glare prediction in daylit spaces with any type of configuration and

dynamic fenestration elements. The last part of the sub-section presents validation of the simulation model using full-scale experimental measurements.

Chapter 4 presents an experimental and simulation investigation of DGP and correlation with daylight metrics in full-scale test offices (Façade Engineering Labs) with dynamic shading. Correlations between measured DGP and horizontal and vertical illuminance metrics are presented for variable sky conditions, two glazing systems, and three different shading controls. The limitations and applicability of simplified glare metrics such as DGPs, and the impact of the contrast term are discussed in detail. Results are presented on the efficiency of two advanced shading controls algorithms in terms of daylight glare protection capabilities. The contents of

Chapter 5 presents two preliminary studies of applying the experimental methods presented in Chapter 3 to obtain visual comfort evaluations in occupied open-plan and private office spaces in the Center for High Performance Buildings. Chapter 5.1 covers field measurements and surveys that were conducted under different sky conditions, and indoor illumination conditions (shading and lighting) for occupants seated in different locations with different view directions. The results include daylight metrics and subject preferences and correlations between visual comfort preferences and existing daylight glare indices. Chapter 5.2 presents experiments conducted in occupied sidelit private offices with different shading and lighting controls. The objective of this sub-chapter is to evaluate the desired interior illuminance and glare conditions according to occupants who had control over their lighting and shading systems.

Chapter 6 presents the experimental investigation of daylight glare for cases when the sun is visible through window shades. An experiment with 41 human subjects and 14

different shading fabrics was performed in order to investigate the impact of fabric properties in the perception of daylight glare, extract ranges of comfort for such conditions, evaluate the applicability of current discomfort metrics based on luminance or illuminance variables, and propose the DGP_{mod} and $GlareE_v$, new indices that can more effectively predict discomfort under such conditions.

Chapter 7 presents the development of a new metric to quantify view clarity through windows with shading fabrics. A separate experiment with human subjects, described in Sections 7.1-7.2, was conducted to obtain view clarity preferences through 14 different shading fabrics for different sky conditions and view distance from the window. The data were processed (Section 7.3) to develop a new metric, the View Clarity Index (VCI), that can be used to characterize common window shades fabrics in terms of view clarity (Section 7.4). This index is only a function of basic shade optical properties and can be used for developing visual environment guidelines when connection to the outdoors is desired.

Chapter 8 proposes a methodology for new designs and retrofits of new spaces, based on visual environment criteria and lighting energy performance. It uses the knowledge obtained by the previous chapters of this Thesis to assess the visual environment of spaces using three main factors: Visual comfort (through the index of Comfort Autonomy), Lighting energy performance (using the Daylight Autonomy) and Connection to the Outside (using the proposed index of the Effective Outside View). The methodology is applied to a private office space with controlled shades and an Open plan office space with fixed permanently closed shading using different objectives for each case.

Chapter 9 includes ideas for future work and potential extensions of this research.

CHAPTER 2. LITERATURE REVIEW

2.1 Evolution of Daylight Glare Indices

One of the earliest studies related to discomfort by “high brightness” was conducted by Luckiesh and Guth (1949). It was an experimental study with results that are considered to be of great importance even in today’s literature.

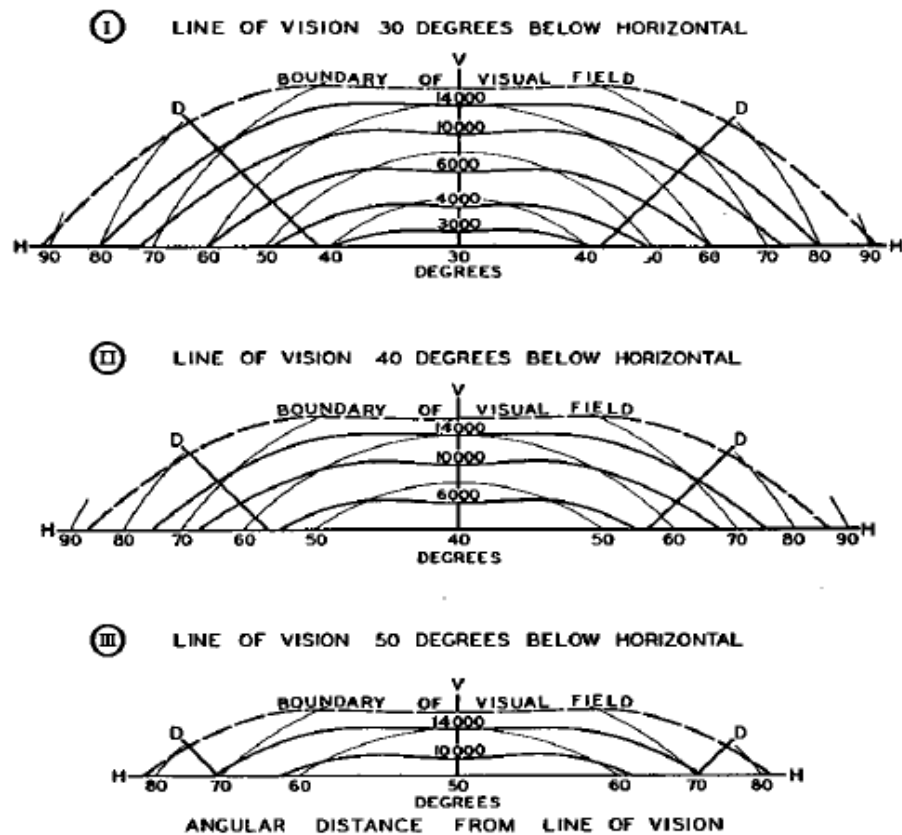


Figure 2.1 Illustration of the extent of the visual field above the horizontal (Lukiesh & Guth, 1949)

Using a specially designed apparatus, they measured the discomfort caused to people by controlled artificial lighting conditions. The criterion that they chose was the so-called “border of comfort and discomfort”, which remains still valid in present practice. The methodology of their study was based on specifying the critical luminance of light sources for which the test subjects were starting to experience discomfort, and the way those values changed depending on several parameters, such as overall field brightness, size of light sources, position of sources, and behavior of multiple and linear sources respectively. In addition, a detailed measurement of the human’s visual field was made (Figure 2.1), which is still followed by visual comfort related research. The importance of this study is obvious considering that the conclusions have been extensively validated in decades of future research and by the fact that several details are used even in present research (e.g., the position index).

Several publications about discomfort and glare followed, which were eventually included in a study of Hopkins (1957). These included the assumption that discomfort should be assessed using the following expression:

$$\text{Glare} = \frac{f(\text{Luminance}_{\text{source}}) \times f(\text{Apparent size}_{\text{source}})}{f(\text{Adaptation Luminance}) \times f(\text{Immediate luminance}) \times f(\text{Angle})} \quad (2.1)$$

Although several indices have been introduced since then, most of them were based on the above expression. Hopkins and Petherbridge (1966) developed the British Glare Index (BGI), based on the glare equation with respect to the four degrees of discomfort: just noticeable, just acceptable, just uncomfortable and just intolerable. Hopkins was charged with transferring the general light discomfort research from artificial lighting and car headlamps to daylight glare due to large windows in buildings,

following the architectural trends of the early 1930s. He investigated the basics of approaching something as subjective as glare giving valuable information, such as the important fact of constancy in the sensitivity of glare over an individual. In his ergonomics-oriented studies, among presenting the details about his glare index, he also specified the most apparent factors that seemed to have an effect in the disturbance of people -not included in that index: window size, brightness and position, interior brightness levels. He also described in detail simple ways to prevent glare such as shades, placing the windows away from the part below the line of sight, using light colors for the room around windows to reduce contrast, etc. These four degrees have been used extensively in most of the future glare indices. Equation (2.2) uses L_s , as the luminance of glare sources, ω_s as the solid angle, P the position index according to Guth (1966) and L_b the background average luminance. These symbols are used to describe the above variables throughout the rest of the chapter. The equation was limited to glare sources sizes of up to 0.027sr.

$$BGI = 10 \log_{10} 0.478 \sum \frac{L_s^{1.6} \omega_s^{0.8}}{L_b P^{1.6}} \quad (2.2)$$

Hopkinson (1972) developed one of the well-known glare indices, Daylight Glare Index or DGI (Eq. 2.3), which is still being used today. The DGI considers visible sky brightness through a window. The sky is supposed to be diffuse. The DGI is weak in describing either direct light conditions from the window or specular reflections from within the room. The methodology of this study involved a diffusing screen which was backlit by a set of fluorescent lamps. Validation studies that followed showed that it generally underestimated the glare from windows compared to the results for artificial light sources.

$$DGI = 10 \log_{10} 0.478 \sum \frac{L_s^{1.6} \omega_s^{0.8}}{L_b + 0.07 \omega_s^{0.5} L_s} \quad (2.3)$$

Nazzal (2005) improved Hopkinson's DGI by adding more factors in the equation, including the mean luminance of the surroundings (L_{adaptive}), the mean exterior luminance (L_{exterior}) and the mean luminance of the window, as the latter was being treated as a uniform glare source. Although DGI_N (Eq. 2.4) is proposed to be an improvement over DGI, it has never been validated by subjects but only correlated to the original DGI.

$$DGI_N = 8 \log_{10} \left\{ 0.25 \frac{\sum L_{\text{exterior}}^2 \times \Omega_{pN}}{L_{\text{adaptation}} + 0.07 \times \left(\sum \omega_N^{0.5} \times L_{\text{window}} \right)} \right\} \quad (2.4)$$

In a study by Einhorn (1979), another glare index was proposed to be used as a standard adopted by CIE. The exponent of solid angles was equal to one to, assuming that dividing a glare source into multiple would produce the same value; direct and indirect illuminance were handled separately.

$$CGI = 8 \log_{10} \left(\frac{2 \left[1 + \frac{E_{\text{direct}}}{500} \right]}{E_{\text{direct}} + E_{\text{indirect}}} \right) \sum \frac{L_s^2 \omega_s}{p^2} \quad (2.5)$$

, where E_{direct} is the direct vertical illuminance from all sources and E_{indirect} the indirect part. The CGI index (Eq. 2.5) was never validated with subjects, but it was correlated with other existing indexes.

UGR or Unified Glare Rating (International commission on Illumination, 1992), shown in Eq. 2.6 is essentially a combination of CGI and BGI indices to assess discomfort by artificial light systems. There is a range for acceptable size of the glare sources when using this equation, and this includes perceived sizes of 0.0003 to 0.1 sr.

$$UGR = 8 \log_{10} \frac{0.25}{L_b} \sum \frac{L_s^2 \omega_s}{p^2} \quad (2.6)$$

2.2 Daylight Glare Probability (DGP)

The Daylight Glare Probability (Wienold and Christoffersen, 2005) is the most recent index of evaluating daylight glare in literature. It was defined as the percentage of people feeling discomfort by daylight glare for a given time and position.

$$DGP = 5.87 \times 10^{-5} E_v + 9.18 \times 10^{-2} \log_{10} \left(1 + \sum_{i=1}^n \frac{L_{s,i}^2 \omega_{s,i}}{E_v^{1.87} p_i^2} \right) + 0.16 \quad (2.7)$$

The index was extracted from 349 responses, using a methodology of grouping results at an increasing value. The equation of DGP (Eq. 2.7) constitutes of three parts: One handling the overall brightness of the visual field, thus being a function of the total vertical on eye illuminance (E_v), one taking into account the cumulative influence of the separate glare sources within the visual field, being a function of the luminance of the glare sources, their geometry, and the total vertical on eye illuminance, and the third part being a constant. The geometry of the glare sources is defined through their solid angle, reflecting the apparent size to the eye, and their position index, reflecting the relative deviation of each source from the line of sight. For the position index, the original study assumed two separate calculation methods for above and below the line of sight in order to comply with the different amount of glare sensitivity (Iwata and Tokura, 1997). Therefore, for the sources located above the line of sight, the position index is calculated as:

$$\ln P = \left(35.2 - 0.31990\tau - 1.22e^{-\frac{2\tau}{9}} \right) \times 10^{-3} \sigma + \left(21 + 0.26667\tau - 0.00296\tau^2 \right) \times 10^{-5} \sigma^2 \quad (2.8)$$

, while for the sources below the line of sight, the equation forms as:

$$\begin{cases} P = 1 + 0.8 \frac{R}{F} & \{R < 0.6F\} \\ P = 1 + 1.2 \frac{R}{F} & \{R \geq 0.6F\} \\ R = \sqrt{H^2 + S^2} \end{cases} \quad (2.9)$$

The symbols are explained in detail in Figure 2.2:

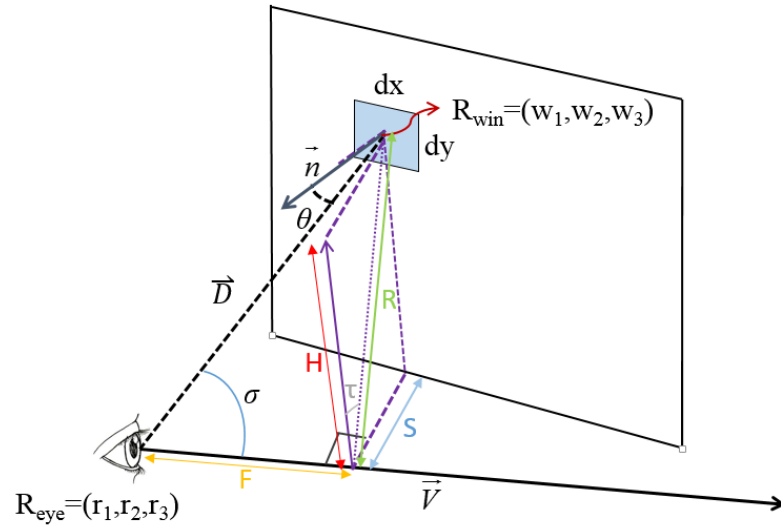


Figure 2.2 Geometry involved in the calculation of position index

Due to the strong correlation of the vertical on eye illuminance with comfort impressions (Figure 2.3), Wienold (2007) introduced a simplified version to approximate DGP which is solely a function of vertical illuminance:

$$DGPs = 6.22 \times 10^{-5} \times E_v + 0.184 \quad (2.10)$$

The above study clearly states the non-applicability of DGPs for instances when direct light hits the observer's eye, with that being a result of a weak correlation between DGP and vertical illuminance for instances of direct radiation. However, it was not clear

whether DGPs could be used for cases of projected direct light on the floor or the walls due to partly opened shades, or in the cases of fabrics with considerable openness which would allow direct light to penetrate the room. Chapter 4 will investigate this matter in detail.

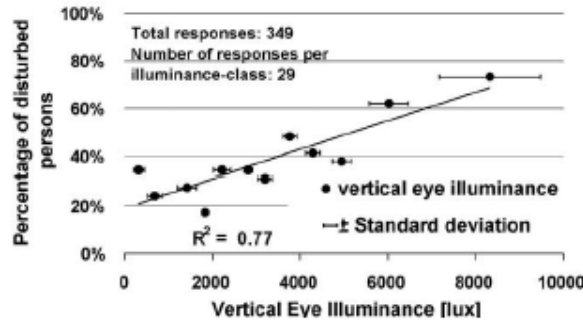


Figure 2.3 Experimental correlation of a linear function of vertical on eye illuminance with percentage of discomfort (Wienold and Christoffersen, 2006)

While the original suggested range for DGP validity was for 0.20-0.80, Wienold (2012) suggested a correction factor to be applied in cases when the vertical illuminance is lower than 320 lux. In these cases, DGP can be calculated as Equation 2.11 suggests:

$$DGP_{\text{low light}} = DGP \times \frac{e^{0.024E_v - 4}}{1 + e^{0.024E_v - 4}} \quad (2.11)$$

Applying this factor solves the issues of having a value of DGP=0.16 for nearly dark conditions, which is inconsistent to the practical definition of DGP as a percentage of discomfort. In addition, in the same study, an age correction factor (Eq. 2.12) is introduced, to account for the variability of glare perception for different age groups.

$$DGP_{\text{age}} = \frac{DGP}{1.1 - 0.5 \frac{\text{age}}{100}} \quad (2.12)$$

As the above two correction factors have been presented in presentation (Wienold, 2013), and not a journal paper, the conditions and settings from which they have been extracted

are not clearly presented. However, they are both available to use in Evalglare (Wienold, 2012).

There have been only very few studies correlating DGP with other lighting metrics; Wienod (2007) presented a correlation of DGP with vertical on eye illuminance, in order to evaluate the applicability of his simplified index. In another study (2009), he suggested comfort classes for glare, based on the annual percentage of discomfort occurrences and using the 95% of best conditions and the average of the rest 5% to define them. Mardaljevic et al. (2012) suggested that the 95% occurrence of DGPs could well correlate with UDI indices. However, in this study there are some major assumptions, such as that DGPs is capable of evaluating annual discomfort in a space. This is not the case, as DGPs cannot handle direct light issues. Annual glare occurrences are currently the best way to grade designs in terms of visual comfort, however more correlations are needed in order to identify simply measureable metrics which could substitute DGP as input for real-time controls.

2.3 HDR imaging for daylight glare evaluation

As all glare indices and comfort approaches include luminance values within the visual field, a prerequisite for obtaining measurements is to be able to perform a detailed luminance mapping of the visual field. This cannot be achieved with luminance point (spot) meters due to the limited area that they can cover and their high cost. If a visual field is the equivalent of a 5MP photograph, an absolutely accurate luminance measurement of a single instance would require the presence of 5 million spot meters.

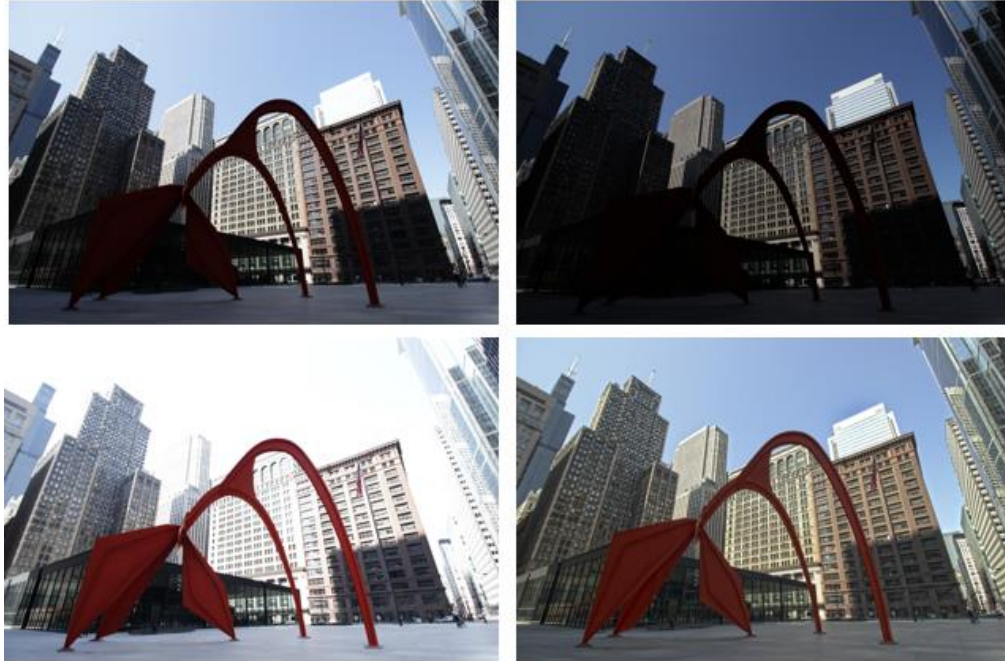


Figure 2.4 Three low dynamic range photographs of normal (top left), darker (top right) and brighter (bottom left) exposure are merged to an HDR image (bottom right) of smooth brightness transition

To overcome this problem, luminance measurements using HDR photography have been adopted. HDR (High Dynamic Range) pictures consist of multiple shots of the same instance of different exposures, usually in terms of variable shutter speeds under constant aperture.

These shots are merged into a unified image that can cover an increased dynamic range in terms of luminance (Figure 2.4). Then, a technique known as radiometric self-calibration relates these pixel values to real-world luminances, using the camera response curve (a function that translates the brightness values of the three basic colors to radiometric intensity). As the camera response curve varies for every combination of camera and lens, the process of radiometric self-calibration has to be repeated for every different case, as well as for different settings (ISO, aperture, etc.).

Uetani and Yoshiaki (2001) provided a thorough literature review of the studies that introduced this technique. A free software often used in literature handling the processes of response function creation and calibration is Photosphere (Ward, 2004). Inanici and Galvin (2004; 2006) performed a thorough evaluation of this measuring methodology by investigating the errors compared to actual luminance measurements using spot meters. The methodology was found to be capable of producing luminance readings at error levels within 10% in average, however there was a considerable variation of the errors depending on the luminance of the target, its color and the overall lighting conditions. This led Borisuit et al. (2010) to suggest separate calibration procedures for different conditions. There are also other factors that influence this accuracy, including vignetting and point spread errors. Vignetting (Fig. 2.5) is the light fall-off experienced in the pixels located at the farthest points from the optical axis.

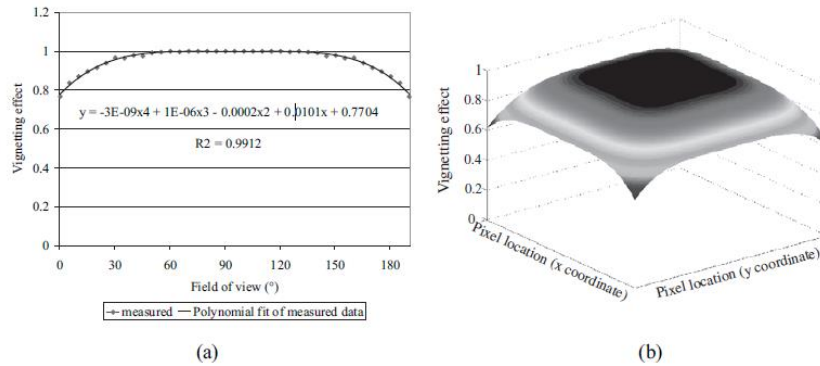


Figure 2.5 The vignetting function of Nikon FC9 fisheye lens for an aperture setting of f/4.0. a) Measured data points and the vignetting function derived to fit the measured points; b) digital filter developed based on the vignetting function (Inanici and Galvin, 2006)

Its correction is based on a function that compensates the luminance of the affected pixels depending on their distance from the optical axis. The vignetting effect is dependent

on the width of the aperture (Inanici and Galvin, 2004; 2006), with smaller apertures generating more controllable and limited vignetting.

Another error that can take place is the result of light that after entering the camera gets spread out and scattered by the optical structure of the lens. The point spread error (Fig. 2.6) was found to be dependent on aperture and eccentricity (distance from the optical center). The authors note that this would lead to problems in cases of bright background surrounding dark targets, which is not usually the case for most architectural applications.

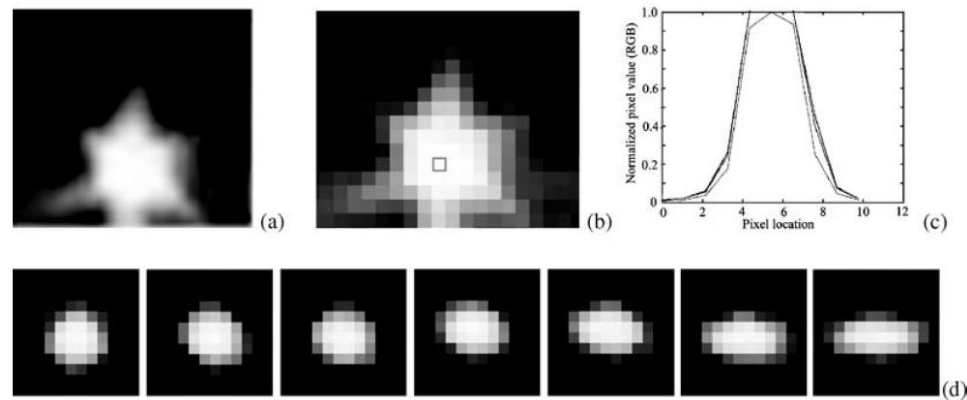


Figure 2.6 a) Close-up view of point spreading; the square in (b) shows the pixel that corresponds to the actual light source. c)PSF as quantified from the HDR image; d) PSF as a function of eccentricity (distance from the optical center) in the camera field of view from 0 to 90° in 15 ° intervals. (Inanici and Galvin, 2006)

However, they do not mention the importance of this error for cases of measuring the solar corona; in these cases, the extreme solar luminance (at the order of 10^6 - 10^7) can affect surrounding pixels causing a much larger apparent size of the solar disc, leading to potential glare overestimations. HDR images including the solar corona have been presented by Inanici (2010), using a methodology introduced by Strumpf et al. (2004). According to the latter study, reasonable readings for the solar luminance can only be obtained by using a technique based on attaching a neutral density (3.0) filter in the area

between the fisheye lens and the sensor, altering the exposures by also altering the apertures, except only modulating shutter speed, and also using a shutter speed as fast as 1/8000 sec (Figure. 2.7). The use of the neutral density filter is essential as, according to the authors, the range between 2 seconds and 1/8000 seconds includes only 14 stops, giving a dynamic range of 2^{14} (16384), which is insufficient for the dynamic range of a sky including the sun.

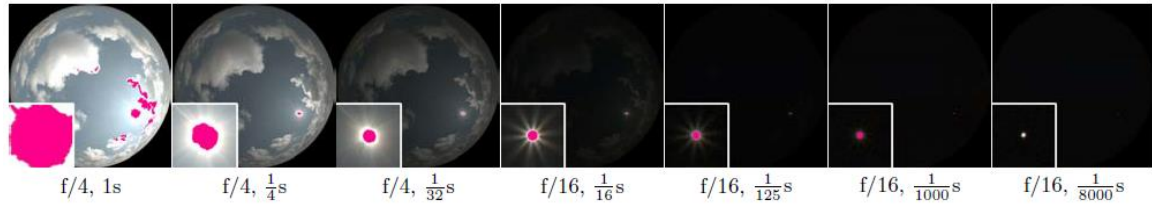


Figure 2.7 HDR sequence and camera settings to span the 17 stops of the sky and sun in 7 exposures. A detailed view of the sun is shown in the bottom left of each image; pink regions indicate saturated pixels. The darkest image is the only image that does not saturate for the sun (Strumpf et al., 2004).

However, there are no cases in literature for HDR images taken from the interior of a room that also include the sun (having so a total range of luminance values from 10 to 10^7 cd/m²). Also, given the errors presented in the study of Inanici and Galvin (2006), the 10% average error observed in exterior conditions can be significant if applied to the extreme luminance value of the sun. It has to be noted that most of the available studies about glare measurements don not mention any other corrections except the one about luminance, and also do not appear to take any extra measures to avoid errors when taking photographs of the sun. Moreover, not only a typical camera has limited dynamic range problems, but also the human eye, as its dynamic range is limited to 10^5 cd/m² (Suk and Schiller, 2013). Therefore, even if a greater dynamic range is achieved in HDR imaging, the practical meaning of this would be questionable. In any case, there are no specific requirements for the cameras used, as even cell phone cameras are used in literature

(Matusiak, 2013), while Konis (2012) presented his measuring methodology based on simple inexpensive cameras.

In a recent study, Jakubiec et al. (2016) presented two different approaches of achieving HDR images of luminance ranges adequate to capture orders of magnitude from 10 to 10^9 cd/m². One was based on combining two HDR images of different ranges for each instance, one normal and one obtained with a ND filter to capture higher values, to obtain a wider range HDR image that would describe the scene more accurately. The second (overflow correction) was based on using a measured value of the vertical illuminance with a photometer mounted on the camera and “reversely calculate” the luminance impact of the bright sources through the difference of the vertical illuminance values obtained by the image and the photometer. These methods however do not come without disadvantages in their use; having to obtain two separate HDR images can complicate the processes for the cases of turbulent weather conditions, where fast luminance acquisition is essential and the two minutes required for the double HDR acquisition are unacceptable. In addition, in the case of simultaneous use of two cameras, there come concerns of practicality, in terms of having two large dSLR cameras near the subject’s head. For the second method of the overflow correction, it is yet to be extensively validated before it is used, and could be also problematic in cases there are more than one sources of extreme luminance in the visual field (for example the sun and a specular reflection somewhere in the interior within the visual field). Overall, these two methods are promising but further advancements and validation are needed before their generalized use can be practically adopted.

2.4 Daylight Glare measurement and experimental studies

There is an extensive amount of literature investigating the measurement methodology of DGP. The vast majority is based on Evalglare (Wienold 2012), a RADIANCE-based freeware that can process HDR calibrated luminance images and calculate metrics such as the average luminance, vertical illuminance, and various glare indices, including DGP, DGI and UGR. Based on Reinhart et al. (2012), the methodology of glare measurements consists mainly of the following steps:

1. 3 or more pictures of variable exposures (in terms of shutter speed) are being shot for the same visual scene, using a camera with a fisheye lens.
2. The pictures are being merged into an HDR image using Photosphere (Ward, 2014), or any other equivalent software solution.
3. The HDR image is being calibrated in terms of luminance using a spot luminance meter and a grey target within the scene.
4. The calibrated HDR image is imported in a glare evaluation tool, which after processing it can calculate the average luminance, the vertical illuminance and the main glare indices. This methodology involves the calculation of average luminance values for certain areas that are acting as threshold for the identification of the glare sources.

Wienold (2012) discusses the Evalglare options and settings. Available options include:

- Cropping of the visual field according to Guth (1966)
- Definition of the fisheye lens geometry in terms of x and y axis span
- Application of the age correction (Wienold, 2012)

- Selection of threshold approach for the glare sources identification (definition of task area coordinates chooser selection between average luminance or constant threshold)
- Creation of a check image with the task area and the glare sources highlighted
- Override of the vertical illuminance extracted from the pictures with a measured value (in cases of lenses with a visual field narrower than 180°)
- Definition of the search radius between pixels where the glare sources are merged into one source
- Application of the smoothing function. Smoothing is an option that can include or darker areas located between glare sources, or merge them with the latter. (Figure 2.8).

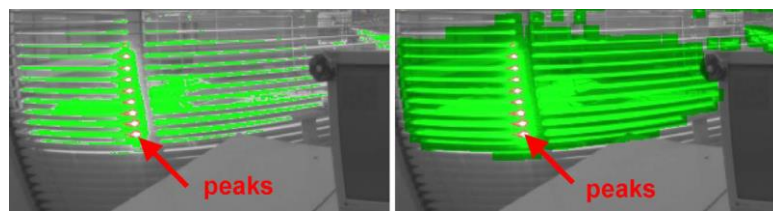


Figure 2.8 Smoothing function (Wienold and Christoffersen, 2006)

About the latter, Wienold (2006) demonstrated that the search radius proves to be not very important towards the correlation level with human impressions, when the radius is less than 0.8 sr (Figure 2.9). For higher values, the correlation drops significantly, as then multiple glare sources are combined to a single one, conflicting this way with the consideration for glare of equation (2.1) by Hopkins (1957). Similar behavior follows the smoothing function, which starts to get important for search radiuses over 0.8 sr.

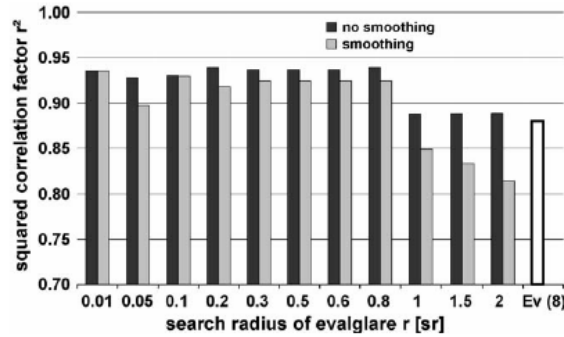


Figure 2.9 Influence of the search radius on the squared correlation of the DGP function.

The black bar is the used search radius of 0.2 sr. The white bar on the right hand side shows for comparison reasons the squared correlation factor for the vertical illuminance only. (Wienold and Christoffersen, 2006)

The fisheye lens is recommended as it most effectively resembles the human visual field. Hirning et al. (2014) suggested the use of a “vision zone”, which is Guth’s total field of view (Guth, 1966). A setting for cropping the visual field accordingly is included in the latest version of Evalglare (2012). However, most studies (Wienold, 2006 and 2009; Van den Wymelenberg et al., 2010; Suk and Schiller, 2013; Reinhart et al., 2012; Jakubiec, 2013) use the complete (180° degrees) visual field. Except for Van den Wymelenberg (2010; 2014) and Hirning (2014), most studies do not mention details about implementing a vignetting correction. The error due to this approximation is highly dependent on the aperture used (Inanici and Galvin, 2004).

A relatively ambiguous issue in DGP measurements is the criterion of the glare sources selection. The original DGP study (Wienold, 2006) investigated three different philosophies:

1. Calculate the average luminance of the visual scene and consider as glare sources the parts with a luminance x -times higher than the average
2. Consider as glare sources the ones with luminance higher than a fixed value

3. Calculate the average luminance of a specific task area (the focus zone of the subject) and consider as glare sources the parts that have x -times higher luminance than this average.

The original study suggested optimal correlation with the occupants' impressions when using a criterion of four times the average luminance of a task area. However, both the extent of this area, as well as the exact multiplication factor constitute a "grey" area, with different approaches followed in different studies. The default setting of Evalglare uses a criterion of five times the average luminance of the visual scene. Hirning (2014) used a "five-times the task luminance" criterion. In addition, he experimented with changing the extent of the task area between a part of the screen, a wider part around the screen, and an area which covered all the parts of the visual field reported as "disturbing" by the subjects. Suk and Schiler (2012) used the default "5 times the task area" criterion, while Van den Wymelenberg (2010) found the best glare sources identifier for DGP to be the comparison with a value of "7 times the task area" luminance. Kleindienst (2009), in a simulation approach, used a criterion of four times the adaptation luminance (based on a specification where the latter is calculated by dividing the vertical on eye illuminance with π). Van den Wymelenberg (2014) presented results using four different identification approaches, which showed negligible differences in terms of final DGP calculation. A possible reason for that is the fact that no high values of contrast-dominated DGP were observed during the test, possibly due to the dominance of the overall brightness term.

The above raises some concerns about the applicability of a metric such as DGP in cases of direct light hitting the eye, due to the presence of the sun within the visual field. Literature about this matter appears to be very scarce. The lack of studies focusing on the

higher range of DGP is a gap in this field of research. It is possible that for the higher end (and the cases when the sun is visible), the glare sensation is too high, causing glare at all times. An approach towards this assumption of an absolute glare factor is discussed in a study of Suk and Schiller (2013). Cases for which the minimum glare source exceeds the value of 5000 cd/m^2 are considered to produce glare independently from other contrast factors. In another study (2012), Suk and Schiller experienced some inconsistencies in their DGP measurements for cases with the sun being within the visual field, resulting to severe under-calculation of vertical illuminance and DGP (Figure 2.10). The reason should be related to the issues of HDR imaging of the solar corona, presented in the previous section. Given the high variety of shading fabrics, in terms of visible transmittance and openness factors, DGP measurement issues for cases including the solar corona should be addressed, in order to investigate a possible relationship of the latter two factors with the glare sensation. The method recently presented by Jakubiec et al. (2016), addressing these issues of HDR imaging, might solve some of these problems in the future.



Figure 2.10 Instance with direct sun, where DGP is calculated as 0.34 (imperceptible), and vertical illuminance extracted by the pictures is calculated as 15486 lux, which is 73% lower than the sensor measured value of 58125.1 lux (Suk and Schiller, 2012)

As for the glare calculation software using measured data, the vast majority of the available studies use the Evalglare software. Use of more than three photographs is generally suggested as it leads to a higher dynamic range for the final HDR image. Another

alternative to Evalglare is Hdrscope (Kumaragurubaran et al., 2013). While it implements the Evalglare algorithm, it introduces a user-friendly graphical interface which allows easier access to Evalglare functions, and some additional statistical processing capabilities.

The objective of glare measurements in the majority of experimental studies is the correlation with subjects' responses. Suk and Schiler (2012), utilized glare measurements to investigate Evalglare, and to introduce their definition of absolute and relative glare (2013), while in the study of Konstantzos and Tzempelikos (2014), DGP measurements are used in order to investigate correlations with other interior illuminance metrics. Borisuit et al. used glare measurements to evaluate the HDR imaging technique in cases of integrated daylighting and electric lighting systems, Matusiac (2013) to evaluate glare in translucent facades, while Clear (2013) used data obtained by the pioneer Lukiesh and Guth study (1949) to investigate the extent in which modern indices can be used to predict it. Kim et al. (2008) investigated the glare from non-uniform light sources to find out that the discomfort glare for a uniform window is higher than in a non-uniform window of the same average luminance.

2.5 Daylight Glare Modeling Approaches

While measurements can provide an accurate description of the extents of glare and discomfort in a visual scene, simulations are essential in order to generalize these results, provide annual predictions, perform parametric analyses or optimization for different materials or shading solutions, evaluate the efficiency of shading controls etc. In order to provide a summary of the main software tools used for these objectives, a short description of the most important modelling approaches must be realized; the sky dome is

characterized by a non-uniform luminance distribution. Any calculation of the illuminance incident to the exterior of façade is derived from the sky model used to quantify this luminance distribution. Moon and Spencer (1942) suggested the first non-uniform CIE standard for overcast sky, with the sun not being visible. Kittler (1967) suggested a luminance distribution for a clear sky with the area around the sun being brighter than any other area. Perez et al. (1990) suggested an all-weather model for different sky conditions. Tregenza and Waters (1983) presented the Daylight Coefficient method. According to that, the sky dome was split in 145 patches of specific luminance. The ratio of the patch luminance to the illuminance due to that patch on a point inside a space was defined as the daylight coefficient. In most annual simulation studies, the latter illuminance is calculated based on the Perez all-weather model using TMY data as inputs. Alternatively, to improve accuracy (Mardaljevic et al., 2000), the daylight coefficient is split into a direct and inter-reflective part, from which the direct part is calculated assuming a more dense splitting of patches.

For the handling of the complex fenestration system (which is constituted by the multiple layers of glass and shading systems, software such as WINDOW (LBNL, 2003) can be used, which calculates the equivalent total angular optical properties, based on a spectral IGDB database supplied by the manufacturers. For the properties of roller shades, most software solutions, like EnergyPlus (LBNL, 2015) assume constant values, independent from the direction of the sunlight –the most recent version, however, has three different models, which can be used to approximate angular properties. In order to achieve higher accuracy by taking into account the off-normal properties of the roller shade fabrics, a semi-empirical model by Kotey et al. (2009) can be used (this model is included in the

newest version of EnergyPlus, but only for solar radiation/thermal calculations). The details and disadvantages of the EnergyPlus models, as well as validation of the Kotey models for lighting calculations are discussed in Tzempelikos and Chan (2016). Then, in order to calculate the final luminance and illuminance mapping in the interior, two methodologies are applied, either separately or combined to improve accuracy: radiosity and ray tracing.

The radiosity method (Goral, 1984) is based on dividing the interior surfaces of the studied space in sub-surfaces which exchange light (and radiation) according to their relative size and orientation. The method assumes that all surfaces are Lambertian (perfect diffusers), therefore they reflect light towards all directions with equal luminous intensity. The proportion of total light that leaves a surface and strikes another one is expressed with the view factor F_{ij} between the two surfaces. As this matrix of values remains constant in most applications, it can be calculated initially and then be recalled for each time step saving calculation load. Therefore, for every sub-surface equation (2.13) applies:

$$M_i = M_{i0} + \rho_i \sum_{j=1}^n M_j F_{ij} \quad (2.13)$$

In the equation above, M_i is the final luminous exitance of sub-surface i , M_{0i} its initial exitance and the sum term accounts for the influence of reflections from every other surface j in the room, visible from surface i . Therefore, for all surfaces, a system of equations is formulated as follows to in order to calculate the final luminous exitances:

$$\begin{bmatrix} M_1 \\ \vdots \\ M_n \end{bmatrix} = \begin{bmatrix} M_{01} \\ \vdots \\ M_{0n} \end{bmatrix} \left[\begin{pmatrix} 1 - \rho_1 F_{11} & \cdots & -\rho_1 F_{1n} \\ \vdots & \ddots & \vdots \\ -\rho_n F_{n1} & \cdots & 1 - \rho_n F_{nn} \end{pmatrix} \right]^{-1} \quad (2.14)$$

Radiosity is a convenient and fast processing method to calculate the final luminous exitances of the interior surfaces, however it has some obvious drawbacks, as there are no real perfect diffusers. Therefore, in cases of surfaces of higher specularity, radiosity can produce inaccurate results (Versluis, 2005). The main problem lies on the assumption that the window is a diffuse source, which is never true, especially when there is direct sunlight, transmitted inside the room.

To address the problems of radiosity's incompatibility with non-Lambertian surfaces, another methodology was developed for specular surfaces based on tracing the path of the rays from (or toward) the light sources. Forward ray tracing (Appel, 1968) assumes that a ray of light is emitted from a source and follows a path to a surface, then gets reflected and, having a reduced intensity, continues its path. This is assumed to be repeated until the reduced intensity is low enough to be neglected (absorbed). The weak side of this approach is that often a significant portion of the rays never actually comes through the point of interest (surface or human eye). Another disadvantage of this method is the high computational time, especially for diffuse light. An alternate approach to address the above issue is the backward ray tracing, where the ray from the eye of the observer to the rest of the environment is being tracked. The drawback of this approach is that often in daylighting analysis more observation points are needed, making the procedure complex and demanding in comparison with the forward approach which is not related with the observer's position. A third method that combines the benefits of both approaches mentioned above is a hybrid approach (Lafortune and Willems, 1996); in that case, a sample of rays is generated and only a portion of them is assumed to be reflected due to

the specularity of a surface. Then, the reflected (or transmitted) ray follows a direction that can be extracted by the optical properties of the surface.

The above mentioned modeling techniques are being used in the most advanced software packages, which usually implement different aspects of the Daylight Coefficients method. Examples of software solutions are EnergyPlus (LBNL, 2015), Ecotect (Marsh, 2006), RADIANCE (Ward and Shakespeare, 1998) and DAYSIM (Reinhart, 2006). Although EnergyPlus includes glare modeling, the majority of literature prefers to use DAYSIM for annual simulations and RADIANCE for detailed modeling of specific visual scenes.

The majority of studies related to simulations and DGP (Wienold, 2007 and 2009; Suk and Schiller, 2012; Jakubiec, 2012 and 2013; Yun et al., 2014, Cantin and Dubois, 2011) use RADIANCE (Ward and Shakespeare, 1998) renderings of visual scenes. Radiance is based on the backward ray tracing methodology. The general modeling approach involves geometry definition and materials selection, the use of Radiance in order to render the scenes for specific instances and finally the extraction of glare indices through the use of Evalglare. This approach is ideal for cases in which accuracy in terms of geometry is essential (Jakubiec, 2013) as a Radiance model can include detailed furniture settings that can moderately affect glare perception. Using this approach, Suk and Schiller (2012) investigated Evalglare by using experimental and simulation results for the same settings, to conclude that Evalglare is a powerful evaluation tool, and needs some improvement in the handling of the lens geometry. The latter issue was however addressed in a later version of Evalglare (Wienold, 2012).

In cases where shading control strategies need to be investigated with the Radiance approach, a time series of all possible shading positions are simulated using DAYSIM and the daylight coefficient method for all time steps and stored in a result-matrix including values for daylight supply, control variables and comfort indices and variables. As DAYSIM can only calculate given points rather than full images, a dense grid of 300x300 calculation points was used in the first study including shading controls as a reference (Wienold, 2007). After the result matrix is created, according to the shading control strategy applied, for each time step, the specific shade positions and calculated results are combined to produce annual data. In the same study, a methodology of only calculating DGPs is presented and correlated with the detailed method. However, as stated by Wienold (2009), with the processing power available after 10 years from the time of the study, it would need around 120-300 hours to render a complete set of annual data (assuming that every year has approximately 4100-4500 hours of daylight).

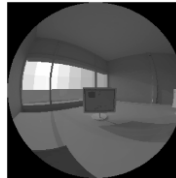


Figure 2.11 DAYSIM calculated picture. The sky subdivisions of the daylight coefficients method used are visible. (Wienold, 2007)



Figure 2.12 Example of glare-causing sources that get isolated instead of rendering the whole image in detail (left) – Flowchart of enhanced simplified methodology (right) (Wienold, 2009)

This was a trigger for the development of an enhanced simplified modeling methodology, based on obtaining the hourly values of vertical illuminance by DAYSIM (Figure 2.11) and include in the rendered image only the parts that will actually act as glare sources (Figure 2.12). However, it is not clearly stated in the study how the glare sources will be selected, but it is reasonable to assume that it covers areas of interest, or that a threshold is extracted from the values of vertical illuminance. This approach minimizes the required number of ambient bounces that is mainly responsible for high computational time.

Kleindienst and Andersen (2009) suggested another simplified modeling approach, using the LSV radiosity engine. As the latter does not include specular material definitions, their approximation is based on three assumptions; first, that any window patch can be assumed to be a potential glare source, second, that due to a hemispheric geometry approach, the adaptation luminance can be extracted by dividing the vertical illuminance by π , and third, that the apparent luminance of the sky patches from the observer's position can be extracted from the known sky luminance distribution data and by creating a line of sight between the sensor and the window patch. Validation with Radiance and Evalglare proved the method to be fairly accurate, most of the time within 5% of error, and therefore much more reliable than DGPs. It has to be noted here that, because of the objective, which was comparing the approximation methodology with the existing simplified index (DGPs), a CIE clear, clear-turbid, intermediate and overcast sky models were used, rendered without sun. However, the authors claim that simulations with rendered sun showed similar behavior, and they were just excluded as irrelevant to the scope of the study.

Chan et al. (2013;2015) used a computational approach based on a hybrid ray-tracing and radiosity lighting model with a glare module using open source language.

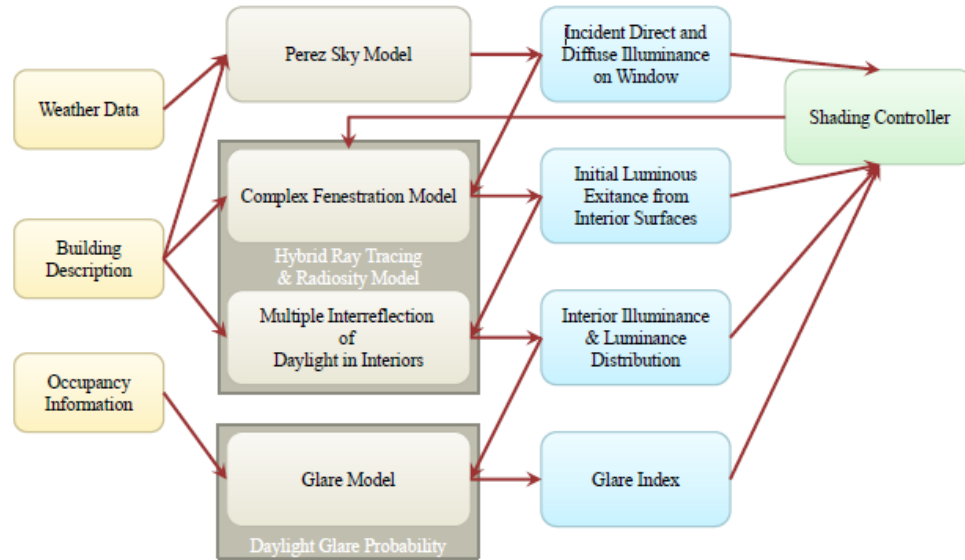


Figure 2.13 Computational approach flowchart (Chan et al., 2014)

The model (Figure 2.13) calculates interior illuminance and luminance data from weather data input, using a sky illuminance distribution derived by the Perez et al. (1990) sky model, and applies the hybrid ray tracing and radiosity method (Chan and Tzempelikos, 2012) to calculate the interior illuminance and luminance distributions. For the modeling of the detailed glazing angular properties, WINDOW (LNBL, 2003) is used, while the angular and specular properties of the roller shades fabrics are addressed by the semi-empirical method introduced by Kotey et al. (2009). Given the detailed illuminance and luminance mapping of the interior, a dense grid of interior surfaces and window patches allows the calculation of glare indices using a similar methodology as the one followed by Evalglare, selecting the glare sources through a variable criterion and applying the respective equations. The model can account for different fenestration approaches (windows, shades, blinds, multi-sectional facades etc.) and customizable shading controls. There appear to be many advantages in this approach, as its flexibility makes it ideal for

optimization, while calculation times are limited compared to other approaches. In addition, it can fully handle the influence of the sun and the increased contrast it creates, something that remains a gray area in the vast majority of RADIANCE-based studies. However, there are some disadvantages due to the fact that, as long as a part of the window constitutes a glare source, then the whole window is identified as one, as well as the fact that it does not take into account furniture, both leading to potential overestimation.

As in the case of experimental studies, the scenes with direct sunlight on the eye are also scarce in related literature. Consideration of such cases is implied in a study of Wienold (2009), where roller shades of considerable openness are used, leading the sun to be visible in RADIANCE renderings and resulting to presented peak values of maximum luminance of $100,000 \text{ cd/m}^2$, and leading to DGP values that can approach 1 (Figure 2.14).

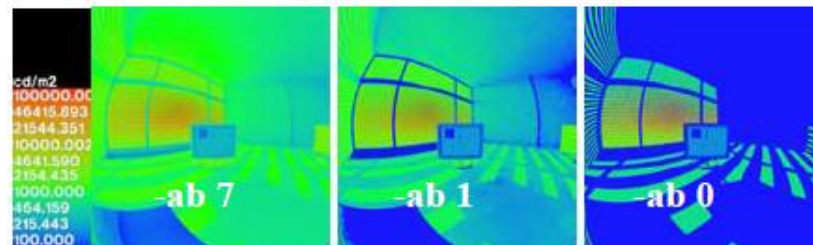


Figure 2.14 High values of luminance due to the presence of sun within the visual field (three images for three different rendering detail settings) (Wienold, 2009)

2.6 Occupant-related daylight glare studies – Validations of indices - Interactions

The initial DGP study (Wienold and Christoffersen, 2006) used a total of 349 responses of 76 subjects to extract the index. Their experimental setting involved two view directions, one parallel to the window and one 45° diagonal towards the window, while the available responses were 4 (imperceptible, noticeable, disturbing and intolerable). In order to overcome the issue of impossible correlations due to the large variation of the

various indices for each response (Figure 2.15), a probability approach was followed, where responses were grouped in 12 classes of 29 samples each with respect to increasing average values for each studied index.

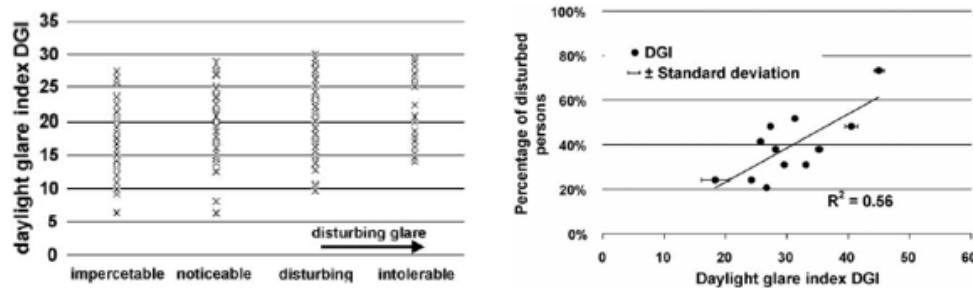


Figure 2.15 Per person correlations of glare index with comfort (left) – Correlation of glare index with grouped responses about comfort (right) (Wienold and Christoffersen, 2006)

Hirning et al. (2014) questioned this approach stating that, in order to follow this grouping, a number of groups equal to the size of each group must be considered, otherwise the system is “overdetermined” and problems of overestimation of the coefficients of determination can occur. Based on this, 419 responses were evaluated, in order to investigate the applicability of the most common glare indices in open plan offices. Subjects were asked to fill a sketch of their visual field (Figure 2.16), indicating their visual disturbances, if any.

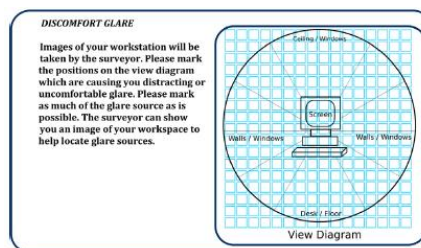


Figure 2.16 Sketch to be completed by subjects in order to record their impressions about visual disturbances (Hirning et al., 2014)

The response was characterized as discomfort if at least one disturbance was indicated, or comfort otherwise, an approach reasonable due to the binary sense of the probabilistic discomfort metrics. DGP achieved a low correlation (0.683), reflecting also the low correlation of vertical illuminance. The authors note the difference in the ranges of vertical illuminance compared to the original DGP study, pointing the fact that open plan offices are characterized by lower light conditions due to the block of furniture or other workstations in the space. They suggest that glare in open plan offices is mostly caused by contrast from luminance sources, rather than vertical illuminance. However, the presented values do not include direct sun instances.

Jakubiec and Reinhart (2013;2015) used a mixed technique using field measurements of occupants with Radiance simulations of existing open plan offices. A major contribution of this study was the consideration of three factors influencing visual comfort, the discomfort glare, the monitor contrast and the direct light falling on the work plane or on the eye. More than 500 respondents were filtered to give their aspect of visual discomfort using a four point scale, while Radiance modeling was applied for the exact same rooms at the same times, using Wienold's enhanced simplified modeling methodology (Wienold, 2007) to calculate DGP, contrast and direct sunlight on the desk or the eye. The results demonstrated the necessity of using a multiple visual comfort criterion instead of only using DGP, as there were instances where only one of the three factors was exceeding the comfort range. (Figure 2.17). In addition, some observations showed the importance of spacing in the room. This study has also been the first attempt to propose some temporal thresholds about constituting a space as intolerable in terms of glare. More specifically, it is stated that occupants experiencing discomfort glare

($DGP \geq 0.4$) for more than 3.5% of occupied hours would evaluate the space as intolerable. In the same scope, occupants who experienced direct sunlight, either on the desk or the eye, of over 1000 lux for more than 5.25% would also constitute the space as intolerable. In terms of low monitor contrast, it would need to be experienced for more than 24% of the given time.

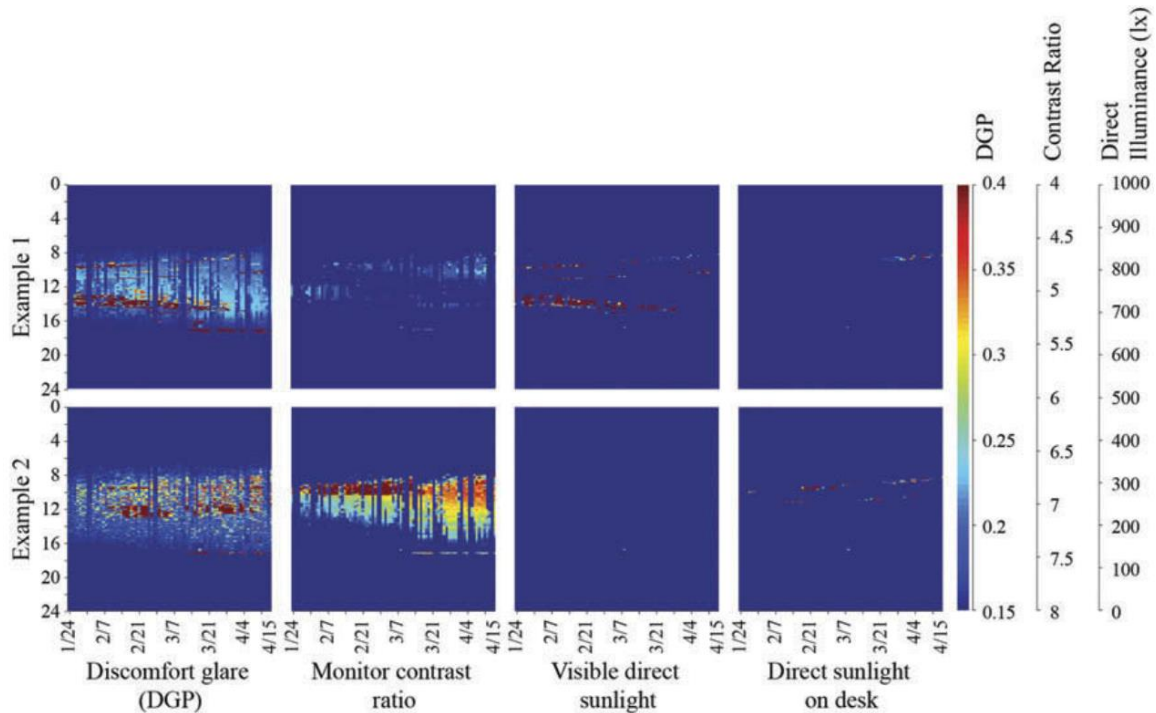


Figure 2.17 Example of instances where monitor contrast issues are present without high DGP values (top) and intolerable DGP values with no significant contrast problems (bottom) (Jakubiec and Reinhart, 2013)

Van den Wymelenberg et al. (2010) used subjects allowing them to adjust their visual (daylighting) conditions using shading, to a ‘perfect’ and a ‘just disturbing’ condition, in order to investigate the parameters that appeared to be significant. DGP performed better than DGI for all cases, however correlations were not as good as the ones obtained by Wienold. The study was mostly based on luminance distributions and three

different approaches were investigated: predetermined absolute luminance value thresholds, scene-based mean luminance value thresholds, and task-based mean luminance value thresholds. The study presented graphs for each case demonstrating whether the selected metric was able to distinguish the “perfect” from the “just disturbing” conditions (Figure 2.18). The best correlation overall was obtained by the metric of the mean luminance of the glare sources identified by a threshold of “7 times the average luminance” of a solid angle-based task area.

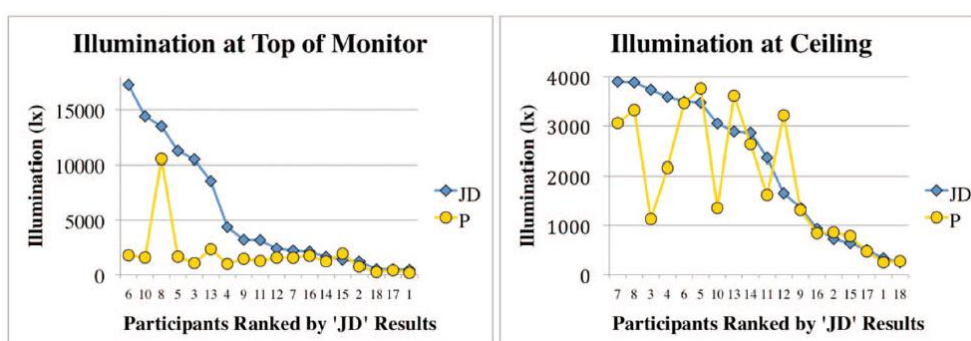


Figure 2.18 Per subject differences in terms of a metric for ‘perfect’ and ‘just disturbing’ conditions. The distinction can be clear (left) or entirely random (right) (Van den Wymelenberg et al., 2010)

Van den Wymelenberg and Inanici (2014) added the influence of electric lighting to the above study. The metric that seemed to correlate better with all the questions was the vertical illuminance in the view direction of the observer, at the top of the screen. The work plane illuminance had some potential of being used as an upper level of comfort, but the authors stated the many cases when even 5000 lux of illuminance was desired by subjects. The importance of luminance-based metrics was noted, but due to the variety of calculation methods for the luminance ratio of the task area, further research is suggested (Figure 2.19). DGP performed better than DGI in general, but still the correlation levels

were not high. The authors also stated the problem that occurs for average or task-based luminance identifications methods; when direct light is included in the reference area, it can lead to severe overestimation of the glare sources threshold, leading thus to an underestimation of the extracted DGP.

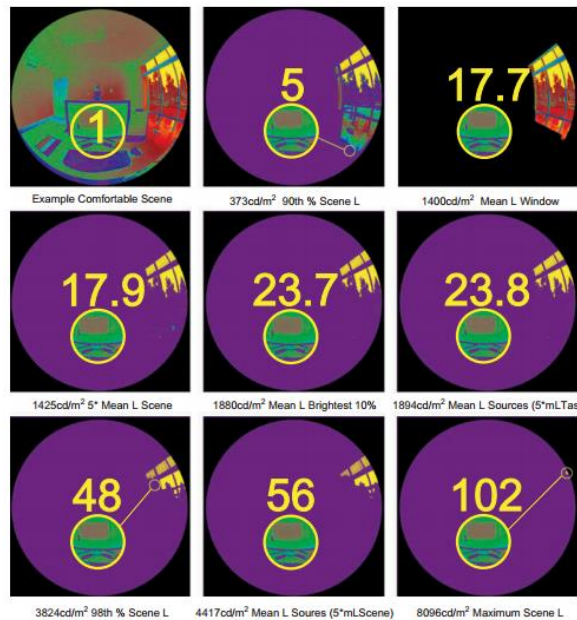


Figure 2.19 Different luminance ratios for a comfortable scene, dependent on the calculation approach. (Van den Wymelenberg et al., 2014)

Karlsen et al. (2015) used reported glare sensations from subjects in order to validate the use of easily obtainable metrics such as vertical and horizontal illuminance or DGPs as predictors for discomfort using a diagonal window facing position. They suggested that there is a statistically significant correlation between the indoor illuminances and glare perception, and suggested thresholds of 1700 lux for the vertical illuminance and 1900-2100 lux for the horizontal illuminance in order to avoid conditions of glare. In the same study, it was reported that DGPs failed to predict discomfort and its equation should be renewed.

Rodriguez et al. (2015) tested the hypothesis that a large area glare source can become an environmental distractor affecting attention, and that glare-sensitive persons would be more affected in terms of attention by such a source. They found that performance was affected in terms of reaction times but there was no significant difference in the sensation of glare between sensitive and insensitive persons. Also, the same study suggested that DGP was capable of describing very bright scenarios, due to a high reported correlation of DGP with Glare Sensation Vote for the bright conditions of the experiment. A few studies focused on the interaction of subjects and visual adjusting devices.

Galasiu and Veitch (2006) presented a literature review about occupant preferences and satisfaction in terms of luminous environment and control systems. They presented the existing findings of a general preference for daylight and a connection to a healthier impression, the general preference towards larger windows, the variability of discomfort perception and preferred illuminance levels and the higher acceptance of automatic systems when there is a way to override them. They indicated several research gaps, including the need to expand the environmental variables measured to other metrics except work plane illuminance. More generalized studies in terms of orientations and locations are needed, in order to compare fully automated systems with to semi-automated systems and observe the benefits of overrides. Also, the concept of conflict in open plan offices towards the design of a more widely acceptable control scheme needs to be studied, among the need for training of the occupants, in terms of comparing the settings they adjust to the ones they report they need. Finally, they suggested that future research should assess trade-offs between glare control, connection to outdoors and energy, towards a more general consideration of visual satisfaction.

Haldi and Robinson (2010) studied subjects in an office building, using an interface questionnaire asking about their thermal and visual comfort as well as satisfaction about air quality. Visual comfort impressions appeared to be distributed almost symmetrically for comfort and discomfort. The authors suggested a distribution of visual sensation S_{vis} with respect to indoor illuminance, which they considered to be the illuminance on the work plane E_{in} (equation 2.15).

$$p(S_{vis} = S_i) = \frac{\exp(a_i + b_i \log(E_{in}))}{1 + \sum_{j=-3}^3 \exp(a_j + b_j \log(E_{in}))} \quad (2.15)$$

, where the summation term reflects the different visual sensation votes, from -3 to 3; a and b are regression parameters.

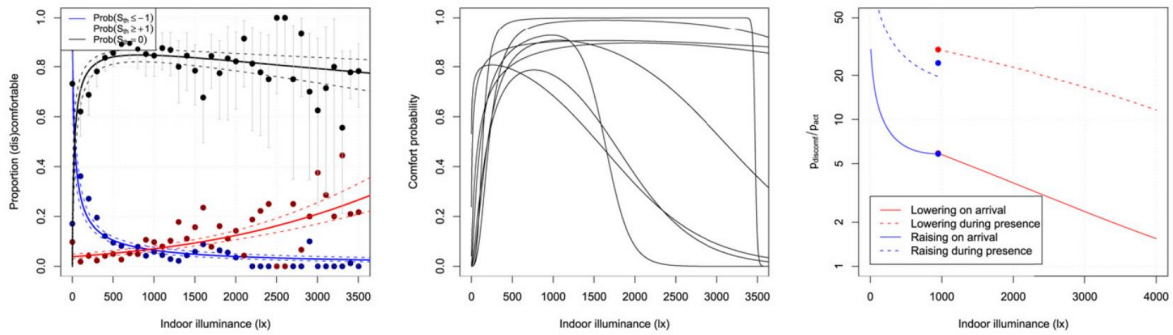


Figure 2.20 Correlation of discomfort sensation, probability, and inertia with indoor illuminance (Haldi and Robinson, 2010)

Some interesting findings included very similar comfort probabilities among subjects about the uncomfortably dark conditions, which was not the case for uncomfortably bright conditions with much higher variation (Figure 2.20 – center). Also, an interesting finding about behavioral trends was the fact that inertia, defined as the subjects' non-willingness for action was more frequent in dark conditions, where they were expected to turn on the

lights. The level of inertia however decreased as interior illuminance was increasing (Figure 2.20 -right).

Konis (2013), used a prototype portable polling station concept on desks in order to investigate the visual comfort conditions in a post-occupancy study of side-lit offices equipped with solar control devices. It was found that, for facades with significant hours of direct sun, direct view of the solar disc should be completely blocked, as the discomfort conditions are intolerable. Also, according to this study, occupant behavior should be a priority compared to the daylighting zone of a room. An interesting fact connected to lighting energy usage was the fact that in perimeter offices, subjects tended to be satisfied with work plane illuminance thresholds below the typical standards. Lastly, connection to the outdoors was proven to be important, as occupants often tolerated discomfort conditions in order to have an improved outside view.

Da Silva et al. (2013) observed the relationship of shading and lighting control actions with metrics such as luminance distributions, illuminance ranges and occupancy patterns. They found occupational dynamics as arrival and departure in the office to be more related to actions than the environmental conditions experienced. In addition, behavioral models were evaluated in terms of successfully predicting the occupants' actions. For electric lighting actions, a significance of the daylight conditions in the office was found towards turning on the light when entering the room, a trend also present in the cases of temporary absence, where lights would be more frequently turned on in cases work plane illuminance was below 500 lux. For shading actions, work plane daylight illuminance, DGP, DGI and transmitted solar radiation were found to be the most related environmental variables. The available prediction models behaved well for the opened states, but failed to predict the

closed states of the shades, while from the behavioral models, only the Pigg model (Pigg et al., 1996) was in qualitative and quantitative agreement with the lighting actions. The authors also pointed the difference of results obtained in real building conditions with the ones obtained in controlled settings.

2.7 Spatial Considerations – Recommendations

Only a few studies have focused on the spatial aspects of DGP.

Jakubiec and Reinhart (2012) defined the concept of an adaptive zone in which occupants can freely adjust their positions and view directions without being exposed to severe glare conditions (Figure 2.21). Such a zone could diminish the annual occurrences of disturbing glare from 20% to less than 1%.

Jakubiec (2013) presented simulations and occupants' responses for open plan offices, demonstrating the diversity in the amount (or the specific way in which) subjects experience discomfort in different positions. Chan et al. (2015) recommended shading fabric properties for different view distances, orientations and locations, based on discomfort criteria related to the total and direct vertical illuminance on the eye level. However, most of the studies note the problem in such considerations which is the furniture settings; different settings can lead to entirely different results, making rules of thumb challenging to achieve. Therefore, the only way would be to include in the recommendations rough details for selected furniture layouts. In addition, discomfort glare is only one of the potential reasons for the lack of visual satisfaction; in cases of suggesting new positioning in offices, other parameters, such as connection to the outdoors should be

considered. Therefore, the introduction of a unified index of visual satisfaction is of the essence as a baseline for introducing guidelines.

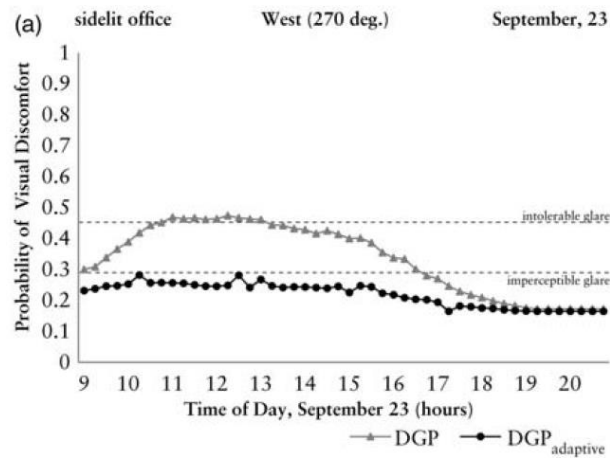


Figure 2.21 Moderate mitigation of glare sensation in terms of DGP when implementing the concept of the ‘adaptive zone’ (Jakubiec and Reinhart, 2012)

Konis (2013), in one of the very few side lit open plan offices studies, issued some initial recommendations for design. He suggested to use external shading devices that can completely block the view of the solar disc and to avoid highly reflective, transmissive or specular materials on the exterior shading surfaces. Also, he encouraged the use of light-redirecting devices (e.g., blinds, louvers etc.) in the upper section of multi-sectional windows, and the need to implement lighting and shading control models early in the design phase. These recommendations about materials are often of less importance compared to the positional aspects of visual discomfort. IES Standard LM-83-12 (IESNA, 2012) also suggests design recommendations in terms of sDA and AES (Annual Sunlight Exposure). Specifically, it dictates a maximum space area of 2% be exposed to direct sunlight of 1000 lux for more than 250 hours annually, but this rule does not apply for

controlled shading cases (which is the most common option in modern office environments).

New detailed recommendations are needed about the placement of workstations related to the orientation and shading systems used.

2.8 Comfort-oriented Control Implementation

Very few studies directly associate glare indices with shading controls. Wienold (2007) used the enhanced simplified DGP approximation to evaluate the efficiency of shading controls towards glare, however the strategies used were not based on glare but only evaluated in terms of it. Yun et al. (2014) used DGP to evaluate blind control strategies towards glare and energy and first stated that E_v is a good alternative to base shading controls on, due to its strong correlation with DGP. However, from their correlations of DGP and DGPs, it is implied that no direct light conditions were met. Obtaining real-time DGP data is quite challenging due to (i) the need of one or more calibrated cameras programmed to shoot pictures, and a computer to process them, extract DGP and send it to the controller and (ii) this process is space- and time-consuming, and expensive to implement in real world buildings. However, as the DGPs approximation uses only one input for vertical illuminance, which can be measured in real time, the potential of a model-based control based on DGPs needs to be investigated (Wienold, 2007). In order to do so, further studies about the applicability of DGPs in cases of direct light projected on the interior surfaces of the room were recently studied (Konstantzos et al., 2015) as described in sections 3.1 and 4.3 of this Thesis. Model-based glare control strategies are also under development (Xiong et al., 2015).

2.9 Daylight metrics

Comfort may be the constraint when designing visual of thermal systems for buildings, but reducing energy costs is always critical. Daylighting can decrease or even eliminate the need for electric lighting, therefore appropriate daylight metrics are required to characterize daylighting performance and assist in evaluation of energy savings from lighting controls on an annual basis.

The oldest index of daylight performance is Daylight Factor. It is defined as the ratio of the horizontal illuminance on a point in the interior of a space to the external horizontal illuminance under a CIE overcast sky (Moon and Spencer, 1942). The benefits of daylight factor is that a designer can estimate daylight conditions based on the worst case scenario of overcast sky. The threshold level for daylight factor according to LEED is 2% (Carrier and Ubbelohde, 2005). There are however flaws involved in this daylight performance metric, as first, it does not take into account factors like season, time, orientation and location, while it does also not consider any shading devices (roller shades, blinds etc.).

The most commonly used metric for annual daylighting performance is Daylight Autonomy (DA). It is defined as the percentage of annual office hours when the interior the illuminance is higher than a pre-defined level. According to the IESNA Lighting Handbook (Rea, 2000), the required minimum level is 500 lux for office spaces. The disadvantage of Daylight Autonomy is that it entirely excludes illuminance values below the specified threshold; that constitutes the specific index not suitable for calculating energy savings due to light dimming.

Continuous Daylight Autonomy (DA_{con}) was a revision by Rogers (2006), which corrected the issue described above, giving partial credit to the times for which daylight illuminance is below the minimum level. This approach is essential when modeling the annual lighting energy savings from dimming controls (Shen and Tzempelikos, 2012).

Maximum Daylight Autonomy (DA_{max}) was defined in order to indicate the percentage of office hours when excessive daylight or direct sunlight are present and probable to cause visual discomfort. The definition of excessive conditions is illuminance levels over ten times the set point (Reinhart et al. 2006).

Useful Daylight Illuminance (UDI) was suggested by Nabil and Mardaljevic (2006) to define the range of daylight between 100 and 2000 lux. The reasoning was the fact that daylight illuminances below 100 lux increase the potential to turn electric lighting fully on, while values over 2000 lux could produce visual discomfort without any apparent benefits.

Spatial Daylight Autonomy (sDA) was suggested to demonstrate the spatial effects of daylight performance. It measures the percentage of a floor area that exceeds a specified illuminance set point level for a specific amount of annual hours. IES standard LM-83-12 (IESNA, 2012) dictates a $sDA_{300,50}$ of over 75% in order for a design to be characterized as ‘preferred’, or over 55% to be ‘nominally accepted’.

2.10 Window Views and Related Studies – Quantity and Quality of View

Another factor directly associated with visual satisfaction is connection to the outdoors, in terms of both amount and clarity of view. Subjective factors, such as view quality, are generally associated with psychological sciences and mainly include preferred outside scenes. Aries et al. (2010) showed that window views rated as “more attractive” can result

in reduced glare; however, this effect can be reversed for occupants seated close to unshaded windows. Tuaycharoen and Tregenza (2007) also attempted to associate discomfort glare with satisfaction from window views, concluding that the perception of glare was lower for “interesting” scenes. Similar findings, connecting the type of view through the window with perception of glare (Shin et al., 2012) or even with job stress and well-being (Leather et al., 1998) or health recovery (Raanaas et al., 2012), have been reported. Konis (2013) noted that despite the presence of visual discomfort, the occupants in the perimeter zones left for most of the time a portion of the window unshaded to maintain connection to the outdoors. Wienold (2007) in his shade control strategies paper concluded that future studies should be focused on investigating occupants’ preferences towards connection to the outdoors.

Objective considerations are more important in urban areas, where there is limited flexibility in choosing the most desired outdoor scenery. Building rating systems (USGBC, 2009) offer credits for outdoor views, without elaborating on details. The only quantifiable elements of connection to the outdoors are (i) the amount of view outside, in terms of relative size of openings compared to opaque walls, and (ii) the view clarity through windows. For the first, Galasiu and Veitch (2006) suggest optimal window sizes of 1.8 – 2.4 m in height and somewhat wider than taller, although window size will vary for different office settings. On the other hand, view clarity through windows with shading devices has not been studied sufficiently. The basic concept of view clarity is even abstract, without a clear definition (Vrabel et al., 1998). Aston and Belichambers (1969) refer to it as a metric of sense of satisfaction, whereas Boyce (1977) defined it as the level of something being “visually distinct and clear”. Early studies associated clarity with

distinctness of detail (Yonemura and Kohayakawa, 1976) or considered the visual clarity of an illuminated scene to be highly correlated with the specific spectral concentration of light sources (Thornton and Chen, 1978).

The clarity of view through actual windows or glass facades depends on the layers of fenestration (glazing and shading systems) and their optical properties. The glazing visible transmittance, which depends on the type of glass and coating used, also determines the ability to see through the glass. Most modern glazing products have a high visible transmittance to allow more daylight into the space, thus their impact on view clarity is not substantial. In contrast, any type of shading (e.g., venetian blinds, roller shades, draperies and screens) significantly affects the clarity of outside view, since they block part of the window and influence the direct-direct and direct-diffuse light transmission. Venetian blinds allow partial direct outdoor view depending on their shape and rotation angle. Tzempelikos (2008) presented a detailed method for calculating the projected outside view for venetian blinds of any shape (flat and curved) as a function of rotation angle, taking into account edge effects and slat thickness. Window shades (fabrics) allow direct outdoor view when they are partially open. However, due to their perforations, they enable some outside view even when fully closed. It is essential to develop guidelines towards the connection to the outdoors, in terms of amount of view and view clarity, as they are both measurable concepts, in contradiction with the quality of view which is subjective and depends on the outdoor landscape.

2.11 Research gaps and aims of Thesis

As seen throughout the previous pages, there is a considerable amount of studies about visual comfort and glare. However, there are specific topics and problems that keep being overlooked in existing literature. First, there is the ambiguous issue of the glare sources identification threshold. Although literature often considers the issue to be not important, this is the result of the fact that most studies evaluate daylight glare without direct sunlight present. As soon as a small portion of direct light hits the eye, the contrast term of DGP or other glare metrics dominates the equation, making the glare identification methodology significant. The latter brings out another deficiency in current literature; discomfort glare connected to direct sunlight through shading fabrics is absent from most related studies. It is unknown at this time the extent to which DGP, as a current preferred index, can be accurate in such (sunlight) conditions. In the initial study (Wienold, 2006) glare sources due to specular reflections and the presence of sun within the visual field were implied. However, the reported values of maximum window luminance (9131 cd/m^2 for specular venetian blinds) and the equipment used could point towards inaccurate readings for the solar corona's luminance. Any attempt to capture the sun without a ND approach between the camera body and the lens would lead to overexposed photographs with unreliable luminance mapping, even in the case of the LMK 98-2 camera with the 10^7 dynamic range capabilities. That may lead to significantly underestimated DGP calculations and thus the higher range of the DGP correlation needs to be further investigated. Solutions such as the one proposed by Jakubiec et al. (2016) are complex and their efficiency needs to be yet validated in human subjects studies.

Shading devices and their effect on glare is a topic of ongoing research. Roller shades are a common solution in commercial buildings and used for reasons of glare protection, thermal comfort, or privacy. However, because of their construction, which involves a noticeable amount of openness, it is unclear whether they can efficiently protect from glare—especially direct sun glare. More research is needed towards this issue in order to develop some guidelines of maximum openness and visible transmittance required for effective glare protection. This requires experimental human subjects studies in order to evaluate the efficiency of current metrics or propose new ones, and modeling work for generalizing results and providing guidelines.

Experimental studies in spaces with roller shades, with DGP measurements using HDR cameras, are needed to further investigate glare evaluation and correlation with daylight metrics. These will be also useful for validating advanced daylight and glare models. Moreover, the issue of different approaches for controlled shades and the impact on glare need to be further studied. More correlations of glare indices, especially DGP, should be attempted on annual basis in order to investigate possible solutions for ‘replacing’ DGP with an easily measurable metric to implement as an input in shading controls. Possible choices include the work plane illuminance or a vertical illuminance near the observer. There is also the question of the reliability of a simplified index such as DGPs applied in cases with shading fabrics. In theory, the direct light penetrating would constitute the use of DGPs (or even DGP) non-valid, but this is an assumption that should be further investigated. DGPs might not be useful in terms of direct light falling into the eye, but it is still unclear whether it can be used for cases of projected light on the interior surfaces under bright conditions with partially open shades, or in terms of high-openness closed shades.

The optical properties of shading fabrics can severely affect the outside view, mostly in terms of view clarity. How fabric properties affect the view clarity performance is unknown. Experimental research is needed to build new empirical models for characterizing the view clarity through windows with shading devices. An equation which could relate fabric properties with view clarity would be a valuable tool in evaluating visual satisfaction during fenestration system design.

There have been very few studies about the spatial aspects of visual discomfort; in many, a simple change of view direction can mitigate glare issues dramatically, often without seriously compromising the daylight availability. It is challenging to issue generalized regulations because of the high complexity of the glare estimation. However, using statistical metrics such as the annual occurrence of visual discomfort, and using simple furniture layouts, it can be possible to grade specific settings using a more holistic index. In order to comply with other aspects of visual satisfaction, the connection to the outdoors should be taken into account in such an index, in terms of amount of view or even considering the final clarity of view through complex fenestration systems (glazing and internal or/and external shading). This, combined with other recommendations about the materials of the interior (wall, floor or desk colors), as well as recommendations concerning the computer monitors used, could improve the overall visual conditions of an office space. The influence of commonly used materials, such as the aluminum used in the window frame towards visual discomfort can be significant, and no study so far has investigated such details.

In addition, more human subjects research is needed in order to better understand the actions induced by visual discomfort. Although there are several studies available, only

a few of them take into account luminance distributions, which appear to be the most significant influence of discomfort. Obtaining more data from test- or real buildings can lead to the development of behavioral models that could significantly improve shading control strategies. An experimental facility of fully controllable and monitored private offices, as the one described in Chapter 3 is an ideal setting for obtaining more luminance related behavioral and interactions data.

Measuring glare has been a challenge so far, as HDR imaging is complex, time consuming and expensive to implement, as explained in Chapter 3. In addition, having a camera close to the eye position of the subject for almost all of the times is not possible, while it is also not applicable for large-scale studies with hundreds of occupants. Developing a reliable method for measuring glare with a few simple cameras, and producing an efficient methodology for processing and correcting the images for estimating daylight glare can lead to new innovative ways of visual comfort mapping in indoor environments.

Based on the above, the detailed aims of this Thesis are:

1. To establish a reliable experimental methodology for measuring visual comfort metrics (glare indices, luminance mapping, etc.) in both daylit test office environments and real office spaces using advanced HDR imaging.
2. To develop and apply detailed and efficient daylight and glare prediction models to generalize results for front - and side lit spaces with any type of dynamic façade systems in terms of glare.
3. Using the aforementioned methodologies, to investigate Daylight Glare Probability (DGP) in spaces with static and dynamic shading on windows; explore its applicability

- and limitations, and the potential of use for simplified versions (DGPs); evaluate shading properties for glare protection; and assess the performance of different shading controls towards minimizing glare.
4. To perform surveys in private and open plan offices with simultaneous monitoring of environmental variables in order to correlate the most important glare indices and other environmental parameters with the sensation of discomfort.
 5. To extend the glare assessment methodology to cases with direct sun visible through shading systems, to evaluate the upper limits of visual comfort for such cases in terms of vertical illuminance or DGP using experiments with human subjects. Additionally, to propose new luminance- and illuminance-based indices that can effectively predict visual discomfort under such conditions.
 6. To develop a new method for quantifying view clarity through windows with common shading fabrics, and develop a new view clarity index associated with basic fabric properties.
 7. To develop an integrated holistic methodology for assessing the overall visual environment and provide guidelines considering visual comfort, daylight provision and connection to the outside.

CHAPTER 3. METHODOLOGY

3.1 Experimental methodology

In this sub-chapter, details about the experimental methodology will be covered, including a thorough description of the experimental facilities, the sensors involved in the experiments and the methods for data acquisition and control.

Overall, three different full-scale facilities were used to achieve the experimental objectives of this Thesis, with different measuring techniques. These include occupied and unoccupied private and open-plan office spaces used for glare measurements, field surveys and occupant monitoring.

3.1.1 Façade Engineering Labs (Architectural Engineering facilities at Bowen Laboratories)

Part of the experiments discussed in this dissertation were conducted in the Architectural Engineering laboratories of Purdue University in West Lafayette, Indiana (Latitude 40°N, longitude 87°W). This research facility was particularly designed for quantifying the impact of facade design options and related controls on indoor environmental conditions and energy use. Two identical, side-by-side test office spaces with reconfigurable facades (Fig. 3.1) were used to compare the impact of different glazing, shading and control options on indoor environmental indices under real variable weather conditions. The dimensions of each room are 5 m wide by 5.2 m deep by 3.4 m high, with

a glass façade (60% window-to-wall ratio) facing south. The façade consists of an aluminum curtain wall framing (Kawneer 1600UT) and three sections of glass, covering a total length of 4.80m and height of 2.10m (Fig. 3.2). The spandrel section extends to 0.6m above the floor, and the total window extends to the ceiling height. There is however a separate upper window section of 0.6m of height. Every component of the façade is easily reconfigurable in order to investigate different settings and their impact on energy and comfort.



Figure 3.1 Exterior view of the twin test offices

In the settings for the glare experiments, the upper section of the window was covered with R-19 insulation board to completely block any daylight from penetrating the room while providing equivalent thermal protection to the opaque envelope sections. Two different glazing systems were used in the initial glare experiments: a SB70XL-clear high

performance glazing unit with a selective low-emissivity coating (visible transmittance: $\tau_v = 65\%$ at normal incidence), as an example of modern solutions used in new buildings, and a double clear glass unit ($\tau_v = 78.6\%$ at normal incidence) as a common product used in existing buildings.

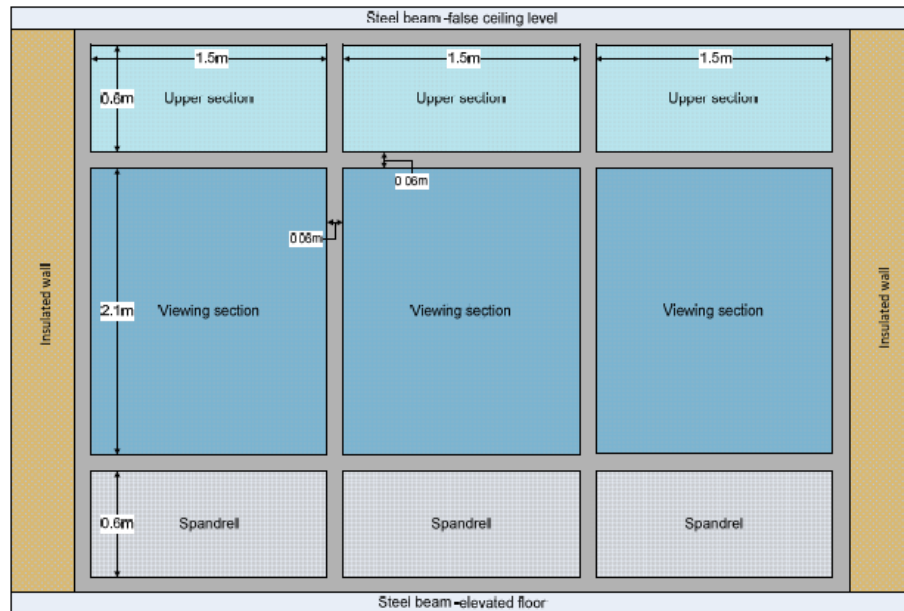
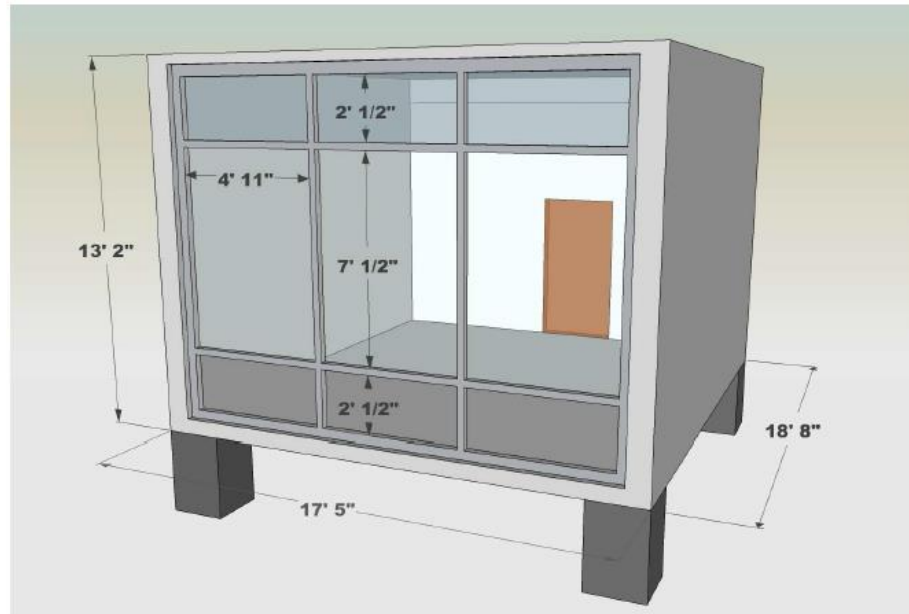


Figure 3.2 3-D model of one lab (top) - Detailed façade sections geometry (bottom)

As the setting is fully modular, depending the objective of each experiment, the glazing units could be replaced in order to be identical for both rooms. Spectral and angular solar and optical properties can be calculated for both glazing systems using WINDOW 7 (LBNL, 2013) based on the manufacturer's specifications (Figure 3.3).

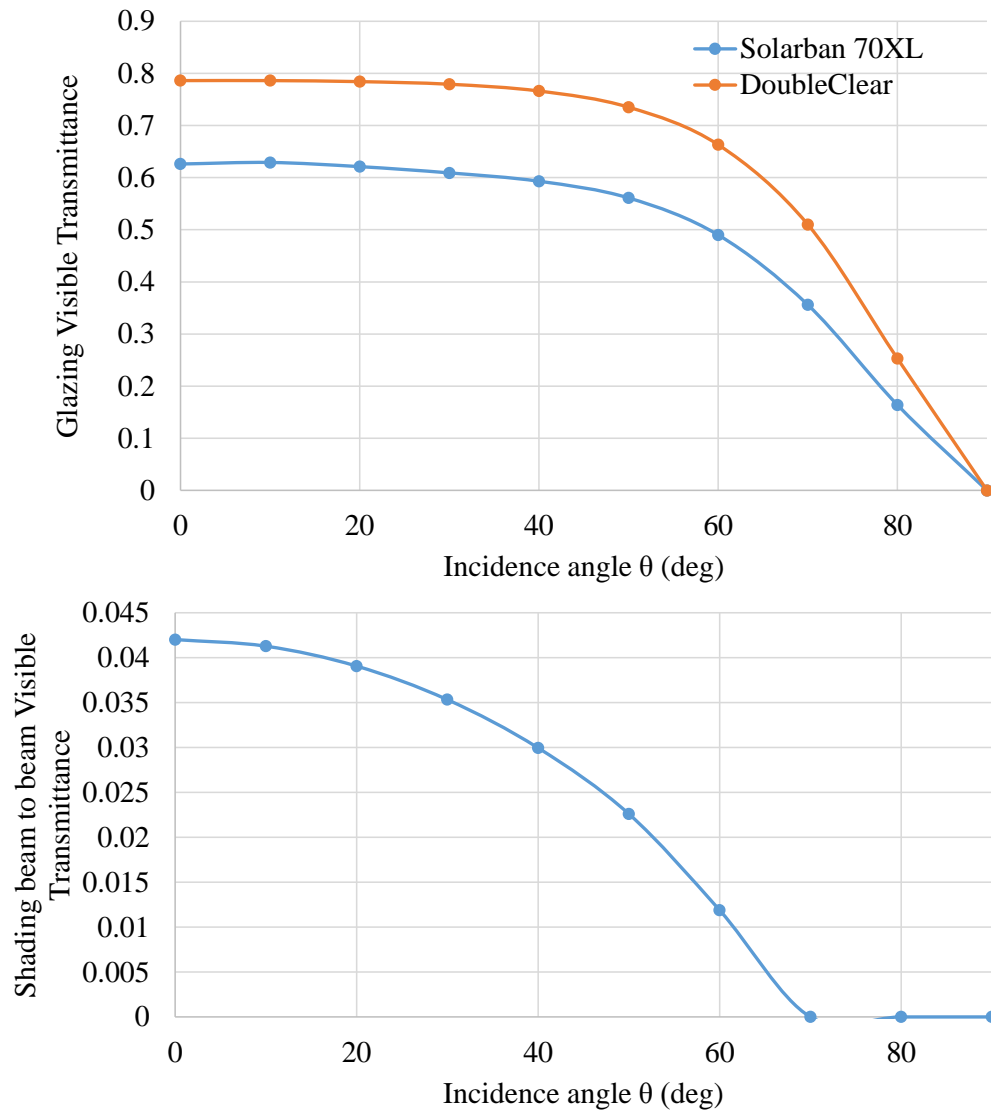


Figure 3.3 Angular visible transmittance of the two glazing systems used (top) and angular beam-beam transmittance of the shading fabric used in the experiments (bottom)

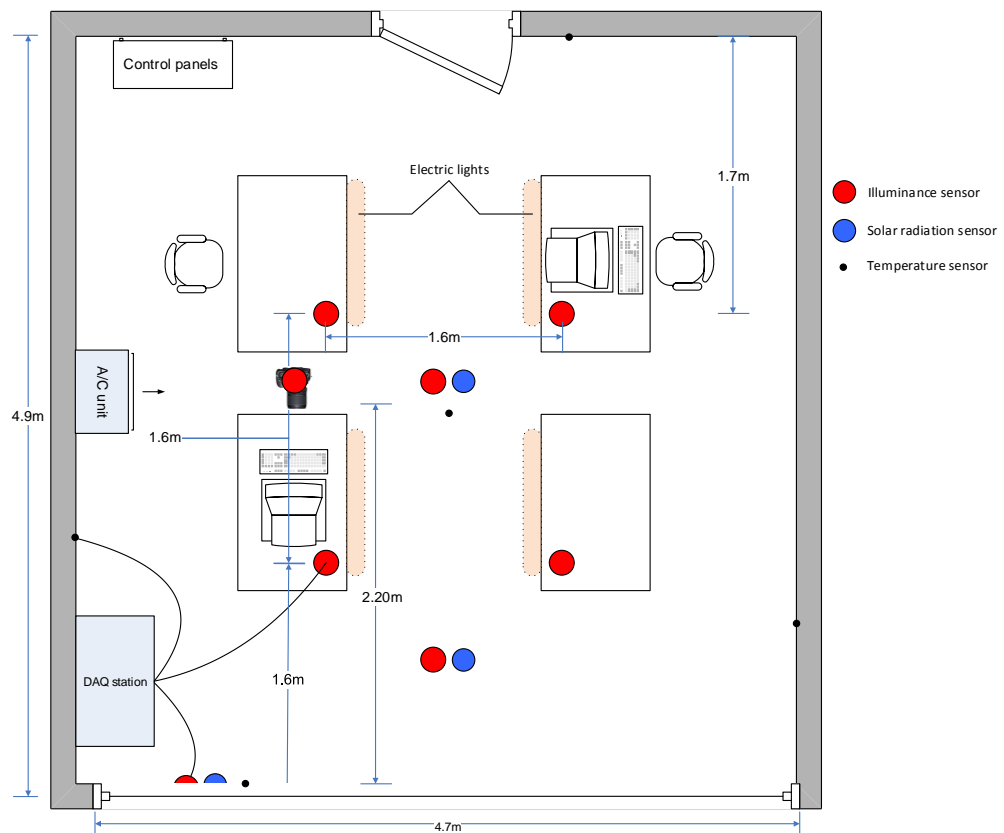
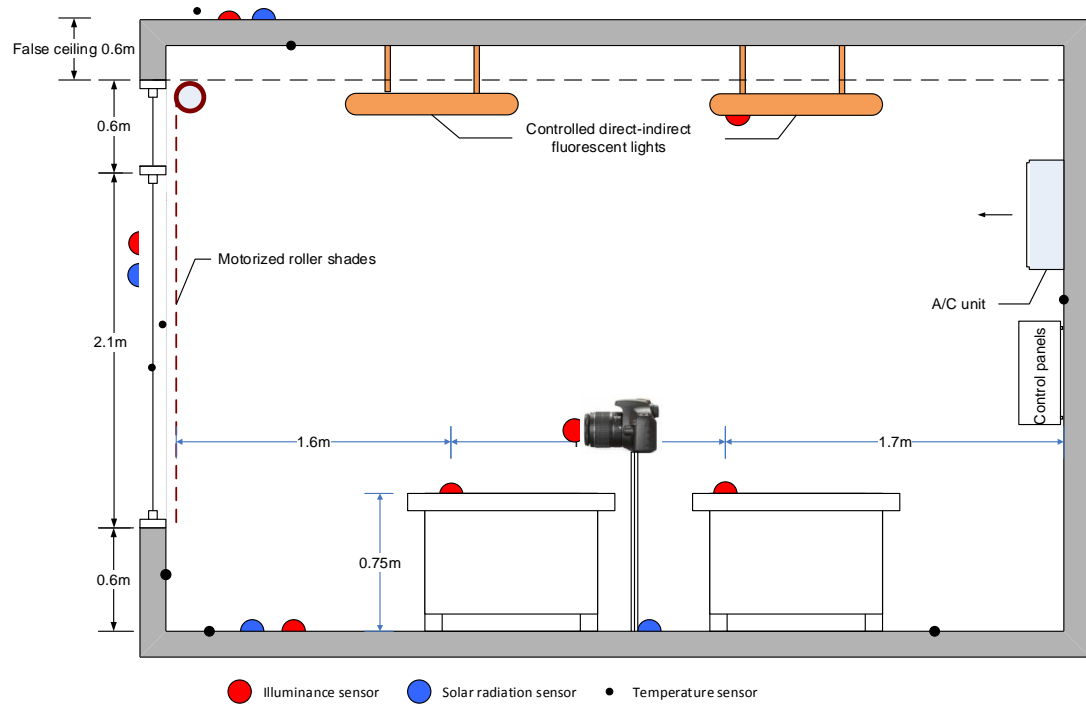


Figure 3.4 Lab vertical intersection (top) and plan view (bottom)



Figure 3.5 SPN1 pyranometer for measuring total and diffuse solar radiation incident on the façade.

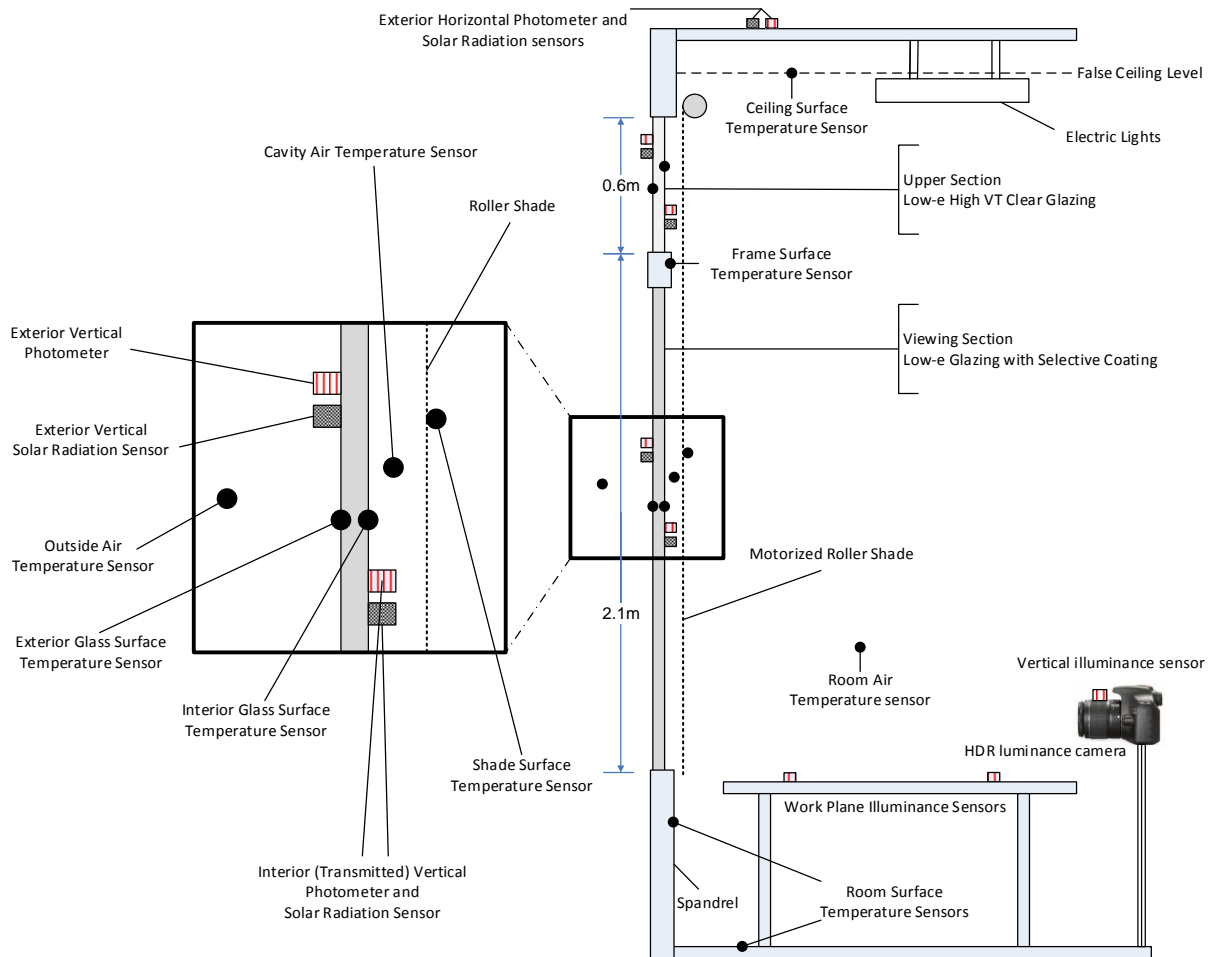


Figure 3.6 Sensor placement and instrumentation in the room

The façade is equipped with motorized roller shades, and Lutron fabrics with total visible transmittance equal to 5% (beam-beam transmittance: $\tau_{bb} = 4.2\%$ at normal

incidence), exterior reflectance equal to 74.5% and interior reflectance equal to 28% (grey color). The detailed spectral and angular properties of the fabrics used in the main experiments (Figure 3.3) were measured with an integrated sphere as described by Collins et al. (2012). The angular properties of these and other fabrics were then modeled using the semi-empirical model of Kotey et al. (2009), as explained in section 3.4.2.2, for use in generalized modeling.

Both rooms are equipped with LI-COR (LI210-SL) calibrated photometers to measure light levels, both exterior (horizontal and vertical illuminance on the exterior wall and roof) and interior (transmitted through window, on the work plane, and on the eye level). The interior window sensors are located on the interior surface of the glass, while for the horizontal work plane illuminance six points are measured in each room, in two rows, 1.6m and 3.30m from the window respectively. Vertical illuminance is measured at the eye height level at a distance of 2.20m from the window (Fig. 3.4). Direct and diffuse portions of incident solar radiation on the façade were also measured with a vertical exterior solar pyranometer (SPN1 by Delta-T), mounted vertically on the exterior south wall (Fig 3.5). A detailed instrumentation schematic is shown in Fig. 3.6). All sensors are connected to an Agilent data acquisition system, accessible through remote access in order to run experiments without interfering with indoor lighting conditions. The shades and lights can be controlled automatically (either standard industry controls provided by the manufacturer or other customized options) or manually. Both measurement and control go through LabVIEW software. According to sensor readings and selected control strategies, the developed program generates commands and sends them through Ethernet or telnet to the control processor for adjustment of shading position and/or light dimming levels (Figure

3.7) The program is also able to communicate with other software (i.e. Matlab) for processing developed models and control façade/lighting components accordingly, as well as getting feedback of operation status.

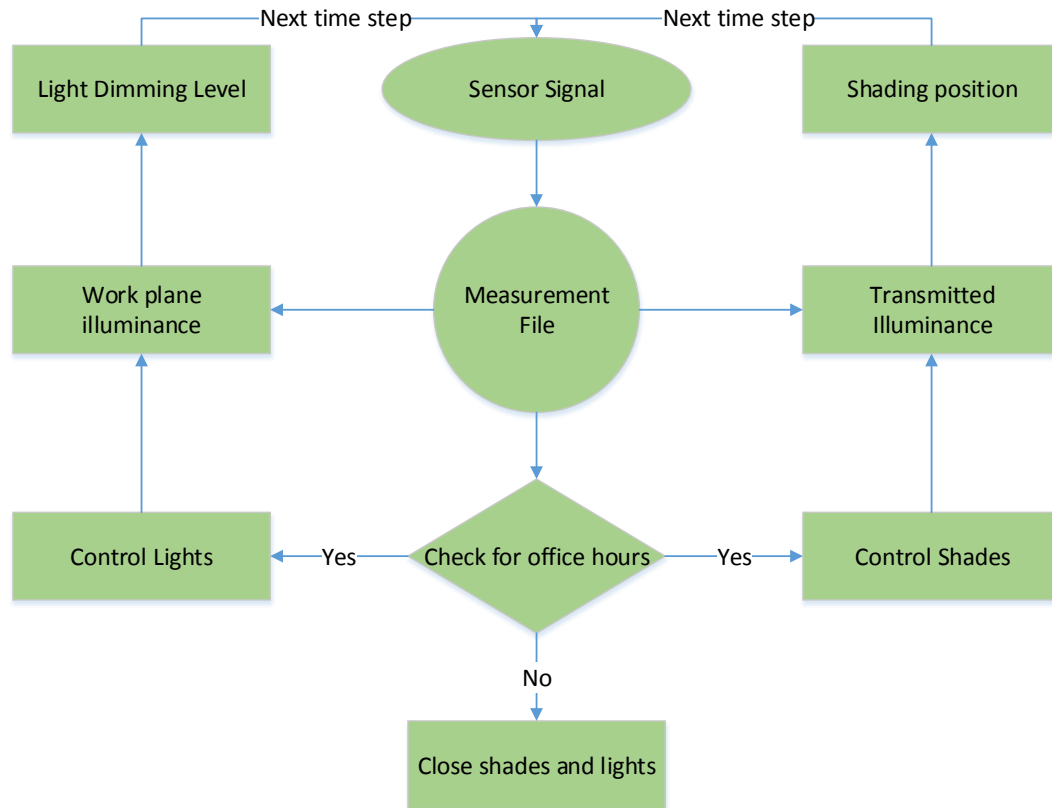


Figure 3.7 Example of measurement and control logic in Labview

The experimental setup described above was used for the non-intrusive experiments of assessing daylight glare with different shading controls. For experiments including human subjects, the space was modified in order to host 6 different isolated partitions, using two identical SB70XL glazing systems for both spaces. More detailed description of these modifications can be found in Chapters 6 and 7.

3.1.2 Living Labs – Herrick Laboratories

In the new Herrick Center for High Performance Buildings, four open plan offices were used for experiments. The four offices (Fig. 3.8), named Living Labs, have identical geometry, and differ mainly in terms of the comfort delivery systems and controls used. Three of the offices have a double skin façade, with a 1.5m wide gap between the facades, and the fourth has a conventional single façade. The Kawneer 1600 framing system is used in all of the offices. The interior façade is equipped with Viracon VE1-2M glazing units with total normal visible light transmittance equal to 70% and total normal solar transmittance equal to 33%. The exterior façade is equipped with clear insulated glazing units with total normal visible light transmittance equal to 79% and total normal solar transmittance equal to 61%. All offices are equipped with automated shading using fabrics of 5% openness and 5% visible transmittance.



Figure 3.8 Living Labs (left) – Space within the double façade (right)

Each lab can host 20-25 work stations for graduate students. Most of these workstations are the main offices of the students, therefore are being used for many hours

daily. As the objective of these spaces were to simulate unobstructed realistic locations, no significant sensor presence was decided.

The automatic shading operation is based on a solar path tracking logic for work plane protection (WPP control described in Section 3.2), but also includes settings for brightness and darkness overrides (based on Lutron Electronics Co Inc standards) which are being controlled through wireless photometers installed on the interior of the glass for each room. Modular lighting fixtures with T5 HO lamps were installed in all rooms. Occupancy sensors are also present in the rooms to enable additional energy savings. Electric lights are automatically controlled (continuous dimming) to provide at least 500 lux on the work plane level. Luminaires are controlled by rows as a function of distance from the windows, but each light fixture is addressable and can be independently controlled for maximum flexibility in studying persona illuminance preferences when needed. Lighting, shading and occupancy operation are all coordinated by Lutron Electronics Quantum© software. Manual overrides for both shading and lighting controls are also possible through wall switches.

3.1.3 Private offices– Herrick Laboratories

Four private occupied offices in the first floor of the Center for High Performance Buildings (Herrick Labs) were used to conduct lighting and glare measurements, and also further investigate occupant interactions with shading and lighting systems (Sadeghi et al., 2016). Each office has a large window on the south side and hosted one occupant, seated facing the side wall (Figure 3.9). The glazing system is Viracon VE1-2M, similar to the interior façade of the Living Lab offices. Dark-colored fabrics with 2.18% openness factor

and 2.5% total visible transmittance were used for these experiments to efficiently protect from glare. Care has been taken in order for all offices to be equipped with the same furniture layout, and for the subjects to have the same visual field (in the extent that was possible). For that reason, similar 19" LCD monitors have been placed in all four offices on four identical desks, all facing the wall and having the window on the left side. 4 HDR cameras with fisheye lenses used for luminance mapping were put on the desks next to the subjects in order to capture as much as possible the same visual field with the one of the subject. For illuminance measurements, Licor LI210SL photometers were installed on the work plane (horizontal), on top of the camera, on the back of the screen and on the interior glass (vertical). The Licor sensors were connected wirelessly with data acquisition modules. The latter, along with the shading, lighting and temperature controllers were connected through JACE controllers with the Building managements system running the Niagara Software Framework (Tridium, 2016), in order to achieve control through web interfaces, manual switches and to continuous record all measured parameters.

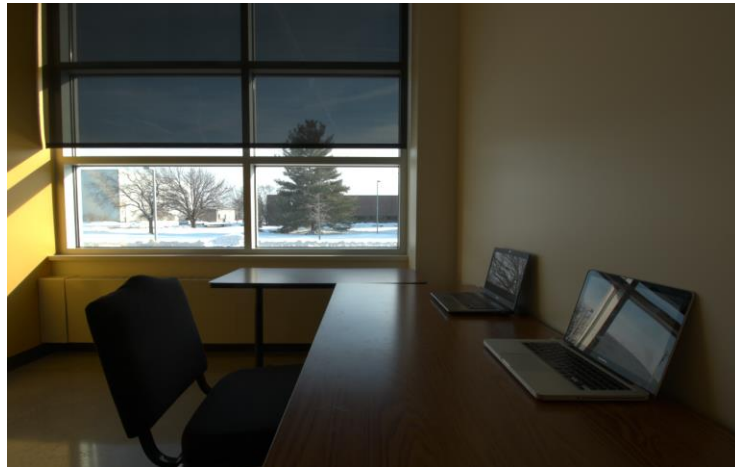


Figure 3.9 View of a private office used in the experiments

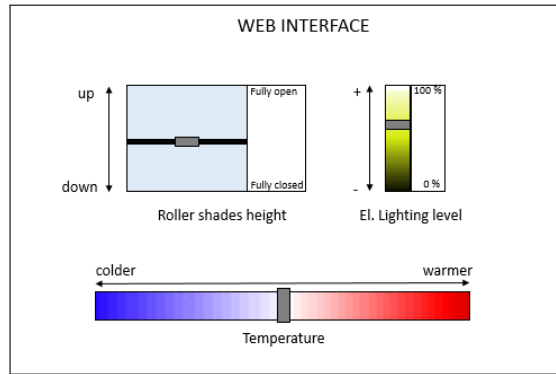


Figure 3.10 Web interface used for control overrides (Sadeghi et al., 2016)

The cameras were mounted on a tripod at 1.2 m height (the average eye height of a seated person) and were facing at the direction of the subjects' view. A vertical photometer was mounted right on the top of the lens, having the exact same view angle, to validate the extracted vertical illuminance values from the camera readings. These values can also be used for overriding the measured vertical illuminance in DGP calculations when the lens is narrower than 180° (Wienold 2012).

As every setup was fully modular, each room could accommodate different types of controls, depending on the objectives of the ongoing experiment. These included:

1. Fully manual controls for light dimming and shading through wall switches
2. Fully manual controls for light dimming and shading through remote controls
3. Fully manual controls for light dimming and shading through web interface (Figure 3.10)
4. Work plane protection (WPP) automatic control for shading and automatic light dimming control based on maintaining 500 lux on the work plane

5. Work plane protection (WPP) automatic control for shading and automatic light dimming control based on maintaining 500 lux on the work plane, both with possibility for overrides through a web interface (Figure 3.10)

3.2 Shading controls

One of the main objectives of this Thesis was glare evaluation and correlation with illuminance metrics in spaces with dynamic shading controls. For this purpose, three different shading control schemes were applied during the experimental measurements in the Façade Engineering test offices and in the simulation model.

1. Fully *closed* shades provides a baseline for comparisons, while it is also a realistic setting in cases of high sky brightness or sunny conditions. This setup was also used for the experiments described in Chapters 6 and 7 of this thesis.
2. Work Plane Protection control (*WPP*): a typical control from industry practice was utilized: shades automatically move to a position that just prevents direct sunlight from falling on the work plane, assuming a certain distance between the working area and the façade. Therefore, shading position at any time is a function of the solar profile angle and the distance between the occupant and the window.
3. Finally, an *advanced* shading control algorithm was studied, aiming to protect the work plane area from direct sunlight, while adjusting the shade height to prevent high work plane illuminances (> 2000 lux) at all times and maximize daylight provision under cloudy sky conditions (Shen and Tzempelikos, 2014). The total “effective” transmitted illuminance through shaded and unshaded window parts, E_{eff} , is plotted against work plane illuminance (for the entire year) to determine a threshold, E_{esp} , to avoid excessive

amounts of daylight on the work plane. If E_{eff} is below this threshold, shading position is determined by the WPP control described above; otherwise, the shades will move to a lower position according to:

$$E_{sh} \times (H - h) + E_g \times h = E_{esp} \times H \quad (3.1)$$

, where H is the entire window height; h is the unshaded window portion; E_g and E_{sh} is the illuminance transmitted through the unshaded and shaded window parts respectively. For the test offices described above, the illuminance threshold is $E_{esp} = 7500$ lux, a value also maintained for the simulation cases.

3.3 HDR imaging

Throughout this thesis, different approaches of luminance measurements have been followed, depending on the objectives of each different study, the equipment available and the requirements in terms of dynamic range, flexibility, automation etc. However, all different approaches were based on three main methodologies that are described in the following sub-sections, Method A, B and C.

3.3.1 Methodology A – LMK system

For the studies performed without subjects in the Bowen Laboratories, as well for the ones performed with subjects in the open plan office studies, where only one camera was required and the sun was never included in the field of view, method A was used for luminance acquisition. Method A was based on the use of an already calibrated Canon 550D dSLR camera, equipped with a Sigma 4.5mm fisheye lens was used for luminance mapping and glare measurements (Figure 3.11). The fisheye lens is recommended since it

better resembles the human visual field. Hirning et al. (2014) suggests a modified human visual field according to the total field of Guth (1966), which is also an option in Evalglare software (Wienold, 2012). Although this approach is reasonable for studies involving human subjects, due to the fact that most of the DGP investigation in this Thesis was focused on measurements and simulations, including correlations with values extracted by photometers having 180° field of view, the original 180° wide visual field was used. A vertical photometer was mounted right on the top of the lens, having the exact same view angle, to validate the extracted vertical illuminance values from the camera readings. These values can also be used for overriding the measured vertical illuminance in DGP calculations when the lens is narrower than 180° (Wienold 2012). The camera is set to shoot three or more pictures of different exposures during each measurement.



Figure 3.11 Method A: dSLR camera setup with vertical photometer and tripod

The Canon 550D camera came as part of an integrated hardware and software luminance measurement set manufactured by Technoteam. The required calibration in terms of luminance, vignetting, point spread error had been already performed by the manufacturer and the calibration data was implemented on the luminance processing software Labsoft 14.3.6 (Technoteam, 2014). Therefore, for that instrument, the readings of the camera were considered to be reliable, and no further calibration was performed for the measurement obtained with the specific device. Labsoft can handle the entire process, from merging the single pictures into HDR images to applying the implemented calibration factor and performing statistical processing to the pictures, covering all steps described in related literature of “Evalglare” (Wienold, 2012; Reinhart et al, 2012).

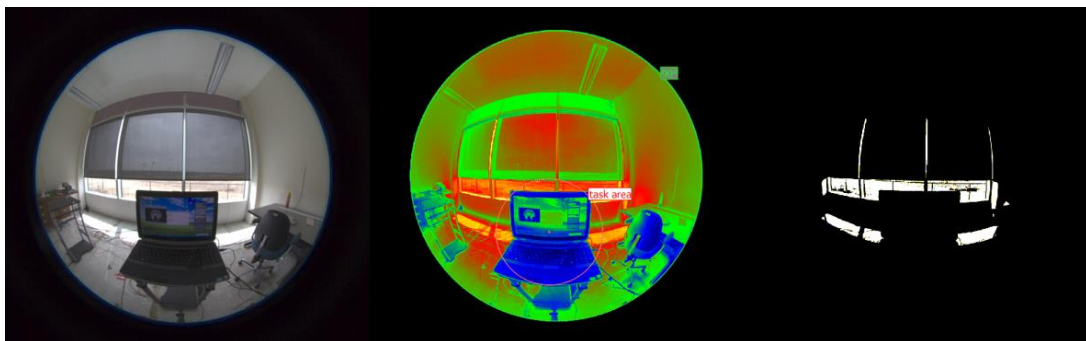


Figure 3.12 HDR image (left) – Extracted luminance mapping and task area definition (center) – Identification of glare sources (right)

An Active-X controlled Excel spreadsheet with Visual Basic was utilized to extract DGP from the measurements, directly communicating with Labsoft to obtain the required luminance per pixel data. The logic followed by the software is the one implemented in Evalglare (2012), as glare sources are identified using a choice of criteria, based on absolute, average or task area based thresholds, and the equation is applied to the visual field, calculating the vertical illuminance and the cumulative influence of the glare sources. The

three steps of processing (HDR merging, luminance mapping and glare sources identification) can be seen in Figure 3.12.

There are certain limitations in the use of Labsoft; first and foremost, Labsoft cannot handle HDR images consisting of more than three exposures, or more than one aperture. This proves problematic for cases when the sun or specular reflections of it are included in the visual field, as multiple apertures could help in order to capture the extreme dynamic range required (Strumpfel et al. 2004). For these cases, Labsoft returned an overdriven image error, expressing the degree of overdrive. This is a common issue in literature, as having in the same image the low values of indoor luminance and the extreme values of the solar corona's luminance requires an extreme dynamic range, which is impossible even for traditional HDR imaging at this time. These images can be unpredictable in terms of measuring; while they usually overestimate the luminance values in certain areas, lower values for DGP can be calculated. The solution suggested by Strumpfel et al. (2004), which involves adding more exposures to each HDR image, modifying apertures additionally to changing shutter speeds, and also adding ND filters on the lens was not followed for Method A, as because of the fact that the experiments were conducted in Fall and Spring, the sun was never included in the field of view to cause any effects like the ones described above. However, a modification of Strumpfel's approach is used in Methodology C (Section 3.3.3), applied for the cases where daylight glare with the sun in the field of view through shading fabrics is investigated (Chapter 6). Another issue in Labsoft was that the correction factors issued by Wienold (2012) for low light and age were not implemented in the evaluation algorithms. While the age factor is controversial and out of scope for this work, the low light correction is critical in cases where correlation

with human subjects' impressions is considered. Therefore, for experiments which included human subjects, the correction was applied after the evaluations. Because of the fact that the majority of literature uses Evalglare for glare evaluation, Labsoft had to be first validated in order to be used. Therefore, validations in terms of DGP, glare sources identification, average luminance and vertical illuminance were performed for a variable visual conditions (Figure 3.13). As it can be seen in the graphs, a satisfactory fit was achieved for all cases. Slight differences are believed to be a result of the slight image processing required for use in Evalglare, due to the suggested 800x800 pixels size.

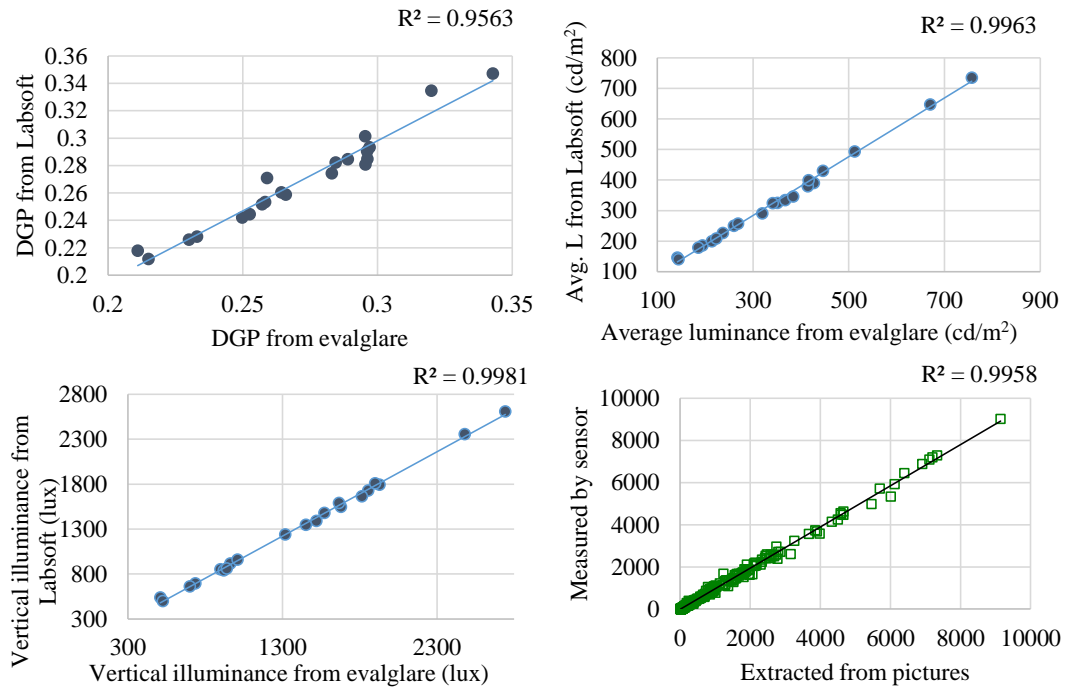


Figure 3.13 Validation of Labsoft results for DGP (top left), average luminance (top right), vertical illuminance (bottom left) using Evalglare – Validation of vertical illuminance extracted from pictures with photometer (bottom right)

The glare sources identification rule used was 4 times the average luminance of a task area (Wienold and Christoffersen, 2006), covering the main part of the laptop screen.

As it can be seen in Figure 3.14, the glare sources identification was a perfect match with the one obtained by Evalglare.

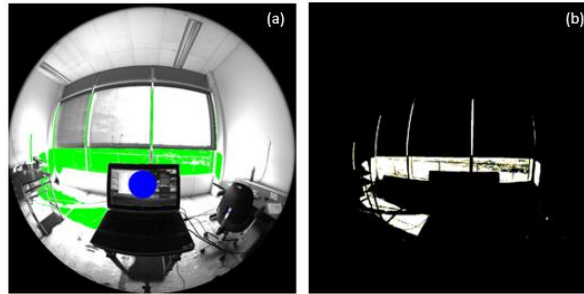


Figure 3.14 Glare sources identification through (a) Evalglare in green and (b) Labsoft in white with partially open shades

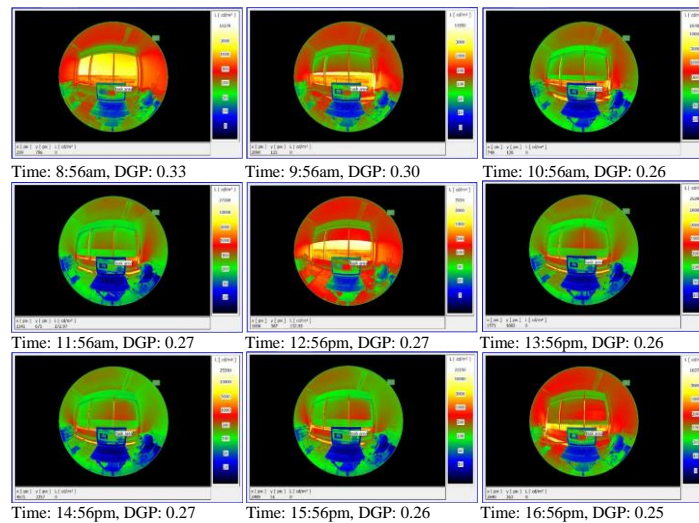


Figure 3.15 Hourly luminance mapping pictures in the test office with automated shading controls enabled.

The HDR images can also be used to calculate vertical illuminance on the eye from the visual field by integrating the total pixels' contribution to the vertical illuminance, as a product of the pixel's measured luminance multiplied by the respective "configuration" factor. The vertical illuminance values extracted by the HDR images using Labsoft were

compared to Evalglare results and also to measured values using the camera-mounted vertical photometer, demonstrating a good fit (Fig. 3.13 – bottom right) and proving the reliability of the HDR luminance measurements.

Taking pictures in the offices had to be automated, to avoid presence that could alter the illumination conditions, and also for convenience due to the high number of images taken during the experiments. For shooting the pictures automatically, a custom firmware (Magic Lantern 2.3) was installed in the camera in order to make use of the implemented intervalometer function. This function allowed shooting in selected intervals of time. An example of luminance images (automated shots) taken every hour in the office with automated shading is shown in Fig. 3.15, with DGP variation.

3.3.2 Methodology B – Calibration of regular dSLR cameras

For the measurements obtained in the four private offices, as 3 of the cameras were not pre-calibrated, the standard calibration approach found in literature was followed, implementing standard Canon 550D (or T2i, according to the American version) cameras available in the market equipped with Sigma 4.5 Fisheye lenses. The multiple exposures were merged into HDR images and afterwards calibrated for luminance using Photosphere (Ward, 2014). Photosphere is a Mac OS only freeware program which has the advantages of performing most of the essential steps for glare evaluation under a user friendly graphical interface. A Konica LS-100 spot meter was used for the calibration, as well as a Macbeth Color Checker Test target (Figure 3.16). It has been found that the accuracy of the procedure was very sensitive to the selection of the baseline surface of the calibration. It is suggested for a small grey target surface to be chosen, as uniform in luminance as

possible and neither very dark nor directly lit by sunlight. In addition, a high range of luminances is desired in the visual field during the calibration, and as a gradual transition as possible between the brightest and darkest parts. The controlled reflectivity surface of Macbeth test target helped obtaining the highest accuracy in calibrations.

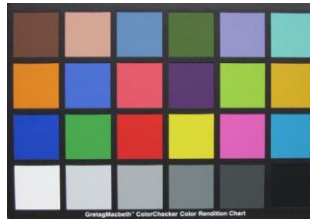


Figure 3.16 Macbeth Color checker target used for calibrations

After extracting the cameras' response curves (Figure 3.17), the extent of vignetting error was investigated. As literature suggests (Inanici and Galvin, 2004), vignetting is less intense for smaller apertures (higher F-values). The experiments were performed with an f/11 aperture, therefore vignetting was controlled and more gradual. In addition, Canon implements a peripheral luminance correction function which aims to eliminate the effect. However, due to the fact that this function was generic, and not for the particular lens, the magnitude of the vignetting effect had still to be investigated. A methodology of having a single grey target and rotating the camera in increments of 5 degrees was followed, to compare the radial decrease function. The decrease, having the correction function on, proved to be negligible and noticeable only at the very end of the visual field (85 degrees from the center of the lens), as seen on Figure 3.18, therefore the peripheral correction function was considered to be reliable enough for the image processing.

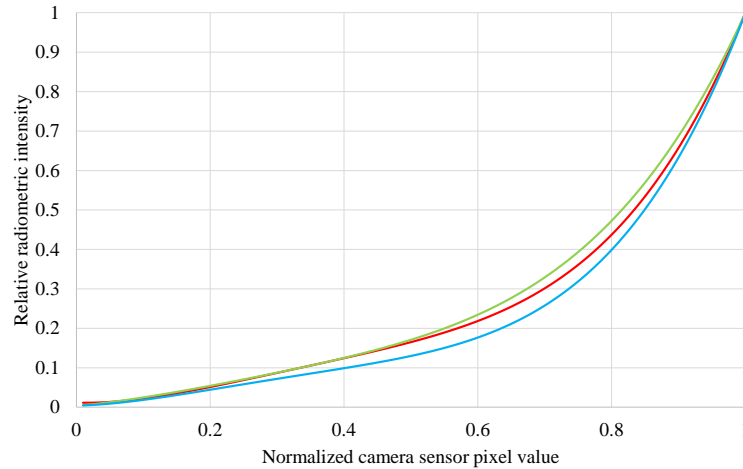


Figure 3.17 Extracted response curve for Canon T2i and Sigma 4.5 fisheye lens (color of lines associated with the three basic colors Red Green Blue).

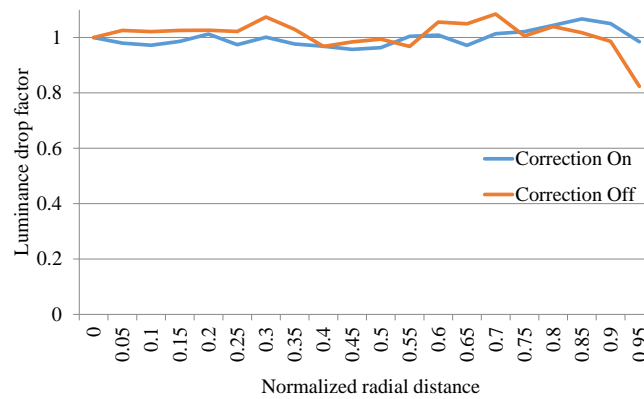


Figure 3.18 Vignetting behavior of Canon T2i + Sigma 4.5 fisheye lens with aperture setting of f/11, with and without the implemented generic correction.

After creating the HDR pictures using the response function of Figure 3.17, they were appropriately cropped to a circumscribed square and resized to 800x800 pixels in order to be used in Evalglare for DGP and other calculations. The inputs of Evalglare include the fisheye geometry of the lens (-vta parameter equal to the 180° total span of the fisheye lens), the position and span of the task area, the optional cropping of the visual field, etc.

For calculating average luminances of areas of interest (window, screen, different task areas etc.), a graphical masking method was followed; the areas of interest were masked with Adobe Photoshop, by being filled with black color, and saved as TIFF images. The latter images were converted to .hdr files through Radiance, resulting to images where the area of interest was solely present. These images were then processed in Evalglare using a negligible glare sources identification threshold, in order for the area of interest to be uniformly identified as a glare source, and the average luminance was obtained by the output file of Evalglare. The steps of the process can be seen in Figure 3.19.

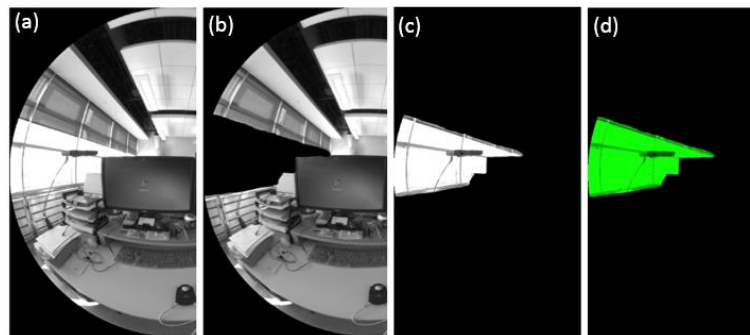


Figure 3.19 Masking methodology for obtaining average luminance of selected areas of interest: (a) Original HDR image – (b) Masking of the area of interest with black color – (c) Isolation of area with Radiance – (d) Calculation of average area luminance with Evalglare

Due to the very high number of pictures to be created and processed (in the order of tens of thousands) in occupied and unoccupied spaces during the experiments, an automation system had to be developed, for both shooting and processing phases. For shooting the pictures automatically, a custom firmware (Magic Lantern 2.3) was installed in the cameras in order to make use of the implemented intervalometer function. This function allowed shooting in selected time intervals. For the automation of HDR creation and processing, and given the fact that HDRgen (Ward) was used, its command line nature

made it possible to be run from within a script. Therefore, a script was created in order to open selected LDR photos, create an indexed HDR photo from the included response function, and then perform all the necessary processing as seen in Figure 3.20.

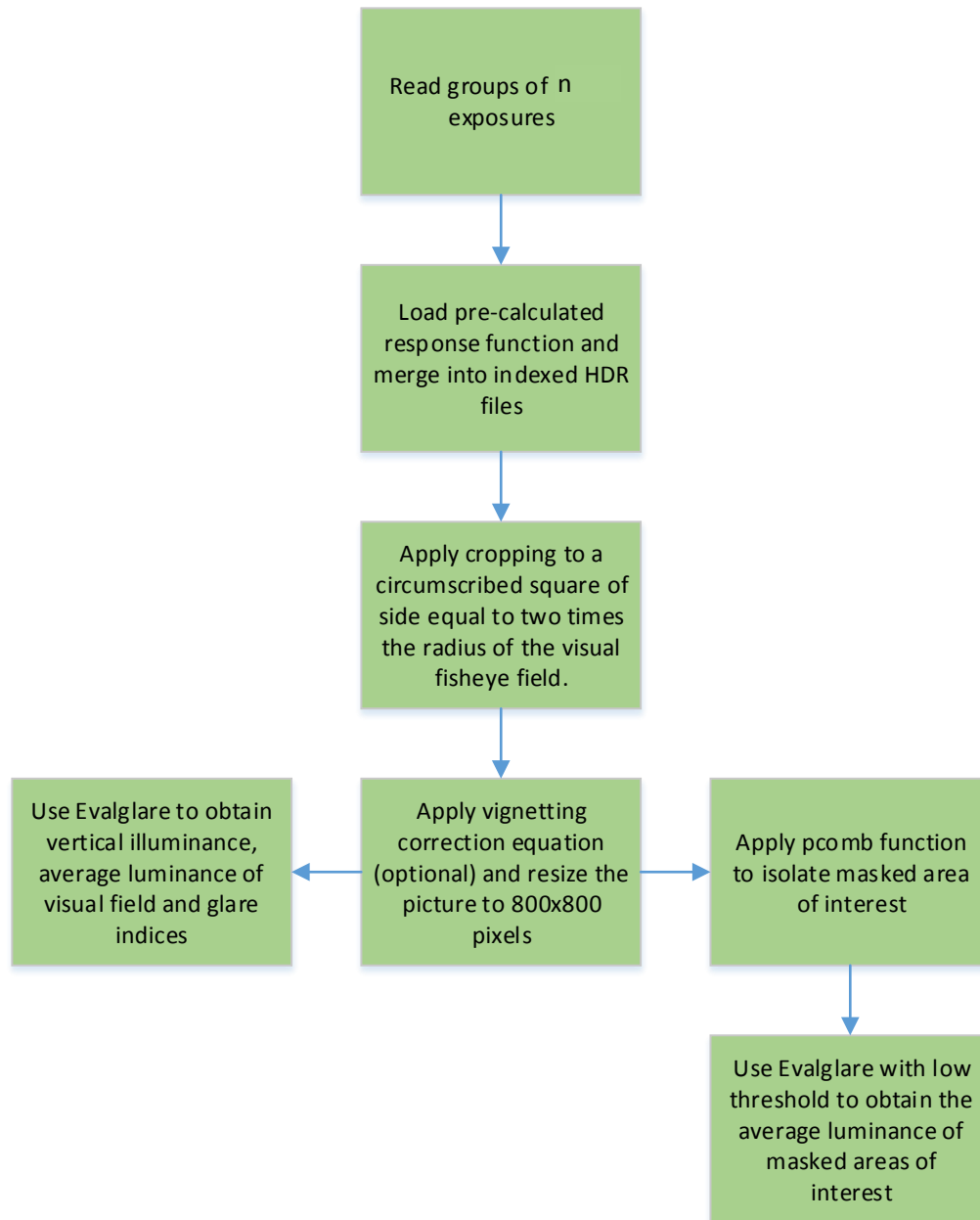


Figure 3.20 Flow chart for automated HDR imaging and processing

In order to validate the calibration performed to the cameras other than the LMK integrated system, the readings of the Konica LS100 spot meter were plotted with the values obtained through the HDR images in terms of luminance. The cameras performed very well, as seen at Figure 3.21.

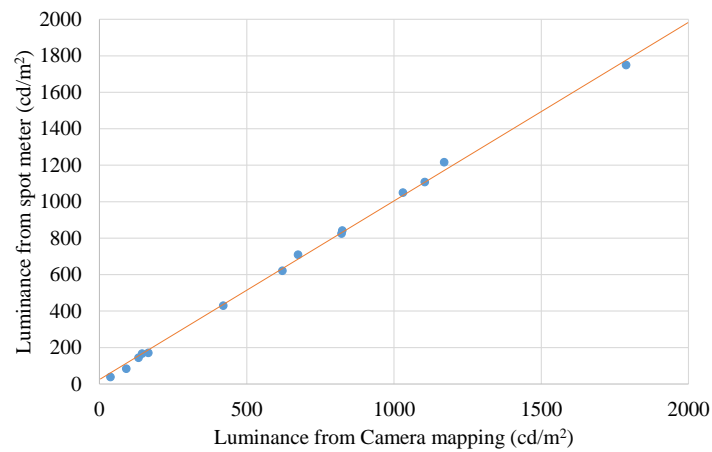


Figure 3.21 Validation of calibration for cameras other than the LMK integrated solution

For the studies performed in the private offices, a cropping according to Guth's total field of view was performed (Figure 3.22).

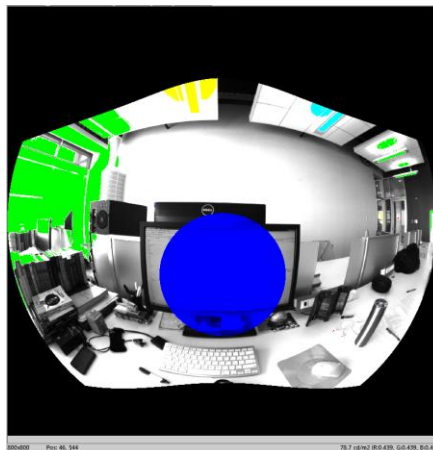


Figure 3.22 Cropping of visual field according to Guth's total field (used in the private offices study)

3.3.3 Methodology C – Including the solar corona through window shades

As mentioned in Chapter 3.3.1, the presence of the solar disc in the field of view introduces several challenges when it comes to HDR luminance acquisition. In order to simultaneously capture the solar corona, at the order of 10^9 cd/m² and the interior of a room (at the order of 100 cd/m²), an extreme dynamic range is required, that cannot be accommodated even by HDR methodologies. The result is that instead of a clear definition of the sun in the pictures, a large area white blob appears, in which the luminance appears to be falsely uniform, and the outline of the sun is not clear. The latter effects are combined with severe under-calculation of the solar corona's luminance, which appears to be at the order of 10^5 cd/m².



Figure 3.23 Overdrive error caused by limited dynamic range, leading to solar corona luminance underestimation for less than 200,000 cd/m² in clear sky conditions (top); and poor luminance mapping in case of sun covered by thin clouds (bottom)

Due to the significance of the solar luminance value for the accurate calculation of glare indices, the above effects make the measurements non-suitable for reliable comfort

research when the solar corona is visible. As one of the main objective of this thesis was the glare evaluation of the sun visible through window shades, this inadequacy of the HDR luminance acquisition methodology had to be addressed. For that reason, Methodology B of Chapter 3.3.2 was extended with slight modifications in order to accommodate such conditions. Indeed, Figure 3.24 demonstrates how the newly developed Methodology C can successfully capture the solar corona through window fabrics, with clear description of the outline of the sun and reasonable luminance values (at the order of 10^6cd/m^2 , as the sun is viewed through a low openness fabric).

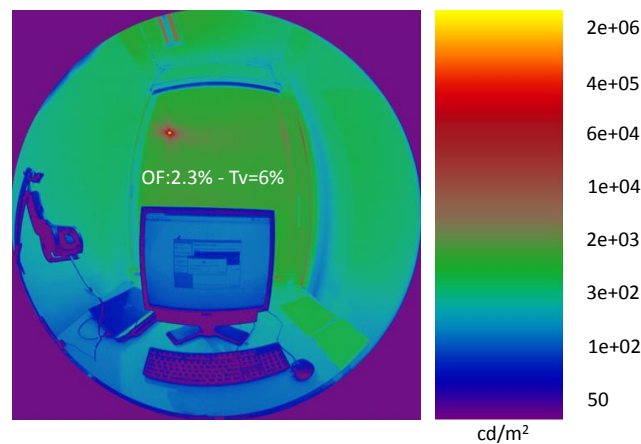


Figure 3.24 HDR image of a partition with fabric E indicating the luminance distribution including the sun visible through the fabric

In order to achieve this result, a Wratten ND 3.0 gelatin neutral density filter was used, mounted between the fisheye lens (Sigma 4.5) and the CCD sensor of the Canon T2i cameras. The addition of this filter causes an exposure drop of 10 stops, transmitting a 0.1% of the original light. The use of such a filter, along with the alteration of the original shutter speeds (using a sequence of 9 exposures, starting from 15 sec to 1/250 sec to compensate for the darker conditions) helped create HDR images that clearly capture the sun without

creating burnt areas of low resolution. The technique is a modification of the methodology suggested by Strumpf et al. (2004), however no variable aperture was used in order to make the process more flexible. Nevertheless, as the experiment was based on observing the sun through relatively low openness fabrics, the dynamic range requirements were found to be able to be accommodated by only varying the shutter speeds. A Konica LS110 luminance sensor, a calibrated LMK Canon 550 HDR measurement system and a Macbeth Color Checker Test target were used for obtaining the camera's response curve under the influence of the ND filter. The script presented in 3.3.2 was extended in order to automatically perform all the stages of HDR imaging, from creating the images from the pictures based on the extracted response function, to cropping and resizing appropriately and then running Evalglare (Wienold, 2014) to calculate the metrics of interest such as DGP.

Since for each measuring point the camera had to be set up at the exact same point with the occupant's head, each case showed slight differences in terms of absolute camera position (due to height differences of the subjects, minor differences in the distance from the screen each subject was choosing, etc.). For that reason, and to avoid inconsistencies between observations due to assuming a fixed uniform task area for all DGP calculations, a fixed glare identification threshold approach was followed instead in Evalglare, using the threshold of 2000 cd/m^2 , which has been found to correlate well with human responses (Van den Wymelenberg et al., 2010). The selection of the specific threshold was to some extent validated by the responses of the subjects when asked to point out any sources of discomfort within their visual field on a sketch in the survey of Chapter 6; assuming lower thresholds (for example 500 or 1000 cd/m^2) would most of the times identify as glare

sources several parts within the visual field that subjects would not consider as sources of distraction whatsoever. As validating the readings would require an instrument with luminance measuring range exceeding the order of 10^7 cd/m², a validation in terms of vertical illuminance (Fig. 3.25) was performed for all of the images. A MSE of 193 lux was calculated and considered satisfactory given the severe conditions (extreme solar corona luminance being partly diffused through the fabric) and the high values of vertical illuminance measured throughout the study.

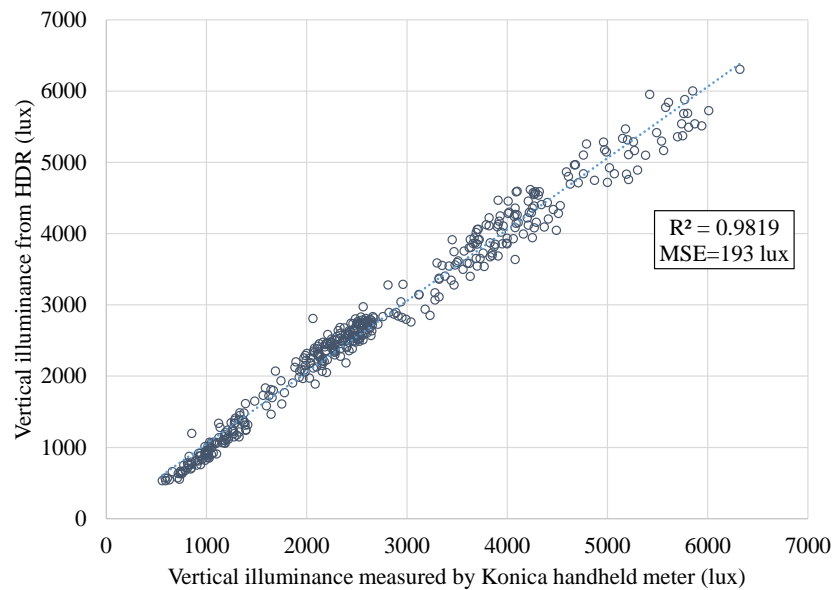


Figure 3.25 Validation of HDR imaging in terms of vertical illuminance

3.4 Simulation Methodology

In order to generalize experimental findings, investigate different scenarios and use optimization methods to suggest guidelines, a hybrid ray-tracing and radiosity daylighting model with a glare module was used. The daylighting model (Chan and Tzempelikos, 2012) uses as inputs TMY3 weather data (alternatively sub-hourly computed or measured

data), building information (geometry, location, orientation, materials) and occupancy details (Figure 3.26).

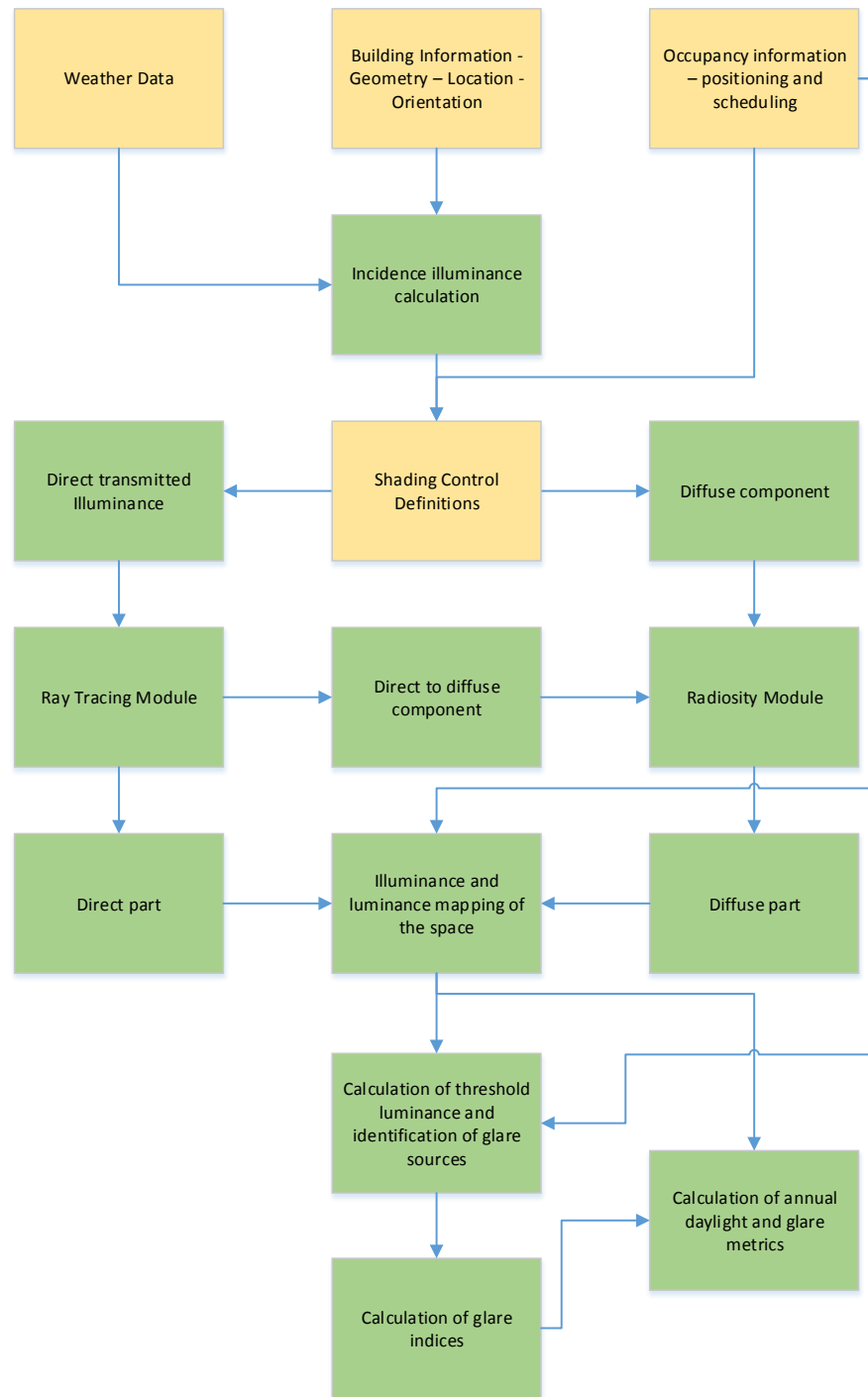


Figure 3.26 Daylighting and Glare model flowchart

3.4.1 Incident illuminance on facade

The weather data for the specific location and orientation is used to calculate the incident illuminance on the façade. The incident illuminance in window is a result of direct sunlight, diffuse daylight from the sky and reflected daylight from the ground. Direct sunlight can be derived from the solar geometry, depending on the location, orientation and time. Then, using the angle of incidence (angle between solar rays and a line perpendicular to the façade), the incident direct sunlight can be extracted.

For calculating the diffuse daylight, the Perez et al. (1990) sky model is utilized. The diffuse total sky illuminance is expressed with the equation:

$$E_{sd} = E_{dh} \left((1 - F_1) \frac{1 + \cos(\beta)}{2} + F_1 \frac{a}{b} + F_2 \sin(\beta) \right) \quad (3.2)$$

, where E_{sd} stands for the sky diffuse illuminance incident on a surface, E_{dh} for the diffuse horizontal illuminance, F_1 for the circumsolar brightening coefficient, F_2 for the horizon brightening coefficient, and a, b factors calculated as function of incidence and altitude angles. For the calculation of ground reflected diffuse illuminance, the total horizontal illuminance is multiplied by the ground reflectance and the view factor between the ground and the surface of the façade.

3.4.2 Interior illuminance calculations

3.4.2.1 Ray tracing method

In order to calculate direct and reflected sunlight in the interior surfaces (floor, walls and work plane), a forward ray tracing method is utilized. After all points of the geometry for the window are defined, a set of rays is randomly generated using the Monte-Carlo

sampling algorithm from the light source (window or sun) representing a specific amount of direct luminous flux per ray equal to:

$$L.flux = \frac{\tau_{dir-win} E_{dir} A_{win}}{N_{rays}} \quad (3.3)$$

, where $\tau_{dir-win}$ is the window's direct visible transmittance, E_{dir} is the direct illuminance, A_{win} the window area and N_{rays} the total number of rays generated.

Each ray is defined by a directional incident vector expressed as:

$$\vec{T} = (\cos(\alpha) \cos(\varphi), \cos(\alpha) \sin(\varphi), -\sin(\alpha)) \quad (3.4)$$

, where α is the solar altitude and φ the solar azimuth. The interior surfaces (walls, floor, ceiling and work plane) are considered as planes defined by a position vector and a normal vector describing their direction. The travel distance of the ray from the window to each one of the surfaces is calculated by the equation, for all planes:

$$t = \frac{(\text{Position Vector of Plane} - \text{Position Vector of Ray}) \cdot \vec{N}}{(\text{Directional Vector of Ray}) \cdot \vec{N}} \quad (3.5)$$

, where N is the normal vector of each plane, Q is the position vector of the ray, P the position vector of the plane and R the directional vector of the reflected ray. The ray is assumed to strike at the plane with the minimum traveling distance.

3.4.2.2 Daylight transmission through shading

Due to the limited information about the detailed angular properties of shade fabrics in the market, in order to effectively simulate the behavior of a roller shades system, the semi-empirical model of Kotey et al. (2009) is utilized to calculate the off-normal beam to

beam, beam to diffuse and diffuse to diffuse properties of the fabrics. The model has been validated with integrated sphere measurements (Kotey et al., 2009) and full-scale experiments (Chan et al., 2014).

The normalized beam-beam component is calculated as:

$$\tau_{bb-norm} = \frac{\tau_{bb}(\theta)}{\tau_{bb}(\theta=0)} = \cos\left(\frac{\theta}{\theta_{cutoff}} \cdot \frac{\pi}{2}\right) \quad \text{for } \theta \leq \theta_{cutoff} \quad (3.6)$$

, where $\tau_{bb}(\theta)$ is the beam-beam component for an incidence angle θ . The “cut-off” angle θ_{cutoff} (angle beyond which transmittance approaches zero) is calculated from:

$$\theta_{cutoff} = 65^\circ + (95^\circ - 65^\circ)(1 - \cos(\tau_{bb}(\theta=0) \frac{\pi}{2})) \quad (3.7)$$

$$\text{, where } b = 0.6 \cdot \cos^{0.3}(\tau_{bb}(\theta=0) \frac{\pi}{2}) \quad (3.8)$$

The normal beam-beam component is assumed equal to the openness factor of the fabric.

The normalized beam-total component is calculated from equation 3.10:

$$\tau_{bt-norm} = \frac{\tau_{bt}(\theta)}{\tau_{bt}(\theta=0)} = \cos^d(\theta) \quad \text{for } \theta \leq \theta_{cutoff} \quad (3.9)$$

, where d is calculated by the following equations:

$$\left\{ \begin{array}{ll} d = 0.133(\tau^{str} + 0.003)^{-0.467} & 0 \leq \tau^{str} \leq 0.33 \\ d = 0.33(1 - \tau^{str}) & 0.33 \leq \tau^{str} \leq 1 \end{array} \right\} \quad (3.10)$$

, and the factor τ^{str} is calculated as:

$$\tau^{str} = \frac{\tau_{bt}(\theta=0) - \tau_{bb}(\theta=0)}{1 - \tau_{bb}(\theta=0)} \quad (3.11)$$

The beam-diffuse component is calculated by subtracting the beam-beam from beam-total for each angle:

$$\tau_{bd} = \tau_{bt} - \tau_{bb} \quad (3.12)$$

The diffuse-diffuse component is calculated by integrating the beam-total component over the hemisphere:

$$\tau_{dd} = 2 \int_0^{\pi/2} \tau_{bt}(\theta) \cos(\theta) \sin(\theta) d\theta \quad (3.13)$$

Direct sunlight entering the room through the fabric is computed from Eqs. (3.6-3.8) and is traced until reflected by interior surfaces. Inter-reflections between the glazing and the shade are considered and are assumed fully diffuse.

3.4.2.3 Radiosity calculations

After all initial luminous exitances of the surfaces are calculated, a 3-D radiosity calculation follows in order to take into account the inter-reflections between the rooms interior surfaces. The surfaces are divided into square sub-surfaces, which are considered diffuse. Therefore, the final luminous exitance of every subsurface is calculated as:

$$M_i = M_{i-0} + \sum_k^n \rho_i \cdot F_{ik} \cdot M_k \quad (3.14)$$

, where M_{i-0} is the initial luminous exitance calculated from the previous steps, k is every other surface, n is the total number of other surfaces viewable by surface i and F_{ik} the view factor between surfaces i and k . The model takes into account shading controls, so that each time step may contain different shade positions. This involves varying view factors between the variable shaded/unshaded portions of the window and the rest of the interior surfaces, which are pre-calculated for all positions in order to improve computational efficiency.

While the direct part of the luminous flux through the window is handled by the ray-tracing method, the diffuse part is also separated to at least two different diffuse sources, corresponding to the luminance of the sky and the ground, rather than following a daylight coefficient detailed approach which would better approach the non-uniformity of the sky but at the same time make the simulation slower. The equations for the luminances of the window sub-surfaces due to the sky and ground are as follows:

$$L_{i\text{-sky}} = \frac{E_{\text{dif-sky}} \cdot \tau_{\text{dif-win}}}{\pi / 2} + \frac{M_i - M_{i-0}}{\pi} \quad (3.15)$$

$$L_{i\text{-gr}} = \frac{E_{\text{dif-gr}} \cdot \tau_{\text{dif-win}}}{\pi / 2} + \frac{M_i - M_{i-0}}{\pi} \quad (3.16)$$

, where $E_{\text{dif-sky}}$ and $E_{\text{dif-gr}}$ are the incident diffuse illuminances due to the sky and ground respectively, and $\tau_{\text{dif-win}}$ is the diffuse transmittance of the window.

Therefore, the contribution of diffuse light to the calculated work plane illuminance is:

$$E_{\text{wp-dif}} = \sum_1^n L_i \cos \theta d\omega \quad (3.17)$$

, where θ is the angle between the line from the virtual sensor to the window and the normal vector to the window.

In case of work plane sensors, having a span of 180° looking upwards, the luminance of the window is entirely due to the sky, while for cases of vertical sensors looking towards the window, sub-surfaces above the line of sight are affected by the sky and sub-surfaces below the line of sight are affected by the ground luminance.

Additionally, in the case of roller shades, the influence of the isotropic direct-diffuse

part of the luminous flux through the fabrics has to be taken into account.

$$L_{i-sky} = \frac{E_{dif-sky} \cdot \tau_{dif-win} \cdot \tau_{dif-sh} (1 - \theta_{dir-dir})}{\pi / 2} + \frac{M_i - E_{dif} \tau_{dif-win} \tau_{dif-sh} (1 - \theta_{dir-dir})}{\pi} \quad (3.18)$$

$$L_{i-gr} = \frac{E_{dif-gr} \cdot \tau_{dif-win} \cdot \tau_{dif-sh} (1 - \theta_{dir-dir})}{\pi / 2} + \frac{M_i - E_{dif} \tau_{dif-win} \cdot \tau_{dif-sh} (1 - \theta_{dir-dir})}{\pi} \quad (3.19)$$

Finally, the total illuminance on a virtual work plane sensor will equal to:

$$E_{wp} = E_{wp-dir} + E_{wp-dif} \quad (3.20)$$

3.4.3 Glare calculation module

Having obtained a detailed luminance and illuminance mapping of the interior gives flexibility in terms of calculating most of the glare indices. An additional input is required, the three-dimensional position of the observer's eye and the respective view direction. The model is able to position the observer on a pre-selected grid of positions on the floor, with any view direction. For the purpose of this study, DGP was selected among the existing glare indices.

$$DGP = 5.87 \times 10^{-5} E_v + 9.18 \times 10^{-2} \log \left(1 + \sum_{i=1}^n \frac{L_{s,i}^2 \cdot \omega_{s,i}}{E_v^{1.87} \cdot P_i^2} \right) + 0.16 \quad (3.21)$$

The location of the observer's eye works as an additional virtual sensor for vertical illuminance, in order to calculate the overall brightness term of DGP. For that reason, a modifiable grid of positions throughout the room is specified. The interior surfaces of the room are then divided into a large number of patches (for this study a grid of 40x40 was used), for which the geometrical details (projected area, solid angle and position index) are pre-calculated for each observer's position, as they remain constant. For the position index

calculation, as described in Chapter 2.2, two different calculation methods are applied, for the patches below the line of sight the method of Iwata and Tocura (1997) is used (Figure 3.27), while for the sources above the line of sight, the classic method of Guth (1966) is applied.

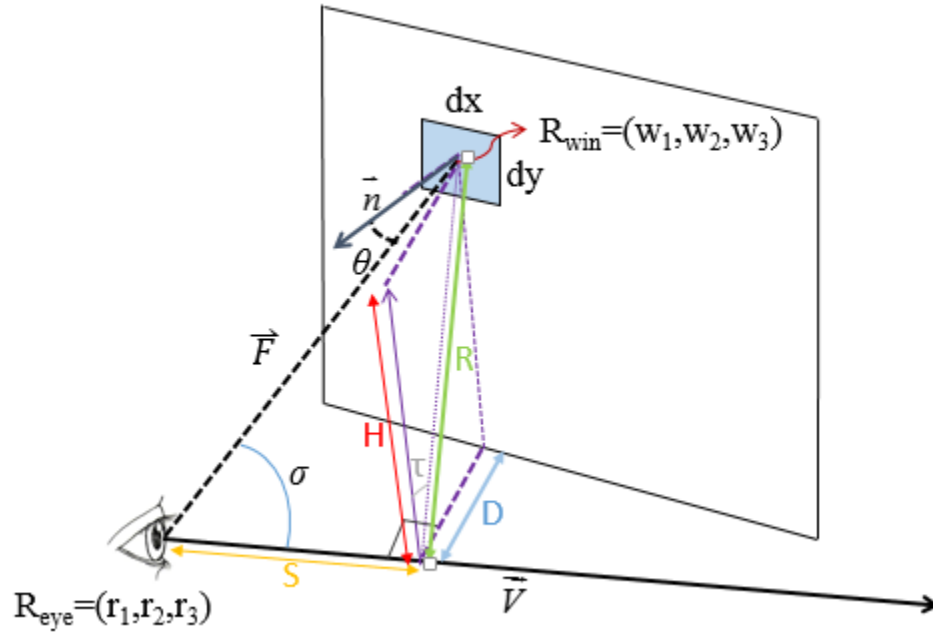


Figure 3.27 Geometry involved in the calculation of position index

Then, for each time step, patches are evaluated by a dual criterion in order to filter which of them act as glare sources. The criteria applied are the following:

- Check if the final luminous exitance of the patch exceeds a threshold (in this study 4 times the average luminance of the work plane in front of the observer (task area equivalent))
- Check if the patch is located within the field of view of the observer. The field of

view is defined as a 3-D cone starting from the eye position and having a half-span of 78°.

The daylighting-glare model calculates the illuminance on the work plane grid and on the eye, for all positions, as well as the luminance of surfaces and the DGP values for any sky conditions and shading positions. Dynamic operation of façade elements (shading control or glazing properties) is automatically taken into account for every time step.

3.4.4 Model Validation

The daylighting model has been validated with full-scale experiments in the test offices of Bowen Labs (for static and dynamic shading controls). The validation can be obtained by overriding the incident illuminance values from the model with the ones measured by the illuminance sensors on the interior of the façade. In order to have a detailed image of the direct and diffuse portions, the readings of the solar pyranometer are used, for a selected period of hours/days. Then, the values of the virtual sensor on the work plane or at the observer's eye are compared with the ones obtained by the illuminance sensors in the labs for the same positions.

Representative daylighting and DGP model validation results for cases with increased complexity –mixed sky conditions and dynamic shading controls employed in the test offices– are presented in Fig. 3.28-3.30, with comparison between camera-measured values (processed with Labsoft) and simulated values for the same exterior conditions (MSE = 0.03). Additional model validation results can be found in Chan et al. (2014).

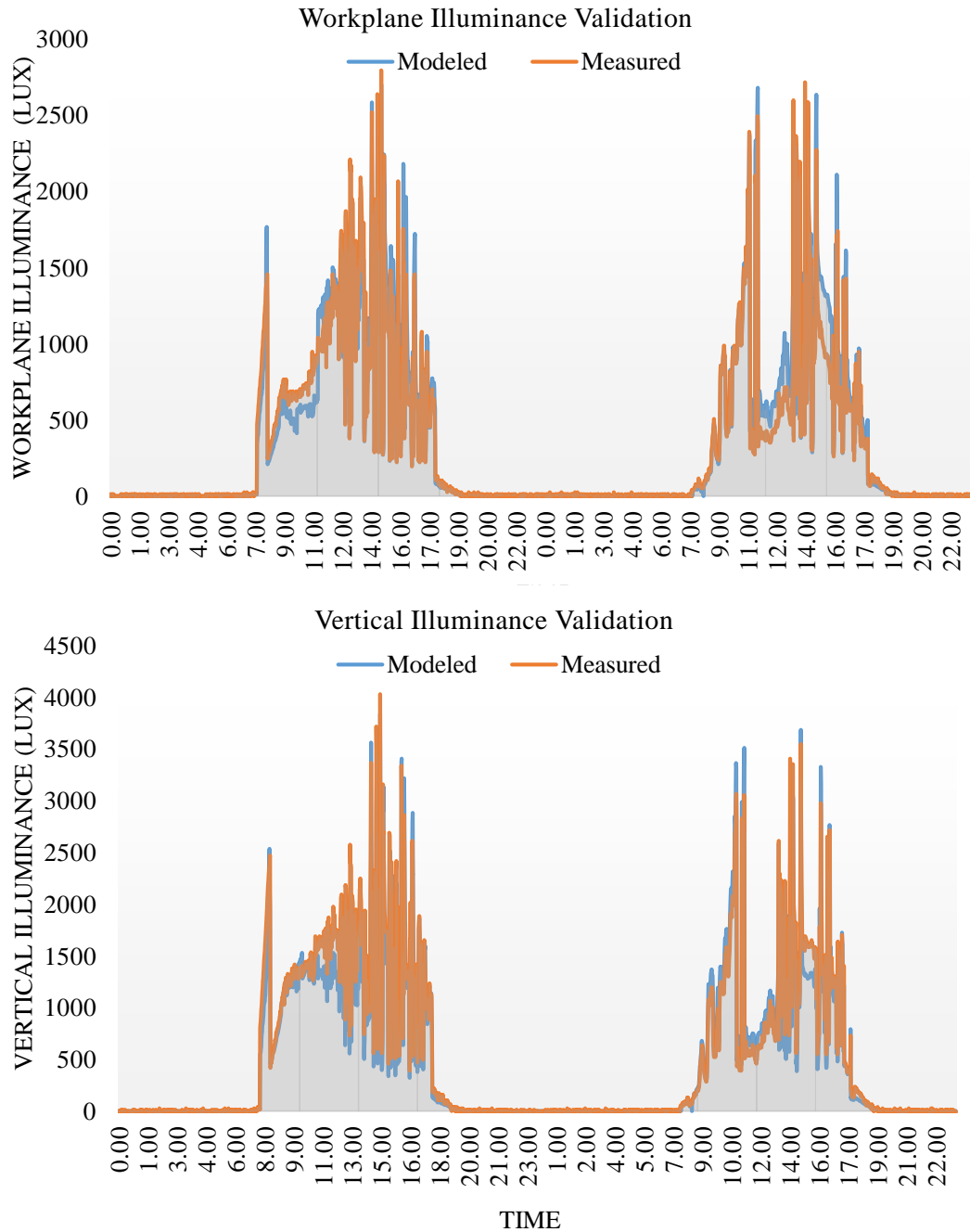


Figure 3.28 Validation for work plane illuminance (top) and vertical illuminance (bottom) for the advanced shading control based on the effective illuminance (presented in Chapter 3.2)

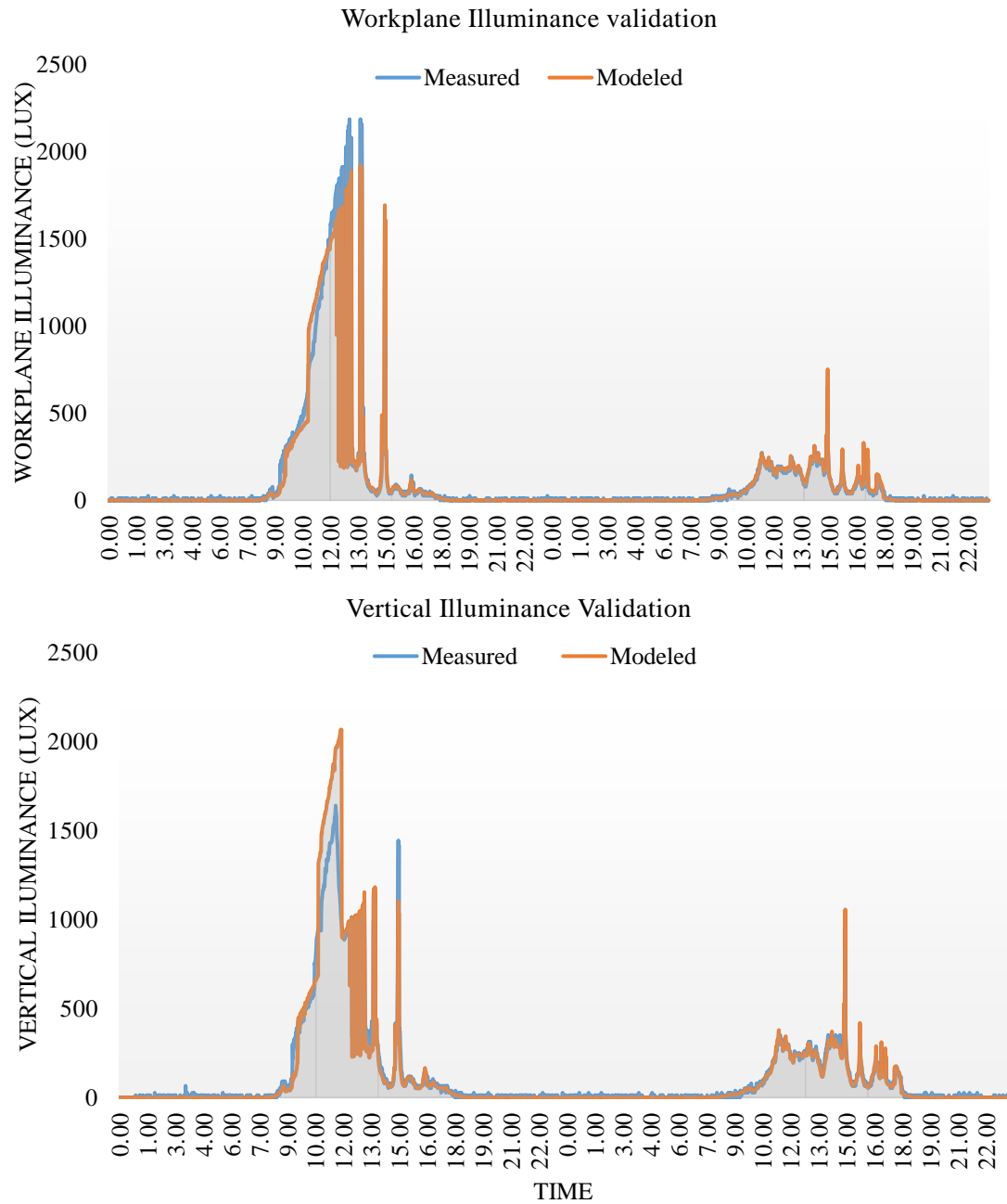


Figure 3.29 Validation for work plane illuminance (top) and vertical illuminance (bottom) for a sunny and a cloudy day (closed shades)

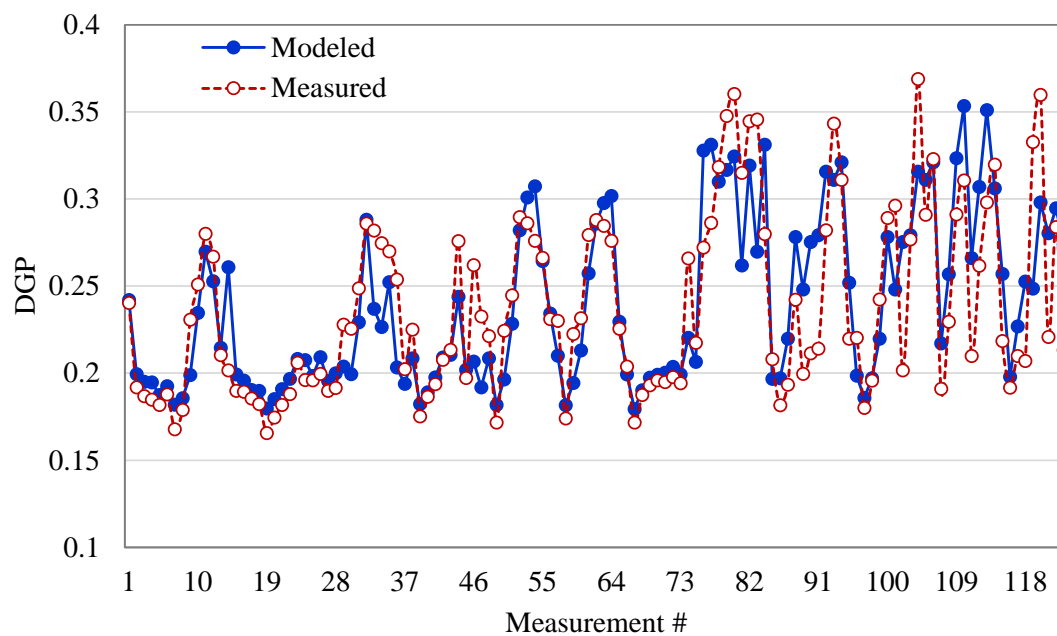


Figure 3.30 DGP model validation –several measurements with mixed sky conditions and shading controls

CHAPTER 4. EXPERIMENTAL AND SIMULATION ANALYSIS OF DAYLIGHT GLARE PROBABILITY IN OFFICES WITH DYNAMIC WINDOW SHADES

4.1 Introduction

This chapter presents new experimental and modeling results for analysis of DGP in spaces with closed and controlled roller shades. Full-scale measurements with an HDR luminance acquisition were conducted in test office spaces under variable sky conditions and shading control operations. The measured data were used to investigate the relative impact of contrast and overall brightness terms, and to derive potential correlations of DGP with design parameters such as indoor illuminances. Strong correlations of indoor illuminances with discomfort predictions are also suggested by Karssen et al. (2015). The applicability of DGP and DGPs in the case of roller shades with openness and partially open windows is discussed. An advanced daylighting model, coupled with a glare prediction model, is validated and used to provide insights on the efficiency of control algorithms and potential simplified guidelines with regards to daylight glare.

4.2 Experimental results of DGP under variable sky conditions

Having a fully equipped twin-office facility allowed a detailed investigation of DGP measurements and illuminance conditions. Experimental data were used to develop

correlations between indoor illuminances and DGP parameters, for different shading control strategies, sky conditions and glazing products. The effects of the contrast term and vertical illuminance are discussed in this context. Later, validated models are utilized to assist in real time model-based glare and luminance mapping, for different façade controls.

The measurements were obtained in the Façade Engineering Labs of Purdue University in Bowen Laboratories (see details in Chapter 3.1.1) during Fall 2013 and Spring 2014. The sun was high in the sky, therefore no cases of the sun included in the visual field were measured. For the purpose of this study, the spaces were unoccupied. For the luminance acquisition, Methodology A was used (Chapter 3.3.1), having the LMK system camera looking toward the window in the center of the room and from a distance of 2.20m from the window (Fig. 4.1)



Figure 4.1 Experimental facility exterior (left), interior (center) and HDR camera placement (right)

4.2.1 Correlations between DGP and work plane illuminance

Deriving a correlation between a design value such as the work plane illuminance and the daylight glare probability would be an interesting opportunity for creating potential guidelines. Representative experimental results for both glazing systems are shown in Fig. 4.2, for the work plane illuminance at the measurement (occupant) location at 2.20m from

the window. The double clear glass results in higher illuminance and DGP values as expected.

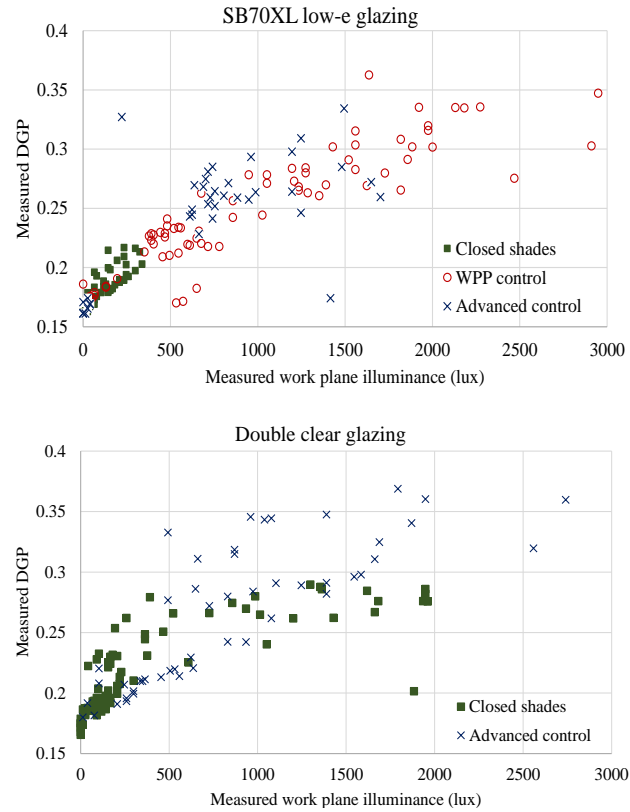


Figure 4.2 Experimental correlation of DGP with work plane illuminance for the two glazing systems and different shading controls

The advanced shading control works well in limiting illuminance values below 2000 lux for almost all cases. Work plane illuminance is related to DGP, however the correlation is not strong. This is expected for several reasons, the most important being the direct sunlight penetrating the space and altering the distribution of work plane illuminance with different controls –in several cases, parts of the window are identified as glare sources and DGP can vary depending on window luminance and contrast between the unshaded portion and other surfaces in the field of view. The fabrics have a direct-direct component

($\tau_{bb} = 4.2\%$) that affects interior illuminance (Chan et al., 2014) and creates significant dispersion of results even for closed shades, especially in early winter for the clear glass case. Except for perfectly diffuse materials, there is no reliable correlation between DGP and work plane illuminance.

4.2.2 DGP-vertical illuminance correlations and contrast influence discussion

As DGP strongly depends on vertical illuminance on the eye (E_v), the correlation is stronger for all the cases of shading controls (Fig. 4.3), but the relationship is still not linear for the reasons mentioned above. For the low-e glass, a good correlation coefficient was obtained. Projections through the unshaded window sections, variable luminance/contrast and especially direct sunlight through the shades would create non-linear trends and significantly weaker correlations. However, as the measurements were obtained in non-winter time, the sun was high and all these effects were negligible. Observing the DGP equation (Eq. 4.1) the index is influenced by the first term, solely a function of the E_v (Eq. 4.2). That was the trigger for introducing DGPs (Eq. 4.4), the simplified glare probability measure (Wienold, 2007). However, its relative weight to the equation remains unclear, especially in terms of whether and when it can be possible for the second term (related to the apparent contrast, Eq. 4.3) to become significant or even outweigh the vertical illuminance term, leading to differences of up to 20% compared to DGP (Kleindienst and Andersen, 2009). This investigation involves many parameters, such as orientation, time of year for the measurements (solar path), ground reflectance, as well as window and shading properties and controls. The influence of contrast for instances with the sun facing the observer can be much stronger, while the perceived contrast when facing a partially shaded window can be significantly higher for dark-colored fabrics if the openness factor

is relatively small. In addition, orientations or climates exposed to lower vertical illuminance values could be more directly influenced by contrast with regards to glare, since the first term is reduced and E_v appears in the denominator of the contrast term.

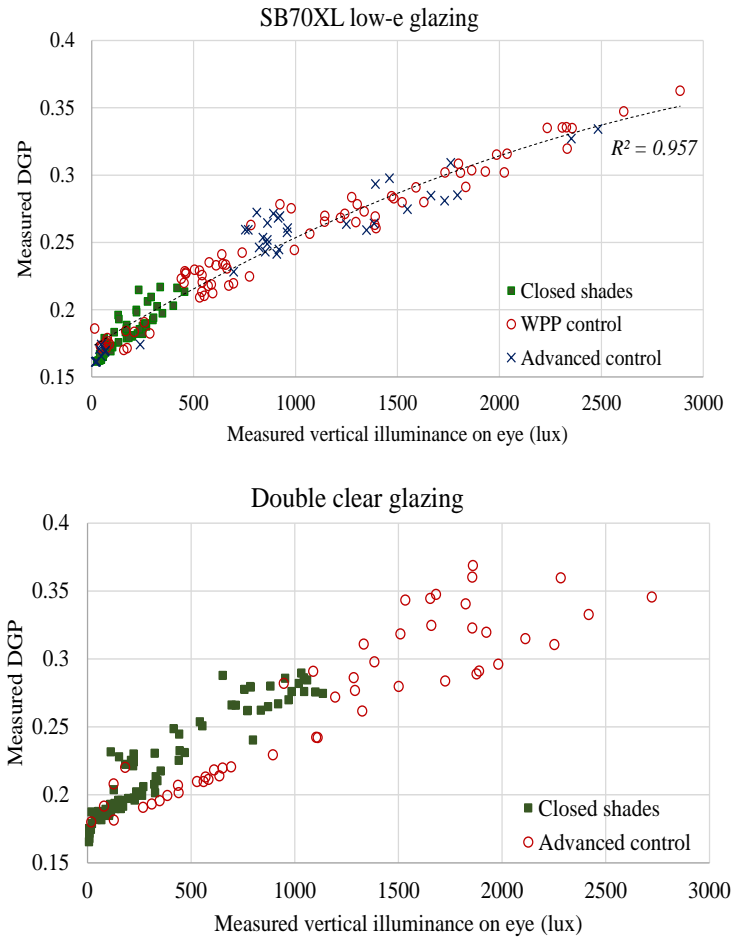


Figure 4.3 Experimental correlation of DGP with vertical illuminance for the two glazing systems and different shading control

$$DGP = 5.87 \times 10^{-5} E_v + 9.18 \times 10^{-2} \log\left(1 + \sum_i \frac{L_{s,i}^2 \cdot \omega_i}{E_v^{1.87} \cdot P_i^2}\right) + 0.16 \quad (4.1)$$

$$ET = 5.87 \times 10^{-5} E_v \quad (4.2)$$

$$CT = 9.18 \times 10^{-2} \cdot \log\left(1 + \sum_i \frac{L_{s,i}^2 \cdot \omega_i}{E_v^{1.87} \cdot P_i^2}\right) \quad (4.3)$$

$$DGPs = 6.22 \times 10^{-5} E_v + 0.184 \quad (4.4)$$

The experimental setting in this study involved a relatively dark (grey) fabric, and due to the south orientation, high values of vertical illuminance were usually observed. In addition, measurements were taken with the sun not visible from the measurement position, therefore the influence of contrast was low, leading to a relatively strong correlation of DGPs with DGP –however, sunlit projections in the space were always present with the two shading controls. Fig. 4.4 shows the results for the case of the low-e glazing using different shading controls.

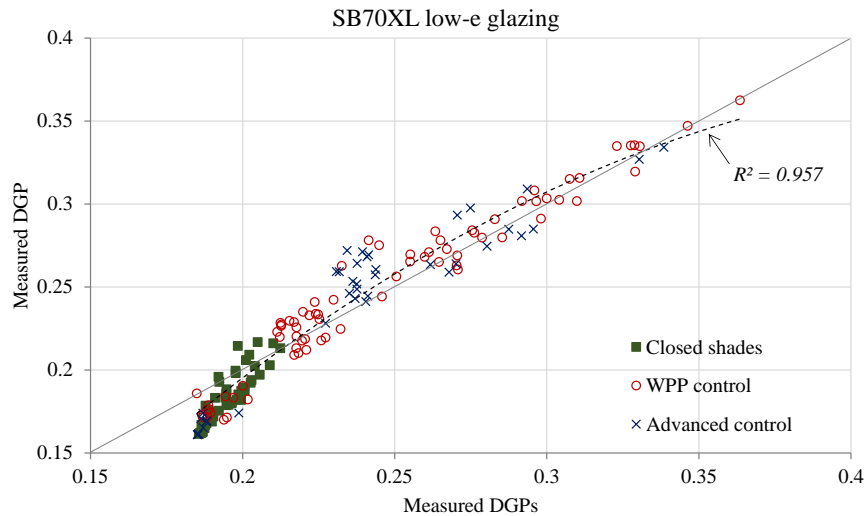


Figure 4.4 Relationship between DGP and DGPs from experimental measurements using different shading control methods

Following the trend of Fig. 4.3, a non-linear correlation provides better results. The ability of using only vertical illuminance as a glare input is useful, especially for real-time glare-based shading controls using a simple sensor input. The data in Fig. 4.4 shows that

sunlight reflections and projections (due to partially unshaded windows when shades are controlled) in the space are not a serious problem for using DGPs (or E_v) to predict glare probability, as long as the surfaces are not highly specular.

4.2.3 Experimental assessment of shading control efficiency in terms of glare

In order to investigate the shading controls efficiency in terms of minimizing daylight glare, a real-time, measurement-aided simulation methodology was followed. The hybrid ray – tracing and radiosity model presented in Chapter 3.4 was utilized for that purpose, using as inputs real measured data obtained by the transmitted illuminance sensors placed on the interior of the glazing system and the shade positions logging from the automatic shading system. Both test offices were used for comparative experiments, one running with the WPP shading control and the other with the Advanced shading control under the same outside conditions for several days. Fig. 4.5 shows the measured data and the shading logs for three selected representative successive days, the first having mixed sky conditions, the second being sunny and the third being cloudy, to cover all cases.

The outputs of the model include detailed illuminance and DGP mapping of the interior, while sample images were taken with the camera for validation purposes. As the measurements took place in March, the sun was never visible from the observer's position, resulting in the absence of high glare instances caused and potentially incorrect DGP values. The variation of measured DGP as a function of time along with measured shade positions is shown in Fig. 4.6 for both offices. Work plane protection control (WPP) cannot always prevent glare since shades open more, causing E_v to reach high values. It can be apparent

by observing Figure 4.6 that the advanced shading control performs better and can protect from glare for most of the daytime.

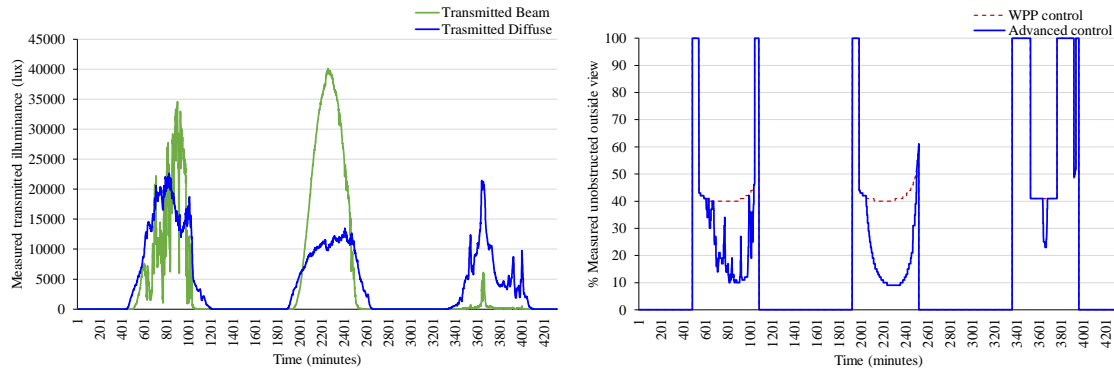


Figure 4.5 Transmitted direct and diffuse illuminance during the comparative experiments (left) – Shade position log for two controls (right)

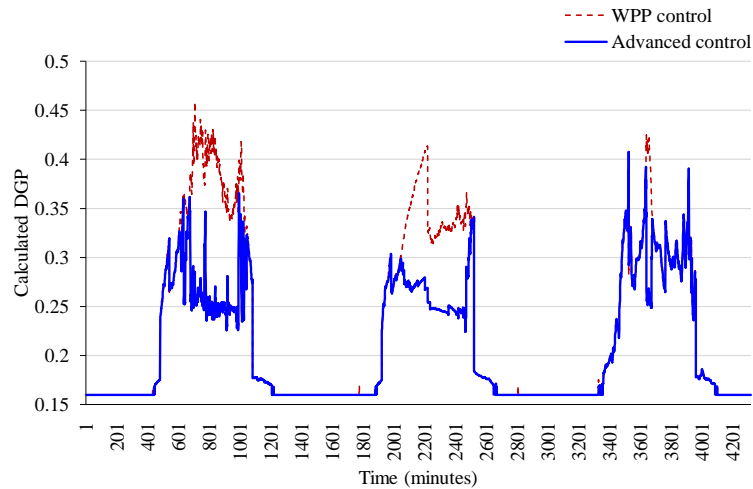


Figure 4.6 Calculated DGP fluctuation for the two office spaces

Higher values during early morning and late afternoon (due to the shading operation in order to maximize daylight) are not of concern because the office is unoccupied during these times. An important result is observed in the third (cloudy) day. The shades open to

allow enough diffuse daylight into the space (work plane illuminances up to 1500 lux in this case), but this is enough to cause “noticeable” glare –note that although the day is cloudy, it is not heavily overcast.

4.3 Generalization of results – DGP simulation for dynamic shading

As the experiments described in 4.2 were mostly performed during Spring and Fall, without the sun present within the visual field, in order to generalize the results simulations were needed. In that scope, the simulation model described in Chapter 3.4 was used. The objective was to investigate the influence of the respective terms of the DGP equation, to find correlations with other easily measurable lighting metrics, to evaluate the applicability of DGPs in special cases and investigate the efficiency of shading controls towards glare. The settings, geometry, materials and location used in the simulations match the experimental test offices in Bowen Labs at Purdue University (Table 4.1):

Table 4.1 Simulation inputs used

Space type	Private office
Location	West Lafayette, Indiana
Glazing type(s)	SB70XL (low-e) plus double clear for experiments
Window-to-wall ratio	60%
Shading properties	Total visible transmittance: 5% Beam-beam transmittance: 4.2% (zero for perfectly diffuse fabric)
Facade orientation	South
Virtual Occupant Position	2.2 m from facade, facing windows
Shading controls	Closed shades WPP (buffer = 1 m from window) Advanced control
Glare sources identification criterion	Sources having 4 times the average work plane luminance

4.3.1 Annual correlations between DGP and work plane illuminance

For the relationship between DGP and work plane illuminance (Fig. 4.7), there is a similar scattering as in the experimental measurements of Fig. 4.2; however three trends are clearly noticeable for each shading control.

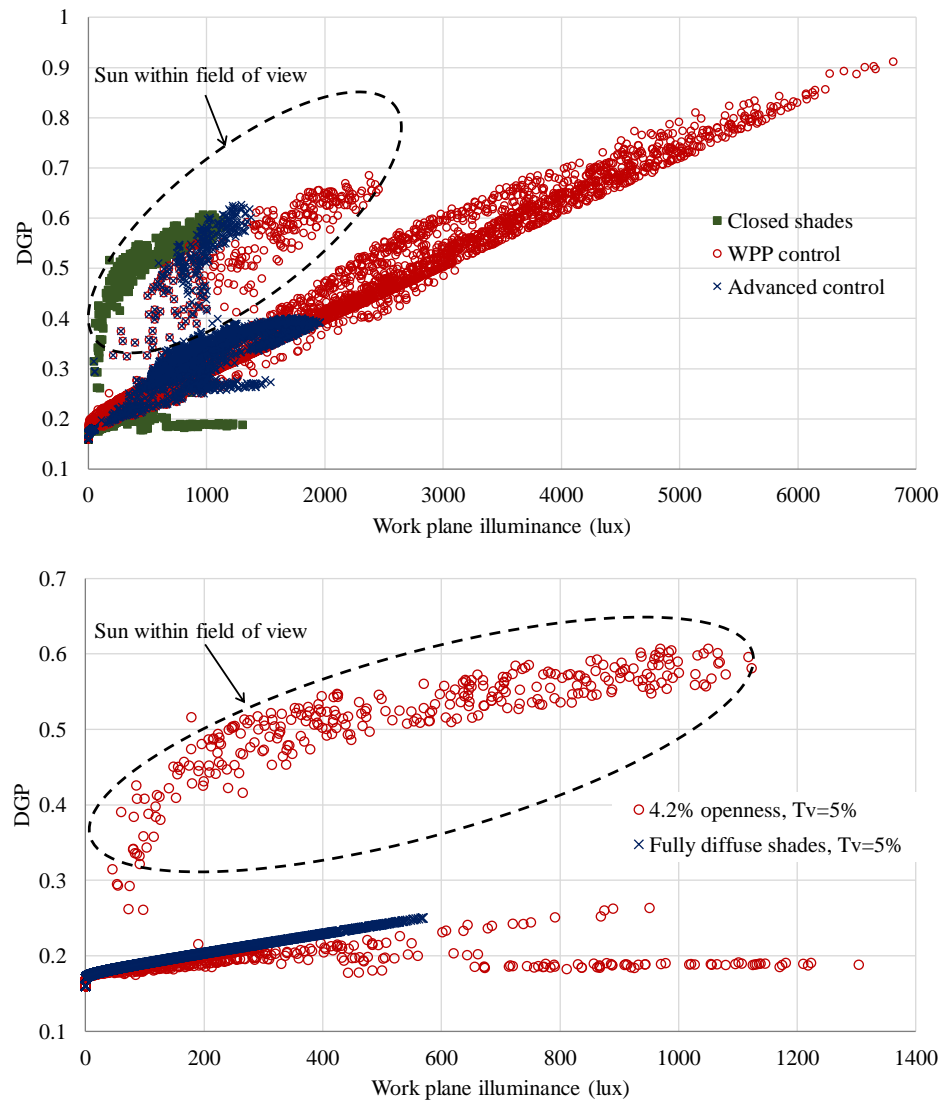


Figure 4.7 Top: Annual DGP-work plane illuminance correlations for the three shading controls – Bottom: Annual DGP-work plane illuminance correlations (closed shades) for the studied shade (4.2% openness, 5% total normal visible transmittance) and a fully diffuse fabric (no beam-beam component)

The upper trend is reflecting the influence of the sun's luminance on the contrast term during winter time. In this case the openness of the fabric leads to excessive glare for all shading controls (including closed shades) and as mentioned before DGP values might be overestimating actual glare. The two lower trends are a result of the modeling approach: the model splits the window into a shaded and an unshaded part. This consideration leads to cases where, due to slight differences in the task area luminance, the entire shaded (or unshaded) area can be either identified as a glare source or not, increasing contrast-induced glare due to the large size of the window. Similar trends can be seen in correlations between DGP and other daylight metrics. In the figure, the difference between the WPP control and the rest cases is apparent, as due to the shades remaining open for a significant amount of time in the summer, the illuminance and DGP levels reach very high values.

Having a flexible dynamic model allows investigation of the assumption that direct sunlight through shades prevents stronger correlations between DGP and work plane illuminance. In that scope, a fully diffuse theoretical shade with the same total visible transmittance (5%) was also modeled. This fabric has no beam-beam component and is equivalent to a translucent material. The results of Fig. 4.7 (bottom) for closed shades show that, in this case, a linear correlation is achieved. This observation has interesting applications for cases of translucent windows or shades with very small openness, since a design parameter like work plane illuminance can be associated with a constraint as daylight glare for different seating positions. In this way, it would be possible to introduce rules of thumb for positioning occupants in spaces equipped with such devices, to minimize the risk of glare –since the sun will not be visible. Although the view quality would be low and this is often not the preferred solution, it could be a design solution for upper window

sections and seating positions/locations preventing low sun view through the lower window section. Also, it can be utilized in special spaces where view to the outside is not of the essence (operating rooms etc.)

4.3.2 Annual DGP-vertical illuminance correlations, DGPs applicability and contrast discussion

The correlation between DGP and E_v , shows some similar behavior, having the same three trends (Figure 4.8 -top).

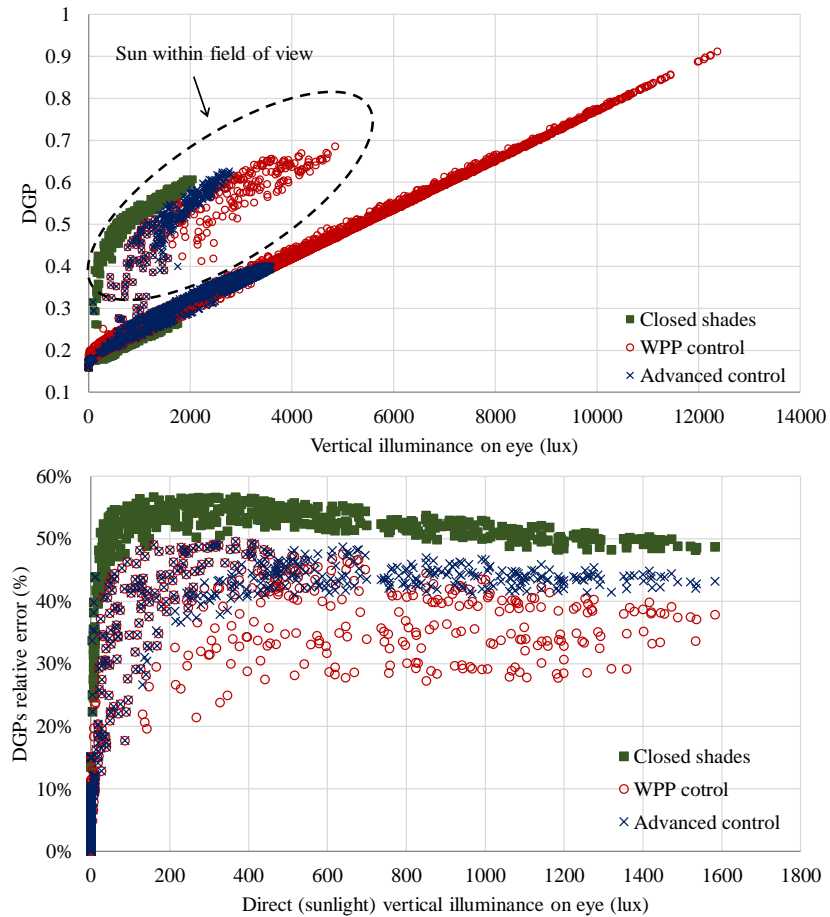


Figure 4.8 Annual DGP-vertical illuminance correlations for the three shading controls (top) –Annual DGPs relative error as a function of direct vertical illuminance on the eye (bottom)

However, the scattering in the non-winter trends is less apparent, reflecting the strong dependence of DGP on E_v . The reason for deviating from a stronger correlation is mainly the sun-facing instances and, to a lesser extent, the contrast effect of the open window portions for the controlled cases.

As a linear function of vertical illuminance, DGPs follows the same trend. Wienold (2007) has already stated the non-applicability of DGPs when specular reflection or direct light hits the eye. Fig. 4.8 (bottom) confirms this claim, showing the DGPs relative error (Eq. 4.5) for the entire year as a function of direct light on the eye of the observer. The error is significant for any amount of sunlight on the eye, independent of shading control type.

$$e = \left| \frac{\text{DGPs} - \text{DGP}}{\text{DGP}} \right| \quad (4.5)$$

In cases without transmitted sunlight on the eye, DGP and vertical illuminance seem to relate well. This includes all instances with direct sunlight falling on interior surfaces and on the work plane, when shades are controlled (or partially open). It is therefore useful to further investigate these cases and shed some light on the applicability of DGPs when sunlit projections are present in the field of view, which is still an area under discussion.

Fig. 4.9 presents the filtered results of DGPs approximation with controlled shades (all cases with sunlight falling on various non-specular interior surfaces and on the work plane but not on the eye) for the entire year, and a comparison between the two shading controls. WPP control allows for much higher DGP values, not shown in Fig. 4.9 for a

straight comparison between the two controls at the important lower DGP range. Overall, a good correlation is observed which proves that DGPs can be used to approximate daylight glare even when sunlight is present in the space (but not on the occupant) –extending Wienold’s findings (2009) for cases with projected light. It is therefore possible to utilize a relatively simple metric, like vertical illuminance, for real-time, glare-based shading control, provided that the sun will not be visible from the occupant position –or that the fabric transmittance is very low, as discussed before. For closed shades and for perfectly diffuse fabrics/materials, a strong linear correlation between DGP and vertical illuminance/DGPs is achieved throughout the year, as the contrast effects of the sun are not present.

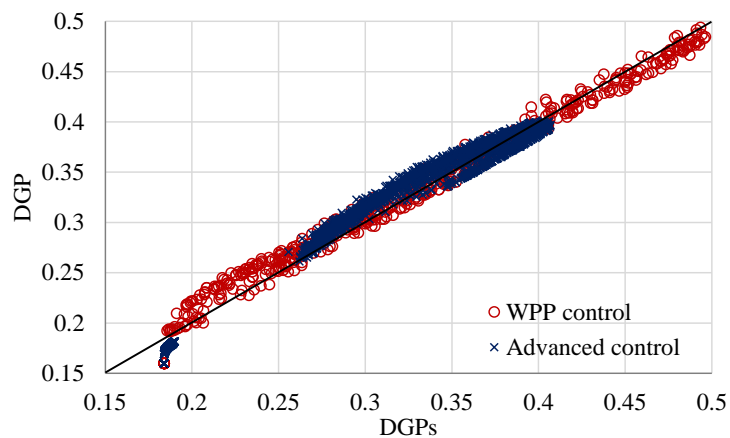


Figure 4.9 Annual correlation between DGP and DGPs for all cases with sunlight falling on various interior surfaces and on the work plane (but not on the occupant) with the two shading controls.

4.3.3 Daylight Glare Probability with the sun within the field of view

Since the annual analysis performed in the simulations includes winter months, when the sun is low in the sky and visible from the occupant position through the shading fabric, it is important to discuss such cases separately.

Unlike glare from non-direct light, which is witnessed mainly due to high E_v values and contrast variation within the visual field (usually between the shaded and unshaded part of the window, or due to the coexistence of dark interior and bright exterior), high DGP values due to sunlight cannot be avoided, even for small amounts of E_v though tight shading fabrics. The reason is the contrast term of DGP, which becomes extremely high when the luminance of the sun is taken into account. In the case of roller shades, using the detailed angular direct transmission through the fabric as suggested by Kotey (2009), and assuming that the sun to be a sphere, therefore its solid angle being constant throughout the solar path, the luminance of the sun observed by the occupant can be approximated by:

$$L_{\text{sun}} = \frac{E_{bb}}{\cos\theta \cdot \omega_{\text{sun}}} \quad (4.6)$$

, where E_{bb} is the beam-to-beam illuminance transmitted through the shades (normalized angularly), θ is the incident angle of the sun to the eye and ω_{sun} is the solid angle of the sun to the observer's eye. As E_{bb} takes into account the openness of the fabric, the perceived solid angle of the sun is a "homogenous" surface of uniform luminance. However, this results to luminances in the order of 10^6 - 10^7 cd/m². Due to the form of the DGP contrast term (second term of the equation reflecting the luminance of the glare sources), these values get squared, resulting to high values of contrast-dominated DGP even for the relatively small sun disc's solid angle, for any E_v value. As a result, DGP values with small E_v due to transmitted sunlight are much higher than those during sunny days with high E_v but with the sun outside the direct field of view (sun higher in the sky). This is illustrated in the modeling results of Fig. 4.10, where all DGP terms (and total DGP values) are plotted hourly during a sunny day in January and a sunny day in June (both with closed shades).

The contrast term alone can reach values higher than 0.3 when small amounts of sunlight are transmitted through the fabric, therefore perceived or even intolerable discomfort glare ($DGP=0.46$) can theoretically occur with very low vertical illuminance on the eye.

This analysis brings two discussion points for further research:

1. It is common experience that no significant glare issues are observed for shading fabrics of 1% openness, while DGP can theoretically reach intolerable levels due to extremely high luminance of the sun considered in the equation. The assumption of a homogenous surface with uniform luminance for the sun disc might not be accurate enough for approximating the luminance of the sun, or the actual ability of the eye to perceive light through low openness fabrics is different.
2. DGP was not developed under direct sun-facing conditions, so its applicability is still unclear and controversial for these cases. Wienold (2009) uses DGP as a baseline to investigate the DGPs applicability in the case of 1% openness fabrics, while Van den Wymelenberg (2013) states that DGP in cases with direct light hitting the work plane can rapidly increase task area luminance leading to misidentifying part of the glare sources. Jakubiec and Reinhart (2012) state that DGP can handle direct light on the work plane (but not necessarily on the eye), and in their next study (2013) they conclude that more than one metric is required for quantifying glare if direct sunlight is present.

Overall, every day experience in working with roller shades makes us believe that sunlight on the eye will cause glare, but as the effect of direct sunlight through shading fabrics on glare has not yet been studied and current DGP models might not be adequate, there might be a need for a correction for these cases, similar to the low-light correction

Wienold suggested (2012). More research is needed in this direction and the experimental facility of the private offices may be used in that scope.

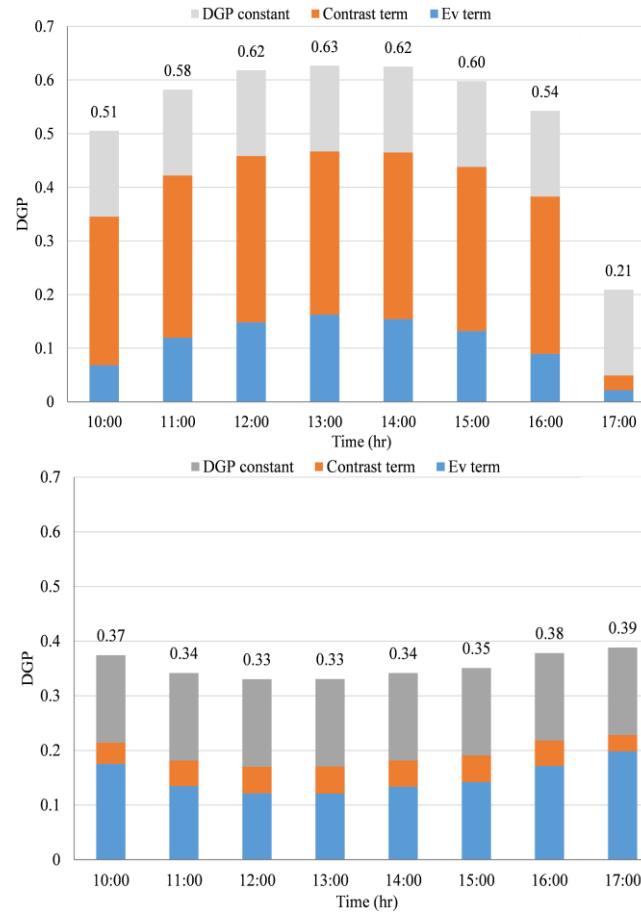


Figure 4.10 Comparison between DGP terms and overall DGP value when the sun is within (top) and outside (bottom) the field of view

4.3.4 Annual evaluation of shading control efficiency towards glare

Finally, the simulation model was used to evaluate the annual glare control performance of the two shading controls and the closed baseline case. The modeling parameters are shown in Table 4.1. Fig. 4.11 presents temporal vertical on eye illuminance and DGP graphs for all shading controls throughout the year.

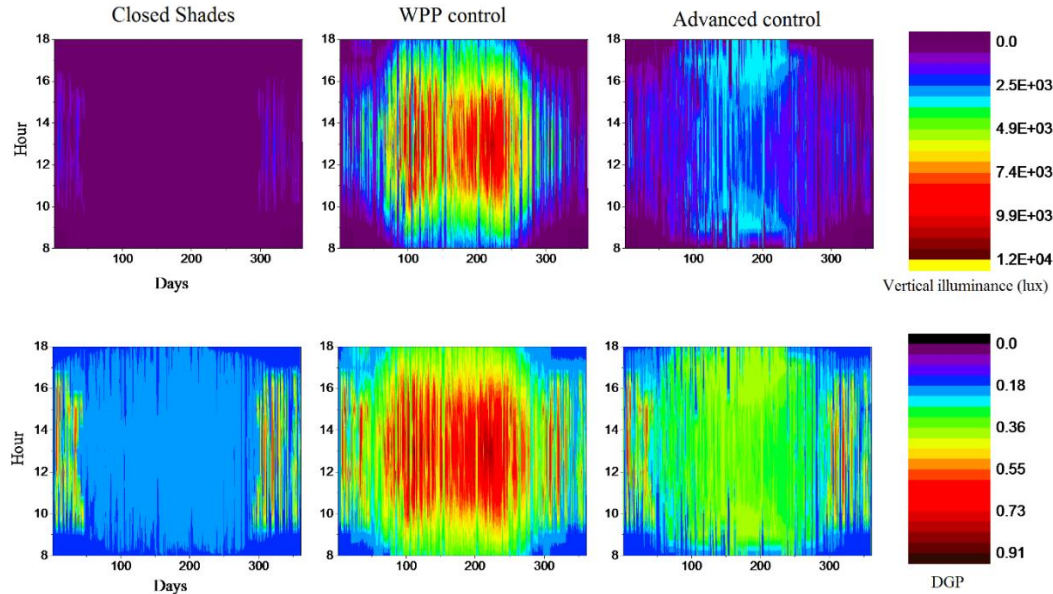


Figure 4.11 Vertical on eye illuminance annual temporal graphs (top) and DGP annual temporal graphs (bottom) with the three shading controls for the selected shade (4.2% openness, 5% total normal visible transmittance)

Higher DGP values are observed during winter months. This is again due to the apparent luminance of the sun seen through the fabric openness even when shades are fully closed. Work plane protection control proves to be insufficient for glare protection, despite the large unobstructed views it can offer when the sun is higher in the sky, with the main reason being the high values of vertical illuminance entering the space (at times over 12000 lux). The advanced shading control achieves satisfactory performance in reducing glare, keeping DGP below 0.35 for most of the time and always below the “intolerable” limit of 0.45, excluding a few instances during winter by maintaining total vertical illuminance below 4000 lux. For the studied position, the direct light on the work plane exceeds 1000 lux for only one hour during the year, while it achieves a satisfactory spatial daylight autonomy ($sDA_{500,50}=0.59$). These results show that the advanced shading control strategy is efficient towards both energy and comfort. Future studies will include integrated

assessment of optimal shading properties and control, considering outside view, visual comfort and energy use.

Assuming that DGP is valid for cases with direct light hitting the eye, leads to the conclusion that, for high openness fabrics, it is impossible to avoid glare when the sun is within the field of view of the observer -therefore very low openness fabrics or venetian blinds should be preferred in such cases. However, as DGP applicability in such cases is still a topic under investigation, further analysis and occupant studies are needed, as everyday experience shows that there are no visual discomfort problems for fabrics of low openness ($< 2\%$), despite high predicted DGP values. Existing guidelines (IESNA, 2012) consider direct sunlight on the work plane (and its spatial frequency) to be a critical metric towards comfort; however, limitations in transmitted direct illuminance do not consider shades or other operable devices.

4.4 Discussion

The detailed simulation study generalized the findings of the experimental study of Chapter 4.2 and managed to (i) identify correlations of DGP with measured and calculated illuminance metrics; (ii) investigate the behavior and applicability of DGP and DGPs for shading fabrics with common openness; (iii) analyze DGP and DGPs ability to capture glare for cases with and without sunlight on the occupant (transmitted through roller shades) and within the field of view (various projections in the space when the shades are controlled) and (iv) study the ability of shading control algorithms to reduce potential glare from daylight. In that scope, some interesting findings were that:

- DGP can potentially predict overestimated results for glare perception when sunlight falls on the occupant, even through shading fabrics of very small openness. Correlations with work plane or vertical illuminance are not useful in this case. Whenever the sun is within the field of view, the luminance term (and DGP) becomes significantly high even if vertical illuminance is minimal. Although the glare trend is reasonable, further research with human subjects is needed for potential modification of the DGP equation coefficients when the observer is facing the sun. Otherwise, more than one metric is needed as suggested by Jakubiec and Reinhart (2013) when sunlight is present. DGPs cannot be used to approximate glare probability even when the slightest amount of sunlight falls on the occupant (directly or transmitted through fabrics of any openness).
- For cases without the sun in the field of view, DGP and work plane illuminance are not well correlated, except for very low openness factors or perfectly diffuse materials. For locations with higher sun angles, facades with translucent panels in the upper window sections are suitable for using these correlations to recommend design guidelines for glare protection.
- For cases without the sun in the field of view, DGP and vertical illuminance are well correlated, even when sunlight falls on interior surfaces (when shades are partially open or controlled). This allows DGPs to be used for all instances except when sunlight directly hits the occupant.
- For shading control strategies that include higher unshaded window fractions, DGP is mostly dominated by the vertical illuminance term, while for controls with more closed positions the contrast term becomes significant, including closed shades, as the

openness of the fabric allows small amount of direct light penetration. For the latter cases of significant contrast, the contrast influence starts to fade when vertical illuminance exceeds a certain value.

- The advanced shading control presented and demonstrated in this study is able to protect from glare for most of the time, while maintaining satisfactory interior illuminance levels. Work plane protection strategies cannot prevent glare, despite maximizing daylight utilization.
- The key factor towards achieving visual comfort appears to be successful control of vertical illuminance, as this is a parameter that may dramatically decrease glare without significantly affecting daylight availability. Model-based controls that include glare evaluation are possible, however dynamic roller shades are a complex case, even compared to venetian blinds –which can redirect daylight, eliminating obvious glare problems.

Integrated simulation and measurement methodologies are useful as they allow detailed DGP mapping using simple measured inputs. In this way, it is possible to perform experiments in private and open plan offices (as well as parametric and optimization studies) without creating obstructions to the subjects, while maintaining a realistic working environment and avoiding expensive and time consuming processes.

Shading design and control strategies for daylit offices need to be carefully studied using annual results of validated detailed models. To completely avoid glare at all times with roller shades, very low openness factors (less than 2%) or fully diffuse materials should be theoretically used, assuming that DGP is an accurate predictor of discomfort for sun facing instances, which still remains unclear. The real challenge is to balance visual comfort,

outdoor view and energy use, therefore future efforts will be made towards this direction, along with more studies with human subjects.

4.5 Recommendations for fabric selection to avoid daylight glare

As mentioned in section 4.3.3, one of the challenges associated with predicting visual discomfort in the case of shading fabrics is the openness factor, responsible for the direct portion of light penetrating the room, and for the direct visibility of the solar corona. The extreme luminance values of the latter create very high DGP values, which could be unsuitable for predicting actual discomfort levels. Triggered by this inconsistency, and to provide fabric selection recommendations aimed to mitigate daylight glare, an alternative discomfort criterion has been suggested;

The annual discomfort frequency (ADF) is defined as the percentage of working hours for which there are conditions creating discomfort, in terms of two factors:

- The direct vertical on eye illuminance being over 1000 lux, a modification of IES-LM-83-12 (IESNA, 2012)
- The total vertical on eye illuminance being over 2760 lux, a value associated with the 0.35 discomfort limit of DGPs (Wienold, 2007).

Although the above factors, especially the one associated with direct light still need to be validated with human subjects, the ADF has the potential to be a more reliable tool to assess discomfort in cases of facing the sun. For the fabric selection recommendations, two levels of strictness for the ADF were applied: a strict set of recommendations for the ADF being 0%, and a less strict one for ADF being 5%. These can be seen on Tables 4.2 and 4.3

respectively. The direct vertical illuminance factor is used to decide the acceptable ranges for the openness factor of fabrics, while both are used for the determination of the acceptable range of visible transmittance.

Table 4.2: Fabric recommendations for 0% annual discomfort frequency (Chan et al., 2015)

Recommended maximum values of shade OF (and VT in parenthesis) for 0% annual visual discomfort frequency.

Buffer zone	Orientation	New York Glazing visible transmittance			Phoenix Glazing visible transmittance		
		0.65	0.5	0.35	0.65	0.5	0.35
0.91 m	S	2% (5%)	3% (7%)	4% (9%)	2% (5%)	3% (6%)	4% (6%)
	SW	2% (5%)	2% (6%)	4% (8%)	2% (4%)	2% (6%)	3% (8%)
	W	2% (5%)	3% (7%)	4% (9%)	2% (5%)	2% (6%)	4% (7%)
	NW	3% (7%)	5% (9%)	7% (11%)	3% (6%)	4% (8%)	6% (10%)
	N	–	–	–	–	–	–
2.74 m	S	2% (9%)	3% (10%)	4% (13%)	3% (9%)	4% (12%)	6% (15%)
	SW	2% (7%)	2% (10%)	4% (12%)	2% (7%)	2% (9%)	3% (12%)
	W	2% (9%)	3% (10%)	4% (13%)	2% (8%)	2% (10%)	4% (12%)
	NW	3% (12%)	5% (14%)	7% (17%)	3% (10%)	4% (12%)	6% (15%)
	N	–	–	–	–	–	–

Table 4.3: Fabric recommendations for 5% annual discomfort frequency (Chan et al., 2015)

Recommended maximum values of shade OF (and VT in parenthesis) for 5% annual visual discomfort frequency.

Buffer zone	Orientation	New York Glazing visible transmittance			Phoenix Glazing visible transmittance		
		0.65	0.5	0.35	0.65	0.5	0.35
0.91 m	S	4% (7%)	6% (8%)	8% (10%)	3% (6%)	4% (8%)	6% (9%)
	SW	4% (7%)	5% (8%)	7% (10%)	3% (6%)	4% (7%)	5% (9%)
	W	4% (7%)	5% (8%)	8% (10%)	3% (6%)	4% (7%)	5% (9%)
	NW	13% (13%)	15% (15%)	16% (16%)	8% (10%)	10% (11%)	13% (13%)
	N	–	–	–	–	–	–
2.74 m	S	7% (14%)	10% (16%)	14% (19%)	12% (12%)	15% (15%)	18% (18%)
	SW	4% (12%)	6% (14%)	9% (16%)	3% (10%)	4% (12%)	6% (14%)
	W	5% (12%)	6% (15%)	9% (17%)	3% (9%)	4% (11%)	5% (15%)
	NW	–	–	–	17% (17%)	–	–
	N	–	–	–	–	–	–

One of the goals of this thesis is to validate if this alternative discomfort criterion is indeed applicable through human subjects research. This goal is addressed by Chapter 6.

CHAPTER 5. VISUAL COMFORT EVALUATIONS WITH HUMAN SUBJECTS

Visual comfort is first and foremost a matter of how humans perceive daylight and glare. Therefore, in addition to the daylight glare evaluation performed in terms of experiments and simulations, presented in the previous chapter, it is fundamentally important to evaluate how actual human subjects perceive the indoor environment from a visual aspect, what are the desirable ranges of interior illuminance to maintain comfort, how effective the current glare indices are in terms of quantifying discomfort, and finally, get some inputs by occupants about the priorities concerning visual conditions in their workplace. In that scope, the experimental facilities of Herrick Laboratories were used, including the Living Labs (presented in detail in Chapter 3.1.2) and the private offices (presented in Chapter 3.1.3). As these spaces were occupied by human subjects, either regularly (Living Labs) or just on an as needed basis (private offices), it was a unique opportunity to expand the experimental methodology presented in Chapter 3 to real settings, investigate the best ways to associate traditional experimental measurements with human perception, through comfort comments and votes obtained using surveys. This chapter will examine visual comfort using two different approaches:

- The preliminary study performed in the Living Labs was based on surveys taken in random moments and positions throughout the four open plan offices, where the indoor conditions were determined by an automated shading control. Therefore for

this data set, both instances of comfort and discomfort were met, so an evaluation of the efficiency of existing indoor illuminance and glare indices as discomfort predictors was possible.

- The study performed in the private offices was based on occupants maintaining their desired indoor visual conditions through having complete manual control over their shading and lighting options. In that scope, and assuming that subjects adjusted their conditions to their satisfaction, the desired ranges of indoor illuminance and glare metrics could be extracted.

5.1 Preliminary study for the evaluation of discomfort predictors in open plan offices

5.1.1 Introduction - Procedure

As stated above, the main objective of the preliminary measurements in the Living Labs was to correlate the perception of comfort of the subjects with known indices of visual comfort and use this to select the most appropriate one to predict comfort in open plan offices, as well as to collect some survey data about the general impressions of the Living Labs occupants, a few months after they moved into their new office. IRB approval (protocol #1311014267) was obtained before conducting these experiments. As the offices were not fully occupied yet, less than 100 data points were collected during this study. Although the number is very limited to obtain conclusive and generalizable results, it was still a good opportunity to evaluate the measuring methodologies, including the luminance acquisition equipment, the questionnaires and procedures, while also obtaining some initial results. Details about the specifications of the Living Labs can be found in the Experimental

methodology chapter. The human subjects participated were the original users of the workstations, all graduate students, who were there performing their everyday work. The measurements were taken during Spring and Fall 2014, capturing sunny, cloudy and mixed days, for different positions in the room and for two main viewing directions, towards the window and towards the side wall.



Figure 5.1 Field measurements setup: HDR camera (left), handheld photometer (center) and moving cart (right)

As the objective of these spaces was to simulate unobstructed realistic locations, no significant sensor presence was decided. Therefore, a moving cart solution was implemented in order to obtain luminance and illuminance readings for the experiments. The cart included the pre-calibrated LMK system discussed in Chapter 3.3.1, based on a dSLR camera (Canon 550D with Sigma 4.5 Fisheye lens to capture the luminance mapping of the visual field of subjects), a Konica – Minolta illuminance sensor (T10) with two measuring probes to measure work plane and vertical (on eye) illuminance, and a laptop which was used as a data acquisition device (Figure 5.1). Due to the availability of a vertical illuminance sensor measuring near the lens, validation in terms of vertical illuminance using the external photometer was possible, giving a resulting MSE of 163lux, considered to be very good. (Figure 5.2).

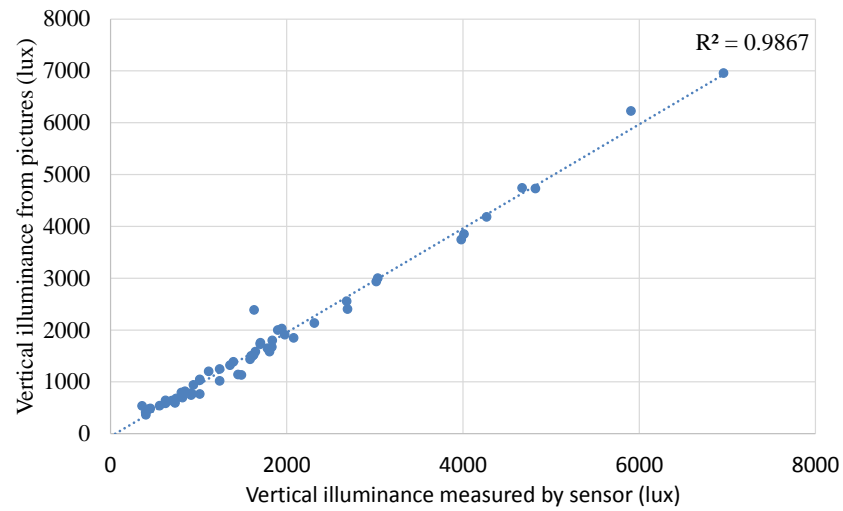


Figure 5.2 Validation of vertical illuminance measurements in Living Labs

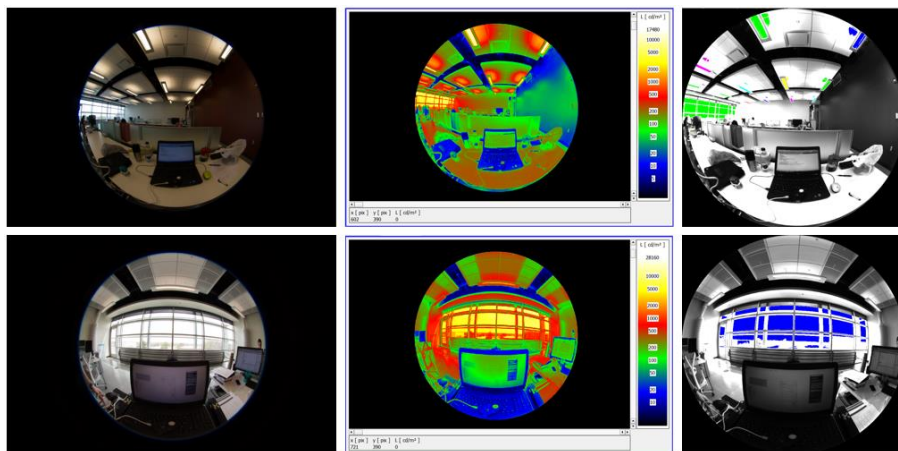


Figure 5.3 LDR image (left) – False color image from Labsoft (center) and Evalglare output (right)

After this step, the pictures were evaluated for glare using both Labsoft and Evalglare, according to the methodology presented before. Figure 5.3 demonstrates one side-lit (wall facing) direction (top) and one window facing condition (bottom).

The experimental procedure was as follows:

- **Step 1:** Subjects were given the questionnaire shown in Figure 5.4 and were asked to complete it by taking into account their current perception of the conditions.
- **Step 2:** Subjects were asked to move away from their desk, and the cart was placed at their seating position with the camera taking three photos at their head's spot, the work plane sensor located on their desk at their keyboard and the vertical sensor being held next to the camera, at the eye level. The illuminance sensor was taking 10 continuous measurements to use the average value. Values for vertical illuminance can be also extracted by the photographs, however the external photometer use can prevent unreliable measurements due to excessive direct light or other random reasons.
- **Step 3:** Subjects were asked to rotate 90 degrees towards the window, and the moving table with the laptop was placed in front of them. Then they were asked to focus on the screen for 1 or 2 minutes (their choice), until they felt that they were adjusted to their new working conditions. When they felt they were ready, they answered again question 7 of the questionnaire ("How satisfied are you in terms of visual comfort (reflections, glare, etc.)?")
- **Step 4:** Subjects got away from the moving desk, and camera was mounted again and took pictures of the extended laptop screen, with illuminance probes on keyboard and next to the camera

In order to minimize bias, the procedure would randomly begin from either facing the window or facing the wall direction. This process was repeated for different test subjects

seated in different locations in the open plan offices. Measurements were conducted under variable sky conditions and shading positions.

INITIAL QUESTIONNAIRE:

SEAT CODE:

Please **circle** the answers that fit better your opinion:

1. How satisfied are you with the automatic shading operation?
Very satisfied Slightly satisfied Satisfied Slightly unsatisfied Very unsatisfied

2. How satisfied are you with the automatic electric lighting operation?
Very satisfied Slightly satisfied Satisfied Slightly unsatisfied Very unsatisfied

3. Overall, does the office layout enhance or interfere with your ability to get your job done?
Yes No

4. How satisfied are you with the lighting conditions in your workspace?
Very satisfied Slightly satisfied Satisfied Slightly unsatisfied Very unsatisfied

5. If unsatisfied, what are the main issues in your opinion (circle as many as needed)?
Too dark Too bright Not enough daylight Too much daylight
Not enough electric lighting Too much electric lighting Not enough light for specific task
Electric light flickering Undesirable light color/temperature Reflections on computer screen

6. Would you prefer:
More natural light Less natural light More electric lighting Less electric lighting

7. How satisfied are you in terms of visual comfort (glare, reflections, etc)?
Very satisfied Slightly satisfied Satisfied Slightly unsatisfied Very unsatisfied
 Please provide brief comments:.....

8. Are you satisfied with occupancy sensors and wall switches?
Satisfied Unsatisfied Don't know/never used them

THANK YOU FOR YOUR COOPERATION!

Figure 5.4 Original questionnaire for comfort and general comments

As one of the objectives of this study was to evaluate the methodology of visual comfort experiments, after the initial pilot data collection was performed, then a smaller questionnaire, without the general comments for the new working space was introduced.

This was done in order to focus more on the environmental variables. The new questionnaire can be seen in Figure 5.5.

Questionnaire

Please select the preferred answer corresponding to your perception at the time of the measurement.

I feel generally pleased with the visual conditions at this moment.

1. Very strongly disagree
2. Strongly disagree
3. Disagree
4. Neither Agree or Disagree
5. Agree
6. Strongly Agree
7. Very strongly Agree

I feel satisfied with the amount of light on my desk

1. Very strongly disagree
2. Strongly disagree
3. Disagree
4. Neither Agree or Disagree
5. Agree
6. Strongly Agree
7. Very strongly Agree

The visual conditions help me successfully handle computer related tasks

1. Very strongly disagree
2. Strongly disagree
3. Disagree
4. Neither Agree or Disagree
5. Agree
6. Strongly Agree
7. Very strongly Agree

The visual conditions help me successfully handle reading or writing based (on the desk) related tasks

1. Very strongly disagree
2. Strongly disagree
3. Disagree
4. Neither Agree or Disagree
5. Agree
6. Strongly Agree
7. Very strongly Agree

I experience glare or reflections within my visual field

1. Very strongly disagree
2. Strongly disagree
3. Disagree
4. Neither Agree or Disagree
5. Agree
6. Strongly Agree
7. Very strongly Agree

Figure 5.5a Updated questionnaire focused on correlations with environmental variables

The white area on the sketch below indicates the extents of your visual field. Your line of sight is indicated with the dot in the center, while the left and the right extents correspond to the positions above your left and right shoulders (The human visual field is known to have a horizontal span of 180°)

Having the above in mind, please, locate with a "X" mark the position(s) of any disturbance(s) within your visual field, if any.

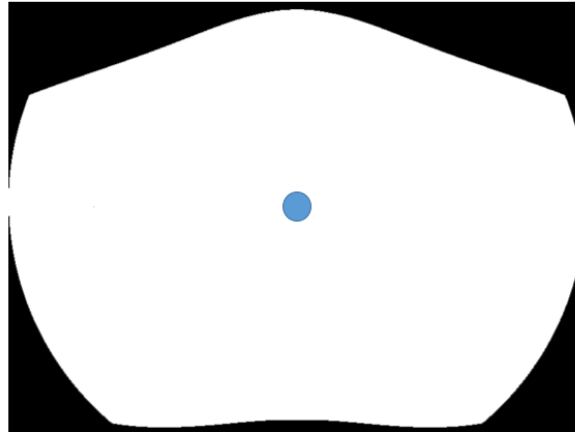


Figure 5.5b Sketch for locating the visual disturbance source

5.1.2 Correlations between visual comfort preferences and known indices

For the correlation of the visual comfort impression with various metrics, the methodology used in the related studies of Wienold (2006) and Hirning (2014) was followed; because comfort is better defined as a probability, the observations of people were first ranked according to the value of each examined parameter and then grouped accordingly. Following Hirning's approach, and eliminating some points that suggested inconsistencies, a total of 81 measurements was split in order to produce 9 groups of 9 persons each. In addition, as a binary consideration is preferred to obtain the clearest results possible, the answers of the subjects (which according to each questionnaire were either a 5 scales range of satisfaction, or a 7 points scale of agreement to the existence of glare and reflections) were converted to two possible answers: YES would indicate either being in a slightly or very unsatisfied condition or agreement (slightly or strongly) to the existence of glare. NO would include all the rest not mentioned above. Labsoft and Evalglare were both

used to obtain the various indices from the HDR pictures. An unanticipated problem was that because of the open plan nature of the experiment, along with the non-controlled conditions, each occupant had a completely different desk to interact with: There were desks with a laptop, others with a tablet, some others with desktop towers on the desk, blocking the view from the window, and many of the subjects had chosen to have multiple screens on their desks, or even work with tablets lying on the desks, rather than standing. This prevented the usual methodology of selecting a universal task area for all cases to extract DGP using a batch routine of Evalglare, as this task area would be different in every person's case. Therefore, for the DGP results using the task area methodology, Labsoft was used, because of its higher flexibility in selecting the task areas, as this is selectable in a GUI, rather than having to simulate it every time in a command prompt based on image coordinates.

The results are presented in graphs of correlations between studied index or light metric and percentage of discomfort, and discussed below:

- Visual comfort of the subjects seems to correlate well with simple light metrics (Figure 5.6). The strongest correlation appeared to be with the logarithm of Vertical on eye illuminance -Ev (0.861), validating the conclusions made in Chapter 4; conditions with the sun not included in the field of view could be efficiently described with vertical illuminance or a function of it, as DGPs. Very good correlations have been also observed for the UGR with 4x average threshold (0.7904), DGP with 6x average threshold (0.8549) and DGI with 6x average threshold (0.7695). It is apparent that the average luminance thresholds perform

better than the absolute ones, with that reflecting the importance of the adaptive part of luminance when it comes to glare perception.

- DGI (Figure 5.8) did perform poorly compared to other indices, while in the case of both DGI and UGR (Figures 5.8-9), there was a significant change of performance with different thresholds. This is a result of the lack of strong adaptation term like E_v in the equation, making the index very sensitive to the glare sources identification method. A more comprehensive recollection of all correlation levels can be observed in Table 5.1.
- There were no clear satisfaction ranges for the work plane illuminance. However, by observing a frequency histogram, it was clear that most unsatisfied subjects were connected to higher values of work plane illuminance. The sample is still small to produce some safer conclusions, therefore the experiments in the private offices will be used to continue this study.
- Similar issues are found in the case of the vertical on eye illuminance, more data is required to draw safer conclusions. The logarithm of vertical illuminance appeared however to have a very strong correlation with the visual comfort (0.86), showing a great potential for using this metric as a comfort definition. A metric measurable with a single sensor, rather than using complicated HDR imaging is more useful for integrating in real time control systems.
- The fact that the measurements took place during Spring and Autumn of 2014, along with the efficient shading control of the Living Labs (based on a solar path tracking algorithm enriched with some overrides for dark or bright conditions) resulted to low brightness conditions for the majority of the measurements. A proof

of this is the fact that only 16 of the total 81 measurements obtained extracted values of DGP over the noticeable limit of 0.35. Therefore, the higher range of the measurements is scarce. However, open plan offices often demonstrate similar behavior (Hirning, 2014) as most occupants are seating far away from the window and now being exposed to very bright conditions.

Table 5.1: Correlation Results

DGP (4x task)	0.763
DGP (4x Average)	0.8193
DGP (6x Average)	0.8549
DGP (500)	0.7967
DGP (1000)	0.7254
DGI (4x Average)	0.5592
DGI (6x Average)	0.7695
DGI (500)	0.6595
DGI (1000)	0.6758
UGR (4x Average)	0.7904
UGR (6x Average)	0.6448
UGR (500)	0.7763
UGR (1000)	0.57
Ev	0.695
log (Average L)	0.695
logEv	0.861
Average L	0.646

It should be noted that the overall sample was small, due to not enough people having moved into the newly built Living Labs at the time when the experiment took place. Therefore, changing a single observation from satisfied to dissatisfied can change the percentage of dissatisfied for the group, affecting significantly the

correlation coefficient. This means that in order to reach accurate conclusions, there should be a much larger sample for the experiment giving a single reading less influence. To make that more specific, to obtain an error of less than 5%, approximately 400 observations should be used, therefore the results presented in this subchapter serve only as preliminary results before proceeding to experiments with more subjects, discussed in Chapter 5.2.

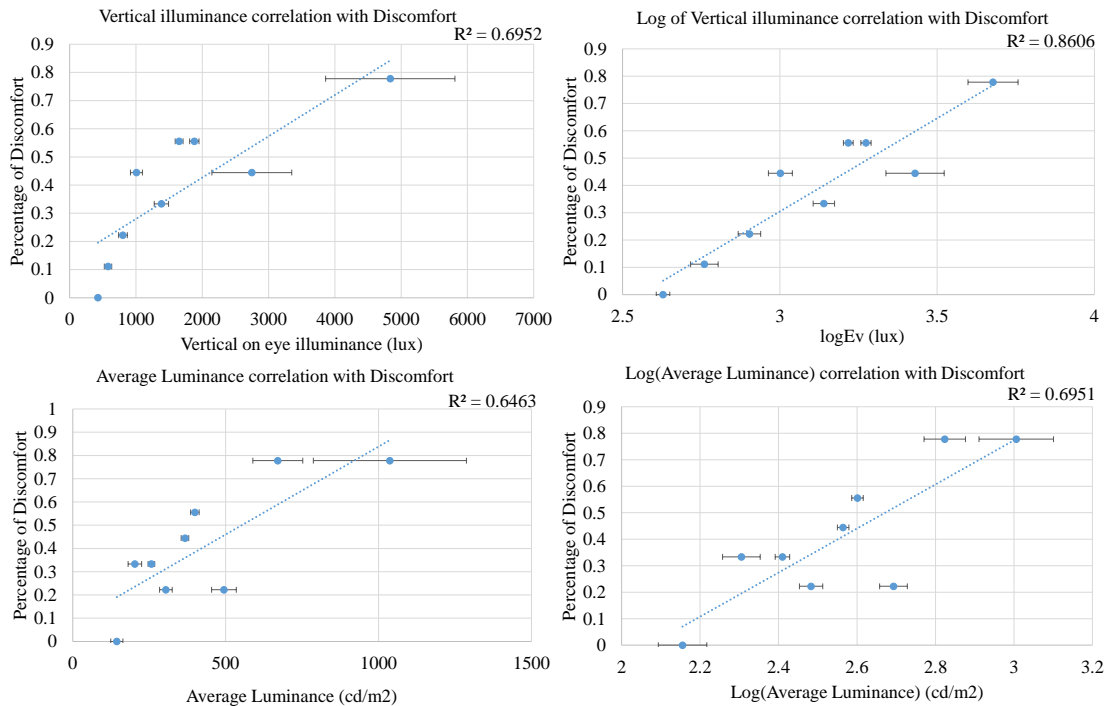


Figure 5.6 Sample correlations obtained in the study between discomfort and glare indices or metrics

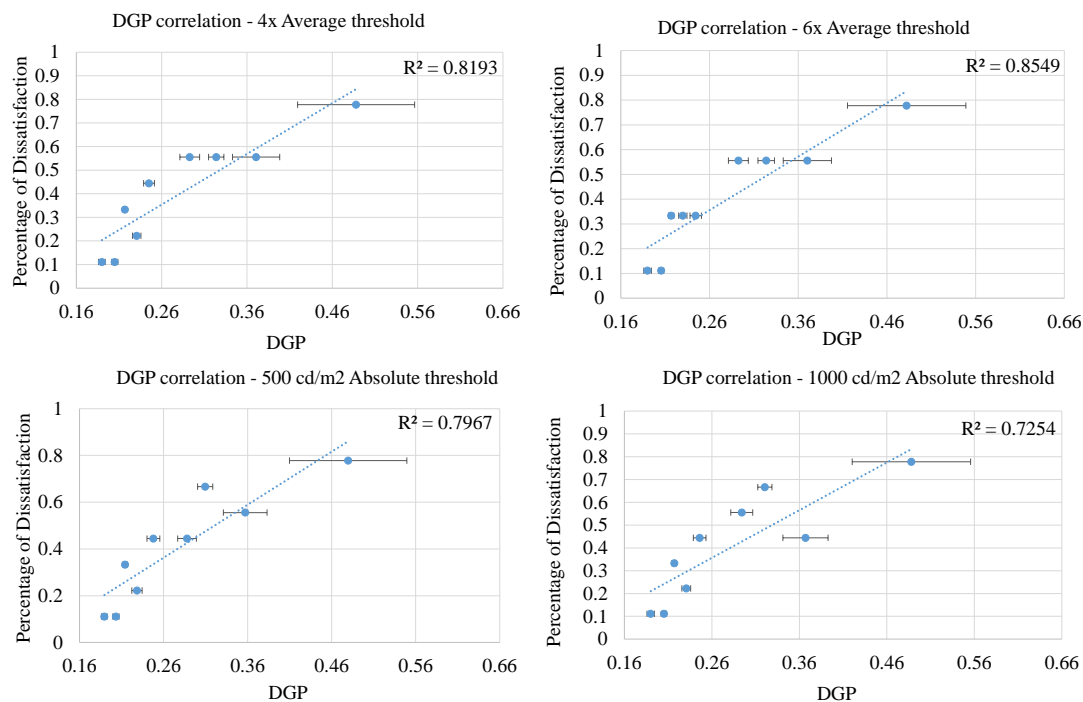


Figure 5.7 Correlations for different thresholds of DGP

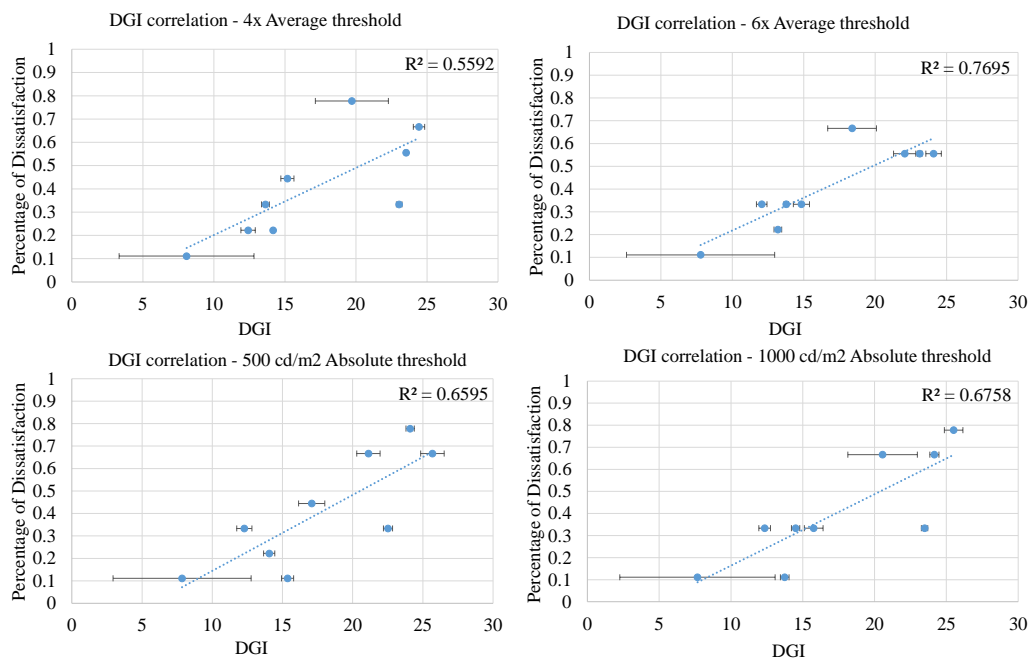


Figure 5.8 DGI correlations for different thresholds

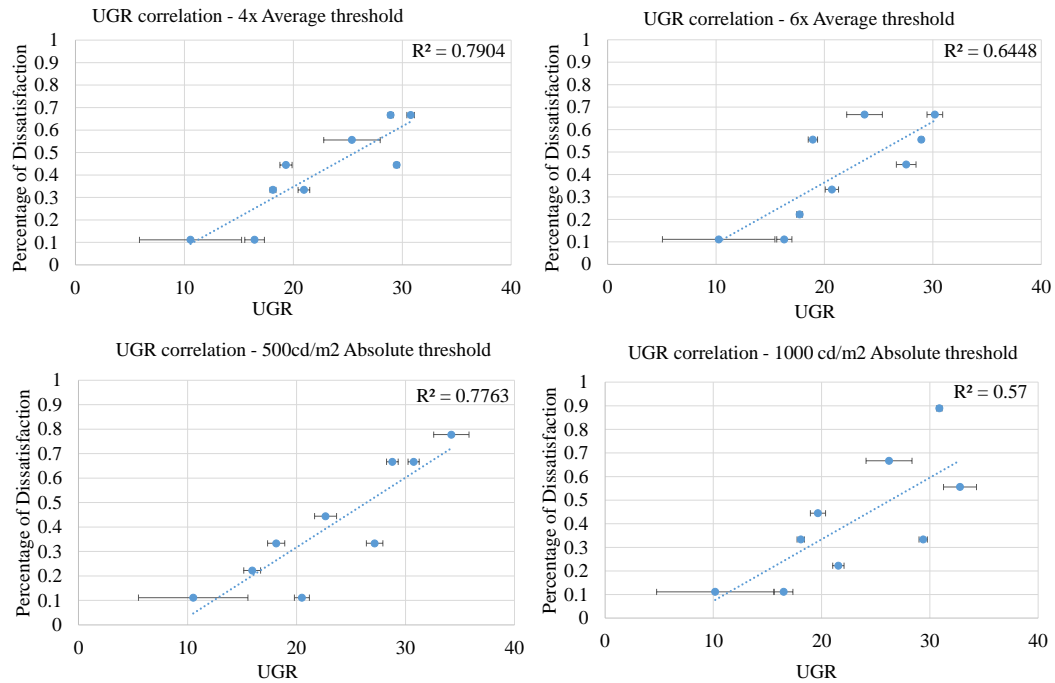


Figure 5.9 UGR correlations for different thresholds

5.1.3 General Impressions

Despite the small number of available test subjects, it was possible to obtain some general impressions and comments about the satisfaction in terms of shading controls, automatic electric lighting, and the occupants' preferences of what they find to be not satisfying and what they would like to correct. As this part of the study was more important for internal use at Herrick Labs, only some interesting results are presented here.

The first two questions were about the satisfaction with the automatic shading and lighting systems. As it can be seen in Figure 5.10, about 77% of the occupants considered the shading system to be working properly while only 33% were slightly or very unsatisfied with the operation. Modifications made in the control system for cases of very high or very low brightness conditions were therefore useful and well accepted. For the automated

lighting, the responses were similar, almost 80% of the participants felt satisfied and 20% more or less dissatisfied. The lighting control used was based on maintaining an average of 500 lux on the work plane, given the current position of the shades.

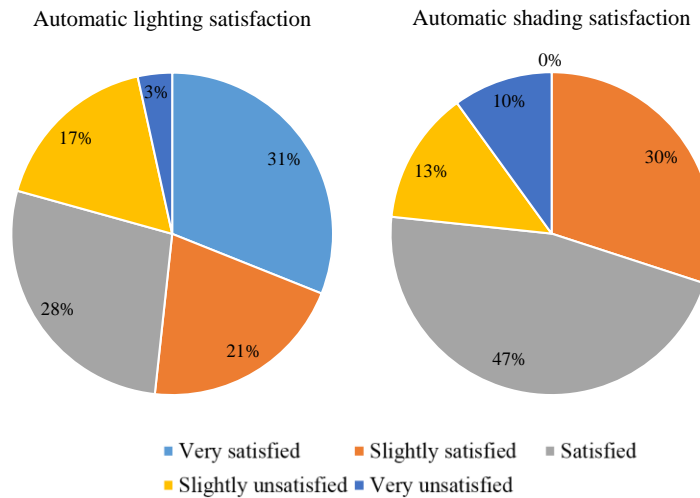


Figure 5.10 Responses to questions 1 and 2.

A third question (Figure 5.11) was asking about whether the office layout interferes with the subjects' ability to get their job done. The purpose of this question was to investigate whether the subjects would be aware of the importance of the layout (orientation, distances between desks, position, etc.) 72% of the participants claimed that this layout influences their productivity, while 28% disagreed.

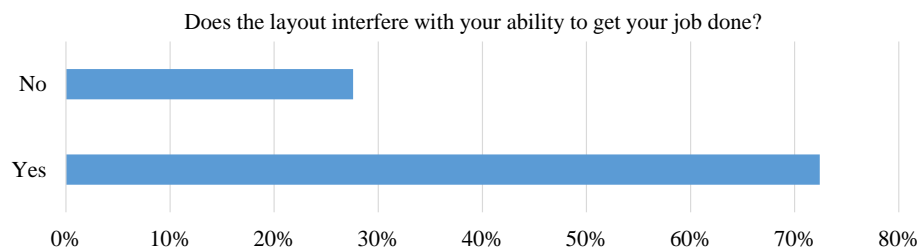


Figure 5.11: Responses to question about layout interference with tasks

The fourth and fifth questions were about the general satisfaction with lighting conditions in the workspace, and the reasons for the lack of satisfaction. In that case, the responses were quite diverse (Figure 5.12); some people reported that the white color of the desk creates unpleasant reflections. However, from the comments it appeared that this question was confusing to the participants, as they did not know whether they should comment about light adequacy, glare, or other issues.

Satisfaction with lighting conditions on workspace

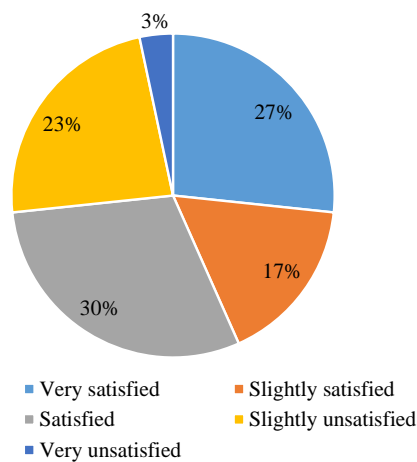


Figure 5.12 Satisfaction with lighting conditions

This ambiguity was however resolved by the fifth question (Figure 5.13) where the occupants specified their most common problems. The most usual problems seem to be the reflections on the screen, pointing out the conflict between designing displays aimed at improved color reproduction (usually glossy) and designing them for optimal office performance (matte). Future recommendations should include that open plan offices with large facades should invest in matte monitors rather than glossy ones. Other reasons of dissatisfaction were the excessive daylight and brightness and also the flickering of electric

lighting. The latter is a strange finding considering the fact that the installed systems were brand new and no flickering problems were otherwise detected.

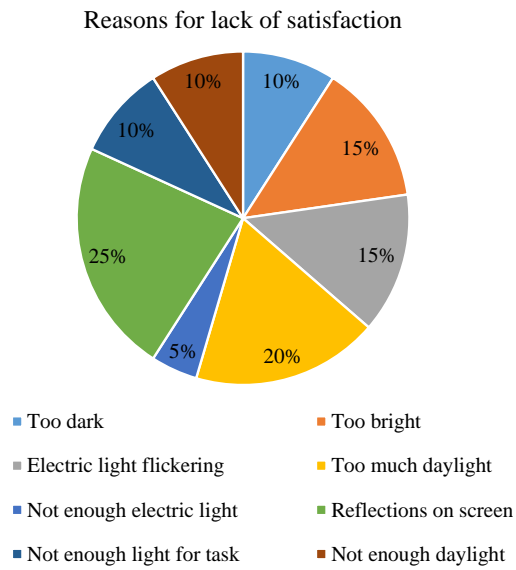


Figure 5.13 Reasons for lack of satisfaction

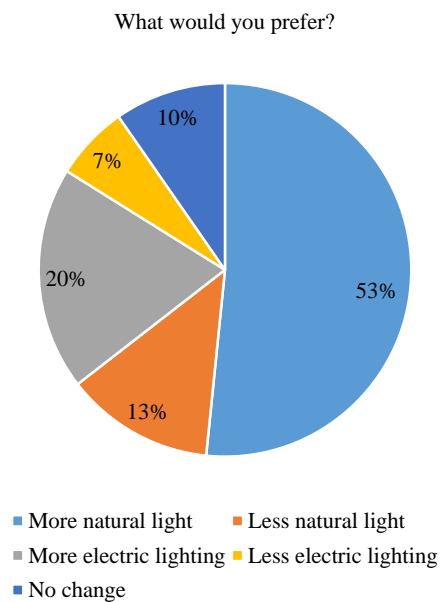


Figure 5.14 Suggested improvements

Finally, there was a question aimed to explore the ideal preferences of subjects (Figure 5.14). The most common answer was the wish for more natural light. However, this should not be confused, as excessive daylight would produce other problems, but it is recorded as the desired setting of the majority of the subjects. People want daylight, as it gives them the impression of a better connection to the outside. Subjects seemed to be confused as they often provided inconsistent answers with question 6, for example, subjects that complained for too much daylight in question 5 asked for more daylight in question 6.

5.2 Preferred indoor illuminance and DGP ranges in private offices with manual visual environment controls

5.2.1 Introduction

In order to conduct measurements in private occupied offices and further investigate occupant interactions with shading and lighting systems, four identical private offices were used in the first floor of the Center for High Performance Buildings (Herrick Labs).

The measurements performed here were part of a wider research project about the interactions of human subjects with control interfaces and the impact of ease of access on their behavioral trends and comfort (Sadeghi et al., 2016), topics that exceed the objectives of this Thesis. However, the fact that part of the data set was extracted using fully manual shading and lighting controls gave a unique opportunity to extract useful ranges for the desired interior lighting conditions in offices. Each office has a large window on the south side and hosted one occupant, seated facing the side wall (Figure 5.15). More information

about the private office setups, characteristics, control options, sensors involved and the data acquisition methodologies can be found in Chapter 3.1.3.



Figure 5.15 Experimental setup in Herrick private offices

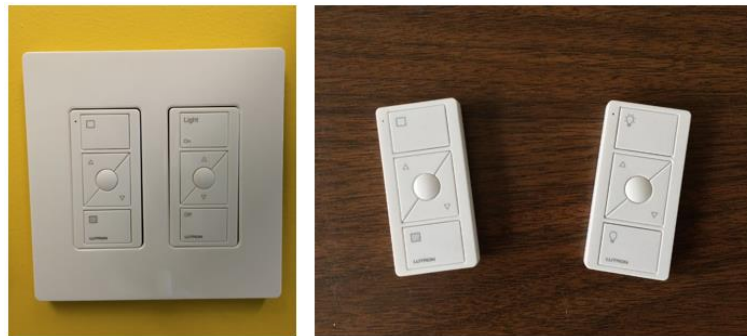


Figure 5.16 Manual controls for shading and light dimming.

The experiment was running from April 1st to June 15th 2015, and 147 different occupants participated for a total of 22 sunny, 10 overcast and 8 mixed days, giving a total number of 7291 data points. During that time, subjects were staying in the offices doing their personal work in computers, while having full control over their lighting and shading through either wall switches or remote controls (Figure 5.16).

The data acquisition system was recording indoor environment values on a 5 minutes basis during the subjects' entire stay in the office. Having this high number of data points obtained under entirely manual controls of the comfort delivery systems was a good opportunity to evaluate the conditions the occupants chose to maintain over their workplace, assuming these were within their borders of comfort. As comparing the different control options was out of the scope of this study, the data sets for the control setup with wall switches and the one with remote controls were combined to one unified data set which was further examined. More details about the differences between control interfaces are discussed in a study by Sadeghi et al. (2015).

5.2.2 Results

As explained in section 5.1, illuminance on the work plane plays a very significant role, as it is the dominant design metric of indoor lighting environment, using a set point of usually 500 lux (Rea, 2000). Figure 5.17 shows the frequency distribution of the total illuminance on the work plane, produced from both daylight and electric lighting.

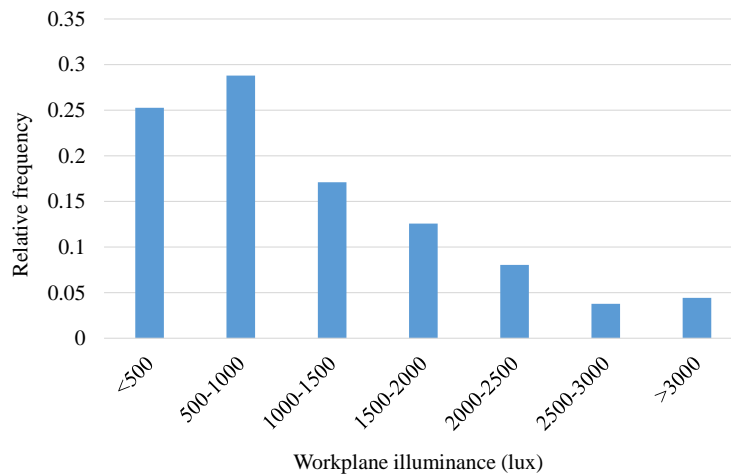


Figure 5.17 Relative frequency histogram of total work plane illuminance

It can be seen that for the majority of the subjects, work plane illuminances of less than 2000 lux were preferred. This validates the selection of the upper limit of 2000 lux on the work plane used by the *Advanced* shading control described in chapter 3.2, while it can also confirm findings of similar studies (Nabil and Mardaljevic, 2009). More specifically, more than half of the occupants were desiring conditions of less than 1000 lux on their work plane.

Figure 5.18 shows the relative frequency distribution of the vertical illuminance on the eye level during the course of the experiments.

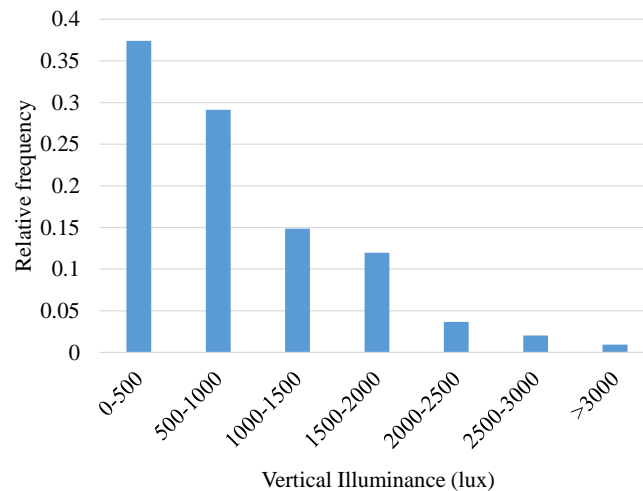


Figure 5.18 Relative frequency histogram of total vertical illuminance

It can be observed that low values were maintained for most of the time, much lower than the 2760 lux threshold which is implied by the definition of DGPs and its discomfort threshold of 0.35. These values however come in line with other studies that proposed lower discomfort thresholds; Karlsen et al. (2015) suggested a threshold of 1700 lux, Van Den Wymelenberg and Inanici (2014) proposed 1250 lux while Konis (2014) suggested 1600 lux). Similar relatively dark preferences can be observed for luminance based metrics.

Figure 5.19 shows the relative frequency distributions of two luminance metrics, the average luminance of the visual field and the average luminance of the visible surface of the window, both also obtained by a large pool of 2384 data points. For the average luminance of the visual field, Figure 5.20 shows the vast majority of the points being lower than 900 cd/m^2 , complying with the identified threshold of 800 cd/m^2 presented by Van den Wymelenberg (2009). In the case of the visible part of the window, most of the data points are within 4000 cd/m^2 . This complies with the findings of Inkarojit (2008) who proposed a logistic model for the closing of blinds, where the probability of closing increases for the average window luminance range of 2500-3500 lux.

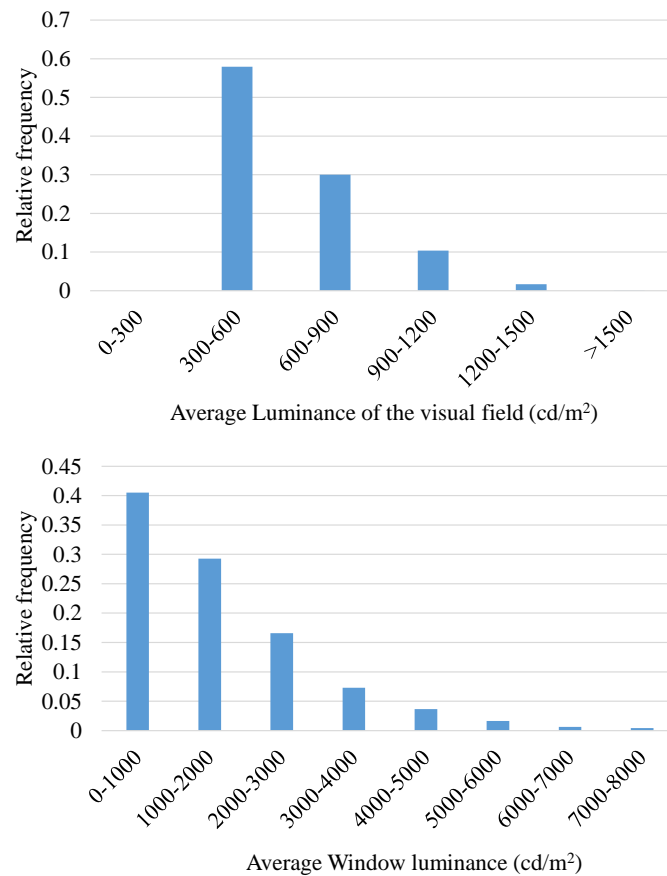


Figure 5.19 Relative frequency histogram of average luminance of visual field (top) and average luminance of the visible surface of window (bottom)

Figure 5.20 shows the relative frequency distribution of DGP (obtained by 2384 data points). It can be seen that all of the data points lie within the 0.35 border of discomfort, as it is defined by Wienold (2007), confirming in some extent the applicability of the DGP for settings like the ones met in this experiment (side wall facing setup with the sun never within the visual field). Due to the nature of the study (subjects with full control selecting their desired conditions), the data points could not be added to the analysis of Chapter 5.1.3 to extend the evaluation of the efficiency of glare predictors, as such a consideration would require a significant presence of discomfort instances.

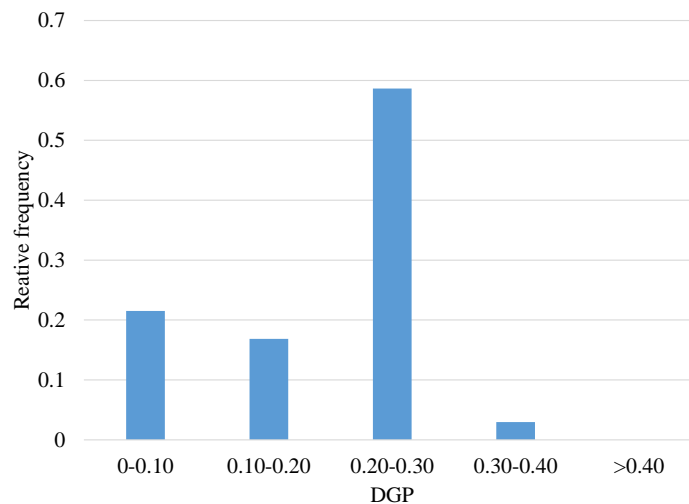


Figure 5.19 Relative frequency histogram of DGP

It has to be noted that for this experiment, the seating layout, facing the wall and having only a slight portion of the window visible could generally lead to reduced ranges of indoor daylight, compared to another seating layout, based on either facing the window, or having a great portion of the window visible. –these could alter the extracted results but would have caused more significant glare conditions.

5.3 Discussion

The two experiments described in the previous sub-chapters were a good opportunity to test the reliability of our experimental methods when it comes to field studies with human subjects. The sensors and data acquisition setup, the camera calibrations, the careful selection of which questions should be asked during human subject surveys, the right balancing of sunny and cloudy days, the automation of procedures, the statistics to be used for the appropriate data analysis and other details were validated through results that comply with current literature and extend the scarce availability of visual environmental data. Especially for the case of the efficiency of discomfort predictors, extending the data availability is of the essence, as meta-analysis of different data-sets could produce useful results, as long as a unified methodology can be proposed (Van den Wymelenberg, 2014). The next experimental parts of this Thesis including human subjects will be based on topics that have been never previously discussed in literature, shedding some light in the impact of fabrics on the view clarity and evaluating the interaction of fabrics properties with the sensation of glare under direct sunlight conditions.

CHAPTER 6. DAYLIGHT GLARE EVALUATION WITH THE SUN IN THE FIELD OF VIEW THROUGH WINDOW SHADES

6.1 Introduction

Shading fabrics are widely used in office spaces to improve visual and thermal comfort, control solar gains and also induce privacy when necessary. They are available in a variety of different colors, materials and weave densities and they can be manually or automatically controlled. The main optical properties that characterize shading fabrics are the openness factor (OF) and the visible transmittance (T_v); the first is an indicator of the weave density and the direct light transmission, whereas the latter indicates the portion of the visible light transmitted through the fabric, characterizing also the fabric's color. Literature focusing on the impact of roller shades on visual comfort is limited and mostly consists of simulation studies; moreover, studies investigating the glare under the presence of sunlight (Rodriguez et al., 2015), with or without shades, are certainly scarce and needed. Wienold (2009) used roller shades among other shading systems to investigate DGP and DGPs, a simplified index approximating discomfort using only the total vertical illuminance as a variable through simulation, while Van den Wymelenberg and Inanici (2010) noted that direct sunlight on the work plane can increase task area luminance and result in misleading use of glare sources when following the standard DGP calculation

approach. Jakubiec and Reinhart (2015) concluded that more than one metric is required for quantifying glare if direct sunlight is present.

As discussed in Chapter 4, for all instances when the sun is not visible by the occupant, DGPs can be used to approximate daylight glare, including cases with sunlight on various surfaces in the space, for any fabric openness and control type. However, the study showed that it is still not clear whether the full DGP index is applicable for the cases when the sun is visible through shading fabrics. Due to the extreme values of the solar corona's luminance, the luminance term of DGP is inflated, predicting discomfort levels that are rather incompatible with everyday practice, especially for the cases of low openness fabrics.

To overcome this potential problem, Chan et al. (2015) suggested an alternative dual visual discomfort criterion for roller shades based on direct and total vertical illuminance on the eye. The reasoning behind the dual criterion is that (i) a threshold for direct eye illuminance could be used to capture the effect of sunlight (or contrast), potentially substituting the luminance terms, and (ii) the total vertical eye illuminance would still be used for the overall brightness term. The proposed threshold values were 2760 lux for the total vertical illuminance (equal to $DGP_s=0.35$) and 1000 lux for the direct vertical illuminance, as a modification of IES Standard LM-83-12 (IESNA, 2012). In this way, the fabric openness factor is directly associated with direct illuminance and the fabric visible transmittance is directly associated with the total vertical illuminance –therefore guidelines for selecting shade optical properties based on glare protection may be developed. Chan et al. (2015) used this approach and identified the appropriate ranges of fabric properties in order to mitigate glare for different orientations, locations, glazing

properties and distances from the window. For instance, it was found that, to entirely eliminate glare when seated close to the window, a fabric of maximum $OF = 2\%$ and maximum $T_v = 5\%$ should be used on south-facing facades, depending on the building location.

However, there are no studies with human subjects, either evaluating glare using different shade fabrics, focused on the actual impact of their properties to the sensation of glare with the sun within the visual field, or exploring the applicability of known metrics in such cases.

This chapter analyzes daylight glare through shading fabrics with the sun within the field of view (through the shades). Fourteen shading fabrics with different light transmission characteristics were evaluated by 41 human subjects. The measured and survey results were used to associate discomfort glare with measured and modeled parameters, test the usability of existing glare indices, examine the efficiency of alternate illuminance-based criteria, and propose corrections in the DGP coefficients for the cases when the sun is visible through the shades. These results can be used for overall glare assessment through roller shades, as well as thresholds for selecting optical properties of shades to ensure glare protection.

6.2 Methodology

6.2.1 Experimental setting, measurements and instrumentation

The experiments were conducted in the two identical, side-by-side office spaces with reconfigurable south-facing facades located in West Lafayette, Indiana, presented in Chapter 3. These are originally designed for quantifying the impact of facade design

options and related controls on indoor environmental conditions and energy use, and were modified in order to host six isolated workstations for testing different fabrics, all facing the exterior façade from a distance of 1.30 m.

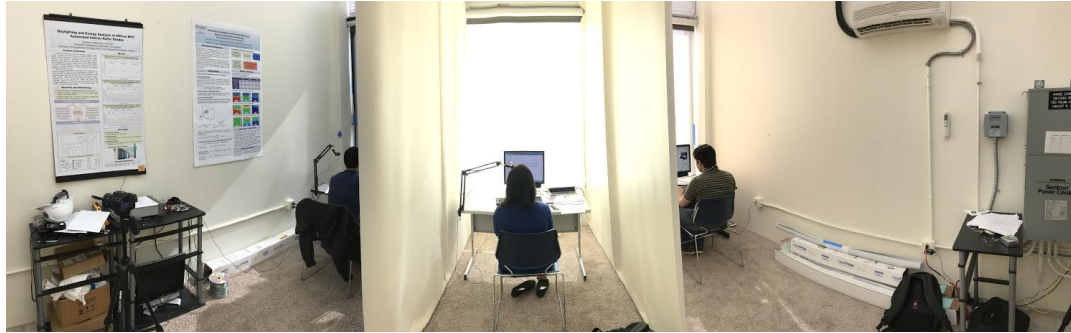


Figure 6.1a Experimental layout of one of the two identical offices used for the study with three partitioned workstations, each equipped with a different shade.

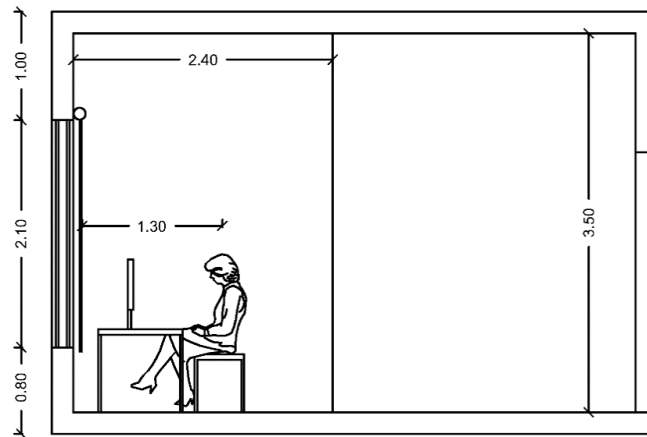


Figure 6.1b Cross section of each of the partitions of the experimental setting; distances of subjects from the glass, depth of partition in the room, and total window and room height can be observed. (in meters)

The placement of the workstations was decided in order to capture the “worst case” scenario for daylight glare in office spaces (view direction), while also providing an adequate time frame of view of the sun through the fabric (distance from window) for each

measuring day. All façade sections were equipped with a SB70XL-clear high performance glazing unit (60% window-to-wall ratio) with a selective low-emissivity coating (visible transmittance: $\tau_v = 65\%$ at normal incidence). The partitions were approximately 1.70×2.40 m, separated by fully opaque dividers having the same color as the walls of the facility. Fig. 6.1a shows a typical experimental setting for each office space, separated in three workstations (6 total), while Fig. 6.1b shows a detailed geometry for each partition.

Several LI-COR calibrated photometers were used to measure illuminance levels during the experiments, for data acquisition and validation purposes. The latter were used in the exterior (mounted on the roof and south wall) measuring the exterior horizontal and vertical illuminance, on the interior of the glass, measuring the transmitted vertical illuminance through the window, and in a small distance next to the subjects' heads, measuring the total vertical illuminance on their eye level. (visible in Fig. 6.1a). For the latter, a Konica T-10s illuminance meter was also utilized as a secondary sensor for reasons of validation, taking a single reading for each measured data point from the exact position of the subject's head. This addition was essential as it could (i) indicate erroneous readings of the Licor sensor due to accidental misplacement to the side etc., (ii) correct the readings of the Licor sensors in some cases of morning or late afternoon measurements, where the sun was on the side of the window, viewable by the subject but not by the Licor sensor and (iii) evaluate the validity of the HDR images through comparison of the extracted vertical illuminance. The latter were obtained by a calibrated Canon T2i HDR camera, and were used to map the luminance distribution of the visual field. As during this study, the sun would be always within the field of view through shading fabrics, from the methodologies presented in Chapter 3.3, only Method C would successfully cover the procedure.

Therefore, this was selected for the luminance mapping of the visual field for each data point. Direct and diffuse portions of incident solar radiation on the façade were also measured with a SPN-1 solar pyranometer, mounted vertically on the exterior south wall. These readings were used to calculate the direct portion of vertical illuminance on the eye, after also correcting for the angular properties of the glass and each fabric (see section 6.2.3). The sensors were connected to a data acquisition and control system (HP Agilent and Labview), accessible through remote access in order to run experiments without interfering with indoor lighting conditions. More details about the connectivity and data acquisition of the sensors are mentioned in Chapter 3.1.1.

6.2.2 Shading fabrics

The purpose of this experiment was to evaluate glare sensation with the sun visible through roller shades (fabrics), therefore the selection of fabric types and properties was critical in order to be able to produce results that cover a wide range of products/optical properties, to generalize the study findings. Roller shades consist of different fabric materials with varying degrees of openness and transmission characteristics, both affecting direct and diffuse light transmission, which in turn have an impact on daylight provision, visual comfort and energy use.

A careful selection of 14 different fabrics was made for the tests. Their properties covered a wide range of OF and T_v values, and shades of white, black and grey. The selected combinations capture the entire range of interest with no specific pattern/relationship between the properties, given realistic limitations. 12 of the fabrics were in the low and middle range of openness factor (0.7% - 4.3%), while two of them had high openness ($OF \approx 7\%$). The reasoning behind this selection was to confirm that fabrics of high openness

would always lead to conditions of glare, and essentially focus on the lower end of the spectrum to closely observe patterns and thresholds. The basic optical properties of the selected fabrics (openness factor and visible transmittance) were measured in detail using an integrated sphere. They were codenamed using letters for reasons of procedural flexibility. Their basic properties are listed in Table 6.1.

Table 6.1 Fabric codes and respective measured optical properties (in %)

Code	A	B	C	D	E	H	I	J	O	P	Q	R	S	T
<i>OF</i>	2.6	0.7	1.6	3.7	2.3	3.9	7	6.7	1.65	4.36	1.15	0.85	1.87	0.95
<i>T_v</i>	2.8	6.4	13.7	4.1	6.6	15.9	7.5	13	7.63	8.57	1.43	12.29	2.18	6.62

6.2.3 Angular fabric transmission properties and direct vertical illuminance on the eye

The angular optical properties of the glazing system were calculated by WINDOW 7.0 software (LBNL, 2013). Shades also have angular light transmission characteristics, which can be modeled either using detailed BSDF data or the semi-empirical model originally proposed by Kotey et al. (2009). The latter is discussed in detail and further validated using integrated sphere measurements and full-scale experiments by Tzempelikos and Chan (2016). This model, which proved to be accurate and reliable for several types of standard (PVC-coated and vinyl) fabrics, calculates the beam-beam and beam-total visible transmittance angular variation as a function of the incidence angle and the normal *OF* and *T_v* properties, provided by manufacturers. The latest version of EnergyPlus (2015) includes this angular model in the “window thermal calculation module”, as part of the new “equivalent layer fenestration model”. In summary, the angular beam-beam shade transmittance (τ_{bb}) is calculated from:

$$\tau_{bb}(\theta) = \tau_{bb}(0) \times \left(\cos \left(\frac{\pi}{2} \times \frac{\theta}{\theta_{cut-off}} \right) \right)^b \quad (6.1)$$

, where θ is the solar incidence angle, $\tau_{bb}(0)$ is the beam-beam transmittance at normal incidence, assumed equal to the *OF* of the fabric (provided by manufacturers), and b and $\theta_{cut-off}$ are parameters that depend on $\tau_{bb}(0)$, as explained in Kotey et al. (2009). The angular beam-total transmittance (τ_{bt}) is calculated from:

$$\tau_{bt}(\theta) = \tau_{bt}(0) \times (\cos \theta)^d, \{ \theta < \theta_{cut-off} \} \quad (6.2)$$

, where $\tau_{bt}(0)$ is the beam-total transmittance at normal incidence (total visible transmittance provided by manufacturers) and d is a parameter that depends on openness factor and total visible transmittance. The cut-off angle should not be applied to light-colored fabrics, to account for direct light scattering at higher angles, while small corrections might be needed for dark-colored fabrics (Tzempelikos and Chan, 2016). The beam-diffuse transmittance, necessary for accurate modeling of light transfer through shades, is then equal to $\tau_{bt} - \tau_{bb}$ for each angle. Finally, integrating τ_{bt} over the hemisphere yields the diffuse-diffuse shade transmittance (τ_{dd}), which cannot be measured or calculated otherwise.

In contrast with total vertical illuminance, which is directly measured, there is no standard way to measure direct vertical illuminance on the eye of the observer (induced by the sun through the glazing and shading) without interfering with the experiment. Instead, the measured transmitted illuminance through the glazing was separated into direct and diffuse parts using the direct/diffuse ratio obtained by the SPN1 pyranometer, while the incidence angle θ was computed for each respective measured data point. The shade

angular transmission model, described above, was then used to calculate the direct and diffuse illuminance through each fabric at each measurement time. In this way, we achieved a reliable estimation of the direct portion of vertical illuminance on the eye with each of the tested fabrics, for the selected position and view direction of the observers. This measurement is needed to evaluate vertical illuminance thresholds and alternate glare criteria when the sun is within the field of view.

6.2.4 Experimental procedure, tests and surveys

The experiments were conducted during sunny days from December 2015 until March 2016. Winter conditions were selected to utilize low sun angles, so that the sun is visible through the fabric during the entire test periods, in order to evaluate glare sensation under the worst case scenario situations. An IRB approval (#1410015323) was obtained in order to recruit human subjects to participate in the study. In total, 41 different subjects participated in the experiment, 25 male and 16 female, all graduate students, while care was taken to achieve the maximum possible diversity in terms of ethnicity. On each test day, the experiments lasted 2-4 hours depending on the number of test subjects and variability in the sky conditions (stable clear sky conditions were necessary for these tests). The test subjects evaluated 6-14 fabrics during each measurement day. The shades were randomly deployed in each workstation every day, although care was taken to ensure a complete range of fabric properties to be present in each measuring day, diminishing the possibility of bias as much as possible.

Each subject was initially assigned to a workstation/partition, in which they would spent 15-20 minutes. This duration should satisfy the need for proper adaptation to the conditions while also providing adequate time to perform specific tasks. The objective was

to simulate regular office activities, including free and time-sensitive tasks. For that reason, the time was split into 3 main parts, including free web browsing period, a character count test and a reading comprehension task, in which subjects had to complete a short questionnaire (Fig. 6.2).

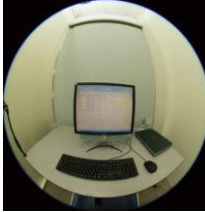
<p>Subject Code: _____</p> <p>Fabric Code: _____</p> <p>Time: _____</p> <p>Date: _____</p> <p>Please read carefully every task and follow the order:</p> <p>1. As you enter the partition, please be seated and start using the computer. You can do anything you like, as long as it is done on the computer. You can browse the internet, check your e-mail, plug in a flash drive to access your files etc. Keep doing that for about 5 minutes or until you are told to proceed to 2.</p> <p>2. Open the .doc file named "Character search" which is located on your desktop. This is a paragraph of random characters. We need you to carefully go through that and count the appearances of the character you'll find in the back of the Fabric code paper. When you finish that, please write the number of appearances in the box below. Be aware that the character asked is lower case!</p> <p>Number of appearances of ____ : <input type="text"/></p> <p>After you're finished with that, proceed to 3.</p> <p>3. Open the .doc file named "Reading comprehension 1" on your desktop. It contains a short passage you have to read carefully, and answer the three simple questions below that. Please mark your answers in the boxes below this line:</p> <p>Q1: <input type="text"/> Q2: <input type="text"/> Q3: <input type="text"/></p> <p>After you're finished with that, or if you're asked to, you can return to your free computer activities until you're told to turn the page and proceed to questions 4, 5, 6 and 7, related to your comfort. Please try to be as accurate as you can in your responses. and continue to the next page.</p>	<p>QUESTIONNAIRE</p> <p>4. Were you satisfied with your visual conditions (<u>brightness, contrast</u>) over the time you spent in this partition.</p> <p>Very unsatisfied <input type="checkbox"/> <input type="checkbox"/> <input type="checkbox"/> <input type="checkbox"/> <input type="checkbox"/> <input type="checkbox"/> <input type="checkbox"/> Very satisfied</p> <p>5. Grade the visual discomfort (glare level), if any, that you experienced <u>overall</u> (any type of visual discomfort: bright objects, high overall brightness, contrast, reflections, shades, etc.) during your stay in the partition, considering that this situation can happen for varying amounts of time in your regular office.</p> <p><input type="checkbox"/> Imperceptible (No feeling of glare – conditions help me focus)</p> <p><input type="checkbox"/> Noticeable (I can clearly feel some glare, but it doesn't really bother me or distract me)</p> <p><input type="checkbox"/> Disturbing (The level of glare is high and can distract me from work after a while)</p> <p><input type="checkbox"/> Intolerable (I experience high glare/discomfort and I cannot focus on my work)</p> <p>6. Grade the visual distraction, if any, that you experienced during your stay <u>specifically due to having the sun visible through the shade fabrics</u>, considering that this situation can happen for varying amounts of time in your regular office.</p> <p><input type="checkbox"/> Imperceptible (No distraction – conditions help me focus)</p> <p><input type="checkbox"/> Noticeable (I can clearly feel some distraction, but it does not really bother me)</p> <p><input type="checkbox"/> Disturbing (The level of distraction is high and can influence my ability to work after a while)</p> <p><input type="checkbox"/> Intolerable (I experience high distraction and I cannot focus on my work)</p> <p>7. The fisheye picture below includes what should approximately be your field of view at the time of your stay in the partition. Please mark with X symbols the areas from which you experienced discomfort (<u>if any</u>). You can mark as many areas as you want.</p>  <p>8. Did you feel affected by the heat of the sun during your stay in this partition?</p> <p>Not affected at all <input type="checkbox"/> <input type="checkbox"/> <input type="checkbox"/> <input type="checkbox"/> <input type="checkbox"/> <input type="checkbox"/> <input type="checkbox"/> Very affected</p>
---	---

Figure 6.2 Questionnaire used in the study and task-related information

As the main reason for including the specific tasks was to make the subjects focus on their screens (performing computer-related activities while the sun is within the field of view through the fabric), the task performance of the subjects is outside of the scope of this study. Towards the end of the session, each subject was asked to lean aside in order for the investigator to place the camera and the handheld sensor in the exact position of the subject's head and shoot the 9 used exposures while also taking a reading with the handheld

illuminance sensor. This way, luminance distribution of the visual field plus a total vertical illuminance reading were acquired for each combination of subject and fabric. As the conditions were assumed to remain constant throughout the 15-20 minutes of the evaluation (due to the clear sky, only negligible fluctuation was observed in the exterior and transmitted illuminances), the readings of the camera and the handheld sensor were assumed to capture the conditions of the entire stay in the partition. At the end of the test period, the subjects were asked to proceed to the second part of the short questionnaire (Questions 4-8), commenting about their visual comfort sensation.

- Question 4 was a 7-point scale satisfaction with the visual conditions (from 1- very unsatisfied to 7- very satisfied)
- Question 5 was a 4-point glare vote (from 1- imperceptible to 4- intolerable) about their overall perception of glare (including any possible source of it, the sun, the fabric, reflections on the desk or within the room, etc.). Keeping the same scale as in the original DGP study allows a systematic comparison with previous results.
- Question 6 asked about the level of distraction because of the presence of the solar disc within the visual field. (4-point scale from 1- imperceptible to 4- intolerable)
- Question 7 requested the subjects to indicate the sources of visual discomfort, if any, on a photo of their workstation, and
- Question 8 asked about whether the subjects felt they were affected by the heat from the sun during their stay in the partition (7-point scale from 1- not affected at all to 7- very affected). The contents are out of the scope of this study, but may be useful in future for thermal comfort evaluation near roller shades.

In total, 425 data points were recorded, with each point being a subject evaluating a fabric. Among these, 355 observations were considered reliable and were used for the main part of the glare evaluation results. The rest were not used, mainly due to (i) subjects that appeared to be entirely insensitive to any change of conditions (ii) data with Fabrics I and J in Table 6.1 that were used just to confirm that high OF or T_v will always result in uncomfortable conditions.

6.3 Results

6.3.1 General impact of fabric properties on glare

In order to investigate in more detail the extent to which the two main fabric properties affect glare sensation, Figure 6.3 shows the behavior of all tested fabrics in terms of the votes obtained by Question 5 (4-point scale overall glare), with the fabrics appearing in order of increasing openness factor.

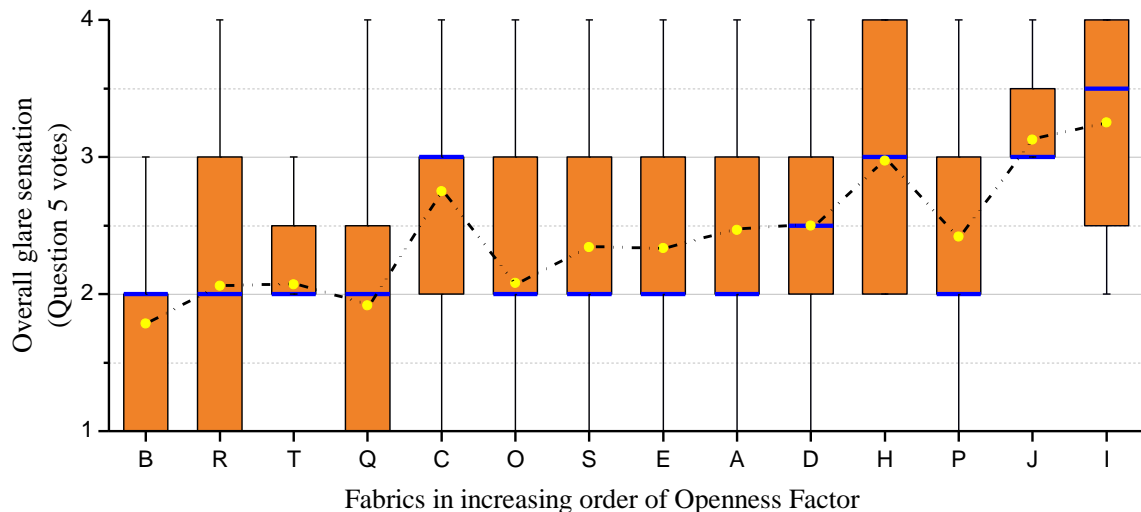


Figure 6.3 Distribution of responses for Question 5 – overall glare sensation (fabrics listed in order of increasing openness factor).

The yellow dots indicate the averaged responses with the median noted by the blue line, while the boxes illustrate the distribution of the results. The two fabrics of high openness factor, I and J, are the only ones with averaged responses that always lie within the discomfort zone, while their distribution is clearly distinguished from the rest of the fabrics. In addition, it has to be mentioned that, while all other 12 fabrics produce a relatively continuous range of direct illuminance, from 119 to 2228 lux, the latter two produce values that lie on an entirely different range (from 2940 to 3558 lux). This inconsistency in terms of ranges, combined with the clear discomfort responses obtained for the two fabrics led to their elimination when it came to the calculation of thresholds or other quantification attempts presented in the next sections.

In order to evaluate the validity of the experimental approach, an analysis of variance was conducted, where the subjects were used as a blocking factor with random effect. However, as described in section 2.5, the logistic complexities of the study, due to the random sequence of days with clear sky prevented the approach of a complete within-subject design, where every subject would end up having evaluated every fabric on the same day. For that reason, care was taken for each subject to encounter a complete range of visual conditions, with respect to direct and total vertical illuminance (which in terms of fabrics can be translated to openness factor and visible transmittance). Within that scope, for the needs of the analysis of variance, the treatments were considered to be four different classes of openness factor and visible transmittance, as shown in Table 6.2, as well as the interaction between them. Table 6.3 shows the ANOVA results for the two overall comfort related questions and for a confidence level of 95%. As expected, the blocking factor (subjects) appears to be significant at all cases, pointing the differences between individual

subjects and the fact that due to the low resolution of the responses (seven points for question 4 and four points for Question 5), it is expected that for a given condition, the responses will be distributed among more than one votes. For both questions 4 and 5 (overall satisfaction/glare perception), both independent variables (classes of OF and T_v) appear to be statistically significant, thus having a strong impact on both visual satisfaction and the overall perception of glare. This result underlines the need for the inclusion of both parameters (in the current or an equivalent form, such as direct and total illuminance) for any discomfort predictor, something that is followed in the next sections of this study. Their interaction, however is not significant, demonstrating the reality of different combinations of OF and T_v potentially leading to similar levels of glare sensation (for example a very dense fabric of very high transmittance or a very open black fabric).

Table 6.2 Classes of fabric properties used in ANOVA

Class	OF (%)	Tv (%)
1	0-1.1	0-5
2	1.1-2.2	5-10
3	2.2-3.3	10-15
4	3.3-4.4	15-20

Table 6.3 ANOVA results

	Variable	df	Sum of Sq.	Mean Square	F Value	p-value
Question 4	<i>Subject</i>	35	257.827	7.366	3.29	<.0001
	<i>OF</i>	3	74.5	24.833	11.08	<.0001
	<i>Tv</i>	3	33.454	11.151	4.98	0.0022
	<i>OF x Tv</i>	3	14.037	4.679	2.09	0.1018
Question 5	<i>Subject</i>	35	50.138	1.433	2.44	<.0001
	<i>OF</i>	3	19.449	6.483	11.02	<.0001
	<i>Tv</i>	3	12.956	4.319	7.34	<.0001
	<i>OF x Tv</i>	3	2.148	0.716	1.22	0.3034

6.3.2 Vertical illuminance, DGP and respective comfort ranges

As described in section 2.5, there were three questions including classic comfort votes, one from a positive aspect (visual satisfaction) and two from a negative aspect (glare and visual distraction). The authors consider the four - point glare scale as defined by Wienold and Christoffersen [7] to be an effective way to assess discomfort. This, combined with the fact that one of the metrics of interest was DGP, led to a 4-point range extraction for the three main metrics investigated (total vertical eye illuminance, direct vertical eye illuminance and DGP) –and their combinations, as shown later. As the objective was to associate the overall sensation of glare with measurable metrics, Question 5 was considered to be most suitable. This decision was corroborated by the fact that, as expected, there was a strong correlation between the responses of Questions 5 and 6 ($R^2=0.74$) and Questions 4 and 5 ($R^2=-0.75$).

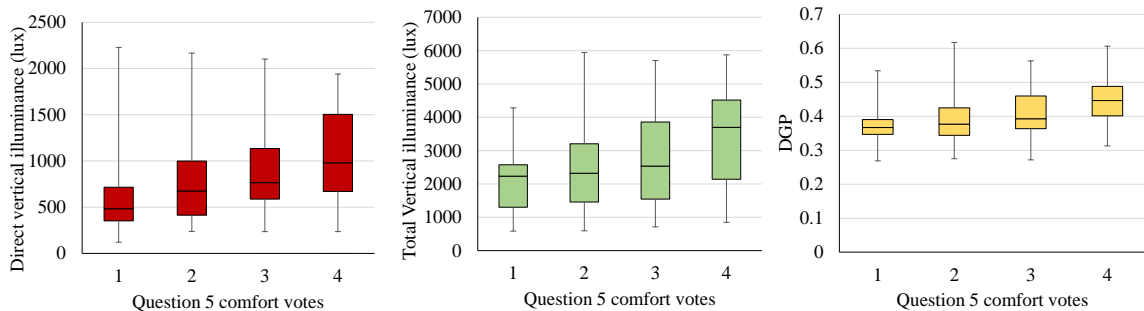


Figure 6.4 Boxplots associating the responses of Question 5 with direct vertical illuminance, total vertical illuminance and DGP respectively for four-point responses.

Figure 6.4 shows the association of the three metrics of interest with visual discomfort according to the responses of Question 5. The selected fabrics indeed resulted in a wide variation for all metrics, which was important for the analysis. More specifically, direct vertical illuminance ranged between 120-2228 lux; total vertical illuminance varied

between 588-5940 lux; and DGP ranged between 0.26-0.62. The standard way to extract thresholds based on the four-point scale requires the mean, standard deviation and upper and lower bound confidence intervals need to be calculated for each vote and for each metric. Although there are clear differences between the different votes, the distribution of the data for each vote did not always approach normality at the desired level, while for the cases of votes 1 and 4, the number of points was significantly lower (Fig. 6.5 – left).

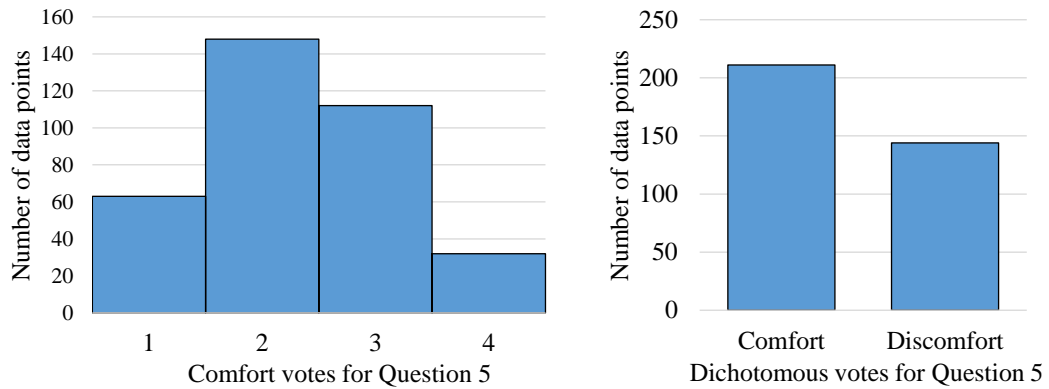


Figure 6.5 Distribution of votes for Question 5 in original form (left) and dichotomous approach (right).

Therefore it was preferred to follow a dichotomous approach (grouping the votes into two groups – comfort for votes 1 and 2 and discomfort for votes 3 and 4), which gives two more equivalent data groups of 211 and 144 points respectively (Fig. 6.5 – right).

Table 6.4 Descriptive statistics and thresholds extraction for discomfort votes

	$E_{v,dir}$	E_v	DGP
Mean	947	2896	0.42
Standard Deviation	490	1420	0.07
Number of points	144	144	144
Confidence Interval (Lower bound)	80	231	0.01
Threshold	867	2664	0.41

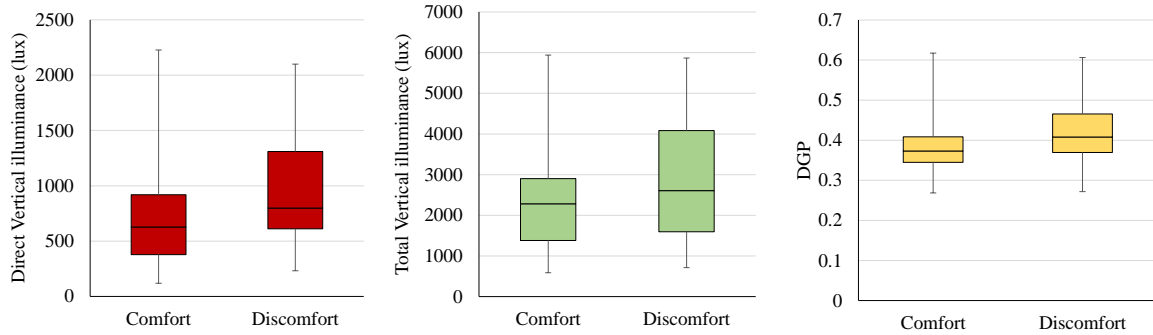


Figure 6.6 Boxplots associating the responses of Question 5 with direct vertical illuminance, total vertical illuminance and DGP respectively using a dichotomous approach.

The results are shown in Fig. 6.6. Table 6.4 shows the descriptive statistics for these dichotomous votes and the lower bound 95% confidence interval for the discomfort group, which indicate the corresponding thresholds for the border of discomfort. The results show that the direct vertical illuminance discomfort threshold for the cases of roller shades and the sun present is around 870 lux. This result provides a first validated insight about the acceptable ranges of direct vertical (sun) illuminance, as recent studies attempt to use a discomfort threshold of around 1000 lux (Chan et al., 2015; Jakubiec and Reinhart, 2015) based on recommendations for direct illuminance on the work plane found in IES LM-83-12 (IESNA, 2012). The threshold cannot be generalized however for other types of shading or daylighting devices without conducting similar studies with these systems. As discussed later, none of the three metrics proves to be appropriate to capture the fluctuation of discomfort by itself, therefore none should be acting as an individual predictor for this special case of conditions.

For the other two metrics, the results show a noticeable agreement with some previous studies; the discomfort threshold for total vertical illuminance lies in the order of

the discomfort threshold for DGP_s (~2800 lux), while the discomfort threshold for DGP was found to be at the level stated in the original DGP study (~0.4). For reference, there are three published studies that propose total vertical illuminance discomfort thresholds: Karlsen et al. (2015) suggested 1700 lux; Van Den Wymelenberg and Inanici (2014) proposed 1250 lux and Konis (2014) suggested 1600 lux. However, these studies used different shading systems and different discomfort scales, the presence of the sun was not consistent and the vertical illuminance ranges were not similar. This shows the need for more related studies with different fenestration systems under variable conditions.

Due to the high deviation, none of the three presented metrics is considered a reliable comfort/discomfort predictor by itself, for the studied case of roller shades with the sun present. The work presented in the next sections aims to bridge this gap.

6.3.3 Correlation of discomfort sensation with existing illuminance- and luminance-based metrics

The results presented in 6.3.2 indicate the extracted thresholds from this study's dataset. However, to effectively evaluate the extent to which a metric can capture the fluctuation of discomfort sensation, the method of ordered grouping of the data points is used. According to that, the data set is first sorted into increasing order of the metric of interest, grouped in n groups of m points per group, and then the correlation of the ordered averages of the groups and the percentage of discomfort per group is evaluated. There is some ambiguity in related literature about the correct approach for creating groups in that sense. Wienold and Christoffersen (2006) split the total 349 data points into 12 groups of 29 points per group. Hirning et al. (2014) states that if the number of groups exceeds the number of data points per group, the system will be underdetermined, leading to lower

correlation results, while for number of data points per group exceeding the number of groups, over-determination will occur. This topic was discussed by Karlsen et al. (2015) who presented both grouping approaches and found differences in the results.

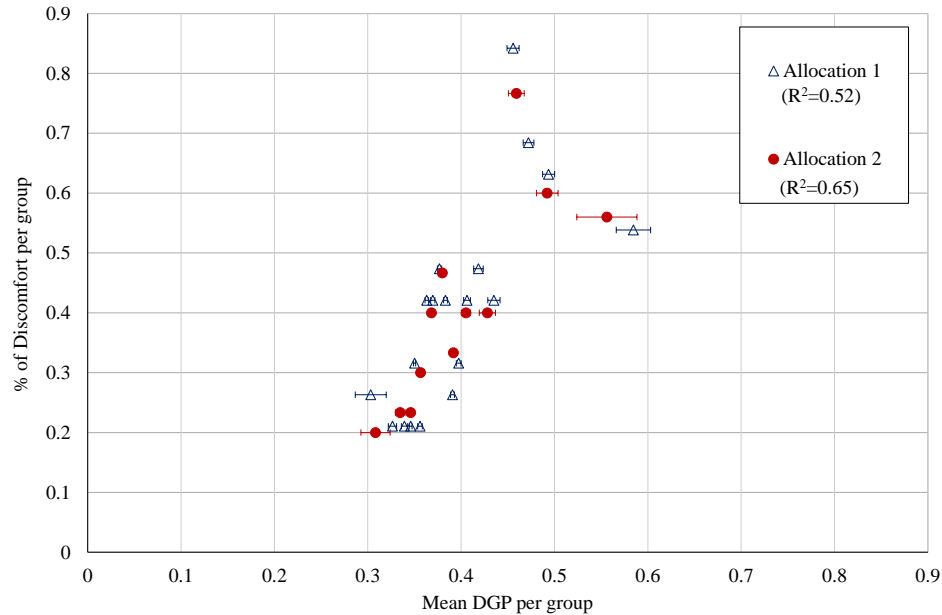


Figure 6.7 Comparison of fits for DGP (2000cd/m² threshold) using two different grouping approaches; Allocation 1 (similar number of groups and points per group) and Allocation 2 (low number of groups with an increased number of points per group).

Indeed, for the data set of this study, Fig. 6.7 shows the “inconsistency” in terms of fit for two different group splitting logics: Allocation 1 shows an approximation of the $n \times n$ rule; as dividing the 355 points data set in n groups of n points was impossible without missing valuable data points, 19 groups were used (18 groups of 19 points and a last group with the remaining 13 points). Allocation 2 shows a split in fewer groups (12) with more points (therefore added reliability) per group (30 points for 11 groups and remaining 25 points for the 12th). Confirming the points made by Hirning et al. (2014), Allocation 1 shows a considerably lower fit of the mean value of metric of each group with the percentage of discomfort ($R^2=0.52$) compared to Allocation 2 ($R^2=0.65$).

The authors of the present study consider that an increased number of data points per group would improve the validity of the results as long as a relatively low deviation around the mean would be observed for all metrics of interest for each group. Also, the same approach should be followed for the evaluation of all existing and newly developed metrics for reasons of fair comparison among them. Within that scope, the 355 total data points were split into 12 groups in total, divided to 11 groups of 30 points and 1 group of 25 points. The deviation was only slightly increased in the boundary points (1st and 12th) with that being a result of the continuity of the data set and the fabrics selection (discrete properties).

A script was created in order to sort all data points (for each metric of interest) from lowest to highest, along with the respective comfort votes, transform the four votes to a binary approach of comfort and discomfort, split the groups according to the approach described above, calculate the averages and standard deviation for each group, along with the percentage of discomfort, and then produce the respective coefficient of determination for each case. Several metrics were evaluated, including vertical illuminance (total and direct), average luminance in the visual field, DGP, UGR and DGI with different thresholds of glare sources identification. The results are shown in Table 6.5, while Fig. 6.8 shows the fit of four of the metrics of interest.

Table 6.5 Evaluation of the fit of some existing illuminance- and luminance-based metrics

Metric	No glare sources			Threshold: 2000 cd/m ²		
	$E_{v,dir}$	E_v or DGP_s	L_{avg}	DGP	DGI	UGR
R^2	0.43	0.49	0.36	0.65	0.79	0.82

As expected, metrics that were not able to describe the influence of the peak luminance of the solar disc did not manage to behave satisfactorily. Similar poor results were observed for metrics that could describe the influence of the sun but not the overall brightness (such as the vertical illuminance). UGR, which was found to perform relatively well in the study of Hirning et al. (2014) and DGI, which was not found to be an adequate metric in related studies (Van den Wymelenberg and Inanici, 2014), showed better fits than DGP. Table 6.5 shows the coefficient of determination results for the evaluated metrics.

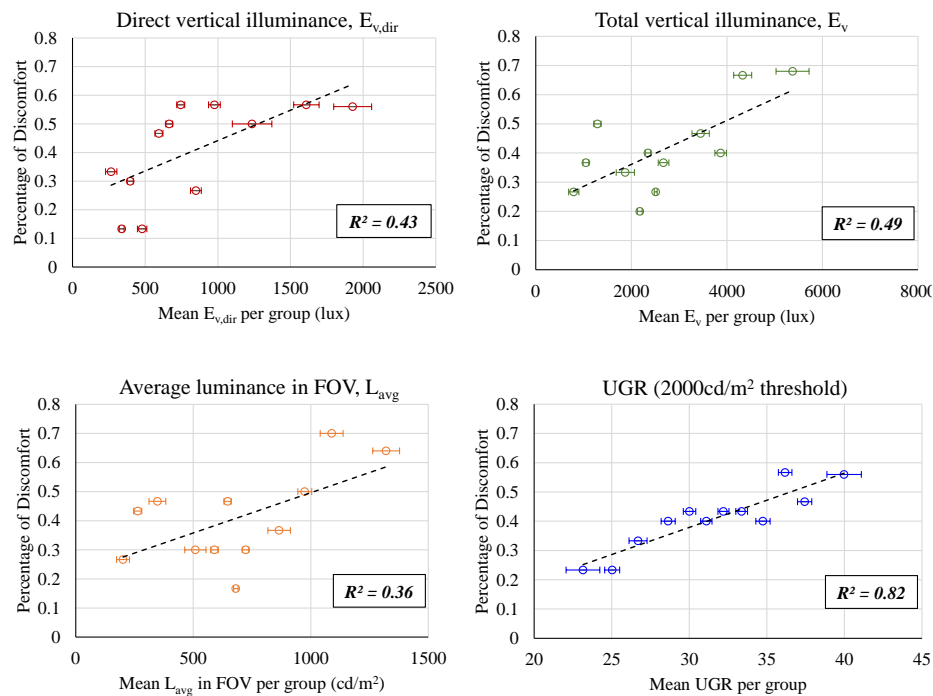


Figure 6.8 Performance of different candidate discomfort predictors

6.3.4 Modification of the DGP coefficients for cases with the sun in the field of view through roller shades

DGP is considered a generalizable glare index, as it simultaneously takes into account the overall brightness of the scene, expressed with the vertical illuminance term, as well as the individual glare sources using the luminance term. The overall brightness is

important when it comes to cases of high vertical illuminance conditions with limited glare sources (such a fully open window inflating the task area luminance). However, the results of Fig. 6.7 and Table 6.5 show a relatively poor fit of the existing DGP index for the studied cases.

For that reason, and assuming that this inconsistency might be a consequence of the specific cases met in this study (glare through fabrics with the sun visible), it was investigated whether the same form of equation could describe the current data set with a modification of its four coefficients. The number of data points was equivalent to the one in the original DGP study (355 compared to 349), therefore such an investigation would show whether indices should be fixed or if a clustering approach should be followed, having different sets of coefficients for fundamentally different kinds of environmental conditions.

An optimization algorithm was created, reading the detailed output of Evalglare, using a 2000cd/m² identification threshold and applying the genetic algorithm approach, with objective to maximize the coefficient of determination for the ordered groups of the modified DGP and the corresponding percentages of discomfort. This investigation showed that the four DGP coefficients can be indeed modified in order to describe our dataset better than any of the metrics evaluated in Table 6.5. The resulting equation with the modified coefficients is shown in Eq. 6.3.

$$\text{DGP}_{\text{mod}} = 8.4 \times 10^{-5} E_v + 11.97 \times 10^{-2} \log \left(1 + \sum_i \frac{L_{s,i}^2 \cdot \omega_{s,i}}{E_v^{2.12} \cdot p_i^2} \right) + 0.16 \quad (6.3)$$

Fig. 6.9 shows the correlation between DGP for each group and respective percentage of discomfort for the original and modified equation coefficients, with obvious improvements.

In addition, the extracted discomfort threshold based on the techniques used in section 6.3.2 is calculated equal to 0.44, slightly higher than the discomfort threshold assumed for the original DGP (0.40). This structure allows utilizing the same fundamental index for cases with and without direct sunlight on the occupant, as a dual function with different coefficients. The authors believe that the general form of the DGP equation is reasonable and adequate, and can be adjusted to account for different cases. Similar approaches may be followed for other shading or daylighting systems and further studies with human subjects are needed for that purpose. It has to be noted that since the equation was extracted from the data set of the current experiment, it can only apply to the conditions met. Using a fabric of very high openness could result to luminances of higher orders of magnitude and therefore severe disability glare, something that was not met during the experiment and could not be assumed to be described with this equation.

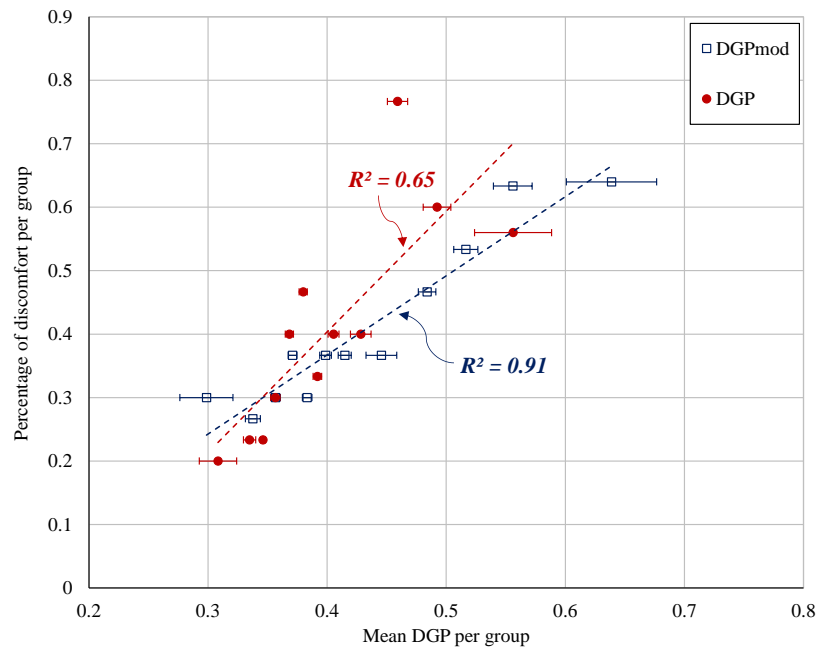


Figure 6.9 Improvement of the fit of DGP using modified coefficients for the current dataset (roller shades and sun within FOV through fabrics).

While Eq. 6.3 shows an obvious improvement in terms of describing this study's dataset over the original DGP equation, it cannot be safely assumed that it will demonstrate the same effectiveness in other studies with slightly different setups. This is an inevitable characteristic of comfort related regression approaches, as hidden factors can affect the results, causing a metric to over- or underperform in different attempts. Although care has been taken in order for the sample to be as random as possible, potential overfitting could never be entirely eliminated in such experiments with finite resources, in terms of recruited subjects and available time. This proves the necessity of a more generalized approach with specific ways of extracting and handling data in order to be possible to even combine different data sets, as discussed by Van den Wymelenberg (2014). That is also the reason why, while a similar approach was investigated for the other two main luminance-based indices (UGR and DGI), their fair fit with the data set in their current form made the formulation of a new modified index vague, as minor improvements in the fit are not necessarily generalizable in any other data sets in order to constitute an improvement.

6.3.5 Formulation of a new illuminance-based metric for assessing daylight glare with the sun in the field of view through roller shades

The final part of this study attempts to assess the efficiency and applicability of a new metric for discomfort glare evaluation, for the cases studied here, based only on vertical illuminance on the eye of the observer. While DGP (especially in its modified aspect presented above) can adequately describe discomfort with roller shades, it requires both extensive field measurements and complicated procedures (calibrated cameras with filters, automation, processing etc.), or, in the case of simulations, heavy computational load for accurate luminance mapping. Although recent computational efforts described in the

simulation methodology (Chapter 3.4) made it possible for fast calculations of luminance and DGP with implementation of real-time, model-based controls (Xiong and Tzempelikos, 2016), illuminance-based metrics would allow faster and simpler calculations and can be directly associated to shade optical properties for development of design guidelines.

As shown in section 6.3.3 and further explained in Chapter 4.3.3, total vertical illuminance or DGP_s are not applicable in cases like the focus of this study. However, a combination of a metric that solely describes the effect of the sun (direct vertical illuminance on eye) and another that captures the overall sensation of brightness (total vertical illuminance on eye) was hypothesized to adequately capture cases including the sun in the visual field but not directly looking at it (as that case would have to be assessed as disability glare). Although the presence of possible minor specular reflections within the room cannot be captured without a detailed luminance distribution, it is reasonable to believe that in the case of fully applied shading fabrics of relatively low openness, the impact of the latter on the direct vertical illuminance on the eye is negligible compared to the part directly induced by the solar disc being in the field of view. This factor, combined with the fact that no highly specular surfaces were present in the experiment, led to the assumption that the impact of projected direct light (on the desk or on the side walls) could be entirely captured by the term of the total vertical illuminance. This assumption can be corroborated by the experimental and simulation results of Chapter 4, where for the case of direct light projected on the interior surfaces, DGP_s (equivalent to total vertical illuminance) was proven to have a very good fit with DGP (extracted by the accurate luminance distribution). The algorithm presented for the modified DGP coefficients was used to associate the direct and total parts of vertical illuminance with their corresponding

comfort votes of question 5, in order to find an equation that would predict discomfort glare based on these two metrics. The two independent variables were chosen to be (i) the calculated direct (sun) part of vertical illuminance, $E_{v,dir(sun)}$, to capture the sun impact, (capturing also the position of the sun as a function of the incidence angle), and (ii) a fraction of the total (E_v) and the direct part ($E_{v,dir(sun)}$) of vertical illuminance in order to capture this interdependence between the color of a fabric, overall brightness, and the apparent intensity of the visible sun. Other combinations of direct and total vertical illuminance were also tried without satisfactory results. The best fit ($R^2 = 0.86$) is expressed by Eq. (6.4) and Fig. 6.10 shows the overall regression with the fluctuation of discomfort in ordered groups, as well as the improvement compared to standard illuminance-based metrics –total vertical illuminance or DGPs.

$$\text{Glare}_{E_v} = 0.13 \cdot E_{v,dir(sun)}^{0.27} + 0.04 \cdot \left(\frac{E_v}{E_{v,dir(sun)}} \right)^{0.84} - 0.48 \quad (6.4)$$

, for $119 < E_{v,dir(sun)} < 2228$ lux and $588 < E_{v,tot} < 5940$ lux

The normality observed in the respective comfort and discomfort groups, allowed the use of the 95% lower bound confidence interval of discomfort for the direct extraction of a discomfort threshold equal to 0.41. Although the fit is not as good compared to the modified DGP coefficients, an illuminance metric on the basis of Eq. 6.4 would simplify annual simulations, eliminating the need for a detailed luminance mapping of the interior, compensating the slight compromise in terms of fit with increased convenience of use. At the same time, it is much more effective than the only other existing illuminance-based glare metric (E_v or DGP_s) for cases with direct sunlight through fabrics.

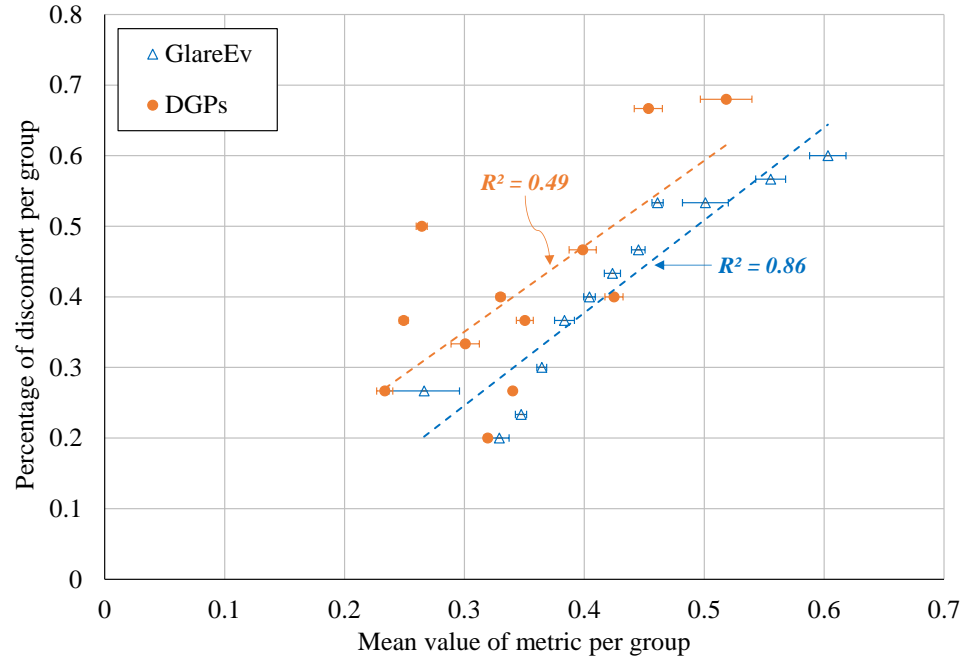


Figure 6.10 Performance of new illuminance-based glare metric compared to DGPs.

Consequently, an index in the form of equation 6 is not proposed as a successor to any of the luminance-based glare metrics -or the modified DGP equation that proved to be the best for the studied cases- but only as one (the only one for the cases studied here) alternative to vertical illuminance or DGPs, that may be used for simpler calculation in cases with direct sunlight through fabrics and relevant practical applications. Considering that the fabric OF relates to direct vertical illuminance and the fabric T_v relates to total vertical illuminance, the discomfort glare thresholds can be directly used to provide design guidelines for selecting fabric properties, as suggested by Chan et al. (2015).

It has to be noted here that Eq. (6) was extracted by calculating the direct (sun) part of vertical illuminance specifically induced by the solar disc being within the visual field, and using the validated model described in section 6.2.3, utilizing as inputs real measured values for the transmitted vertical illuminance through the glazing. This variable for Eq.

(6.4) was proposed in order to eliminate the need for heavy calculations (in case of simulations) or extensive calibrations and image processing (when it comes to field measurements), steps required for the extraction of an accurate luminance distribution). Therefore, any future use of Eq. (6.4) should be based on the assumptions discussed above, as it cannot be generalized for other methods of obtaining the overall direct part of vertical illuminance (as Evalglare does, including the impact of all identified glare sources).

6.4 Conclusion

This chapter provides new insights on daylight glare evaluation for cases with the sun in the field of view through window shades. 41 human subjects were tested while performing specific office activities near a south-facing façade equipped with 14 shade products of different openness factors and visible transmittance values (direct and total light transmission characteristics). The fabrics were carefully selected to cover a wide range of properties (OF and T_v), resulting in a large variation of vertical illuminance values on the eye and DGP ranges, to study worst case scenario situations in order to establish discomfort thresholds.

The measured variables and survey results were first used to associate discomfort glare (based on a 4-point scale) with measured direct and total vertical illuminance on the eye and with DGP. Although clear differences exist between the votes, a large deviation was observed and it was preferred to follow a dichotomous approach (comfort for votes 1 and 2 and discomfort for votes 3 and 4). This allowed the extraction of glare discomfort thresholds for direct vertical illuminance (870 lx), total vertical illuminance (2800 lux) and DGP (0.4). While these can be used as rough estimates, none of the three individual metrics

is considered entirely adequate to be a sole discomfort predictor for the studied case of roller shades with the sun present. That was also confirmed by a statistical analysis, following the method of ordered grouping. Existing metrics which are only luminance-based or only illuminance-based showed a poor performance in that regard, while DGI and UGR showed better results.

To further investigate other options for improved glare assessment metrics for the studied cases, a modified DGP equation was developed, using optimized coefficients, based on the ordered groups of the current dataset. The new equation showed the best agreement with the discomfort votes and this allows utilization of the same fundamental index for cases with and without direct sunlight on the occupant through shades, as a dual function of DGP with different coefficients. Moreover, it is reasonable to believe that the general form of the DGP equation is reasonable and adequate, and can be adjusted to account for different cases, by clustering different sets of coefficients for different environmental conditions or fenestration systems.

Finally, a new glare discomfort index was developed for the studied cases with fabrics and the sun visible through them, based on direct and total-to-direct vertical illuminance on the eye. The direct illuminance captures the impact of sunlight whereas the second variable captures the interdependence between the color of a fabric, overall brightness, and the apparent intensity of the visible sun. The new index can simplify annual simulations, eliminating the need for a detailed luminance mapping of the interior, and can be directly associated with fabric optical properties for development of design guidelines.

The results presented in this study are only applicable to roller shades. Combining illuminance-based metrics and existing glare indices can result in a more realistic glare

evaluation covering all cases with and without the sun through shading fabrics, and potentially through other systems. Further similar human subject studies with different datasets and similar or higher numbers of observations are needed to apply the new equations and metrics, further validate the respective discomfort thresholds and hopefully extend the present findings

CHAPTER 7. A METHOD FOR QUANTIFYING VIEW CLARITY THROUGH WINDOWS WITH SHADING FABRICS

7.1 Introduction and Experimental Methodology

Visual comfort may be a priority in design, however the overall satisfaction of occupants is also depending on one other important field, the connection to the outdoors. Occupants want to be able to see outside and have the impression of direct contact with the exterior environment. This can either be established by shading controls which can keep a considerable portion of the window unshaded, or with fabrics that allow clear outside view. Clarity of view is a topic not well studied, especially when it comes to windows with shading fabrics. For that reason, an experimental field study with the participation of eighteen subjects, was performed.

The subjects were 23 to 55 years old, while six of them were female and twelve male. An approval from Institutional Review Board was obtained (IRB #1410015323) before starting the experiments. All participants in this study were reported to have satisfactory visual acuity, as the ones that were using visual aids (glasses or contact lenses) were all equipped with them during the experimental sessions. Additionally, in order to verify this consideration, a reference objective test case without shading was tested for each session. The experiments were conducted in the Façade Engineering Labs at Bowen Laboratories, Purdue University. The rooms were slightly modified in order to have six (3

in each room) separate and view-isolated partitions for subjects to evaluate each fabric (Figure 7.1).



Figure 7.1 Modified room with three partitions (left) – Attached charts with Landolt-C tests (right)

Two separate sets of “external” parameters were considered in the experiments: Different sky conditions and different distances from the window for the subjects. As sky conditions affect the overall outside luminance and illuminance levels, different tests were conducted for sunny and cloudy days in order to investigate the potential impact of exterior conditions and differences between the studied cases.

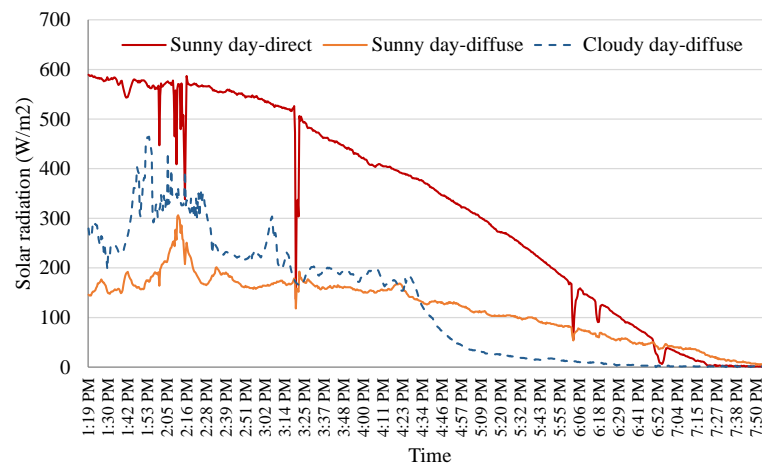


Figure 7.2 Typical variation of direct and diffuse solar radiation on the windows with installed shading fabrics during the field tests.

Figure 7.2 shows typical solar radiation values during the periods of testing (early afternoon). It was decided, during the experiment to prevent the sun from being within the direct field of view of the participants, as the potential influence of glare on view clarity impression was out of the scope of this pilot study.

The tests were conducted under standard office lighting conditions. The F54T4HO lamps were automatically controlled to provide at least 500 lux of horizontal illuminance on the work plane, in order to provide realistic luminance and contrast conditions for the interior. It has to be noted that electric lighting can have a significant influence in the perception of view. High electric light levels with relatively dark exterior conditions can lead to the perception of less clear views compared to dark interior with bright exterior conditions. However, due to the experimental setup (2 rooms that accommodated simultaneously three fabrics each), and the fact that luminaires in the rooms were not assigned in a way where each luminaire was over one specific partition, it was impossible to maintain at the same time 500 lux for all partitions. Therefore, and in agreement with the fact that, while there is a minimum work plane illuminance level for almost all different spaces, there is no such standard value about the maximum illuminance, a decision was made to recalibrate the electric lighting system in order for all partitions to have at least 500 lux at the work plane.

Empirical observation from everyday practice have shown that in the case of fabrics, the weave construction can affect the perception of clarity. The amount of weave density viewable from the observer is depending on the position of the latter; subjects that are standing very close to the fabric tend to observe the knits, while for further distances, the subjects tend to focus more to the exterior (Fig. 7.3). Therefore, to capture this effect, the

testing for all cases was repeated for two viewing positions (both facing the window): 1 m and 2.4 m away from the window. The analysis of variance performed, shown in detail in the next subchapter, showed that the viewing distance was indeed a significant factor. It has to be noted that Brand (2006) states that the importance of sitting close to a window relates to the percent exterior view made available. Office workers might be seated close or further away from windows, therefore this parameter was worth studying.



Figure 7.3 Outside view impression (camera images) with a light-colored shade for different viewing distances from the window: 0.5m (left), 1m (middle) and 2m (right).

The participants were randomly separated into three groups of six, to conduct the field study efficiently using the six partitioned areas. Each group was tested under sunny and

cloudy conditions and two viewing positions (close and further away from the windows), for all selected shading fabrics, following a within subjects approach. Sunny day testing preceded cloudy day testing in all cases due to convenience and availability of weather conditions. In the beginning of each testing day, a short presentation of the procedure was made, and shades were removed from one of the partitioned sections, to provide the participants with a baseline of “maximum” view clarity (and later normalize all total view clarity scores), as well as to confirm that none of the subjects was visually impaired. One of the fabrics (E), empirically considered to have intermediate level of clarity was selected for repeated measurements during all the sessions to ensure the reliability of results. Therefore, for each measuring day (sky conditions), each participant was given 32 questionnaires (14 different fabric tests plus one repeated fabric test and one test without shades, all for each view position).

Each testing set (specific group and sky conditions) consisted of three sessions, arranged as follows. First, all six participants in the group completed the questionnaires for the two viewing positions with each fabric: after finishing the test with the first fabric, they rotated clockwise (moved to adjacent partitioned area with a different fabric), and repeated the procedure until all six shades had been experienced by all six participants. Then, the next set of six shades were installed on the windows and the entire procedure was repeated. The order of participants and fabrics was randomized. The third session included three general impression/preferences questions (not used in the results). The exact same process was followed for each group, for different measurement days (outside conditions).

The fabrics were products in the market, of variable openness factor from 0.8% to 13% and visible transmittances of 2.8% to 25.1%, selected to cover the most

commonly used range, and four different main colors (black, white, grey and brown). The selection of the fabrics can be seen in Table 7.1. The questionnaires used in the main procedure were in the form of Fig. 7.4. Eight questions were used in total. The data collected from the first six questions was used for the quantitative part of the study, while questions 7 and 8 were related to the general impression of visual comfort and clarity satisfaction, potentially useful for future studies and correlations.

Table 7.1 Fabrics used in the View Clarity study

Fabric code	Product code #
A	S3030-E-1
B	S0207-E-1
C	S0202-E-1
D	S3030-E-3
E	S0710-M-3
F	S3071-E-3
G	S3271-KB-3
H	S0202-E-3
I	S3030-E-5
J	S0207-E-5
K	S0202-E-5
L	S3030-E-10
M	S0207-E-10
N	S0202-E-10

7.2 Questionnaires – Data collection

The first three questions were of subjective nature, using a 7-point Likert scale and asking about the individual perception of clarity of view, visibility of the exterior sky conditions and vividness of the outside colors. This inclusion of color rendering, discrimination and border sharpness was a result that the above reflect the impression of view clarity (Vrabel et al., 1998).

Fabric Code _____

F

1. How clear is your outside view through the window and shade?

Not clear at all ☐ ☐ ☐ ☐ ☐ ☐ ☐ Very clear

2. Can you tell the sky conditions outside by what you can see (sunny/cloudy/extends of clouds)?

Not clear at all ☐ ☐ ☐ ☐ ☐ ☐ ☐ Very clear

3. How would you grade the vividness of the outside colors?


Not vivid at all ☐ ☐ ☐ ☐ ☐ ☐ ☐ Very vivid

4. Which outside objects can you distinguish from the following: Fence, Street, Power cables?
-
- Please circle
- all that apply
- :

None Fence Street Power cables

5. Can you clearly distinguish the color of moving cars on the street?

Yes No

6. Observe the target outside the window, and count how many
- 
- symbols you can clearly distinguish for each line:

1st line _____ 2nd line _____ 3rd line _____ 4th line _____ 5th line _____

7. Are you satisfied with the visual comfort conditions (glare, reflections, etc)?

Not at all ☐ ☐ ☐ ☐ ☐ ☐ ☐ Very much

8. How would you comment about this fabric? (Circle
- all that apply
-):

Too bright Too dark Good color
Too open Too opaque Good openness/transparency

Figure 7.4 Questionnaire used in the main procedure

The first three questions were of subjective nature, using a 7-point Likert scale and asking about the individual perception of clarity of view, visibility of the exterior sky conditions and vividness of the outside colors. This inclusion of color rendering, discrimination and border sharpness was a result that the above reflect the impression of

view clarity (Vrabel et al., 1998). Questions 4 and 5 were of more objective nature, asking for the visibility of three specific “layers of view”, objects at different distances from the window and the perception of the color of cars moving on the road about 30m away. The trigger of question 6 was the conclusion of a study by Hellinga and Hordijk (2014) that the more layers visible, the higher the quality of view.

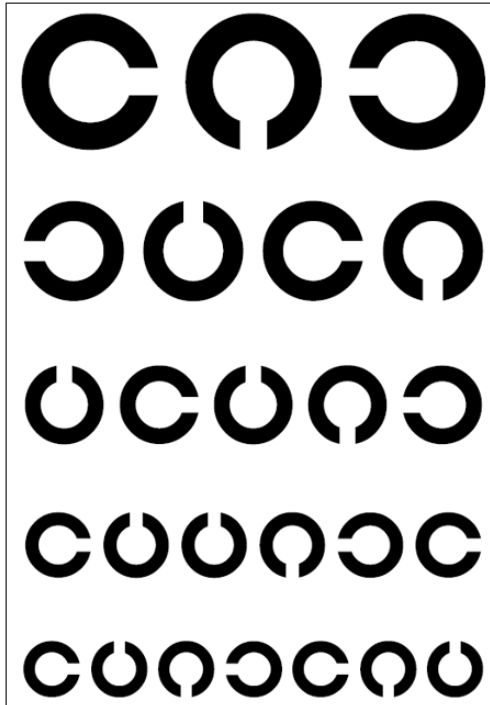


Figure 7.5 Example of modified Landolt–C test used for collecting data for Question 6.

Question 6 was entirely objective, as at the same time, it was asking for specific information and also allowed the investigators to measure the accuracy of the responses. Based on a modified Landolt-C visual acuity test (Bondarko and Danilova, 1997), it asked from the subjects to count the instances of a certain direction of the C symbol on every line, observing vertical view boards mounted on a fence averagely 4.5m away from the window (Fig 7.1 - right). Different variations and symbols were used in different view sections

(partitioned areas). To eliminate possible effects of variation in terms of sharpness of vision, only the first 5 lines of the typical Landolt-C test's 10 lines were used (Figure 7.5). In order to prevent subjects from remembering the amount they counted for the back position, the amount of instances of another rotation of the symbol was asked for the front position, while every partition had a different board attached in front. The responses were graded as the number of lines for which the number of symbols was identified correctly, independent from the line sequence. Therefore, the scoring for that specific question varied from 0 to 5. Questions 7 and 8 were not included in the analysis and the rankings, but were added as general impressions questions, to potentially associate view clarity impressions with other parameters such as glare sensation or fabric color for future studies.

7.3 Total scores and fabric rankings

1152 questionnaires were used in the analysis (18 participants, 16 shade test cases, 2 viewing positions and 2 sky conditions), with 6912 total responses for all questions collected. Since different questions had different numbers of possible answers (Appendix A), all answers were normalized to a scale from 0 to 1 (e.g., for the 7-Likert scale, minimum rating of 1 corresponds to normalized score of 0). In absence of similar studies in existing literature, the total responses from the six main questions were weighted equally. The averaged normalized scores for the two sky conditions and the two viewing positions (to capture the effect of view distance) were used to develop a total view clarity score. As the glazing was highly transparent in the visible spectrum, the test scores for unshaded windows were used to account for small errors (0.03%) in the total view clarity scores due to visual acuity/experimental procedure.

The analysis led to the development of the *View Clarity Index (VCI)*, a new metric that can be used to evaluate the perceived clarity of view through window shades, for any type of common glazing product. The overall rankings for all studied fabrics (including their measured optical properties) and the *measured total normalized view clarity score* can be seen in Table 7.2.

Table 7.2: Measured view clarity score and ranking of all fabrics with properties

Rank	Fabric code	Fabric Color	Measured OF	Measured T_v	Normalized view clarity score
1	L	Black	11.30%	12%	0.893
2	I	Black	7.00%	7.30%	0.817
3	D	Black	3.70%	4.10%	0.73
4	M	Grey	12.60%	19.90%	0.682
5	N	White	12.50%	25.10%	0.585
6	J	Grey	6.70%	13.00%	0.56
7	G	Brown	3.90%	5.90%	0.531
8	A	Black	2.60%	2.80%	0.527
9	F	Brown	3.00%	4.50%	0.42
10	K	White	5.90%	18.20%	0.298
11	E	Grey	2.30%	6.60%	0.212
12	H	White	3.90%	15.90%	0.187
13	C	White	1.60%	13.70%	0.026
14	B	Grey	0.70%	6.40%	0.013
N/A	P	N/A	N/A	N/A	1

It is apparent that openness factor, color, and visible transmittance all play a role in total view score and preferred clarity of view. The three top ranked shades are dark-colored, but their OF values are quite different. However, the OF and T_v values are close (indicating small direct-diffuse light transmittance), which is considered in the development of a view clarity model presented later – note that this is not the case for fabric A that has a smaller OF . The next three white or grey-colored fabrics also rank high, and their properties are again diverse. Light-colored shades with low openness factors have the lowest view clarity scores.

7.4 Descriptive statistics

In order to ensure that participants responded thoughtfully to the questions, a few tests with the same fabrics were repeated. For Fabric E, which was repeatedly tested during both sunny and cloudy conditions for all participants, a reliability analysis with Cronbach's alpha showed acceptable results (> 0.7), indicating that responses are consistent. All variables were tested for normality and had both skewness and kurtosis values less than ± 3 . The mean normalized view clarity score was equal to 0.413 ($\sigma=0.265$). Fig. 7.6 presents the normalized score distributions for each fabric, separately for sunny and cloudy conditions (including responses from all participants).

The bar colors represent the actual fabric colors, while the bar texture density reflects the fabric weave density (more tight fabrics with low OF appear in more dense textures). Case P (no shading) shows a clear ceiling effect without dispersion, proving that the responses were reliable and that visual acuity was not an issue. For both sky conditions, darker fabrics with higher openness factors generally achieve higher scores with some

exceptions (e.g., fabrics D, J, M, and N). Overall, the score distribution varies for different fabrics without following an apparent trend, proving that the impact of the combined shade properties is complex. Only in the cases of fabrics B and C there is negligible deviation; these are the lowest-ranked fabrics (light color, tight weave) and are better suited for privacy instead of outside view. In Fig. 7.6 one can also observe the differences in scoring distributions between sunny and cloudy conditions, which are discussed next.

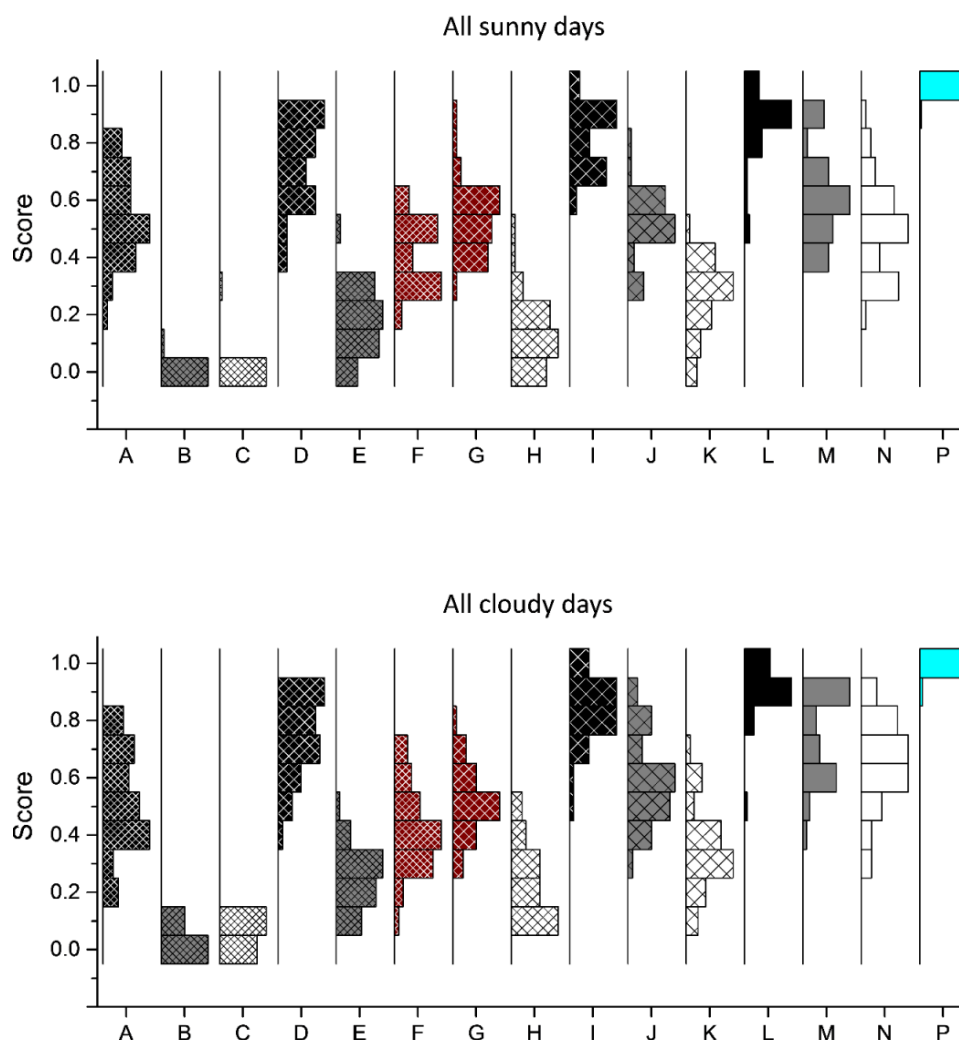


Figure 7.6 Distributions of normalized view clarity score for each fabric for all measurements during sunny days (top) and cloudy days (bottom). Bar colors reflect actual fabric colors and bar texture density indicates fabric knit/weave density.

7.5 An empirical model for predicting the view clarity index

The processed results of the field study were also used to develop an equation that calculates the *View Clarity Index* for window shades, using only the basic shade properties (openness factor and normal visible transmittance) as inputs. These properties are usually provided by manufacturers; therefore, the developed model can be directly used to characterize common window shade products. It has to be noted here that manufacturers actually provide inaccurate values of these properties due to lack of measurements and labeling standards in the industry.

Table 7.3 Differences between labeled and measured fabric properties used in the study

Label	Fabric Card		Actual measured	
	OF	Tv	OF	Tv
A	1%	1%	2.30%	2.80%
B	1%	6%	0.70%	6.40%
C	1%	11%	1.60%	13.70%
D	3%	4%	3.70%	4.10%
E	3%	7%	2.30%	6.60%
F	3%	7%	3.00%	4.50%
G	3%	7%	3.90%	5.90%
H	3%	13%	3.90%	15.90%
I	5%	4%	7.00%	7.30%
J	5%	9%	6.70%	13.00%
K	5%	17%	5.90%	18.20%
L	10%	12%	11.30%	12.00%
M	10%	18%	12.60%	19.90%
N	10%	22%	12.50%	25.10%

Table 7.3 presents listed and detailed measured values for 14 different fabrics, with evident differences in both OF and Tv values. This inconsistency may lead to incorrect architectural and design specifications decisions with respect to selecting specific fabrics

for glare protection. The above underlines the need for a standardized approach in labeling properties among manufacturers.

As explained above, the relationship between openness factor (OF), color (R_v), and visible transmittance (T_v) is non-linear and cannot be simply formulized. Consequently, the impact of these parameters and their interactions need to be included in the empirical model. The view clarity results of Table 7.2 show that darker fabrics with noticeable OF (considerable direct-direct light transmission) are ranked highest, followed by light-colored fabrics with high OF and T_v , and then dark or colored fabrics with small OF ; light-colored fabrics with low OF (significant direct-diffuse light transmission) received the lowest scores. An empirical model was developed from the measured clarity scores in order to capture these effects, considering also the need for a relatively simple form that contains only the basic shade properties and parameters that have a physical meaning.

The model uses only two parameters: the OF and a parameter representing the fraction of direct-to-total light transmission (OF/T_v). This ratio is also related to fabric reflectivity – it is maximized for dark-colored fabrics and minimized for light-colored fabrics. Note that $OF < T_v$ for any shading device. Following this approach, the following form was considered, since view clarity should increase non-linearly with both parameters:

$$\text{View Clarity} = a \cdot (OF)^b + c \cdot \left(\frac{OF}{T_v} \right)^d + e \quad (7.1)$$

A very satisfactory fit (Fig. 7.7) with experimental results was obtained for $a = 1.43$, $b = 0.48$, $c = 0.64$, $d = 1.09$ and $e = -0.22$. Several other forms were investigated, including fabric visible reflectivity as a parameter, without improving the model accuracy. The above

regression model was thus considered the most reliable and the following equation is used to define the *View Clarity Index*:

$$VCI = 1.43 \cdot (OF)^{0.48} + 0.64 \cdot \left(\frac{OF}{T_v} \right)^{1.1} - 0.22 \quad (7.2)$$

Eq. (7.2) can be used to calculate the View Clarity Index for any common window shade or fabric product using basic, publicly available information. The permitted values of the equation range from 0 to 1, as for diffuse fabrics the clarity is by definition equal to zero, while in the experimental procedure, 1 was the grade given to the unshaded baseline case. The overall comparison between measured scores and VCI values is shown in Fig. 7.7, for all 14 measured window shades. Given the partially subjective nature of this metric, the agreement is quite satisfactory ($R^2 = 0.970$ and $SSE = 0.03$), while the fit of the residues with normality can be observed in Fig. 7.8. A 2-D representation of the VCI variation with OF and T_v is shown in Fig. 7.9.

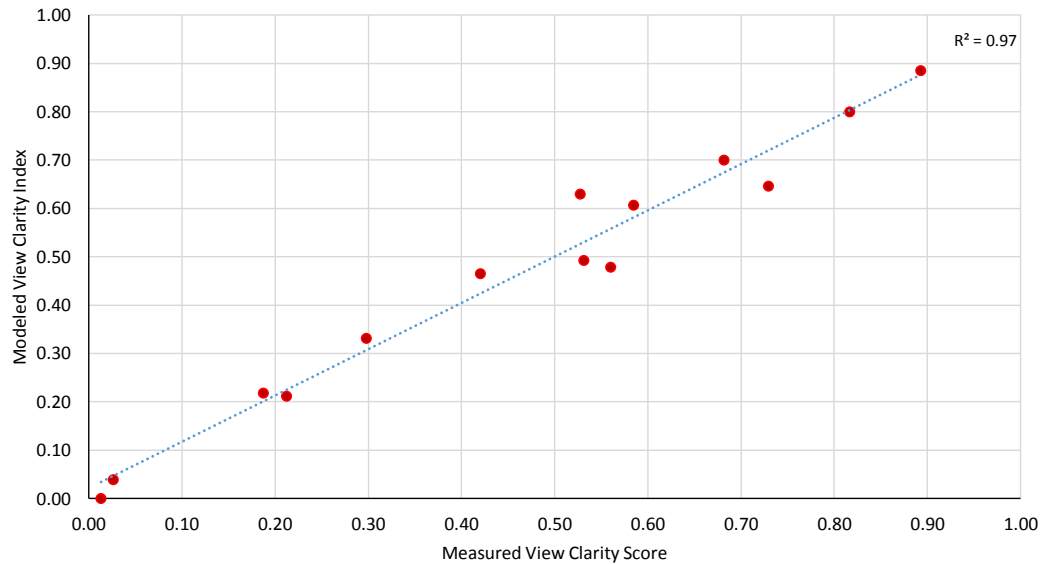


Figure 7.7 Overall comparison between measured view clarity scores and View Clarity Index for all studied window shades.

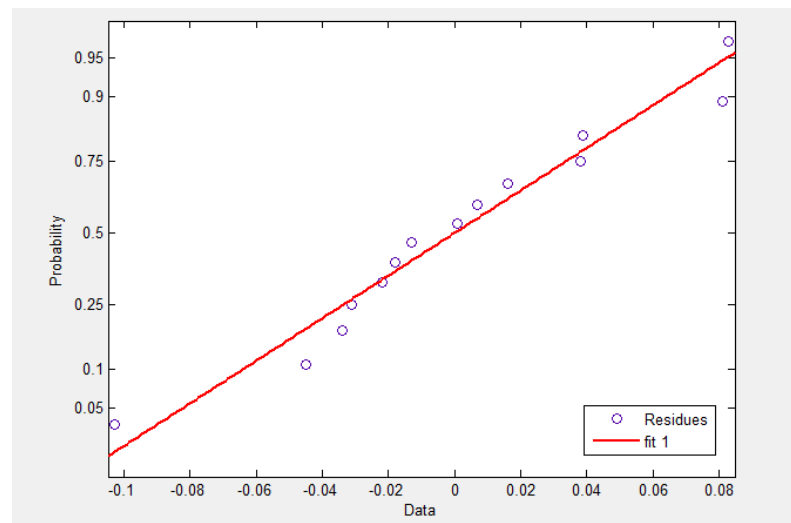


Figure 7.8 QQ plot – Residues are approaching normality even with the limited number of data points

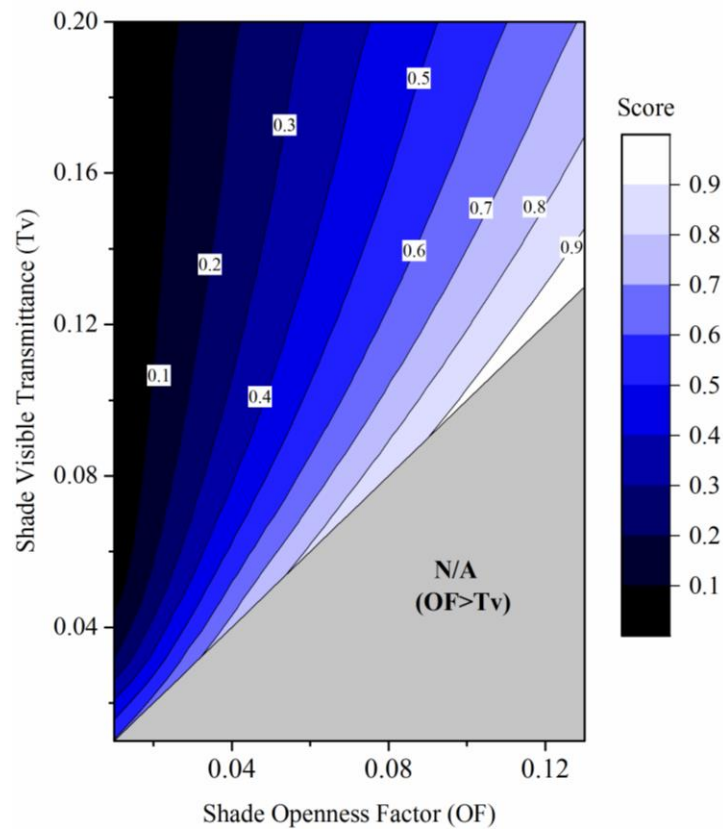


Figure 7.9 View Clarity Index as a function of fabric OF and T_v . The gray area is not applicable since T_v must be higher than OF.

7.6 Analysis of variance results

As mentioned above, two “external” parameters were considered, exterior sky conditions and distance from the window. Having a detailed quantitative view of their dependence was out of the scope of this study, as, especially in the case of exterior sky conditions it was impossible to conduct a controlled study with variable sky covering. For similar reasons, distance from glass was not a parameter that could be included in the equation, as in every office, especially in open plan cases, seating is random. Therefore, these parameters were only studied in terms of significance to clarify the necessity of future studies based on them. Because the study used a within-subject design in which each participant received all conditions, a repeated-measures analysis of variance (ANOVA) with a 2 x 2 x 15 factorial design was conducted, in order to explore dependencies of view clarity on variables such as weather conditions or distance from the fabric.

Table 7.4 ANOVA results for the overall view clarity score

Independent Variables	Df	F	p	η^2
Fabric	5.7, 97.2	203.33	0	0.923
Weather	1, 17	27.757	0	0.62
Distance	1, 17	38.44	0	0.693
Fabric * Weather	4.8, 82.1	6.556	0	0.278
Fabric * Distance	6.7, 114.2	4.215	0	0.199
Weather * Distance	1, 17	0.008	0.929	0
Fabric * Weather * Distance	6.7, 113.1	0.844	0.548	0.047

Such an ANOVA includes subjects as a blocking factor and extracts the between-subjects variability from the within-subject error terms. The independent variables were (i) sky conditions (sunny vs. cloudy), (ii) viewing distance (near vs. far) and (iii) fabrics (14 different shading fabrics plus one case P without shading). Primarily, the analysis (Table 7.4) revealed a main effect of fabric, which confirms that the fabrics were indeed different from each other in terms of view clarity. Yet, in a few cases, such as fabrics B and C, the differences were negligible as the view clarity score approaches zero. The results incorporate the Greenhouse-Geisser correction for deviations from sphericity (Abdi, 2010).

The main effect of sky conditions proved to be significant as well. Specifically, slightly higher scores were generally observed for cloudy conditions. Note that the cloudy sky tests followed the sunny sky tests; therefore, a possible sequence effect cannot be neglected. Nevertheless, both cloudy and sunny tests were conducted on different (and random) days for each group of participants. Post hoc paired samples t-tests were conducted to observe the differences between fabrics. The alpha level of the t-tests was adjusted to 0.00166 using the Bonferroni (1936) method to avoid alpha-error inflation, which would otherwise create significant results by chance. The fabrics H, E, J, M and N showed significantly higher scores for cloudy conditions. For other fabrics, a numerical trend in this direction was also noticed (Fig. 7.10), but did not reach the level of significance, which is probably due to the selected conservative alpha-level. Moreover, the effect of sky conditions does not severely affect the overall ranking. Fabrics M and N have the highest OF and T_v , and direct-diffuse light transmission effects are dominant.

Viewing distance was also a significant factor: a longer distance (2.4 m from window) achieved higher view clarity than a smaller distance (1 m from window) for the majority

of fabrics (Fig. 7.11). The post hoc analysis of the interaction between fabric and viewing distance showed significantly higher scores at a longer distance for fabrics E, F, G, J, D, M and N. The viewing distance did not affect the overall ranking. It should also be mentioned that the interaction of sky conditions and viewing distance was not significant, and neither was the higher-order three-way interaction. This indicates that these factors are independent and so is their influence on the different shading fabrics.

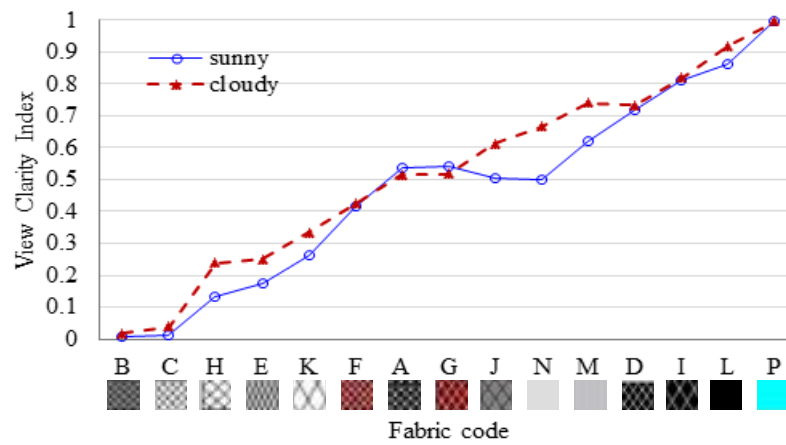


Figure 7.10 Interaction between sky conditions and shading fabrics.

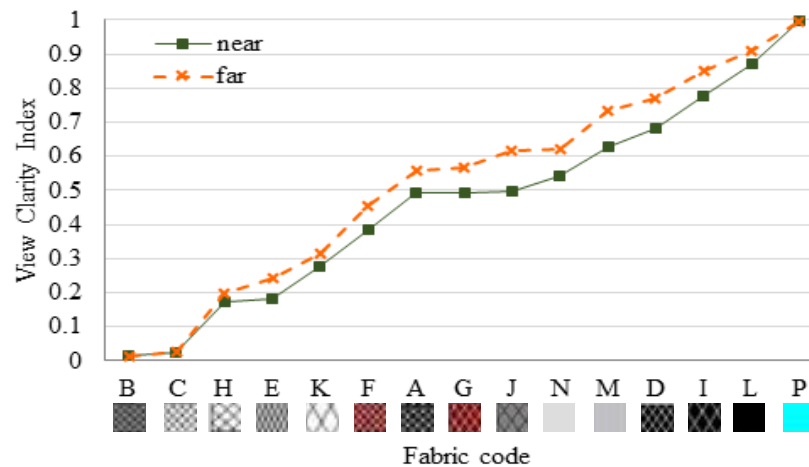


Figure 7.11 Interaction between viewing distance and shading fabrics.

As Question 6 (Landolt-C test) provided an objective set of responses in the field study (by asking for specific symbol appearances and having the responses corrected), these results were analyzed separately, to examine potential inconsistencies between these responses and the overall view clarity score. The same 2 x 2 x 15 repeated-measures ANOVA was conducted for the entire set of objective observations (Table 7.5).

Table 7.5 ANOVA results for the objective (C-chart) scores

Independent Variables	df	F	p	η^2
Fabric	14, 238	194.365	0	0.92
Weather	1, 17	1.625	0.22	0.087
Distance	1, 17	56.975	0	0.77
Fabric * Weather	14, 238	4.35	0	0.204
Fabric * Distance	14, 238	9.935	0	0.369
Weather * Distance	1, 17	2.914	0.106	0.146
Fabric * Weather * Distance	14, 238	1.66	0.065	0.089

Similar to the overall score analysis, the main effects of fabric, and viewing distance were significant. It should be mentioned here, that the latter effect is even underestimated in this analysis, because the Landolt-Charts were fixed, while the participants moved backwards in the back viewing position. This means, they saw a comparably smaller Landolt-Chart than in the previous position. The main effect of sky conditions was not present in this objective measurement. The interactions of fabric and sky conditions, and fabric and viewing distance were again detected. The deviation in the main effect of sky conditions (but not in the weather and fabric interaction) suggests that the subjective fabric ratings are more influenced by sky conditions compared to the objective tests. Still, the fabric-weather interaction is present and fabrics J, M, N and H show higher view clarity scores for cloudy conditions in the post-hoc analysis: $t(17) > 2.51$; $p < 0.0011$ (adjusted significance-level=0.00167).

Overall, the ANOVA results showed that the data were appropriately collected, as an acceptable level of reliability was reached. Significant differences in view clarity scores for different fabrics were observed as expected. Some fabrics had a very high score (e.g., fabrics L, I and D), whereas the clarity of view was almost zero for others (e.g., fabrics B and C). Furthermore, the hypothesized influence of viewing distance and sky conditions was confirmed. For most fabrics, the view clarity score was higher for the farther viewing distance, and similarly for cloudy conditions. Nevertheless, the rank order is not affected by sky conditions or viewing distance, allowing the development of a formula for prediction of *View Clarity Index*, based on elimination of these parameters using average values instead, as described next, applicable to different sky conditions and viewing distances up to 2.5m. A more meticulous analysis of the influences of distance and outside sky conditions was outside the scope of this study, which aimed to suggest a methodology of evaluating clarity of view from commonly available fabric properties. This kind of analysis would require more viewing distances and a high variety of data about transmitted illuminance from the window, amount of clouds, etc.

7.7 General Impressions

For reference, subjects after each measurement day answered three general questions (Fig. 7.12) to give their overall impressions of the fabrics they have been evaluating.

The first question was asking whether the color of the fabric was affecting the clarity of view, the second was about the subject's color preferences in fabrics, and the third was about general preferences on opaque or open fabrics. Figure 7.13 shows the

overall responses (as there were no significant differences for sunny or cloudy measuring days). Overall the subjects reported that color plays a significant role in terms of clarity, showed a slight preference towards dark colors (48.57% against 40% for bright), and a strong preference towards transparent fabrics against opaque (85.71%).

General questionnaire (used once for each measurement day)

1. Do you think that the fabric color influences the clarity of the outside view?
 - a. Yes
 - b. No
 - c. I don't know/I'm not sure
2. Do you generally prefer the lighter or the darker fabrics?
 - a. Lighter
 - b. Darker
 - c. I don't care/I'm not sure
3. Do you generally prefer the more transparent or the more opaque fabrics?
 - a. More transparent
 - b. More opaque
 - c. I don't care/I'm not sure

Figure 7.12 General Impressions questionnaire

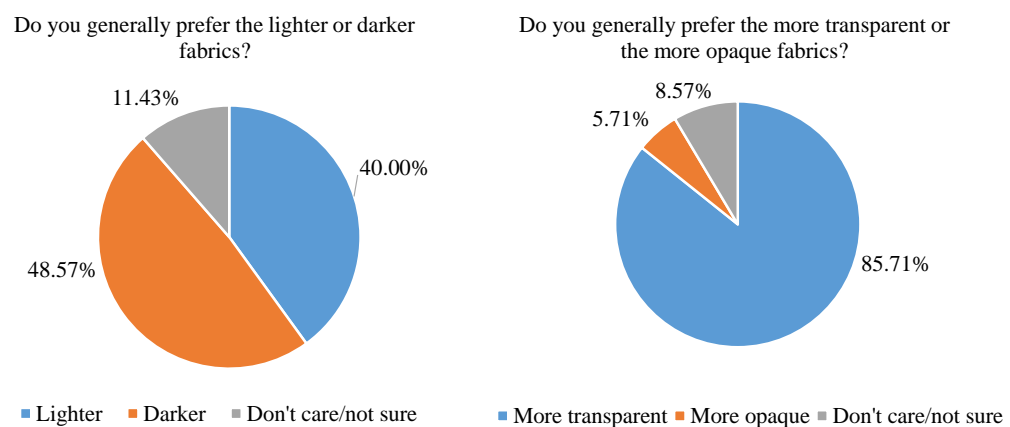


Figure 7.13 General impressions responses

7.8 Visual comfort, color and transparency preferences

Two more questions were included in the surveys, as mentioned above. These questions were neither participating in the grading of the fabrics nor in the regression procedure, as they both were entirely subjective and targeting to get the impressions of the participants concerning a very vague field as the visual comfort and the color and transparency of the fabrics.

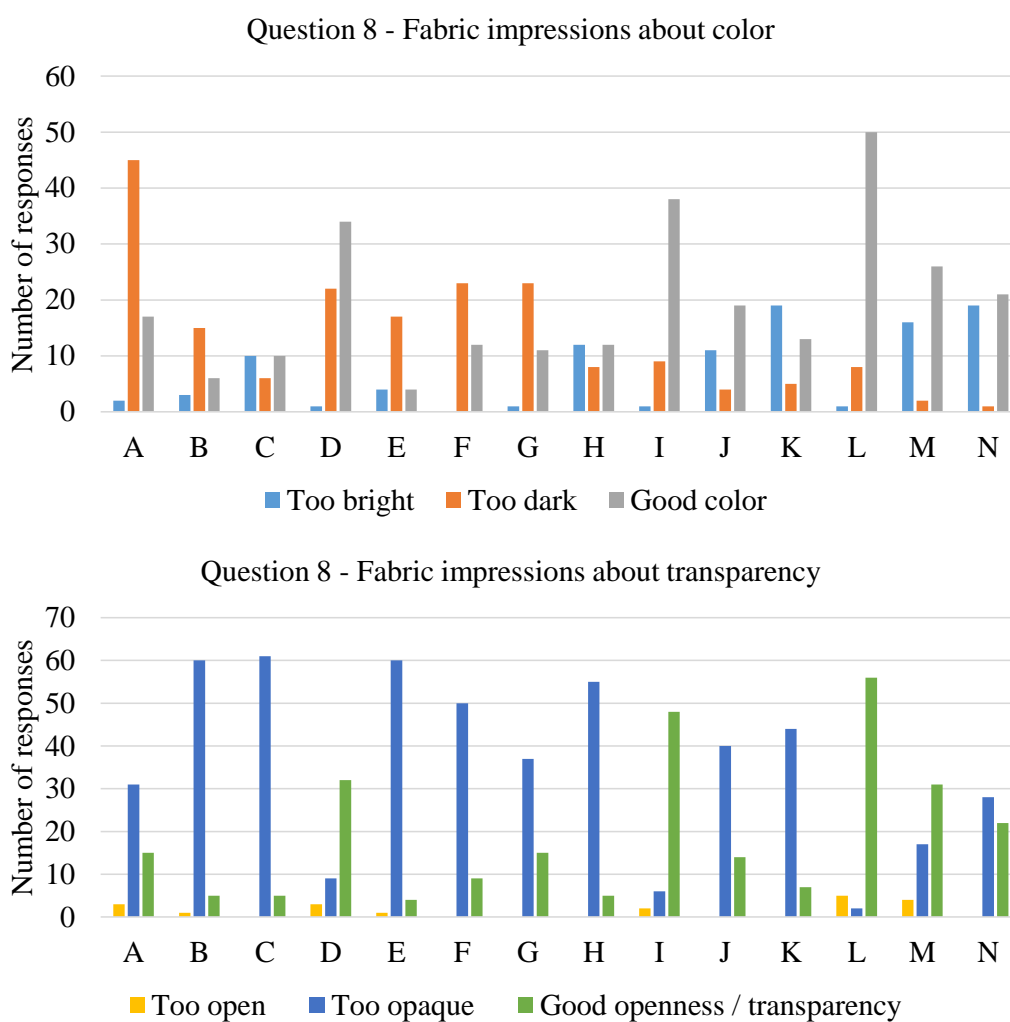


Figure 7.14 Responses for Q8 in terms of color (top) and transparency (bottom)

For the visual comfort question, the impressions were consistent to the general ranking of the fabrics, putting the black fabrics with OF relatively similar to Tv in the first three places. That proves a common and proven belief, that discomfort glare, in cases when the observer is not facing the sun in the interior (therefore without direct light hitting the eye), is more apparent in cases of bright colored fabrics with high direct-diffuse component. These impressions should however by no means be associated with high glare performance for these fabrics; In cases where the sun is within the field of view (winter time for south-facing facades or most of the year for west-facing cases), high values for OF allow direct light to reach the eye of the occupants, resulting in intolerable levels of discomfort. In addition, as the scope of this study was strictly related to the clarity of view, the participants were asked to focus their vision on the targets outside, something entirely inconsistent with the common practice in glare evaluation, where subjects are usually focusing on their work areas.

For the question concerning fabric impressions, the graphs of Figure 7.14 show the total recorded number of instances for each characterization regarding impressions about color and transparency. The data extracted from question 8 is generally consistent with the rest of the grade-participating questions, verifying the validity of the experiment:

- The dark black fabrics are indeed showing the optimal transparency/openness (D,I,L), something that verifies the ranking of them as top three in the results
- The black fabrics also have the highest ‘good color’ proportions, indicating a general preference to black color. (also consistent to the ranking)
- The characterization of too dark did not show any specific trend for color, as highest scores were for fabrics A (black), F (brown), D (black), E (grey) and G (brown).

However, all the above fabrics had a measured visible transmittance of 3-8 %, relatively consistent with the characterization.

- Fabrics B, C, E, F, H, J and K were also characterized as too bright. Leaving the inconsistencies for E and F (which were also said to be too dark), C, H, J and K had higher visible transmittances. However B was considered to be too bright with a small transmittance of 6%, having however the lowest openness in the test (0.67%). This shows the importance of the factor H_o/T_v .
- Fabrics B, C, E, F, H which are characterized as ‘too opaque’ received scores below 0.5 and standing in the last places of the ranking table.
- None of the fabrics has a significant ‘too open’ characterization, showing that, at least to the extent that participants understand, openness at this range (1.60%-12.60%) is never too high.

7.9 Limitations

Although this study covered a wide range of openness factors and visible transmittance values, it was impossible to include an entirely diverse variety of materials, colors and styles. Future studies should include other materials and shading types, as well as tests with obstructed views (in dense areas with high-rise buildings), to provide more data towards a unified View Clarity Index in buildings.

It has to be noted that the majority of products tested in this study were of the same type (thickness and weave configuration), common for most commercial applications. It is reasonable to believe that no meaningful differences would be observed for other fabric styles, as the values for openness and visible transmittance represent the characteristics of

the fabric, as used in the current developed VCI model, but future studies are needed to confirm this assumption. The range of openness factor and visible transmittance values tested in this study (0.7-13% and 3-25% respectively) are considered to cover a complete range of common products used in commercial buildings. Extreme values for these properties were not tested, since they will result in significant glare problems. Also, very low openness values (0-0.5%) accompanied by high values of visible transmittance would result to apparent “negative” values of the VCI. These values should be considered to be equal to zero, as there is no practical meaning of VCI for values except the range 0 to 1. In addition, only interior shades were included in this work. Exterior products may consist of different materials (e.g., aluminum) and will result in different perception of view clarity for several reasons (different reflectivity, possible specularly, luminance, construction, light transmission, etc.).

The developed model is supposed to cover different fabric colors (and reflectivities) with high accuracy. However, it is possible that fabrics with vivid colors (other than variations of black, grey, brown, cream and white used here), although rarely used in commercial buildings, can affect visual impression in alternate ways. In such cases, as well for some dual-sided fabrics, fabric visible reflectivity might be required as an additional factor in Eq. (7.2) to obtain better results, although this property is not currently provided by manufacturers (solar reflectivity is sometimes given, but differs from the visible values).

The tests in this study were conducted under standard office lighting conditions. The electric lights (typical office luminaires with F54T5HO lamps) were automatically controlled to provide around 500 lux on the work plane, which also provide realistic contrast/luminance conditions. Nevertheless, the amount of electric lighting will have an

impact on the perception of view due to changes in the luminance of the fabrics and contrast levels. For example, high electric light levels would result in higher interior luminances that would affect the perception of view clarity. The effect of higher/lower electric light levels was not studied, and future research on this topic would provide useful results for different interior lighting scenarios.

Although the developed model works very well for the studied sky conditions (sunny and cloudy) in North America, its applicability in other locations with different sky luminance distributions, window products and sociocultural factors is uncertain. Similar studies in other parts of the world are needed to develop a universal model for view clarity through shading fabrics.

CHAPTER 8. DESIGN RECOMMENDATIONS

8.1 Introduction

Throughout the previous chapters of this Thesis, useful results were presented mostly concerning the visual comfort aspect of design, along with the energy performance improvement due to the utilization of daylight and details about the impact of the properties of roller shades on visual comfort and visual clarity. However, the overall feeling of being connected to the exterior is an important aspect that should not be neglected; a variety of studies (described in detail in Chapter 2.10) showed the importance of outside view, which can at times even reduce the perception of daylight glare (Tuaycharoen and Tregenza, 2007; Konis, 2013). Successfully assessing the visual environment and designing spaces focused on daylight provision requires the consideration of all three parameters, as shown in Figure 8.1.

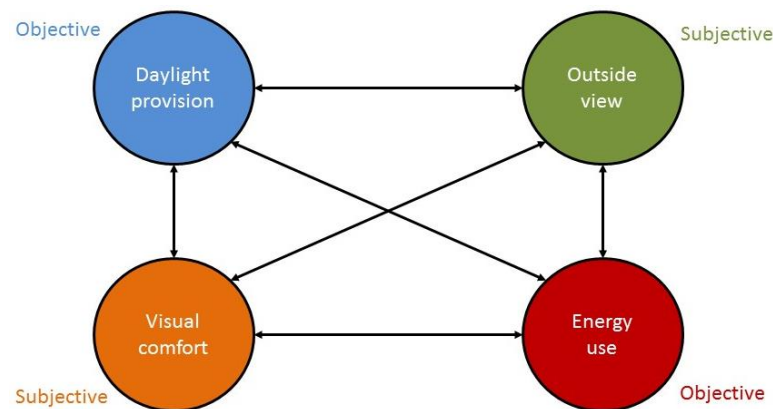


Figure 8.1 Interactions between main criteria for evaluating visual environment

Considering the above, this chapter comes back to the end-goal of the Thesis, to include most of the newly acquired knowledge presented in the previous chapters in a triple criterion in order to select the most effective design visual environment approach for a private and open plan office spaces with respect to visual comfort, lighting energy performance and connection to the outdoors.

A strategy of maximizing lighting energy performance and connection to the outdoors while keeping visual comfort as a constrain constitutes a straightforward decision making process, which can be used either in existing buildings, in terms of retrofitting and positional layouts or also optimize the design of new spaces, in terms of orientations, façade configurations, control methods or even spatial layouts according to the specific needs and functions of the space. The above can be all linked in one main annual metric, the Visual Environment Index (VEI), which consists of three parts: VEIc, related to visual comfort, VEIe, focusing on lighting energy performance and VEIv covering the connection to the outdoors (outside view). The approach under which each of the three parts are handled is discussed in section 8.2

8.2 A suite of metrics for the holistic evaluation of the visual environment

8.2.1 Visual Comfort Autonomy (VCA)

The Visual Comfort Autonomy or VCA is defined as the portion of working hours when a person in a specific position and under a selected viewing direction is under visually comfortable conditions. There are multiple approaches that can be followed in order to evaluate visual comfort and extract VCA. As explained in Chapter 4.3.3, there is some controversy regarding the use of DGP in the cases of direct sunlight penetrating the room

through roller shade fabrics; although the common experience states that fully closed roller shade fabrics of low openness lead to comfortable conditions for most of the time, DGP can predict discomfort instead. This is caused by the solar corona's luminance which can reach extreme values, even when observed through low-openness fabrics, and therefore inflates the luminance term of DGP, causing the prediction of higher glare level compared to everyday practice, especially for the cases of tight fabrics. Therefore, alternate criteria should be preferred in the cases of spaces equipped with shading fabrics, especially for evaluations where the sun will be within the field of view through window shades for a significant portion of the time. DGP_{mod} and its 0.44 border of discomfort, proposed in Chapter 6.3.4 are at this point only validated for fully applied shading fabrics, and should not be used for controlled cases, where part of the window will be unshaded. For these cases, a more general approach is suggested, based on thresholds for DGPs to account for the overall brightness of the space, and for the direct part of vertical illuminance hitting the eye, to account for the influence of the extreme luminance of the solar disc. As DGPs is a linear function of the total vertical illuminance on the eye, the above criterion is translated to a double illuminance (Direct and Total) criterion. The results of Chapter 6.3.2 proposed discomfort thresholds for direct and total vertical illuminances (870 and 2710, respectively), but it has to be kept in mind that they were referring to conditions of fully applied shading, that may or may not have interfered with the glare perception. For that reason, and until other validated approaches shed some light for the case of partly opened shades, the proposed thresholds are (i) 0.35 for DGPs (translated to a 2760 threshold for vertical illuminance and (ii) 1000 lux for the direct vertical illuminance, as a modification of the IES Standard LM-83-12 (IESNA, 2012). For the threshold used in the case of DGPs,

a conservative approach is followed, using the 0.35 “noticeable” glare limit. This selection is irrelevant for closed shades of low visible transmittance, as the upper limits of vertical illuminance penetrating the fabrics are usually within the noticeable limits. In addition, the vertical illuminance threshold associated with this limit (2760 lux) is a better fit with the validated threshold presented in Chapter 6 for fully closed shades. However, for cases of controlled shades, with higher or lower portions of the window remaining unshaded, this threshold might interfere with the annual discomfort hours. Therefore, it should be the designer’s decision whether to follow a more conservative approach or not. For the direct vertical illuminance, the threshold is already mentioned in literature (Jakubiec and Reinhart, 2015). The latter study is also the only one in current literature that proposes a temporal threshold for conditions of high glare; specifically, it is stated that occupants experiencing discomfort glare of $DGP > 0.4$ or direct sunlight on the eye or the workplane over 1000 lux for more than 5.25% of working hours would evaluate the conditions as intolerable. However, as mentioned above, it is yet to be determined whether such long term temporal thresholds should be based on the noticeable or disturbing limits of DGP, as well as the required duration or magnitude for a human study to validate them. Therefore, for the needs of the presentation of the methodology, it is proposed that in order to constitute a seating layout as usable, VCA must be more than 95% throughout the annual working hours. Therefore, only seating layouts that comply with that constrain should be further evaluated for the secondary objectives (lighting energy savings potential and connection to the outdoors). The decision about which of the latter two should be a priority belongs to either the architect or the building manager.

For the case of private offices, where the selection of the optimal position is of the essence, the VEIc index for each combination of position and viewing direction is considered to be equal to the VCA, as described above. Therefore:

$$VEIc_i = VCA_i \quad (8.1)$$

For the case of open-plan offices, in order to be able to directly compare two different overall layouts, a single index should be considered, presenting the usability potential of the space in terms of visual comfort. This can be seen in equation 8.2, with the comfort sub-part of the Visual Environment Index, showing the portion of the open-plan footprint that can be utilized with workstations.

$$VEIc = \frac{\sum_{i=1}^n i}{n} | VCA_i > 95\% \quad (8.2)$$

8.2.2 Lighting Energy Performance

In order to account for daylighting provision and lighting energy use reduction, the annual index of continuous Daylight Autonomy is used. This metric is more suitable for obtaining light energy use for offices with light dimming control systems, a common practice nowadays. A threshold of 300 lux on the work plane is used, complying with IES recommendations (IESNA, 2012). For the case of positioning alternatives in a private office, the cDA₃₀₀ for each possible seating position is evaluated (spatial variation) so the lighting energy savings potential of each position can be compared, as seen in Eq. (8.3).

$$VEIe_i = cDA_i \quad (8.3)$$

For the case of an open plan office, where the overall evaluation of the office layout is of the essence, the spatial average cDAs of all points of the usable grid, as they are defined

by VEI_e is used. The latter constitutes the energy sub-part of the Visual Environment Index, shown in Equation 8.4.

$$VEI_e = \frac{\sum_{i=1}^n cDA_i}{n} \mid i \cap (n \in VCA > 95\%) \quad (8.4)$$

8.2.3 Connection to the outdoors

The Effective Outside View or EOV is introduced in order to quantify the connection to the outdoors in terms of amount of view and quality of view for the case of fully applied shading. As quality of view depends on a variety of highly subjective parameters, including scenery, location, orientation etc., the authors decided to include as the sole quality parameter the clarity of view, quantifiable by the View Clarity Index (VCI), presented in Chapter 7. The latter (Eq. 8.5) associates the two commonly available fabric properties (openness factor and visible transmittance) with the level of visual clarity while looking towards the exterior through a specific fabric.

$$VCI = 1.43 \cdot (OF)^{0.48} + 0.64 \cdot \left(\frac{OF}{T_v} \right)^{1.1} - 0.22 \quad 0 \leq VCI \leq 1 \quad (8.5)$$

, where OF is the openness factor and T_v is the normal total visible transmittance of the fabric as provided by the specifications.

According to the Effective Outside View definition, the amount of view is defined as the portion of the occupant's visual field that is covered by a window, corrected by the clarity of view through the particular fully applied shading fabric, if any. In that scope, and in order to provide a sense of measure against visual field having a full connection to the exterior, the projected solid angle of the visible part of the window (for each position and

view direction of interest) is normalized with the overall solid angle of the human visual field, Ω_{FOV} (approximated as a circular cone with a half-angle of 78°). To make calculations more efficient, the window is discretized into rectangular fragments to approximate the total solid angle of the window as the sum of the respective solid angles of the fragments (Figure 8.2). An algorithm rejects all window fragments that extend beyond the field of view of 78° and includes the rest in equation 8.4 which gives the Effective Outside View for cases of fully applied shading, considering both the amount and the clarity of outdoor view for any seating position, view direction and shading fabric.

$$\text{EOV} = \frac{\sum_{i \in \text{FOV}} \Omega_{i \in \text{FOV}} \cdot \text{VCI}}{\Omega_{\text{FOV}}} = \sum_{i \in \text{FOV}} \frac{A_i \cos \theta_i \cdot \text{VCI}}{2\pi(1 - \cos 78^\circ) \cdot |\vec{D}_i|^2} \quad (8.6)$$

,where A_i is the area of each visible window fragment i , θ_i is the angle between the normal to the window and the line connecting the eye and the fragment, and D_i is the distance between the eye and the fragment as shown in Fig. 8.2.

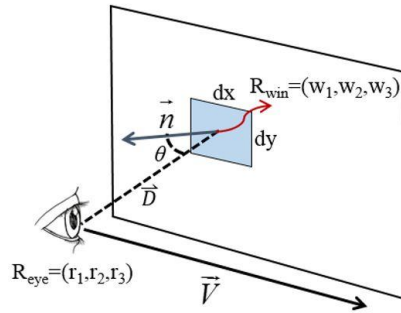


Figure 8.2: Calculation of differential solid angles and projected solid angle of each window segment in the direction of the observer.

In the cases of dynamic shading, either manual or automated, the EOV can be modified with equation 8.7 in order to cover partly shaded windows.

$$EOV(t) = \frac{\sum \Omega_{i \in SA}(t) \cdot VCI_s + \sum \Omega_{i \in UA}(t) \cdot VCI_g}{\Omega_{FOV}} \quad (8.7)$$

, where SA is associated with the shaded area and UA with the unshaded area of the visible part of the window, respectively. EOV is a function of time in cases of controlled shades. In all other cases (always open or always closed), it keeps constant over time for a single position. For that case (as well as the case of fully unshaded fenestration), the view clarity of the glass is considered to be equal to 1, complying with the assumption presented in Chapter 7. While this can be considered to be reasonable for often used glazing systems (both clear, tinted or coated), it has to be modified for light-redirecting systems and translucent materials using human subject studies similar to the one presented in Chapter 7.

Differences in shading controls in terms of dominant opened portions can be reflected in clearer way when investigated in a longer term basis. For that reason, an annual evaluation is suggested to draw safer conclusions about the differences between control strategies. In that scope, for the case of a private office with specific seating positions of interest, the Effective Outside View can be evaluated on an annual level using the average value of the index over the annual working hours for each position, as shown in equation 8.8. The strict consideration of working hours is essential, as in most control strategies roller shades are returned to either fully closed or fully open positions when the space is unoccupied. Consideration of these states in annual basis comparison would mask the actual differences by including approximately 4015 annual hours with identical shading positions.

$$EOV_{an,i} = \frac{1}{n_{w.hours}} \sum_1^{n_{working\ hours}} EOV_i(t) \quad (8.8)$$

In that scope, the “connection to the outdoors” part of the VEI for the case of private offices with controlled shades is based on the value of eq. (8.8) for every position and viewing direction of interest:

$$VEIv_i = EOV_{an,i} \quad (8.9)$$

It has to be noted that due to the high dependence of solid angle to the distance, EOV is rapidly decreasing when moving away from the window. This leads to reduced values even for relatively small distances from the window, especially in the side wall facing layout. However, it is still to be investigated whether the proximity to the window plays a significant role to subjects through experimentation. EOV is developed to serve as an effective quantification index for the connection to the outdoors. The absolute level of the sensation of connection to the outdoors is yet to be investigated with human subjects. For that reason, the authors suggest for the values of EOV to be used in a relative level to find the better of two different configurations. The impact of shading controls on EOV can be clearly reflected in Figure 8.3, for (a) facing the window and (b) facing the side wall, for a controlled and a fully open shades case respectively.

For cases when the objective is the overall grading of a space in terms of the connection to the outdoors, a spatial consideration of the EOV, referring only the usable area of the space as it is defined by VEI_c can be used. This constitute the third sub-part of the visual environment index, and is described in equation 8.10.

$$VEIv = \frac{\sum_{i=1}^n EOV_{an,i}}{n_{grid}} | i \cap (n \in VCA > 95\%) \quad (8.10)$$

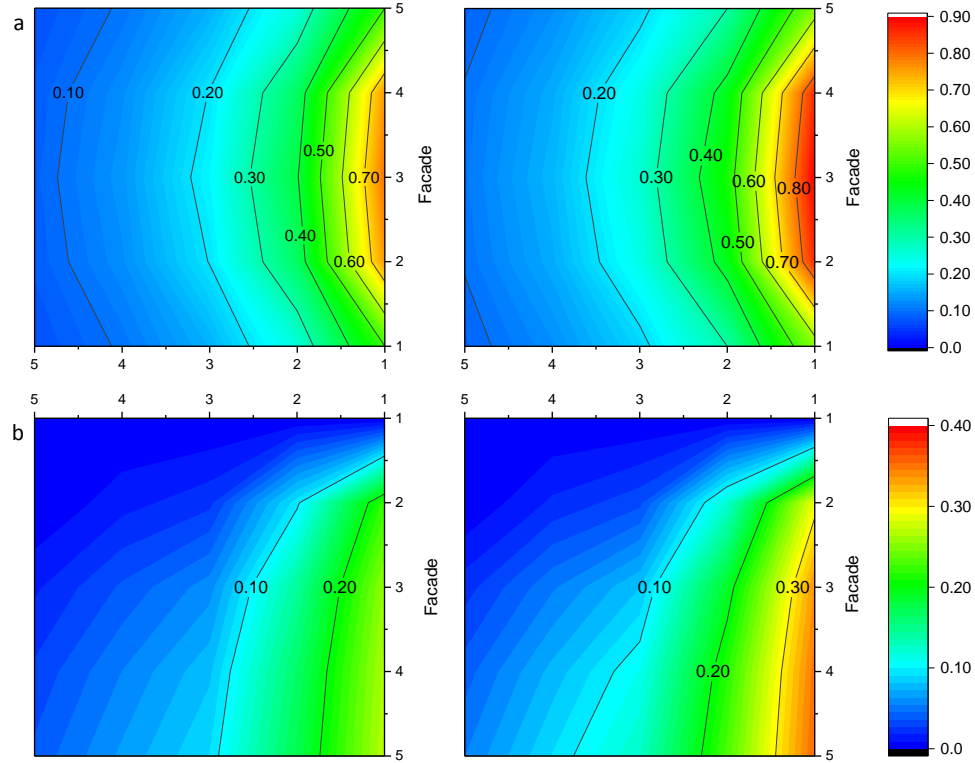


Figure 8.3: Annual Effective Outside View spatial distribution for controlled (left) and for fully open (right) shades respectively for (a) viewing direction towards the window and (b) viewing direction towards the side wall. The two axes indicate a 5x5 grid of the room.

8.3 Using the suite of metrics as a triple visual environment criterion

The suite of the visual environment metrics presented in 8.2 can be used for a wide range of applications, for direct comparisons of two or more different space configurations. These can include differences in terms of envelope design, complex fenestration systems, orientations, shading controls, seating layouts etc. The most objective way to evaluate these

different setups is through annual results using any desired modeling approach. For the needs of this thesis, and in order to present two different case studies of using the triple criterion, the hybrid ray-tracing and radiosity daylighting model presented in Chapter 3.4 is used for the calculations of interior illuminances, glare indices, VCA and continuous daylight autonomy. For the calculations of the EOV index, a separate 3D geometry model was used, discretizing the window as described in section 8.2.3 and calculating the effective outside view. For the cases of dynamic shading, an additional input vector was the shade position for each time step.

The shading controls presented in the case studies are described in detail in Chapter 3.2

8.3.1 A private office case study

In this case study, the visual environment in an existing perimeter office space in Chicago will be investigated, in terms of fabrics, shading controls and positioning in the room. This is a common case where perimeter spaces with fixed characteristics (orientation, window to wall ratio, glazing type etc.) need to be revisited in order to improve visual comfort and lighting energy performance potential.

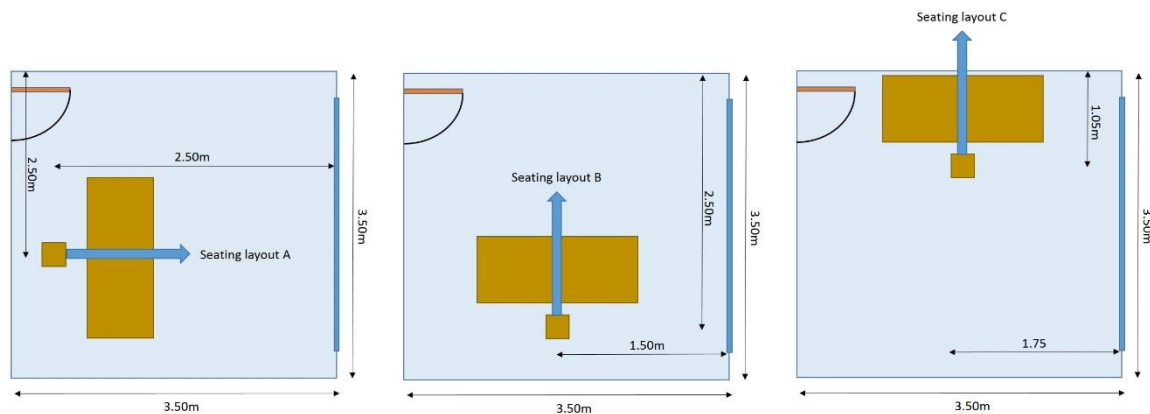


Figure 8.4 Three different layouts investigated for this case study

A typical 3.5mx3.5mx3.5m high private perimeter office space is investigated, facing towards the south and having a 60% window to wall ratio. The glazing is assumed to be a regular double-clear module, often used in existing buildings. In the analysis, three typical seating layouts will be investigated: one facing the window from a distance of 2.50m, one facing the side wall but having part of the window within the visual field, and one facing the wall without having the window within the visual field (Figure 8.4). A layout facing the back wall was considered to be out of the scope of the study, as, while facing the back of the room solves the discomfort glare problems, it entirely eliminates any view outside. A shading fabric (OF of 4.2% and visible transmittance of 5%) was used on the windows.

Table 8.1: Case study 1 simulation results

		South Window			North Window		
		VEIc	VEIe	VEIv	VEIc	VEIe	VEIv
Case I	Layout 1	0.43	0.9	0.15	0.65	0.9	0.15
	Layout 2	0.57	0.9	0.08	0.95	0.9	0.08
	Layout 3	0.79	0.9	0.03	1	0.9	0.03
Case II	Layout 1	0.98	0.29	0.1	1	0.21	0.1
	Layout 2	1	0.4	0.05	1	0.21	0.05
	Layout 3	1	0.38	0.02	1	0.2	0.02
Case III	Layout 1	0.74	0.79	0.13	0.66	0.9	0.15
	Layout 2	0.87	0.81	0.07	0.95	0.9	0.08
	Layout 3	1	0.81	0.03	1	0.9	0.03
Case IV	Layout 1	0.98	0.68	0.11	1	0.62	0.12
	Layout 2	1	0.7	0.07	1	0.63	0.07
	Layout 3	1	0.69	0.02	1	0.63	0.03

The results for the three indices are shown in Table 8.1, for a south and north orientation, in order to point out the fundamental differences regarding the suggested retrofit solutions. Table 8.1 shows that for each orientation, although more than one layout and control approach can be acceptable in terms of the main constrain (VCA), the methodology can at

the same time provide information about the other two important design factors, making the final decision more efficient.

For the south orientation, it is apparent from the results of Case I that a shading system is necessary, even for a side wall facing layout. Although Case II (fully closed) can provide comfortable conditions for all layouts, it leads to very dark conditions (therefore increased electric lighting usage), while the connection to the outdoors is also reduced compared to Case I. Using the Advanced control (Case IV) for the shades and applying the seating Layout 1 will give at the same time comfortable conditions, acceptable lighting energy performance and only slight loss for the connection to the outdoors compared to the fully open window, therefore it can be considered to be the optimal choice. For the North orientation however, it can be seen that even Case I (no shading) could be acceptable when using Layouts 2 and 3 (facing the side wall). This gives an example of how just adjusting the layout, can give significantly improve comfort without any installation cost. As the case study building is located in the northern hemisphere, direct sunlight exposure during the winter is not an issue, therefore the standard control approach (Case III) operates identically to Case I.

This holistic approach is useful for cases of renovations as well as for new designs, where more parameters can be altered, such as WWR, glazing systems, room geometry, orientations etc. Having a complete image of the visual environment of a space allows better prioritizing and more efficient handling of the needs of the spaces and the budget.

8.3.2 Application in open-plan offices – A case study

The main difference of the design approach for open plan offices is that all seating positions are of interest, therefore the scope moves from selecting the best spot to selecting

the configuration that could better utilize the available space. Therefore, the methodology can slightly differentiate, as follows:

The spatial variation of the three metrics (VCA, cDA and EOv) is used to calculate respective annual Visual Environment Indices for comfort, energy use and outdoor view (VEI_c, VEI_e and VEI_v) as described in 8.2. Visual comfort is the main priority, therefore VEI_c (Eq 8.2) is first defined as the portion of comfort-autonomous area (number of seating locations satisfying the VCA criteria for 95% of the working hours). For that area only, VEI_e and VEI_v are calculated from cDA and EOv respectively, averaged over the remaining usable seating location grid, to obtain average VEI “scores” for each directional seating layout.

For each directional layout, the output is a triplet of VPI factors, which can be compared with results for alternate layouts on a relative basis, for an overall visual environment evaluation of any space with a given geometry, orientation, glazing and shading properties. The process is described in Fig. 8.5.

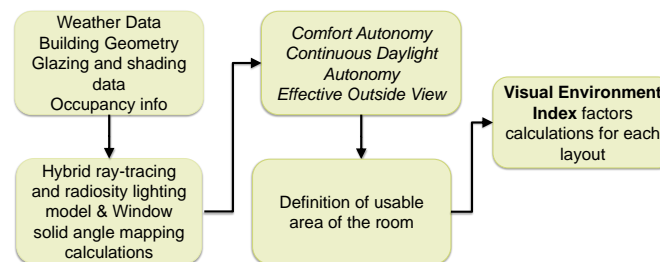


Figure 8.5 Flowchart of simulation methodology and VPI factors

For this case study, a 10 m x 10 m x 4 m high open-plan office space is considered, with a 75% of the façade covered by double clear windows. A dark-colored shade is used with high OF=4.37% and Tv=4.37%, which has a high VCI (0.74) and provides good connection

to the outside even with closed shades. The simulation was performed for West Lafayette, Indiana, for different façade orientations and for two directional workstation layouts (facing the left side wall and facing the window).

The full results can be seen in Table 8.2 while some representative spatial mappings are shown in Figures 8.6-8.7. Orientation plays a significant role: for south-facing façades (Fig. 8.6), due to the increased sunlight exposure and low winter sun, a significant portion of the space (37%) does not satisfy the visual comfort autonomy criteria ($VCA > 95\%$) for window-facing positions. For the rest of the (acceptable) space, $VPI_e = 12.7\%$ and $VPI_v = 7.4\%$, as all positions near the window (which contribute to higher effective view) are outside the “comfort-autonomous” zone.

However, for left side wall facing positions, the entire space is within acceptable comfort limits ($VPI_c = 100\%$), therefore VPI_e increases to 24% and VPI_v only negligibly decreases to 7%. (Figure 8.7).

Table 2: Results for all orientations of Case study 2

	VEI _c		VEI _e		VEI _v	
	Window	Wall	Window	Wall	Window	Wall
South	0.63	1.00	0.13	0.24	0.07	0.07
North	1.00	1.00	0.12	0.12	0.18	0.07
West	0.56	0.76	0.13	0.16	0.07	0.03
East	0.65	1.00	0.10	0.19	0.08	0.07

For north-facing facades (Fig. 8.7), where the sun is not visible in the winter and the brightness conditions are lower, the entire space is “comfort-autonomous” for both viewing directions and therefore the resulting VEI_e remains stable. However, the spatial EO_V is more than twice as high for window-facing layouts, which makes this configuration more appropriate. East orientations show a behavior equivalent to the one of the south façade,

making side wall facing layout more appropriate, while west facing is the worst scenario, as the increased presence of the sun makes none of the layouts efficient, so for that case an alternative light redirecting shading device, as venetian blinds should be preferred.

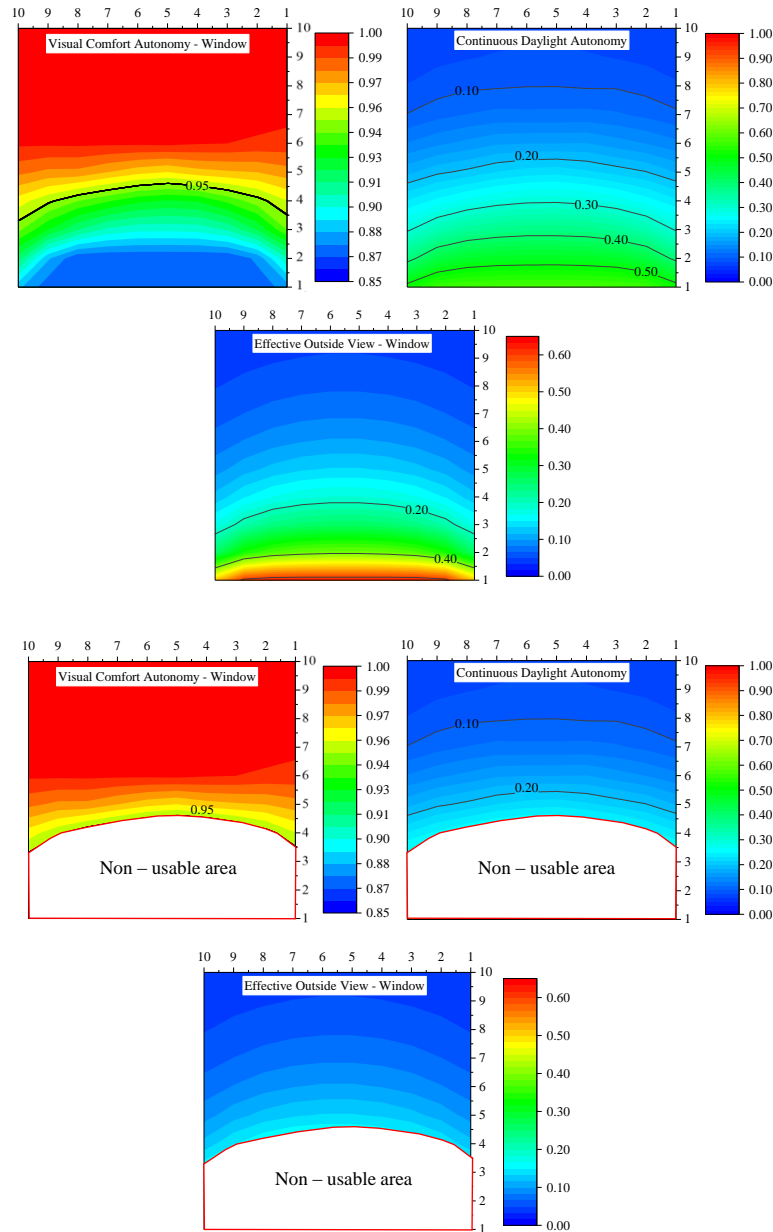


Figure 8.6: Visual Environment Indices for South facing façade before (top) and after (bottom) subtracting the non-usable area due to VCA < 95%. Window is in the bottom of each map.

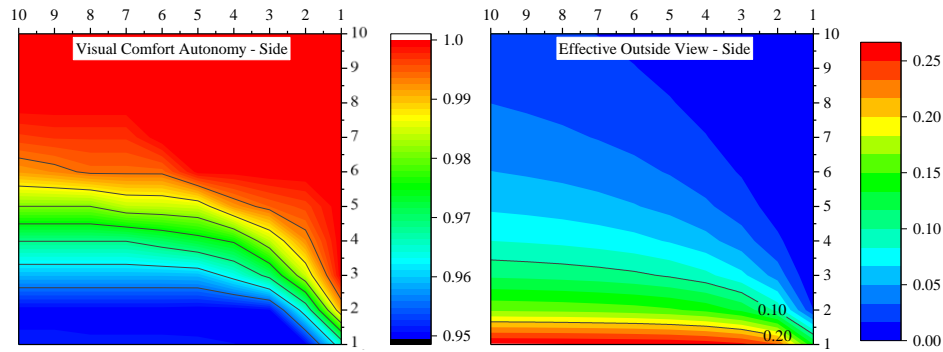


Figure 8.7: VCA and EOV mapping for side wall facing layout and south orientation – Entire floor plan is usable – Window is in the bottom of each map.

8.4 Discussion - Limitations

This chapter suggests a new methodology for evaluating the overall visual performance in offices based on visual comfort, lighting energy use and outdoor view criteria. The method can be used either during the design phase, to compare different envelope configurations, or for existing buildings, to make decisions about the directional layout of workstations. A carefully selected layout can lead to higher space usability, lower lighting energy use and higher connection to the outdoors. This study part of ongoing research, aiming to provide more conclusive regulations for perimeter offices in terms of comfort, energy and connection to the outdoors.

The methodology also introduces some limitations, the solution to some of which is an essential part of future work.

- The permitted annual amount of discomfort hours (here assumed to be 5%) has not been extensively studied; Jakubiec and Reinhart present a value connected to direct vertical illuminance exceeding 1000 lux and discomfort, however this is

not based on an annual test, but in a long exposure in the workstations. Long term experiments with human subjects are needed in order to define a specific annual threshold.

- The EOV index is a strictly geometrical quantification of the amount of outdoor view corrected with the clarity of view, for fixed or dynamic fenestration systems. While VCI is extracted by human subjects experimentation, the acceptable ranges of the amount of view are still unclear; the extent in which the distance from a window affects the satisfaction of occupants if the whole window is still within the visual field is yet to be investigated, along with the extent of compromise a partly shaded window can cause to the sensation of connection to the outside, even with a very high VCI fabric. It has to be noted that for very clear fabrics (VCI close to 1), the importance of the shading control is not effectively captured by EOV, as the shaded and the unshaded portions are almost counted as identical. All the above remarks have yet to be investigated with human subjects, being an important part of the future work of the author.
- The study does not take into account possible reflections of the sun on the screens in the cases of side viewing directions. This effect is highly dependent on the type and positioning of the screen, while different subjects choose to have their screens right in front of them or at a slight angle, while others may prefer to use their laptops instead of regular monitors, leading to a multitude of possible scenarios that extend beyond the scope of the study. As a general recommendation, non-reflective screens should be used in all side wall seating layouts, independent from the shading controls used, as a significant amount of

the solar direct light will still penetrate the room, except the case of using very low openness fabrics.

CHAPTER 9. FUTURE WORK

9.1 Development of a standard framework for glare evaluations

Chapters 5 and 6 of this thesis cover extended surveys targeted to glare evaluation of different conditions. As it happens in all comfort-related research studies, the data sets are rather small, with this being a result of limited resources, in terms of human subjects, budget, availability of facilities, weather conditions, etc. Small data sets as the ones presented in this Thesis always involve the risks of bias and possible overfit. In addition, the ordered grouping approach for the evaluation of metrics requires as many data points as possibly available, a fact that does not permit further cross-validations. All the above signify the necessity of proposing a standard method of obtaining data, in order for different data sets from around the globe to be able to be combined and processed in meta-analyses. This need is also expressed in a recent study by Van den Wymelenberg (2014) where the deficiencies of current glare research are analyzed.

9.2 Glare evaluation with the sun visible through diffuse fabrics.

Most chapters of this Thesis investigate daylighting for cases of dynamic or static shading with regular shading fabrics, with small but significant openness. As it is stated in Chapter 4, and also implied in the results of Chapters 5 and 6, fully diffuse fabrics could

lead to entirely different results, in terms of glare (solar disc will create a different effect), view clarity and daylight provision. Although such a hypothesis can be easily confirmed in terms of glare and daylight performance with the use of simulation approaches like the one described in Chapter 3.4, it also needs to be validated with human subjects' experimentation, equivalent to the ones presented in Chapters 5&6.

9.3 Fabric selection guidelines

The new methodology presented in Chapter 6 sheds light to the unexplored territory of the interaction of fabric properties with glare sensation for cases of the sun being within the visual field. Using the newly developed glare indices, a fabric properties selection methodology can be proposed, equivalent to the one suggested by Chan et al. (2015), but also enhanced with the addition of the impact of view clarity (analyzed in Chapter 7). Using the three parts of the visual environment index of Chapter 8, a unified grading system for fabrics can be developed, with respect to visual comfort, lighting energy performance and connection to the outdoors.

9.4 Luminance and glare evaluation using smartphones

Measuring glare has been a challenge so far, as HDR imaging is complex, time consuming and expensive to implement, as explained in Chapter 3. In addition, having a camera close to the eye position of the subject for almost all of the times is not possible, while it is also not applicable for large-scale studies with hundreds of occupants. Developing a reliable method for measuring glare with simple cameras, and producing an

efficient methodology for processing and correcting the images for estimating daylight glare can lead to new innovative ways of visual comfort mapping in indoor environments. The methodology and performance of luminance measurements through a smartphone will be investigated, with all necessary detailed corrections (luminance, vignetting). If possible, instead of only using the smartphone to take pictures manually, an application will be developed that will shoot pictures in a way appropriate for high detail HDR pictures creation. Then, if possible, HDRgen code will be implemented in the smartphone app, among pre-calculated response curves for the most important smartphone models and optional combinations with fisheye cameras, in order to create a complete and accurate luminance measurement system within the smartphone. Image processing will then be performed to extract glare metrics. This approach would provide instant measurements (and recording) of visual conditions and preferences in every building. Occupants would then be able to report their visual impressions online, building a huge database that could be used to develop new visual comfort guidelines for different scenarios. This project is challenging, since it involves correcting phone cameras for correct measurements, automatic picture shooting and configurations, and HDR creation through an app (requiring programming using the smartphone interface), plus image processing for glare evaluation embedded in the application.

REFERENCES

REFERENCES

- Abdi, H. (2010). "Greenhouse-Geisser correction". In N. Salkind (Ed.), *Encyclopedia of Research Design*, pp. 544-548. Thousand Oaks, CA: Sage.
- Appel A. (1968). "Some techniques for shading machine renderings of solids." *AFIPS Conference Proc.* 32 pp.37-45
- Aries, M. B., J. A. Veitch, et al. (2010). "Windows, view, and office characteristics predict physical and psychological discomfort". *Journal of Environmental Psychology* **30**(4): 533-541.
- Aston, S.M., Belichambers, H. (1969). "Illumination, colour rendering and visual clarity". *Lighting Research and Technology* **1** (4), 259-261.
- Bonferroni, C. E. (1936). "Teoria statistica delle classi e calcolo delle probabilità". *Pubblicazioni del Istituto Superiore di Scienze Economiche e Commerciali di Firenze* 8, 3-62.
- Borisuit A., Scartezzini J-L., Thanachareonkit A. (2010). "Visual discomfort and glare rating assessment of integrated daylighting and electric lighting systems using HDR imaging techniques". *Architectural Science Review* **53**(4), 359-373.
- Boyce, P. (1977). "Investigations of the subjective balance between illuminance and lamp colour properties". *Lighting Research and Technology* **9**(1): 11-24.
- Brand, J.L. (2006). "An easy, effective and useful measure of exterior view: toward a user-centered perspective for assessing occupancy quality". *Proceedings of the Human Factors and Ergonomics Society 50th Annual Meeting*, pp. 799-803.

- Cai H. (2013). "High dynamic range photogrammetry for synchronous luminance and geometry measurement". Lighting Research and Technology **45**, 230-257.
- Cannavale A., Fiorito F., Resta D., Gigli G. (2013). "Visual comfort assessment of smart photovoltachromic windows". Energy and Buildings **65**, 137–145.
- Cantin F., Dubois F.C. (2011). "Daylighting metrics based on illuminance, distribution, glare and directivity". Lighting Research and Technology **43**, 291-307.
- Carrier, K. and Ubbelohde, M.S. (2005). "The Role of Daylighting in Leed Certification: A Comparative Evaluation of Documentation Methods". 2005 Solar World Conference, Orlando.
- Chan Y.-C., Konstantzos I., Tzempelikos A. (2014). "Annual daylight glare evaluation for typical perimeter offices: simulation models versus full-scale experiments including shading controls". Proceedings of ASHRAE Annual Conference, Seattle, Washington.
- Chan Y.-C., Tzempelikos A. (2012). "A hybrid ray-tracing and radiosity method for calculating radiation transport and illuminance distribution in spaces with venetian blinds". Solar energy **86**(11), 3109-3124.
- Chan Y-C., Tzempelikos A. (2013). "Efficient venetian blind control strategies considering daylight utilization and glare protection". Solar Energy **98**(C), 241-254.
- Chan Y.-C., Tzempelikos A., Protzman B. (2014). "Solar optical properties of roller shades: modeling approaches, measured results and impact on daylighting and visual comfort". Proceedings of 3rd International High Performance Buildings conference at Purdue, West Lafayette, Indiana.
- Chan, Y. C., Tzempelikos, A., & Konstantzos, I. (2015). "A systematic method for selecting roller shade properties for glare protection". Energy and Buildings, **92**, 81-94.
- CIE (1992) "Discomfort Glare in the Interior Lighting", Commission Internationale de l'Eclairage (CIE), Technical committee TC-3.13, Division 4, Interior Environment and Lighting Design, Vienna, Austria.

- Clear R.D. (2013). "Discomfort glare: what do we actually know?" Lighting Research and Technology **45**, 141-158.
- Collins M., Wright J.L., Kotey N. (2012). "Off-normal solar optical property measurements using an integrating sphere". Measurement **45**(1), 79-93.
- Da Silva, P. C., V. Leal, et al. (2013). "Occupants interaction with electric lighting and shading systems in real single-occupied offices: Results from a monitoring campaign". Building and Environment **64**: 152-168.
- Einhorn, H. (1979). "Discomfort glare: a formula to bridge differences". Lighting Research and Technology **11**(2): 90-94.
- Energy Plus (2015). "Energyplus Engineering Reference – the reference for Energyplus Calculations", Lawrence Berkeley National Laboratory (LBNL).
- Galasiu, A. D. and J. A. Veitch (2006). "Occupant preferences and satisfaction with the luminous environment and control systems in daylit offices: a literature review". Energy and Buildings **38**(7): 728-742.
- Goral, C.M., Torrance, K.E., et al. (1984). "Modeling the interaction of Light between Diffuse Surfaces". ACM SIGGRAPH Computer Graphics, ACM.
- Guth S.K. (1966). "Computing visual comfort ratings for a specific interior lighting installation". Illuminating Engineering, pp. 634-642.
- Haldi, F. and D. Robinson (2010). "On the unification of thermal perception and adaptive actions". Building and Environment **45**(11): 2440-2457
- Hirning M., Isoardi G., Cowling I. (2014). "Discomfort glare in open plan green buildings". Energy and Buildings **70**, 427-440.
- Hopkinson, R. (1957). "Evaluation of glare". Illuminating Engineering **52**(305): 329-336.
- Hopkinson, R.G., Petherbridge, P., et al. (1966), "Daylighting", Heinemann.
- Hopkinson, R. G. (1972). "Glare from daylighting in buildings" Applied Ergonomics **3**(4): 206-215

IESNA (2012). “IES Standard LM-83-12. Approved method: IES Spatial Daylight Autonomy (sDA) and Annual Sunlight Exposure (ASE)”. Illuminating Engineering Society of North America, New York, USA.

Inanici M. (2006). “Evaluation of high dynamic range photography as a luminance data acquisition system”. Lighting Research and Technology **38**(2), 123-134.

Inanici M., Galvin J. (2004). “Evaluation of high dynamic range photography as a luminance mapping technique”. LNBL Report 57545.

Inkarojrit, V. (2008). “Balancing Comfort: Occupants’ Control of Window Blinds in Private Offices” (Doctoral Dissertation). Retrieved from escholarship.org database – University of California

Iwata, T., Tokura, M. (1997). “Position Index for a glare source located below the line of vision”, Lighting Research and Technology **29**(3) 172-178

Jakubiec J.A., Reinhart C.F. (2013). “Predicting visual comfort conditions in a large daylit space based on long-term occupant evaluations: a field study”. Proceedings of IBPSA 2013: 13th Conference of International Building Performance Simulation Association, Chambéry, France.

Jakubiec J.A., Reinhart C.F. (2012). “The ‘adaptive zone’ – a concept for assessing discomfort glare throughout daylit spaces”. Lighting Research and Technology **44**(2), 149-170.

Jakubiec J.A., Reinhart C.F. (2015): “A concept for predicting occupants’ long term visual comfort within daylit spaces”. Leukos **2724**, 1-18.

Jakubiec J.A., Inanici, M., Van den Wymelenberg, K., Mahic, A. (2016). “Improving the Accuracy of Measurements in Daylit Interior Scenes Using High Dynamic Range Photography”. Proceedings of PLEA 2016, Los Angeles.

Karlssen, L., Heiselberg, P., Bryn, I., Johra, H. (2015). “Verification of simple illuminance based measures for indication of discomfort glare from windows”. Building and Environment, **92**, 615-626.

- Kim W., Kim J.T. (2011). "The scope of the glare light source of the window with non-uniform luminance distribution". Indoor and Built Environment **20**(1), 54–64.
- Kim W., Kim J.T. (2012). "The variation of the glare source luminance according to the average luminance of visual field". Indoor and Built Environment **21**(1), 98–108.
- Kittler, R. (1967). "Standardisation of Outdoor Conditions for the Calculation of Daylight Factor with Clear Skies". Conference sunlight in Buildings, Rotterdam, Netherlands.
- Kleindienst S.A., Andersen M. (2009). "The adaptation of daylight glare probability to dynamic metrics in a computational setting". Proceedings of Lux Europa 2009 - 11th European Lighting Conference, Istanbul, Turkey.
- Konis, K. (2012). "A method for measurement of transient discomfort glare conditions and occupant shade control behavior in the field using low-cost CCD cameras". American Solar Energy Society (ASES) National Solar Conference, Denver, Colorado.
- Konis, K. (2013). "Evaluating daylighting effectiveness and occupant visual comfort in a side-lit open-plan office building in San Francisco, California". Building and Environment **59**: 662-677.
- Konis, K. (2014). "Predicting visual comfort in side-lit open-plan core zones: results of a field study pairing high dynamic range images with subjective responses", Energy and Buildings. **77** 67-79."
- Konstantzos I., Tzempelikos A. (2014). Daylight Glare Probability measurements and correlation with indoor illuminance in a full-scale office with dynamic shading controls". Proceedings of 3rd International High Performance Buildings conference at Purdue, West Lafayette, Indiana.
- Konstantzos, I., Tzempelikos, A., & Chan, Y. C. (2015). "Experimental and simulation analysis of daylight glare probability in offices with dynamic window shades". Building and Environment **87**, 244-254.
- Kotey N.A., Wright J., Collins M.R. (2009). "Determining off-normal solar optical properties of roller blinds". ASHRAE Transactions **117** (1), 10 pages.

- Kumaragurubaran V., Inanici M. (2013). "Hdroscope: high dynamic range image processing toolkit for lighting simulations and analysis". Proceedings of IBPSA 2013: 13th Conference of International Building Performance Simulation Association, Chambéry, France.
- Lafortune, E.P., Willems, Y.D. (1996). "Rendering Participating Media with Cidirectional Path Tracing". Rendering Techniques '96, Springer: 91-100.
- LBNL (2013). "WINDOW 7 simulation manual". Lawrence Berkeley National Laboratory. <http://windows.lbl.gov/software/window/7/>
- Leather, P., Pyrgas, M., Beale, D., Lawrence, C. (1998). "Windows in the workplace: sunlight, view, and occupational stress". Environment and Behavior **30**, 739-762.
- Luckiesh, M., & Guth, S. K. (1949). "Brightness in visual field at borderline between comfort and discomfort (BCD)". Illuminating Engineering **44**(11), 650-670.
- Mardaljevic J. (2000). "Beyond Daylight Factors: An Example Study Using Daylight Coefficients". Proc. CIBSE National Lighting Conference, York, UK.
- Mardaljevic J., Andersen M., Roy N., Christoffersen J. (2012). "Daylighting metrics: is there a relation between useful daylight illuminance and daylight glare probability?" Proceedings of BSO12 -Building Simulation and Optimization Conference, Loughborough, UK.
- Marsh, A. (2006). "Ecotect." London, UK: Square One Research (2006).
- Matusiak B.S. (2013). "Glare from a translucent facade, evaluation with an experimental method". Solar Energy **97**, 230-237.
- Moon, P. and Spencer, D. E. (1942). "Illumination form a Non-Uniform Sky". Transactions of the Illumination Engineering Society **37**.
- Nabil, A. and Mardaljevic, J. (2006). "Useful Daylight Illuminances: A Replacement for Daylight Factors". Energy and Buildings **38**(7): 905-913.
- Nazzal, A. A. (2005). "A new evaluation method for daylight discomfort glare". International Journal of Industrial Ergonomics **35**(4): 295-306.

Perez, R., Ineichen, P., Seals, R., Michalsky, J., & Stewart, R. (1990). "Modeling daylight availability and irradiance components from direct and global irradiance". Solar energy **44**(5), 271-289.

Pigg S., Eilers, M., Reed, J. (1996). "Behavioral aspects of lighting and occupancy sensors in private offices: a case study of a university office buildgin", ACEEE 1996 summer study on energy efficiency in buildings 8, p.8, 8161-8171.

Raanaas, R.K., Patil, G.G., Hartig, T. (2012). "Health benefits of a view of nature through the window: a quasi-experimental study of patients in a residential rehabilitation center". Clinical rehabilitation **26** (1), 21-32.

Rea, M.S. (2000). "The IESNA Lighting Handbook: Reference and Application"

Reinhart, C.F. (2006). "Tutorial on the Use of Daysim Calculations for Sustainable Design". Institute for Research in Construction, National Research Council Canada, Ottawa.

Reinhart, C.F., Mardaljevic, J. et al. (2006). "Dynamic Daylight Performance Metrics for Sustainable Building Design". Leukos **3**(1):1-25

Reinhart C.F., Doyle S., Jakubiec J.A., Mogri R. (2012). "Glare analysis of daylit spaces: recommendations for practice":

http://web.mit.edu/tito/_www/Projects/Glare/GlareRecommendationsForPractice.html. Last accessed April 2014.

Rodriguez R.G., Pattini A. (2014). "Tolerance of discomfort glare from a large area source for work on a visual display". Lighting Research and Technology **46**(2), 157-170.

Rodriguez RG, Yamí'n Garreto' JA, Pattini AE. (2015). "Glare and cognitive performance in screen work in the presence of sunlight". Lighting Research and Technology DOI:10.1177/1477153515577851.

Rogers, Z. (2006). "Daylighting Meric Development Using Daylight Autonomy Calculations in the Sensor Placement Optimization Tool". Boulder, CO: Architectural Energy Corporation.

- Sadeghi, SA, Karava, P., Konstantzos, I., Tzempelikos, A. (2015) "Occupant Interactions with Shading and Lighting Systems using different control interfaces: A Pilot Field Study." Building and Environment **97**, 177-195
- Shen, H. and Tzempelikos, A. (2012). Daylighting and Energy Analysis of Private Offices with Automated Interior Roller Shades. Solar Energy **86**(2): 681-704
- Shin, J.Y., Yun, G.Y., Kim, T.J. (2012). "View types and luminance effects on discomfort glare assessment from windows". Energy and Buildings **46**, 139-145.
- Suk J-Y., Schiler M., Kensek K. (2013). "Development of new daylight glare analysis methodology using absolute glare factor and relative glare factor". Energy and Buildings **64**, 113-122.
- Suk J-Y., Schiler M. (2012). "Investigation of Evalglare software, daylight glare probability and high dynamic range imaging for daylight glare analysis". Lighting Research and Technology **45**, 450-463.
- Stumpfel J, Jones A, Wenger A and Debevec P. (2004). Direct HDR capture of the sun and sky. Proceedings of 3rd International Conference on Virtual Reality, Computer Graphics, Visualization and Interaction in Africa, Cape Town, South Africa.
- Technoteam, LMK Labsoft 14.3.6. Last accessed May 2014.
http://www.technoteam.de/product_overview/lmk/software/lmk_labsoft/index_eng.html
- Thornton, W.A., Chen E. (1978). "What is visual clarity?" Journal of the Illuminating Engineering Society **7** (2), 85-94.
- Tregenza, P. and Waters, I. (1983). "Daylight Coefficients". Lighting Research and Technology **15**(2): 65-71.
- Tridium Inc. Niagara AX Software.
<http://www.tridium.com/en/productsservices/niagaraax>.
- Tuaycharoen N., Tregenza P.R. (2007). "View and discomfort glare from windows". Lighting Research and Technology **39**(2), 185-200.

- Tzempelikos, A., (2008). “The impact of venetian blind geometry and tilt angle on view, direct light transmission and interior illuminance”. Solar Energy **82**, 1172–1191.
- Tzempelikos A, Chan Y-C. (2016). “Estimating detailed optical properties of window roller shades from basic available data and modeling implications on daylighting and visual comfort”. Energy and Buildings **126**:396-407.
- Uetani, Y. (2001). “Measurement of cie tristimulus values xyz by color video images-Development of video colorimetry”. Journal of Architecture Planning and Environmental Engineering **543**, 25-32.
- USGBC, L. (2009). “New Construction and Major Renovations”. USGBC–United States Green Building Council, Washington, DC (2011) (updated November 2011).
- Van Den Wymelenberg K., Inanici M., Johnson P. (2010). “The effect of luminance distribution patterns on occupant preference in a daylit office environment”. Leukos **7**(2), 103-122.
- Van Den Wymelenberg, K., & Inanici, M. (2014). “A critical investigation of common lighting design metrics for predicting human visual comfort in offices with daylight.” Leukos **10**(3), 145-164.
- Versluis, R. (2005). “Ray-Tracing Vs. Radiosity Modeling of Venetian and Pleated Blinds and the Influence of the Energetic Properties of Windows.”, IBPSA-NVL Conference. Delft, Netherlands.
- Vrabel, P.L., Bernecker, C., Mistrick, R.G. (1998). „Visual performance and visual clarity under electric light sources: Part II—visual clarity”. Journal of the Illuminating Engineering Society **27** (1), 29-41.
- Ward G. Anywhere Software. Photosphere v1 8. <http://www.anywhere.com>. Last accessed April 2014.
- Ward, G. J. and Shakespeare, R. (1998). “Rendering with Radiance. The Art and Science of Lighting Visualization.” Morgan Kaufmann Publishers

Wienold J. (2007). “Dynamic simulation of blind control strategies for visual comfort and energy balance analysis”. Proceedings of IBPSA 2007 Conference, Beijing, China, pp. 1197-1204.

Wienold J. (2012). EvalGlare Version 1.0. Fraunhofer Institute for Solar Energy Systems, Freiburg.

Wienold J., Christoffersen J. (2006). “Evaluation methods and development of a new glare prediction model for daylight environments with the use of CCD cameras.” Energy and Buildings **38**(7), 743-757.

Wienold J. (2009). “Dynamic daylight glare evaluation.” Proceedings of IBPSA 2009 conference, Glasgow, Scotland, pp. 944-951.

Wienold J. (2013). “Glare Analysis and Metrics”. Last accessed October 2016: https://www.radiance-online.org/community/workshops/2013-golden-co/wienold_glare_rad_ws2013.pdf

Xiong J., Chan Y-C., Tzempelikos A. (2015). “Model-based control algorithms for optimized shading and lighting operation considering visual comfort and energy use.” Proceedings of CISBAT15 Conference, Lausanne, Switzerland.

Yonemura, G., Kohayakawa, Y. (1976). “A new look at the research basis for lighting level recommendations.” US Department of Commerce, National Bureau of Standards Washington, DC.

Yun G.Y., Yoon K.C., Kim K.S. (2014). “The influence of shading control strategies on the visual comfort and energy demand of office buildings. Energy and Buildings **84**, 70-85.

VITA

VITA

IASON KONSTANTZOS

EDUCATION

Ph.D. Purdue University – Lyles School of Civil Engineering – (2012 – 2016)

M.Eng. National Technical University of Athens (NTUA) – Design of and Construction of Underground structures – School of Mining Engineering and School of Civil Engineering (2011)

B.Eng. National Technical University of Athens (NTUA) – School of Civil Engineering (2009)

PUBLICATIONS

PUBLICATIONS

REFEREED JOURNAL PUBLICATIONS

1. **Konstantzos, I.**, Tzempelikos A. (2016). “Daylight Glare Evaluation with the Sun in the Field of View through Window Shades”, Building and Environment. In press
2. Sadeghi, SA, Karava, P., **Konstantzos, I.**, Tzempelikos, A. (2015) “Occupant Interactions with Shading and Lighting Systems using different control interfaces: A Pilot Field Study.” Building and Environment 97, 177-195
3. **Konstantzos, I.**, Chan, Y. C., Seibold, J., Tzempelikos, A., Proctor, R. W., & Protzman, B. (2015). View Clarity Index: a new metric to evaluate clarity of view through window shades. Building and Environment. 90, 216-214
4. Chan, Y. C., Tzempelikos, A., & **Konstantzos, I.** (2015). A systematic method for selecting roller shade properties for glare protection. Energy and Buildings, **92**, 81-94.
5. **Konstantzos, I.**, Tzempelikos, A., & Chan, Y. C. (2015). Experimental and simulation analysis of daylight glare probability in offices with dynamic window shades. Building and Environment **87**, 244-254.

REFEREED CONFERENCE PROCEEDINGS

1. **Konstantzos, I.**, Tzempelikos, A. (2016). “A holistic Approach for Improving Visual Environment in Private Offices”. Proceedings of SBE 16, Thessaloniki 2016.
2. **Konstantzos, A.** Tzempelikos, (2015) Design recommendations for perimeter office spaces based on visual performance criteria, CISBAT International Conference, Lausanne, Switzerland, September 2015.
3. **Konstantzos, I.**, Tzempelikos, A. (2015) “Daylight Glare Probability Measurements in Offices with Dynamic Facades”, ASHRAE Winter Conference, Chicago, January 2015.

4. Y-C. Chan, **I. Konstantzos**, A. Tzempelikos, “Annual Daylight Glare Evaluation for Typical Perimeter Offices: Simulation Models versus Full-Scale Experiments Including Shading Controls”, ASHRAE Annual conference, Seattle, June 2014.

NON-REFEREED CONFERENCE PROCEEDINGS/PRESENTATIONS

1. **Konstantzos, I.**, Tzempelikos, A. (2014). “Daylight glare evaluation when the Sun is Within the Field of View through Window Shades”, Proceedings of 4th High Performance Buildings conference at Purdue, July 2016.
2. **Konstantzos, I.**, Tzempelikos, A. (2014). “Daylight glare probability measurements and correlation with indoor illuminances in a full-scale office with dynamic shading controls”, Proceedings of 3rd High Performance Buildings conference at Purdue, July 2014.
3. **Konstantzos, I.**, “Integration of Humans into Building Design and Operation”. International Living Future conference, Seattle, May 2016.
4. Chan, Y. C., **Konstantzos, I.**, Tzempelikos, A., “Visual Comfort Assessment in Spaces with Smart Façade Controls”, Poster presented at the Herrick IAC Annual Meeting, November 2013.
5. Chan, Y. C., **Konstantzos, I.**, Tzempelikos, A., “The Impact of Roller Shade Properties on Daylighting and Visual Comfort”, Poster presented at the Herrick IAC Annual Meeting, November 2014.
6. **Konstantzos, I.**, Tzempelikos, A., “Design recommendations for perimeter office spaces based on visual performance criteria”, Poster presented at the Herrick IAC Annual Meeting, November 2015.
7. **Konstantzos, I.**, Tzempelikos, A., “Daylight Glare Evaluation with the Sun in the Field of View through Window Shades”, Poster presented at the Herrick IAC Annual Meeting, October 2016.

AWARDS

ASHRAE Graduate Student Grant-in-Aid Award (2014-2015)

3rd Paper Award: 3rd International High Performance Building Conference at Purdue University (2014)